U.S. Department
of Transportation
**National Highway
Traffic Safety
Administration**

NHTSA
www.nhtsa.gov

DOT HS 811 521A

September 2011

Objective Tests for Automatic Crash Imminent Braking (CIB) Systems

Appendices
Volume 2 of 2

CAMP

Crash Imminent Braking Consortium

Ford

GM

Continental

DELPHI

Mercedes-Benz

DISCLAIMER

This publication is distributed by the U.S. Department of Transportation, National Highway Traffic Safety Administration, in the interest of information exchange. The opinions, findings, and conclusions expressed in this publication are those of the authors and not necessarily those of the Department of Transportation or the National Highway Traffic Safety Administration. The United States Government assumes no liability for its contents or use thereof. If trade names, manufacturers' names, or specific products are mentioned, it is because they are considered essential to the object of the publication and should not be construed as an endorsement. The United States Government does not endorse products or manufacturers.

Technical Report Documentation Page

1. Report No. DOT HS 811 521A	2. Government Accession No.	3. Recipient's Catalog No.
4. Title and Subtitle Objective Tests for Automatic Crash Imminent Braking (CIB) Systems Appendices Volume 2 of 2		5. Report Date September 2011 6. Performing Organization Code
7. Authors Carpenter, Michael G., Feldmann, Michael, Fornari, Thomas M., Moury, M. Todd, Walker, Christopher D., Zwicky, Timothy D., and Kiger, Steven M.		8. Performing Organization Report No.
9. Performing Organization Name and Address Crash Avoidance Metrics Partnership on behalf of the Crash Imminent Braking Consortium 39255 Country Club Drive, Suite B-40 Farmington Hills, MI 48331		10. Work Unit No. (TRAIS) 11. Contract or Grant No. DTNH22-05-H-01277
12. Sponsoring Agency Name and Address U.S. Department of Transportation National Highway Traffic Safety Administration 1200 New Jersey Avenue, SE Washington, DC 20590		13. Type of Report and Period Covered Final Report September 2007 – August 2010 14. Sponsoring Agency Code
15. Supplementary Notes		

16. Abstract

This report documents the work completed by the Crash Avoidance Metrics Partnership (CAMP) Crash Imminent Braking (CIB) Consortium during the project titled "Objective Tests for Imminent Crash Automatic Braking Systems." Participating companies in the CIB Consortium were Continental, Delphi Corporation, Ford Motor Company, General Motors, and Mercedes-Benz. The purpose of this project was to attempt to define minimum performance requirements and objective tests for crash imminent braking systems and to assess the potential benefits of various system configurations and performance capabilities.

17. Key Word	18. Distribution Statement Document is available to the public from the National Technical Information Service www.ntis.gov		
19. Security Classif. (of this report) Unclassified	20. Security Classif. (of this page) Unclassified	21. No. of Pages 271	22. Price

Form DOT F 1700.7 (8-72) Reproduction of completed page authorized

Table of Contents

Appendix A Supplier Survey Invitation Letter A-1

Appendix B CIB Technology Survey Questionnaire B-1

Appendix C Cost and Complexity Assessment for Candidate CIB Sensing and Braking Systems C-1

C.1 Sensing System Cost and Complexity Assessment C-1

C.2 Braking System Cost and Complexity Assessment C-2

Appendix D Candidate Sensing Systems for the CIB Project D-1

Appendix E Candidate Braking Systems for the CIB Project E-1

Appendix F CIB Target Development F-1

F.1 Vehicle Target F-2

F.2 Pole/Tree Target F-8

F.3 Pedestrian Target F-8

Appendix G Target Tow System G-1

G.1 Overview G-1

G.2 Motor and Capstan Assembly / Power Supply and Control Unit G-2

G.3 Motor and Capstan Assembly (Part 1) G-2

G.4 Control Unit (Part 2) G-6

G.5 Test Procedure G-6

G.6 Typical Setup G-7

Appendix H Pedestrian Mannequin Testing Report H-1

Appendix I Balloon Car Radar and Visual Properties I-1

Appendix J Correlation of Radar Return Characteristics of 3rd - Generation Balloon Car to Real-World Passenger Car J-1

J.1 Method J-1

J.2 Results of Evaluation J-2
J.3 Summary J-7
Appendix K Standard Testing Conditions and Equipment... K-1
K.1 Standard Conditions for Testing of CIB Systems K-1
K.2 Equipment for Testing of CIB Systems K-2
Appendix L Functional Test Methods..... L-1
L.1 Rear-End – Lead Vehicle Stopped (LVS).....L-1
L.2 Rear-End – Lead Vehicle Moving (LVM).....L-14
L.3 Rear-End – Lead Vehicle Decelerating (LVD).....L-26
L.4 Pedestrian Scenarios.....L-34
L.5 Straight Crossing Path (SCP) L-42
L.6 Left Turn Across Path – Opposite Direction (LTAP-OD).....L-54
L.7 Opposite Direction (OD) L-63
L.8 Pole / Tree L-74
L.9 Rear End – Cut-In.....L-97
L.10 Final Test Procedures for Validated Test Methods.....L-99
Appendix M Comparison of Data Acquisition Systems Used in LVD Scenario..... M-1
Appendix N Conduct Real-World Operational Assessment Data (ROAD) Trip and Recommend Operational Test Methods..... N-1
N.1 ROAD Trip Overview N-1
N.2 ROAD Trip Data Analysis N-1
N.3 Environmental Conditions Not Assessed by the ROAD Trip .. N-56
Appendix O Operational Test Scenarios O-1
O.1 Operational Test Procedure for Objects-in-Roadway O-2
O.2 Operational Test Procedure for Stationary Object at Curve Entrance O-4
O.3 Operational Test Procedure for Stationary Object at Curve-Exit O-7

O.4 Operational Test Procedure for Roadside Stationary Objects .. O-10
O.5 Operational Test for Overhead Signs and Bridges..... O-12
O.6 Operational Test Procedure for Short-Radius-Turns O-14
O.7 Operational Test Procedure for Lead Vehicle Deceleration (LVD)..... O-16

List of Figures

Figure 1: Balloon Cars Used during Testing F-2
Figure 2: Vehicle Foam Pillows Used during Testing F-3
Figure 3: Flip-down Corner Reflector Used during Testing F-4
Figure 4: Hanging Target Testing Simulator F-5
Figure 5: Crash Simulator Used during Testing F-5
Figure 6: Balloon Car Carrier F-6
Figure 7: Balloon Car Puller System Block Diagram F-6
Figure 8: Target Tow System - Overview G-1
Figure 9: Target Tow System - Detail G-2
Figure 10: Target Tow System on Truck Rear Hitch G-3
Figure 11: Front View of the Target Tow System G-4
Figure 12: Rear View of the Target Tow System G-5
Figure 13: Simplified Test Flow Chart G-7
Figure 14: Balloon Car on Ground Sheet with Rope, PVC Guide Pipes, Steel Cables, Zip Ties and Cords G-8
Figure 15: Target Tow Setup on Truck Rear Hitch (Pedestrian Scenario) G-8
Figure 16: Target Tow Setup on Truck Rear Hitch (LVM Scenario) G-8
Figure 17: Anchored Base Plate for Steel Cables G-9
Figure 18: Anchored Base Plate for 90 Degree Rope Pulleys G-9
Figure 19: End Pulley with Safety Spring G-9
Figure 20: Capstan Drum Assembly with Tow Rope, End Pulley, Safety Spring and Encoder Wheel G-10
Figure 21: Complete Setup of Target Tow System for LVM Scenario G-10
Figure 22: 2nd-Generation Balloon Car Front, Side and Rear Views I-1
Figure 23: 3rd-Generation Balloon Car Front, Side and Rear Views I-2
Figure 24: 3rd-Generation Balloon Car Rear View I-2
Figure 25: Methodology for Balloon Car Evaluation J-1
Figure 26: Speed Reductions and Braking/No Braking Distribution J-3
Figure 27: Rear-End Radar Signature of Real Car / Balloon Car J-4
Figure 28: Side Radar Signature of Real Car / Balloon Car J-5
Figure 29: Front End Radar Signature of Passenger Car / Balloon Car J-6
Figure 30: Radar Return Intensity with Angle Deviation J-7
Figure 31: Distance at Brake Initiation for Three Different Targets and Baseline Vehicles A, B, C at 20 and 30 mph L-3
Figure 32: Rear View of Orange Balloon Car with Additional Reflective Material L-7
Figure 33: 2nd-Generation Balloon Car, Front, Side and Rear Views L-8
Figure 34: 3rd-Generation Balloon Car; Front, Side and Rear Views L-8
Figure 35: All Test Track Results for LVS Scenario L-9
Figure 36: All Speed Reductions for LVS Runs for Vehicle E L-10
Figure 37: Stage 1 vs. Stage 2 Braking of Vehicle F in LVS Scenario L-11
Figure 38: Vehicle F Speed Reductions and Distribution of Braking vs. No Braking for LVS L-12
Figure 39: Vehicle G Speed Reductions for LVS Runs L-13

Figure 40: Comparison of Speed Reductions for All Vehicles and Initial Test Speeds with Different Target Systems L-16
Figure 41: Balloon Car Carrier with Additional Radar Reflective Parts L-17
Figure 42: Lead Vehicle Moving Setup L-19
Figure 43: 3rd-Generation Balloon Car with PVC Guide Tubes and Ground Sheet L-20
Figure 44: All Track Test Results for LVM Scenario L-21
Figure 45: All Speed Reductions for Vehicle E LVM Runs, including Simulation Results L-22
Figure 46: Speed Reductions for Vehicle F in LVM Runs L-23
Figure 47: Stage 1 vs. Stage 2 Braking in Vehicle F LVM Scenario Runs L-24
Figure 48: All Speed Reductions for LVM Runs, including Simulation Results, for Vehicle G L-25
Figure 49: System Vehicle with an Additional Target Carrier Vehicle L-27
Figure 50: Sample Test Data from Lead Vehicle Deceleration Scenario L-28
Figure 51: LVD Speed Reductions and Standard Deviations for All Test Vehicles L-29
Figure 52: LVD Runs with and without Brake Activations L-30
Figure 53: All Track Test and Simulation Results for LVD Scenario L-32
Figure 54: Support Structure Proposal for Pedestrian Cross-Path Testing L-35
Figure 55: Upper Support Bracket Assembly L-36
Figure 56: Tow Line Routing for Pedestrian Support Structure L-36
Figure 57: Tow-Motor Side of the Tow Line Routing L-37
Figure 58: Lower Pulley on Tow Motor Side of Tow Line Routing L-37
Figure 59: Return Side of Tow Line Routing L-38
Figure 60: Application of Tow Motor Assembly for Pedestrian Testing L-38
Figure 61: Test Equipment and Setup for Pedestrian In-Path Testing L-39
Figure 62: Test Equipment and Setup for Pedestrian In-Path Testing L-40
Figure 63: All Track Results for Pedestrian Cross-Path and Pedestrian In-Path Testing L-41
Figure 64: CIB System Test Vehicle with a Mobile Target L-43
Figure 65: Balloon Car with Tow System for Straight-Crossing Path Testing of PIP Vehicles L-47
Figure 66: 2nd-Generation Balloon Car Front, Side and Rear Views L-50
Figure 67: Test Method Sequence of Events for the SCP Test Scenario L-51
Figure 68: Test Method System Components for the SCP Test Scenario L-52
Figure 69: Track Test Results for SCP Scenario L-53
Figure 70: System Vehicle with a Towed Balloon Car as the Target L-54
Figure 71: Baseline LTAP OD Test Sequences: Balloon Car Pulled by Rope (Top); Rope Brakes Away, Balloon Car Begins Turning (Center); Balloon Car Follows Arc and Hits Test Vehicle (Bottom) L-55
Figure 72: Balloon Car is Pulled by Pull Vehicle, Scene 1 - Short Time Before Impact, Straight Pulling along Steel Cables L-56
Figure 73: Balloon Car is Pulled by Pull Vehicle, Scene 2 - At the Time of Impact, Balloon Car Rotates Around Pivot Point L-56
Figure 74: Balloon Car Pulled by System Vehicle Just Prior to Impact L-57
Figure 75: 3rd-Generation Balloon Car Front, Side and Rear Views L-58
Figure 76: Test Method System Components for the LTAP-OD Test Scenario L-59

Figure 77: Test Sequence of Events for the LTAP-OD Test Scenario – Wide View....L-60
Figure 78: Test Sequence of Events for the LTAP-OD Test Scenario – Close View ...L-61
Figure 79: CIB System Test Vehicle with a Mobile Target L-64
Figure 80: Balloon car with Tow System for Opposite Direction Testing of PIP Vehicles.....L-69
Figure 81: 2nd-Generation Balloon Car Front, Side and Rear Views L-72
Figure 82: Test Method System Components for the OD Test Scenario L-73
Figure 83: Baseline Testing with Large Pole/Tree Target.....L-75
Figure 84: Baseline Testing w/ Target Suspended from Boom of Hanging Apparatus L-76
Figure 85: Support Structure for Pole/Tree Tests w/ PIP Vehicles L-78
Figure 86: Staking Method Used for Anchoring the Post Base Plate.....L-79
Figure 87: Chain Link Attachment Connecting the Towline and Upper Tension Cable L-80
Figure 88: Radar-Absorbing Foam Added to Support Posts L-81
Figure 89: Telephone Pole Sample Supported at Target Location.....L-82
Figure 90: Position of PIP Vehicle at Start of Correlation Data Measurement.....L-82
Figure 91: Beginning of Correlation Data Measurement of Telephone Pole Sample ...L-83
Figure 92: Correlation Data Measurement Using Metal Pole L-83
Figure 93: Small Pole Target Design.....L-84
Figure 94: Correlation between Sample Metal Poles and the Small Pole Target.....L-85
Figure 95: Large-Pole Target 1st Iteration Using Cardboard Cylinder L-86
Figure 96: Large-Pole Target 2nd Iteration Using Bundled Foam Tubes L-87
Figure 97: Correlation between Simulated Large Pole/Tree Target and Actual Poles L-88
Figure 98: Pole/Tree Target Configurations.....L-91
Figure 99: All Track Test Results for Small Pole.....L-92
Figure 100: All Track Test Results for Large Pole.....L-93
Figure 101: Small and Large Pole Data Chart for Vehicle E L-94
Figure 102: Small and Large Pole Raw Data Chart for Vehicle F L-95
Figure 103: Small and Large Pole Raw Data Chart for Vehicle G.....L-96
Figure 104: Comparison of Brake Activations of Baseline Vehicles with Early and Late Cut-Ins L-98
Figure 105: Test Vehicle with Stationary Target.....L-100
Figure 106: Test Vehicle with Moving Target L-101
Figure 107: Test Vehicle with Decelerating Target.....L-103
Figure 108: Target Tow System Configuration for Measuring Speed and Position..... M-1
Figure 109: Comparison of Distance between Balloon Car and Test Vehicle when Balloon Car Starts Decelerating..... M-3
Figure 110: ROAD Trip Speed Distributions for Vehicle E..... N-2
Figure 111: ROAD Trip Speed Distributions for Vehicle H N-2
Figure 112: Actual ROAD Trip Speed Distribution vs. RWUP Predicted Distribution N-3
Figure 113: Radar-only Precharge Events (by Scenario) N-5
Figure 114: Radar-only Intervention Events (by Scenario)..... N-6
Figure 115: Objects in Roadway Detected as In-Path Targets N-7

Figure 116: Vehicle Speed Distribution for Objects-in-Roadway N-7
Figure 117: Yaw Rate Distribution for Objects in the Roadway N-8
Figure 118: False Activation on Stationary Object during Curve-Entry N-9
Figure 119: Speed Distribution for Radar-Only-Based, False Activations – Curve-Entry N-10
Figure 120: Yaw Rate Distribution for Radar-Only-Based, False Activations – Curve-Entry N-11
Figure 121: Radius of Curvature Distribution for Radar-Only-Based, False Activations – Curve-Entry N-12
Figure 122: False Activation on Stationary Object during Curve-Exit N-13
Figure 123: Speed Distribution for Radar-Only-Based, False Activations – Curve-Exit N-14
Figure 124: Yaw Rate Distribution for Radar-Only-Based, False Activations – Curve-Exit N-15
Figure 125: False Events Caused by Roadside Objects N-16
Figure 126: False Activation on Stationary Object Due to Roadside Objects N-17
Figure 127: False Activation on Stationary Object Due to Overhead Object N-18
Figure 128: Speed Distribution for Radar-Only-Based, False Activations – Overhead Signs and Bridges N-18
Figure 129: False Activation during Short Radius Turn N-19
Figure 130: Speed Distribution for Radar-Only-Based, False Activations – Short-Radius Turn N-20
Figure 131: Yaw Rate Distribution for Radar-Only-Based, False Activations – Short-Radius Turn N-21
Figure 132: Radius of Curvature Distribution for Radar-Only-Based, False Activations – Short-Radius Turn N-22
Figure 133: Scenario Classifications for Mono-Vision-Only False Interventions N-24
Figure 134: Scenario Distribution for Mono-Vision-Only, False-Intervention Events N-25
Figure 135: Scenario Classifications for Mono-Vision-Only, False, Precharge Events N-26
Figure 136: Scenario Distribution for Mono-Vision-Only, False, Precharge Events ... N-27
Figure 137: Turn Lane Arrow Influencing Vision Measurement N-28
Figure 138: Line on Road Influencing Vision Measurement N-29
Figure 139: Shadow-on-Road Influencing Vision Measurement N-30
Figure 140: Change-in-Vehicle Pitch Influencing Vision Measurement N-31
Figure 141: Vehicle Reflection Influencing Vision Measurement N-32
Figure 142: Vehicle Shadow Influencing Vision Measurement N-32
Figure 143: Ghost Targets N-33
Figure 144: Scene Complexity Influencing Vision Measurement N-33
Figure 145: Speed Distribution for Mono-Vision-Based, False-Intervention Events N-34
Figure 146: Speed Distribution for All Mono-Vision-Based False Events N-35
Figure 147: Yaw Rate for Mono-Vision False Events N-36
Figure 148: TTCs for Mono-Vision-Based False Events N-38
Figure 149: Target Range for Mono-Vision-Based False Events N-40

Figure 150: Target-Range Rate for Mono-Vision-Based False Events N-42
Figure 151: Scenario Classifications for Fusion False Precharge Events..... N-44
Figure 152: Scenario Classifications for Fusion False Precharge Events (Normalized) N-45
Figure 153: False Precharge Event at Baseline Sensitivity Due to Roadside Object ... N-46
Figure 154: "LVD" Precharge Event at Baseline + 50%..... N-47
Figure 155: "LVD - Target Turns Out-of-Path" Precharge Event at Baseline + 50% N-47
Figure 156: Speed Distribution for Fusion Precharge Events N-48
Figure 157: Speed Distribution for LVD Events N-48
Figure 158: Speed Distribution for LVD – Target Turns Out-of-Path Events N-49
Figure 159: Yaw Rate Distribution for Fusion Precharge Events N-49
Figure 160: Example Recording #1 Triggered as a Result of the "Horizon Line Estimator" Function Removal..... N-51
Figure 161: Example Recording #2 Triggered as a Result of the "Horizon Line Estimator" Function Removal..... N-51
Figure 162: Example Recording Triggered as a Result of the Path Estimation Error .. N-52
Figure 163: Example Recording Triggered as a Result of Overestimated Longitudinal Velocity N-53
Figure 164: Distribution of Resimulated Stereo Vision System Recordings N-54
Figure 165: Example Image from an Event Recording Obstructed by Rain N-55
Figure 166: Example Image from an Event Recorded in Low-Light Conditions..... N-55
Figure 167: No Evidence of Obstruction on the Outside of the Fascia N-56
Figure 168: One Icicle on the Inside of the Foam Block N-57
Figure 169: False Targets are Circled in Red N-57
Figure 170: Plastic Strips Used to Emulate Partial Ice Blockage N-58
Figure 171: Test Vehicle with Objects-in-Roadway O-3
Figure 172: Stationary Vehicle Located at Curve Entrance O-5
Figure 173: Stationary Vehicle at Curve Exit..... O-8
Figure 174: Roadside Stationary Vehicles..... O-11
Figure 175: Overhead Sign/Bridge O-12
Figure 176: Short-Radius Turn O-15
Figure 177: Operational Test for LVD On-Road Features O-17
Figure 178: Operational Test for LVD Over Shadows-on-Road..... O-18
Figure 179: Detail of Shadow on Road..... O-19
Figure 180: Operational Test for LVD During CIB-Vehicle-Pitch-Change O-20
Figure 181: Operational Test for LVD with Target-Vehicle-Shadows O-20
Figure 182: LVD Target Turns Out-of-Path Operational Test O-21

List of Tables

Table 1: Target System Definition for Target Used in Objective Testing.....F-8
Table 2: Target System Definition for Target Used in Objective Testing.....F-9
Table 3: Dimensions of Balloon Car Compared to an Actual Small Passenger Car J-1
Table 4: Summary of Step 1 and 2 Results..... J-2
Table 5: Required Instrumentation Accuracies / Collection Rates..... K-3
Table 6: Velocities for Lead Vehicle Stopped Scenarios L-1
Table 7: Target Systems for Lead Vehicle Stopped Scenario L-2
Table 8: Results of LVS Test Runs with Vehicle E using a Deceleration Setting of 0.9g and different TTC Settings L-5
Table 9: Results of LVS Test Runs with Vehicle F.....L-5
Table 10: Results of LVS Test Runs with Vehicle G using a TTC Setting of 1 S L-6
Table 11: Detailed Lists of Results for Vehicle E in LVS Scenario.....L-10
Table 12: Detailed Lists of Results for Vehicle F in LVS Scenario.....L-12
Table 13: Detailed Lists of Results for Vehicle G in LVS Scenario L-13
Table 14: Velocities for Lead Vehicle Moving Scenarios.....L-14
Table 15: Target Systems for Lead Vehicle Moving Scenario.....L-15
Table 16: Comparison of Brake Activations for LVM and LVS of Hanging Target....L-15
Table 17: Vehicle F Results for Lead Vehicle Moving L-17
Table 18: Vehicle G Results for Lead Vehicle Moving L-18
Table 19: Detailed Lists of Results for Vehicle E in LVM Scenario L-22
Table 20: Detailed Lists of Results for Vehicle F in LVM Scenario.....L-23
Table 21: Vehicle G in LVM Scenario Detailed Lists of Results.....L-24
Table 22: Velocities for Lead Vehicle Decelerating Scenarios L-26
Table 23: Following Distance between System Vehicle and Target System L-27
Table 24: Deceleration Rate for Target System.....L-27
Table 25: Target Systems for Lead Vehicle Deceleration Scenario L-28
Table 26: Results for Vehicle F Lead Vehicle Deceleration Runs L-31
Table 27: LVD Speed Reductions and Standard Deviations for All Test Vehicles L-31
Table 28: Detailed Lists of Results for Vehicle E in LVD Scenario L-32
Table 29: Detailed Lists of Results for Vehicle F in LVD Scenario L-33
Table 30: Detailed Lists of Results for Vehicle G in LVD Scenario.....L-33
Table 31: Vehicle G Results for Pedestrian Cross-Path and In-Path Tests L-41
Table 32: Longitudinal Velocities for Straight Crossing Path Crash Scenario Test Method L-43
Table 33: Target System Used for Straight-Crossing Path Testing with Production Vehicles.....L-44
Table 34: Straight-Crossing Path Tests Results for Baseline Production Vehicles Target SCP1 – Towed Balloon Car with Tow Vehicle.....L-46
Table 35: Longitudinal Velocities for Straight-Crossing Path Crash Scenario L-48
Table 36: Target Systems used for Straight-Crossing Path Testing with PIP Vehicles L-48
Table 37: Detailed Lists of Results for Vehicle E in SCP Scenario L-53
Table 38: Longitudinal Velocities for Opposite Direction Crash Scenario.....L-64
Table 39: Target Systems used for Opposite Direction Testing with Production Vehicles L-65

Table 40: Opposite Direction Tests Results for Baseline Production Vehicles Target OD1 – Hanging Corner Reflector....L-66
Table 41: Opposite Direction Tests Results for Baseline Production Vehicles – Target OD2 Balloon Car Carrier....L-67
Table 42: Opposite Direction Tests Results for Baseline Production Vehicles – Target OD3 Towed Balloon Car....L-67
Table 43: Speed Reduction for each of Three OD Cases (OD1, OD2, and OD3)....L-68
Table 44: Longitudinal Velocities for Opposite Direction Crash Scenario....L-69
Table 45: Opposite Direction Tests Results for PIP Vehicles – Target LVS2A Towed Blue Balloon Car....L-71
Table 46: Opposite Direction Tests Results for PIP Vehicles – Target OBC Towed Orange Balloon Car....L-71
Table 47: Baseline Vehicle B Test Results for Small Pole Scenarios....L-77
Table 48: PIP Test Results for Small Pole Target....L-89
Table 49: PIP Test Results for Large Pole/Tree Target....L-90
Table 50: Stereo Vision Test Results for Pole Targets....L-90
Table 51: Small and Large Pole Raw Data Summary for Vehicle E....L-94
Table 52: Small and Large Pole Raw Data Summary for Vehicle F....L-95
Table 53: Small and Large Pole Raw Data Summary for Vehicle G....L-96
Table 54: Velocities for Cut-In Scenarios....L-97
Table 55: Distance between System Vehicle and Target System at Cut-In....L-97
Table 56: Test Speeds for Lead Vehicle Stopped....L-100
Table 57: Test Speeds for Lead Vehicle Moving....L-101
Table 58: Test Speeds for Lead Vehicle Decelerating....L-103
Table 59: Additional Test Parameters for Lead Vehicle Decelerating....L-103
Table 60: Test Data Summary for Stereo-Vision System in Vehicle E....L-105
Table 61: Distance between Balloon Car and Test Vehicle when Balloon Car Starts Decelerating....M-2
Table 62: TTC Settings for Precharge and Intervention Braking....N-5
Table 63: Parameters for Objects-in-Roadway Operational Test....O-3
Table 64: Test Parameters for Curve-Entrance Operational Test....O-5
Table 65: Test Parameters for Curve-Exit Operational Test....O-8
Table 66: Test Parameters for Roadside-Object Operational Test....O-11
Table 67: Test Parameters for Overhead Sign/Bridge Operational Test....O-13
Table 68: Test Parameters for Short-Radius-Turn Operational Test....O-15
Table 69: LVD Scenario Physical Conditions....O-23

List of Acronyms

AAAM	Association for the Advancement of Automotive Medicine
AIS	Abbreviated Injury Scale
CAMP	Crash Avoidance Metrics Partnership
CAN	Controller Area Network
CDS	Crashworthiness Data System
CI	Cut-In
CIB	Crash Imminent Braking
CIBC	Crash Imminent Braking Consortium
COTS	Commercial Off-the-Shelf
DGPS	Differential Global Positioning System
ECU	Electronic Control Unit
EDR	Event Data Recorder
EHB	Electro-Hydraulic Braking
EMB	Electro-Mechanical Braking
F-B	Front- to-Back
F-F	Front-to-Front
FARS	Fatality Analysis Reporting System
FCW	Forward Collision Warning
FHWA	Federal Highway Administration
FOT	Field Operational Test
FoV	Field of View
FYL	Functional Years Lost
GES	General Estimates System
GIDAS	German In-Depth Accident Study
GPS	Global Positioning System
HLE	Horizon Line Estimator
HMI	Human-Machine Interface

IRB	Institutional Review Board
KE	Kinetic Energy
LD	Lateral Direction
LIDAR	Light Detection and Ranging
LTAP	Left Turn Across Path
LTIP	Left Turn Into Path
LVD	Lead Vehicle Decelerating
LVM	Lead Vehicle Moving
LVS	Lead Vehicle Stopped
MAIS	Maximum Abbreviated Injury Scale
NASS	National Automotive Sampling System
NBSM	Never-Before-Seen-Moving
NCAP	New Car Assessment Program
NHTSA	National Highway Traffic Safety Administration
NIST	National Institute of Standards and Technology
OBC	Orange Balloon Car
OD	Opposite Direction
PBA	Panic Brake Assist
PC	Personal Computer
PCDS	Pedestrian Crash Data System
P-CP	Pedestrian – Crossing Path
P-IP	Pedestrian – In Path
PIP	Performance Improvement Prototype
PVC	Polyvinyl Chloride
RCS	Radar Cross Section
ROAD	Real-World Operational Assessment Data
RTIP	Right Turn Into Path
RWUP	Real-World User Profile
SCP	Straight Crossing Path

SIM	Simulated
SAM	Specific Anthropomorphic Mannequin
SAR	Specific Absorption Rate
TMT	Technical Management Team
TRK	Track
TTC	Time to Collision
UMTRI	University of Michigan Transportation Research Institute
UTC	Coordinated Universal Time
VRTC	Vehicle Research and Test Center

Appendix A Supplier Survey Invitation Letter

CAMP
Crash Imminent Braking

39255 Country Club Drive, Suite B-40
Farmington Hills, MI 48331-3419
Telephone: (248) 848-9595
Fax: (248) 848-9533
Email: cibsurvey@crashavoidancemetrics.org

April 4, 2008

To Whom It May Concern,

The National Highway Traffic Safety Administration and the Crash Avoidance Metrics Partnership - Crash Imminent Braking Consortium (CIBC, consisting of Continental, Delphi, Ford and General Motors) are conducting a three year cooperative research program to develop minimum performance requirements, objective test procedures and methods for estimating the potential safety benefits of autonomous Crash Imminent Braking systems.

The CIBC is conducting a survey of safety system manufacturers to better understand currently available and anticipated near term technologies and control strategies and is soliciting XYZ's input into the project. It is the goal of the project that the resulting performance requirements and test procedures be attainable utilizing near term sensor technologies, algorithms and components. To assist in this goal, please complete the applicable sections in the attached survey form for each candidate system you feel should be comprehended in defining system performance requirements and objective test procedures and return to the address listed above by April 25, 2008. The CIB team will compile all responses into a comprehensive list that will define the latest sensor set and control algorithms that will be installed and field tested as part of the program.

Thank you in advance for your participation,

Mike Carpenter
Principle Investigator

Appendix B CIB Technology Survey Questionnaire

Detailed analysis of NHTSA databases has resulted in the following crash scenarios. Please identify if this particular scenario can be detected by your sensor(s) and at what maximum delta closing speed. Please comment on the required sensor set and any unique features or constraints.

Please indicate how you would address the following:		Detectable?	Delta Speed?	Range ?	Sensor Set/Comments
Vehicle-to-Object Crashes:					
	Pedestrian				
	Minimum Height (cm)		-	-	
	Minimum Weight (Kg)		-	-	
	Pole/Tree				
	Minimum Diameter (cm)		-	-	
	Road Side Structure				
Vehicle-to-Vehicle Crashes:					
	Opposite Direction – Front to Front		-	-	
	Stationary				
	Moving				
	Rear End – Front to Back		-	-	
	Stationary				
	Moving				
	Left Turn Across Path / Opposite Direction				
	Straight Crossing Path		-	-	
	Stationary				
	Moving				

CIB Sensor Survey – Radar Information

Mechanical Parameters	**Value**	**Unit**	**Remark**
Size			
Height		m	
Width		m	
Depth		m	
Weight		Kg	
Mounting			
Others			

Interface Parameters		**Unit**	**Remark**
Operating temp.		°C	
Storage temp.		°C	
Operating Voltage		V	
Operating current		I	
Mechanical			
Data interfaces			
Control interfaces			

Key Parameters		**Unit**	**Remark**
Transmitter Frequency		GHz	
Transmitter Power			
Waveform			
Scan mechanism			
Cycle time		ms	
Number of beams		beams	
Horizontal Performance			
Field of view		Degrees	
Beam width		Degrees	
Accuracy		Degrees	
Separation		Degrees	
Resolution		Degrees	
Vertical performance			
Field of view		Degrees	
Beam width		Degrees	
Accuracy			
Resolution			
Ranging and detection			
Distance		m	
Accuracy		m	
Separation		m	
Resolution			
Measuring of relative speed			
Coverage		m/s	
Accuracy		m/s	
Separation		m/s	
Resolution		m/s	
Measuring of relative acceleration			
Coverage		m/s^2	
Accuracy		m/s^2	
Resolution		m/s^2	
Handling of stationary objects			

CIB Sensor Survey - LIDAR Information

Mechanical Parameters	**Value**	**Unit**	**Remark**
Size			
Height		m	
Width		m	
Depth		m	
Weight		Kg	
Mounting			
Others			

Interface Parameters		**Unit**	**Remark**
Operating temp.		^{o}C	
Storage temp.		^{o}C	
Operating Voltage		V	
Operating current		I	
Mechanical			
Data interfaces			
Control interfaces			

Key Parameters		**Unit**	**Remark**
Frequency		GHz	
Range		m	
Waveform			
Wavelength		nm	
Resolution		beams	
Horizontal Performance			
Field of view		Degrees	
Beam width		Degrees	
Accuracy		Degrees	
Separation		Degrees	
Resolution		Degrees	
Vertical performance			
Field of view		Degrees	
Beam width		Degrees	
Accuracy			
Resolution			
Ranging and detection			
Coverage		m	
Accuracy		m	
Separation		m	
Resolution			
Measuring of relative speed			
Coverage		m/s	
Accuracy		m/s	
Separation		m/s	
Resolution		m/s	
Measuring of relative acceleration			
Coverage		m/s^2	
Accuracy		m/s^2	
Resolution		m/s^2	

CIB Sensor Survey – Camera Information

Mechanical Parameters	**Value**	**Unit**	**Remark**
Size			
Height		m	
Width		m	
Depth		m	
Weight		Kg	
Mounting			
Others			

Interface Parameters		**Unit**	**Remark**
Operating temp.		^{o}C	
Storage temp.		^{o}C	
Operating Voltage		V	
Operating current		I	
Mechanical			
Data interfaces			
Control interfaces			

Key Parameters		**Unit**	**Remark**
Technology	CMOS		
Spectral sensitivity		nm	
Resolution			
Pixels			
Size of chip			
Optics			
Field of view		Degrees	
Zoom			
Focal length		m	
Sensitivity			
Dynamic range			
intra-scene		db	
inter-scene		db	
Accuracy			
Resolution			
Illuminator			
Wavelength		nm	
Acquisition delay		mS	
Update rate		Hz	

Appendix C Cost and Complexity Assessment for Candidate CIB Sensing and Braking Systems

C.1 Sensing System Cost and Complexity Assessment

System	Sensor Code	Sensor System Description	Relative Cost	Integration Complexity	Component Lead Time
A	R1	Short Range Radar	Low	Low	Low
B	R2	Long Range Radar	Low	Low	Low
C	R1, R2	Short + Long Range Radar	Mid	Mid	Low
D	R3	Mid&Long Range Radar	Mid	Low	Mid
E	R1, R3	Short + Mid&Long Range Radar	Mid	Mid	Mid
F	L1	Lidar	Low	Low	Low
G	C1	Mono Camera	Mid	Low	Low
H	R3, L1	Mid&Long Range Radar + Lidar	Mid	Mid	Mid
I	R3, C1	Mid&Long Range Radar + Mono Camera	High	Mid	Mid
J	L1, C1	Lidar + Mono Camera	Mid	Mid	Low
K	R3, L1, C1	Mid&Long Range Radar + Lidar + Mono Camera	High	High	Mid
L	R1, R3, L1, C1	Short + Mid&Long Range Radar + Lidar + Mono Camera	High	High	Mid
M	R4	Mid&Long Range Radar	Mid	Low	Mid
N	C2	Mono Camera	Mid	Low	Low
O	R4, C2	Mid&Long Range Radar + Mono Camera	High	Mid	Mid
P	R5	Long Range Radar	Low	Low	Mid
Q	C3	Mono Camera	Mid	Low	Mid
R	C4	Stereo Camera	Mid	Low	Mid
S	C5	Stereo Camera	Mid	Low	Mid
T	R6, C6	Mid&Long Range Radar + Stereo Camera	High	High	Mid

C.2 Braking System Cost and Complexity Assessment

System	Brake System Description	Relative Cost	Integration Complexity	Component Lead Time
A	Active Vacuum Booster w/ auto braking algorithm	Low	Low	Low
B	Hydraulic Accumulator w/ auto braking algorithm	High	Mid	High
C	Hydraulic Pump w/ auto braking algorithm	Low	Low	Low
D	EHB, EMB, Electric Booster w/ auto braking algorithm	High	High	High
E	Active Vacuum Booster w/ pre-fill & auto braking algorithm	Low	Low	Low
F	Hydraulic Accumulator w/ pre-fill & auto braking algorithm	High	Mid	High
G	Hydraulic Pump w/ pre-fill & auto braking algorithm	Low	Low	Low
H	EHB, EMB, Electric Booster w/ pre-fill & auto braking algorithm	High	High	High
I	Active Vacuum Booster w/ pre-brake & auto braking algorithm	Low	Low	Low
J	Hydraulic Accumulator w/ pre-brake & auto braking algorithm	High	Mid	High
K	Hydraulic Pump w/ pre-brake & auto braking algorithm	Low	Low	Low
L	EHB, EMB, Electric Booster w/ pre-fill & auto braking algorithm	High	High	High

Appendix D Candidate Sensing Systems for the CIB Project

Candidate Sensing Systems

System	Sensor Code	Sensor System Description	Detectable/Classifiable Crash Scenario[1] (D=detectable only, X=detectable & classifiable)							Supplier
			Pedestrain	Pole/Tree	Side Structure	Opposite Direction	Rear End	LTAP/OD	Straight Crossing Path	
A	R1	Short Range Radar	D [2]	D [2]	D [2]		x	x	x	2
B	R2	Long Range Radar	D	D	D	x	x		x	2
C	R1, R2	Short + Long Range Radar	D	D	D	x	x	x	x	2
D	R3	Mid&Long Range Radar	D	D	D	x	x	x	x	2
E	R1, R3	Short + Mid&Long Range Radar	D	D	D	x	x	x	x	2
F	L1	Lidar	D	D			x			2
G	C1	Mono Camera	x	x	x	x	x			2
H	R3, L1	Mid&Long Range Radar + Lidar	x	x	x	x	x	x	x	2
I	R3, C1	Mid&Long Range Radar + Mono Camera	x	x	x	x	x	x	x	2
J	L1, C1	Lidar + Mono Camera	x	x		x	x			2
K	R3, L1, C1	Mid&Long Range Radar + Lidar + Mono Camera	x	x	x	x	x	x	x	2
L	R1, R3, L1, C1	Short + Mid&Long Range Radar + Lidar + Mono Camera	x	x	x	x	x	x	x	2
M	R4	Mid&Long Range Radar	D	D	D	x	x	x	x	3
N	C2	Mono Camera	x	x[3]		x	x	x		3
O	R4, C2	Mid&Long Range Radar + Mono Camera	x	x[3]	D	x	x	x	x	3
P	R5	Long Range Radar		D	x	x	x		x	6
Q	C3	Mono Camera	x	x[3]		x	x	x		4
R	C4	Stereo Camera	x		x	x	x	x	x	1
S	C5	Stereo Camera	x	x	x	x	x	x	x	5
T	R6, C6	Mid&Long Range Radar + Stereo Camera	x	x	x	x	x	x	x	1, 2, 3, 5

Note 1: System capabilities shown are based upon the survey responses from Task 3. Actual performance can vary due to environmental conditions, vehicle speed and other factors.
Note 2: Two short range radars required
Note 3: Capability will be added to future software versions

Appendix E Candidate Braking Systems for the CIB Project

Candidate Braking Systems

System	Brake System Description	Relative Performance	Supplier
A	Active Vacuum Booster w/ auto braking algorithm	Mid	Delphi & Continental
B	Hydraulic Accumulator w/ auto braking algorithm	High	
C	Hydraulic Pump w/ auto braking algorithm	Low	
D	EHB, EMB, Electric Booster w/ auto braking algorithm	Mid	
E	Active Vacuum Booster w/ pre-fill & auto braking algorithm	Mid	
F	Hydraulic Accumulator w/ pre-fill & auto braking algorithm	High	
G	Hydraulic Pump w/ pre-fill & auto braking algorithm	Mid	
H	EHB, EMB, Electric Booster w/ pre-fill & auto braking algorithm	Mid	
I	Active Vacuum Booster w/ pre-brake & auto braking algorithm	High	
J	Hydraulic Accumulator w/ pre-brake & auto braking algorithm	High	
K	Hydraulic Pump w/ pre-brake & auto braking algorithm	High	
L	EHB, EMB, Electric Booster w/ pre-fill & auto braking algorithm	Mid	

Appendix F CIB Target Development

The following general methodology and guidelines were followed as much as applicable for the CIB Target development, which includes consistent target system correlations. For each test method, representative objects were identified and analyzed which includes mid-size vehicles, tree, metal and wood pole. A brief review of pedestrian targets is discussed in the last section of this appendix.

1. Vehicle target must have a low enough mass such that it is capable of being moved by a tow system.
2. Vehicle target must have a reasonable cost such that a suitable number of replacement spare targets can be acquired.
3. Vehicle target must be durable and thus capable of maintaining radar or visual profiles after being hit repeatedly by a test vehicle, such that the need for replacement targets are minimized. In addition, target must not damage the test vehicle.
4. Vehicle target must have a radar profile correlated to that of a real motor vehicle. For each surrogate object, radar power return values were measured at different distances within the range of the radar sensors using the Performance Improvement Prototype (PIP) vehicles. To obtain radar power return measurement variation data, three sample values were recorded for each vehicle.
5. Specific test targets were identified, then experimented with by attaching combinations of reflective material until the radar power return measurements closely matched the values of the original target within the variation measured from the original target.
6. Vehicle target must have visual properties similar to a real vehicle in order to ensure that a machine vision system would recognize the target as a motor vehicle. Vision sensor target reports were reviewed to determine whether the camera systems acquired the same target.
7. Vision sensor target reports were then verified to ensure the camera systems acquired the same target and categorization as resulted in Step 6.
8. If necessary, target visual characteristics were modified until the vision systems were able to track the target in the same manner as resulted in Step 6.
9. After completing the target correlation, limiting values for TTC and brake deceleration levels were calculated for the test scenarios to ensure measurement of potential maximum and minimum system performance without reaching full vehicle stop prior to impact with the target.
10. The test matrices for the specific scenarios were then run with each PIP vehicle using various TTC and vehicle deceleration settings within the limits established in Step 9. Vehicle deceleration was accomplished by use of the foundation brakes on the vehicle.

F.1 Vehicle Target

The following CIB vehicle targets were reviewed and developed over the course of the project. As defined below

F.1.1 Balloon Cars

For vehicle-to-vehicle scenarios, several types of balloon cars were evaluated for static testing targets a shown in

Figure 1. These targets were selected for initial evaluation based on their ease of use and their ability to replicate vehicle characteristics in all orientations, including visual and, with the addition of metallic reflective material, appropriate radar response.

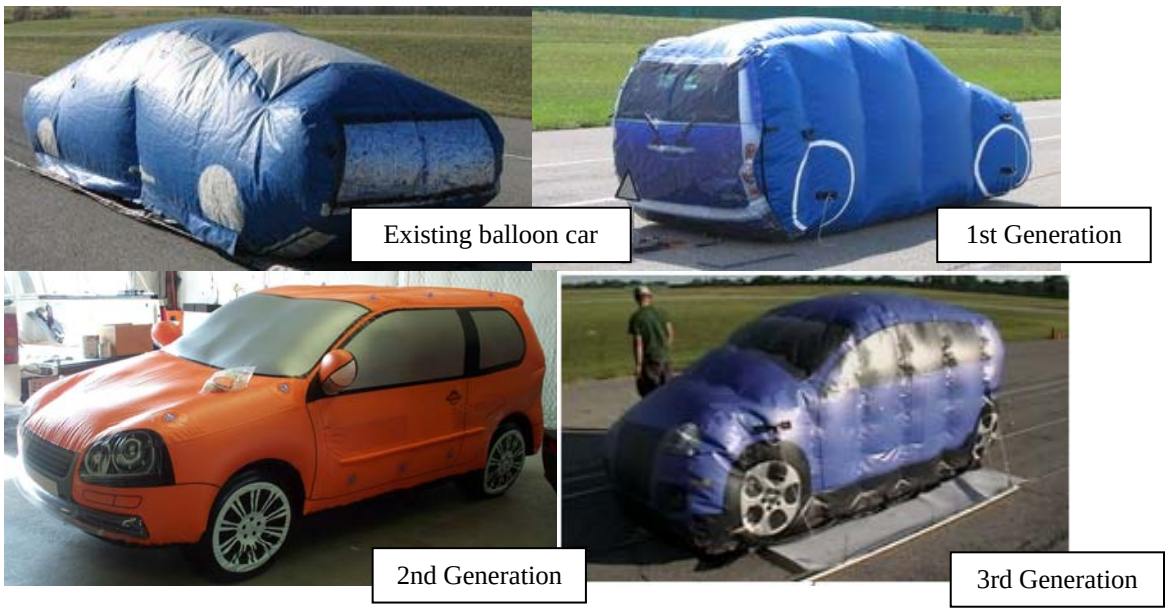

Figure 1: Balloon Cars Used during Testing

The 1st-generation balloon car had minimal lifelike visual characteristics and was painted with aluminized paint for radar reflectivity. The 2nd-generation balloon car, shown in Table 2, was visually more lifelike, but the robustness and radar reflectivity of this target were not suitable for the CIB tests. The 3rd-generation balloon car target, shown in Table 2, came closest to meeting the vehicle target requirements. This target had good, visual, lifelike properties, contained internal radar reflective material and was made of a thick, canvas-reinforced material that dramatically improved the durability of the target relative to the previous balloon cars developed. Since the 3rd-generation balloon car target was in development when the "test method validation" portion of the CIB Project was initiated, the 2nd-generation balloon car was used for the test validation runs prior to the availability of the 3rd-generation target. Appendix I provides a discussion of the radar return and visual property characterizations for the 3rd-generation balloon car. Appendix J presents the correlation of this balloon car to an actual vehicle.

F.1.2 Vehicle Foam Pillows

Like the balloon cars, the foam pillows were selected for initial evaluation due to their ease of use and their ability to replicate vehicle visual characteristics and, with metallic reflective material between the foam and outer skin, the radar reflective characteristics. These targets (Figure 2) are currently only available as two-dimensional representations of the back of a vehicle and are held together by hook and loop closures and are designed to break apart when struck by the test vehicle.

Figure 2: Vehicle Foam Pillows Used during Testing

F.1.3 Flip-down Target

The Flip-down target works as a combination of a main unit, light barrier, and a power supply (see Figure 3). The main unit includes the radar corner reflector mounted to a mechanism which allows it to rotate. The flip-down corner reflector is activated by a light beam located at a defined distance from the radar corner reflector. An electromagnet in the main unit is connected to the power source. While under current, the electromagnet keeps the reflector from flipping down. As soon as a vehicle moves through the light barrier, the electromagnet is disconnected from power, the reflector flips down, and the test vehicle drives over the target.

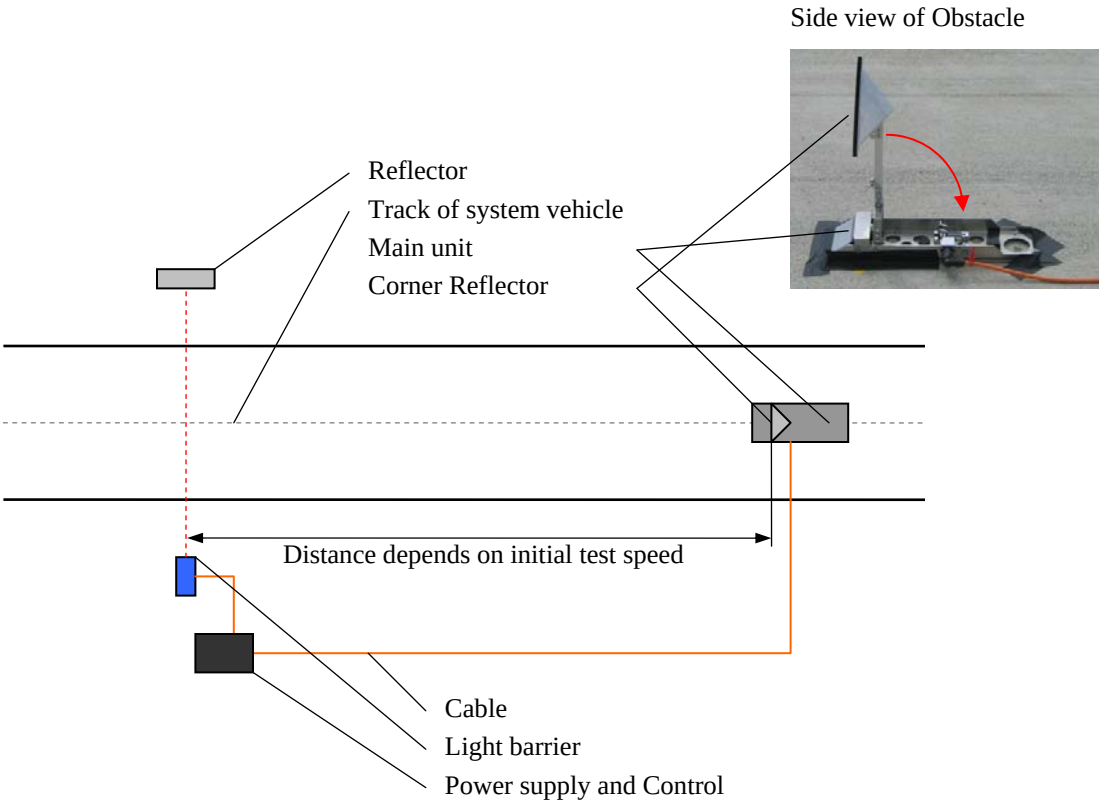

Figure 3: Flip-down Corner Reflector Used during Testing

F.1.4 Hanging Target Simulator

The hanging target simulator uses a boom mechanism that "hangs" a corner reflector in an adjacent lane, as shown in Figure 4. The corner reflector provides radar feedback to the vehicle under test and is mounted to a soft structure which is capable of being hit by an oncoming vehicle at closing speeds up to 35 mph. The mechanism is capable of flipping up and will rotate out of the way to allow the test vehicle to pass under the boom mechanism. This mechanism can be connected to the front or rear of the vehicle so that "oncoming vehicle" tests can be performed as well as the "following vehicle" cases. Initial evaluations of pole and tree targets could also be evaluated by replacing the target insert with various diameter foam targets wrapped with metallic reflective material correlated to actual pole and tree obstacles.

Figure 4: Hanging Target Testing Simulator

F.1.5 Crash Simulator

The Crash Simulator as shown in Figure 5 and was used for both the static and movable target testing up to 45 mph. When contact is about to occur with the simulator dummy, the dummy is released and swings up very quickly out of the vehicle path. The simulator uses compressed springs on a main shaft that are held in place by electromagnets. When the power to the magnets is switched off, the spring force is released and the dummy swings up and out of the way of the approaching test vehicle.

Figure 5: Crash Simulator Used during Testing

F.1.6 Balloon Car Carrier

For this application, a specially constructed balloon car is attached to a cantilevered truss which is suspended from a second vehicle driving in the adjacent lane (see Figure 6). A quick release clamping mechanism holds the balloon in place and releases it when the balloon is struck by the test vehicle. The clamping mechanism can be reversed to allow testing in opposite direction scenarios. The maximum velocity for this test apparatus is approximately 35 to 40 mph and can also be used for static object testing.

Figure 6: Balloon Car Carrier

F.1.7 Dynamic Vehicle-to-Vehicle Scenarios

For the dynamic vehicle-to-vehicle scenarios, a system was developed to convey the test targets in a manner representative of the priority crash scenarios. A tow system for the inflatable targets (note: this tow system was also used for vehicle-to-object targets) was designed and fabricated. This system is depicted in Figure 7. The tow system major components are highlighted in the block diagram in Figure 7 and are described below.

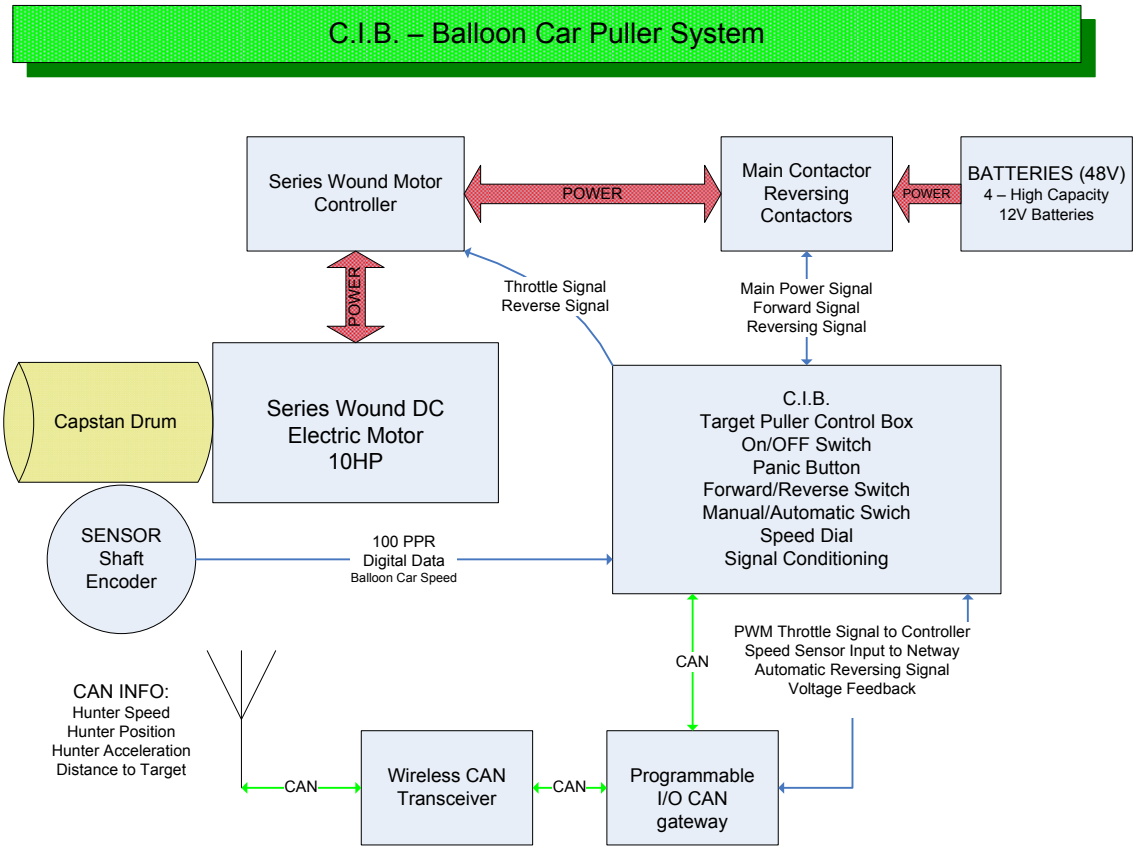

Figure 7: Balloon Car Puller System Block Diagram

Series Wound DC Electric Motor
The 10HP Electric motor provides the torque that drives the capstan drum pulling the balloon car down the track. This motor was chosen because of ready availability, high torque output and 48V DC operation.

Capstan Drum
The capstan drum is connected to the DC motor via drive belt. The capstan drum pulls the rope which is connected to the balloon car by providing friction through the geometry of the capstan drum. The ratio from motor to capstan is 1:1.5, which has been shown to pull the balloon car at speeds up to 25 mph.

Motor Controller
The motor controller is an off-the-shelf controller for series wound DC motors. This controller was chosen because it is currently in mass production and has been used to control the electric motor used in our design. This controller is capable of providing 650 Amps of DC current to the motor and is capable of slowing and or reversing the DC motor while in the forward mode, enabling the LVD scenarios to be more easily conducted.

Main Contactor and Reversing Contactors
The main contactor allows the current from the 48V battery pack to be sent to the motor controller and provides a means for a safety shutdown via the emergency stop button on the control box. The reversing contactors provide directional flow for the motor via the motor controller that can modulate the field current to control braking force.

Series Shaft Encoder
The shaft encoder is used as a “feedback” device for controlling the speed and position of the balloon car by monitoring the speed of the pulling rope.

Controller Area Network (CAN) Gateway
The CAN Gateway provides the automatic control for the motor control unit. When in automatic mode, the Gateway box receives inputs from the CAN bus, which provides distance and speed information on the test vehicle and determines the settings for the motor controller. The relative information is extracted from the CAN bus and combined with the feedback from the encoder and translated into a direction output signal used by the motor controller.

CIB – Target Puller Control Box
The control box is the main interface between the user and the target puller machine. The control box houses the signal conditioning for both the throttle input to the motor controller and the digital signal from the shaft encoder to the Gateway. The control box allows the user to switch between manual mode and automatic mode via a three-position switch on top of the box. When in manual mode, the user can select forward or reverse from a switch on the side of the control box as well as throttle position from a dial mounted on the top of the control box. The control box houses the relays which allow automatic control as well as the “Emergency Stop” button which, when pressed, will switch off power to the motor system by causing the main contactor to open.

Wireless CAN Transceiver
The CAN transceiver provides access to the test vehicle's CAN output which contains all the relative information regarding the speed, acceleration and distance between the test vehicle and a fixed "target" point. By using this information, the Gateway can calculate the relative distance and speed between the test vehicle and the balloon car it is pulling.

Batteries – 48V
There are four, deep-cycle, 12V batteries connected in series to create a 48V DC power supply that are constantly being charged by a four-bank battery charger.

F.2 Pole/Tree Target

The pole and tree targets also incurred considerable development during the course of the project. The graphic in Table 2 shows the third iteration of the pole/tree foam targets.

Table 1: Target System Definition for Target Used in Objective Testing

Name	Brief Description	Photograph
Foam Pole/Tree Target	Used with radar and vision systems. Static target that is struck. Target diameters 12 inches and 4 inches.	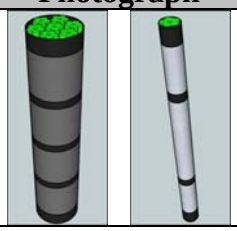

F.3 Pedestrian Target

This section provides a summary of the pedestrian target system, beginning with a list of the primary pedestrian target requirements.

- Pedestrian target must have a radar profile correlated to that of an adult human. Adults were the primary pedestrian struck in forward impacts based on the PCDS data analysis. Project timing did not permit the examination of child pedestrian targets. Because of this constraint, the focus of this work was on a generic pedestrian size.
- Pedestrian target must have visual properties similar to an adult human in order to ensure that a machine vision system would recognize the target as a pedestrian.
- Pedestrian target must have a low enough mass such that it is capable of being moved by a tow system.
- Pedestrian target must be durable and thus capable of maintaining radar or visual profiles after being hit repeatedly by a test vehicle, such that the need for replacement targets are minimized. In addition, the target must not damage the test vehicle.
- Pedestrian target must have a reasonable cost such that a suitable number of replacement spare targets can be acquired.

An outside research firm performed a significant amount of work to develop a pedestrian target to meeting these requirements. This work is summarized in Appendix H. The resulting target consisted of a low-cost, air-filled mannequin resembling a human adult. A set of radar-reflective clothing and copper tape were added to the mannequin in order to provide a pedestrian target with a radar return signature similar to that of an adult human. The correlation of the target was found to be within ±1 standard deviation of the mean radar return measured for the 50th percentile adult subjects. This target modification allowed correlation to a human for both 24 GHz and 76 GHz radar frequencies which represent the radar systems used in this project. The resulting target, based upon the development effort, is shown below (see Table 2). This target was used in the testing for the Pedestrian In-Path and Pedestrian Cross-Path test scenarios.

Table 2: Target System Definition for Target Used in Objective Testing

Name	Brief Description	Photograph
Inflatable Pedestrian Target	Balloon mannequin representation of a human adult with correct radar cross section. Used with radar and vision systems. Towed with the tow system.	

Appendix G Target Tow System

The following section briefly describes the setup and operation of the target tow conveyance system that was used during CIB track testing for all test scenarios that required either a vehicle or pedestrian moving target.

G.1 Overview

The target tow system is designed for scenarios that require a moving, simulated, car sized balloon target or other moving targets such as a pedestrian mannequin (see Figure 8). This tow system can be used primarily for tests in which the target is traveling in a straight line at speeds from 0 to 30 mph. The target tow system is composed of 3 major parts:

1. Motor / Capstan Assembly / DC Power supply (Battery Pack)
2. Control Unit
3. Ropes / Pulleys / Cables

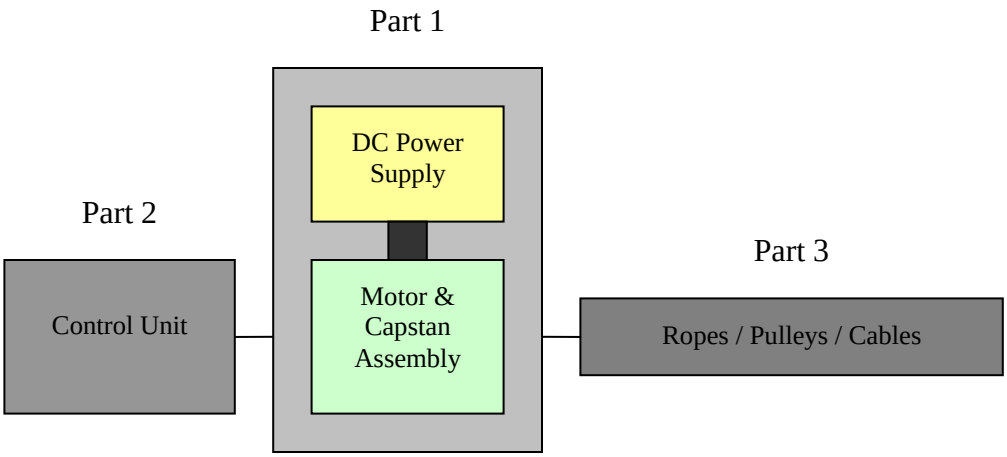

Figure 8: Target Tow System - Overview

A list of the test scenarios utilizing this conveyance system is provided below, which highlights the flexibility of this system:

1. Lead Vehicle Moving
2. Lead Vehicle Decelerating
3. Opposite Direction
4. Left Turn Across Path - Opposite Direction
5. Straight Crossing Path
6. Pedestrian Cross-Path
7. Pedestrian In-Path

G.2 Motor and Capstan Assembly / Power Supply and Control Unit

The main inputs for the target tow system are power and the measured speed of the target system. Additional inputs are the speed, position (distance to target) and acceleration of the test vehicle.

The target tow system operator can select either the manual mode or the automatic mode. In manual mode, the system can be controlled by the operator and allows the operator to conveniently reset the target to start position or experiment with and develop new scenarios. In automatic mode, the system operates autonomously based on measured speed and distances of target system and test vehicle. This mode enables carefully, controlled, repeatable testing of CIB systems for a given test scenario (see Figure 9).

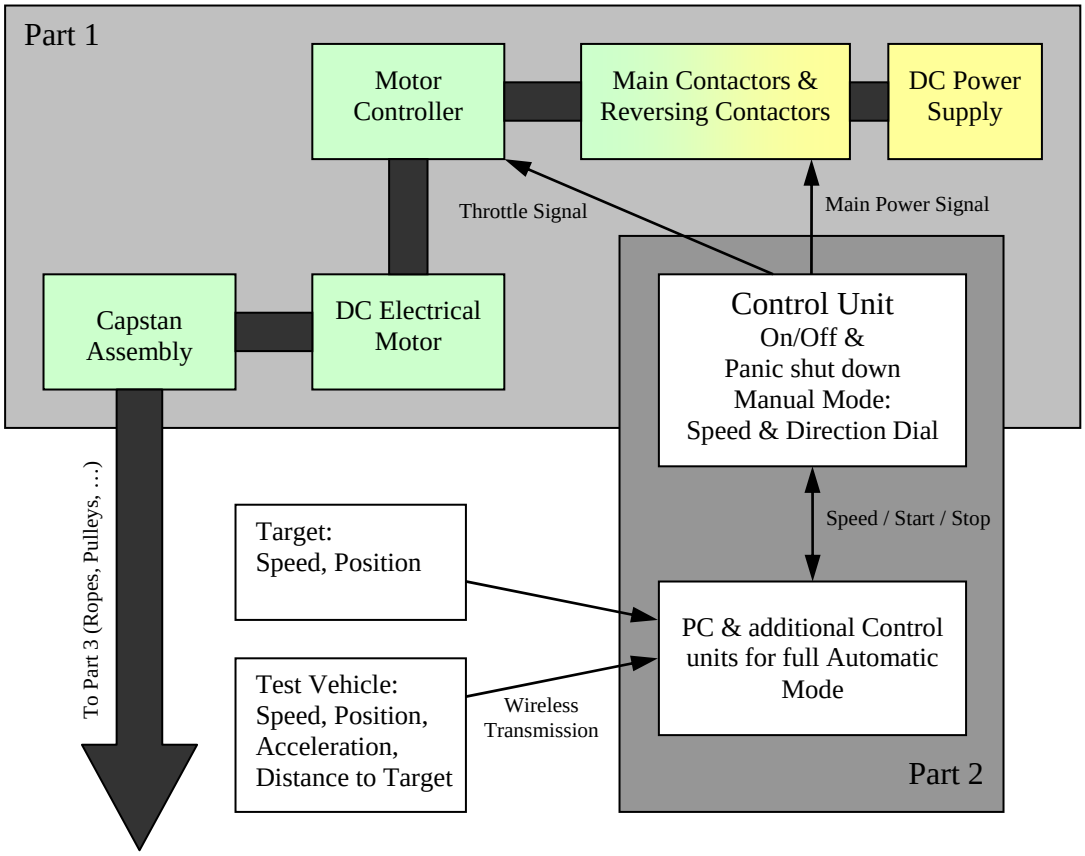

Figure 9: Target Tow System - Detail

G.3 Motor and Capstan Assembly (Part 1)

Within this project, the target tow system was developed and designed such that it could conduct all required test scenarios. The resulting system is comprised of a motor/capstan assembly that is attached to the hitch of a support vehicle (see Figure 10). This approach provides a stable anchor as well as a method for tensioning the main towing rope. Additionally, this approach allows flexibility in test setup and ease in equipment

relocation. The usage of off-the-shelf materials (i.e., aluminum framing, drive pulleys, belts, electrical golf cart drive motor / controller) enabled efficient and timely development of this approach.

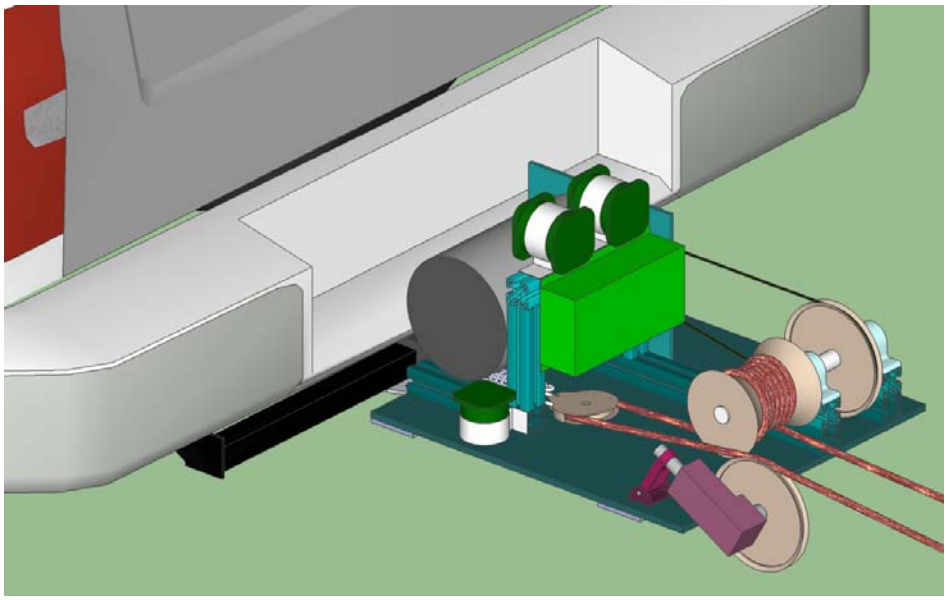

Figure 10: Target Tow System on Truck Rear Hitch

The following list describes the components of the motor/capstan assembly (see Figure 11 and Figure 12).

1. Aluminum Mounting Plate
2. Aluminum Framing
3. 48V DC Electric Motor
4. Motor Controller
5. Main Contactor
6. Directional Contactors
7. High Current Wiring
8. Signal Wiring
9. Capstan
10. Capstan Drive Shaft
11. Capstan Drive Shaft Bearings
12. Motor Drive Pulley
13. Capstan Drive Pulley
14. Motor/Capstan Drive Belt
15. Encoder Wheel Assembly

16. Motor/Capstan Assembly Hitch Mounting
17. Tensioning Spring
18. Tensioning Pulley
19. Encoder Pulley

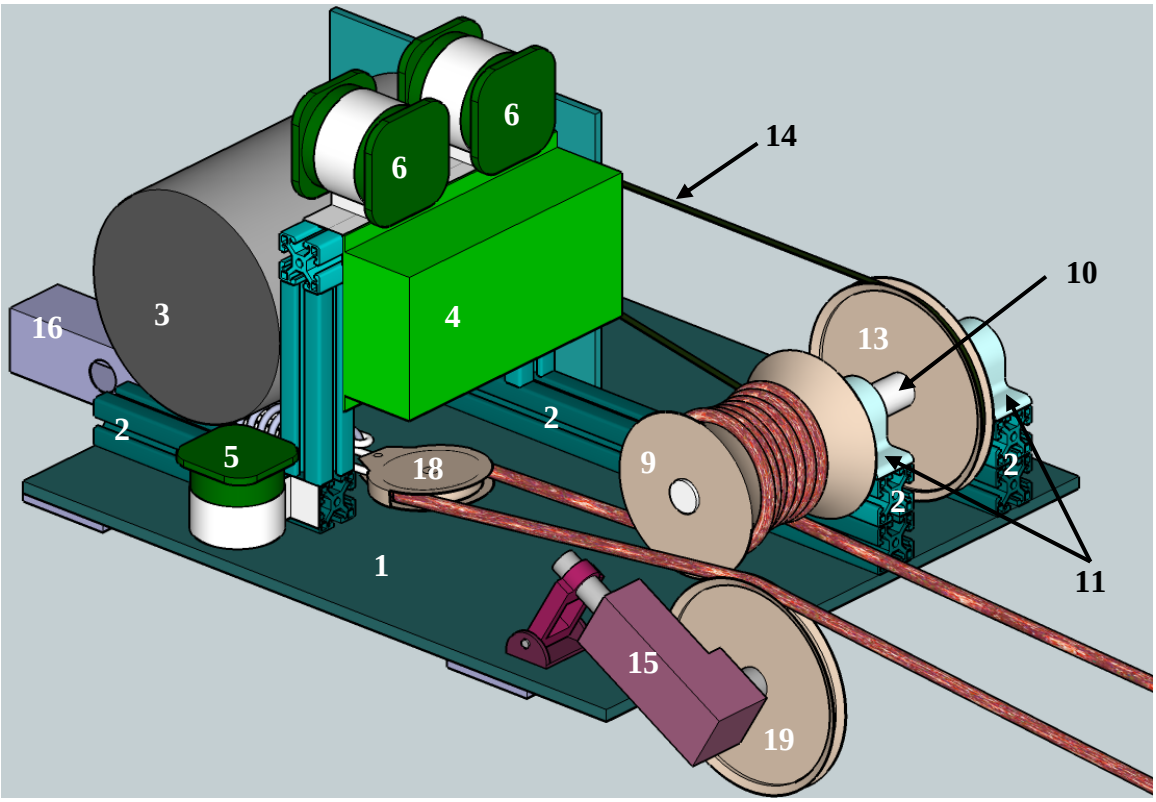

Figure 11: Front View of the Target Tow System

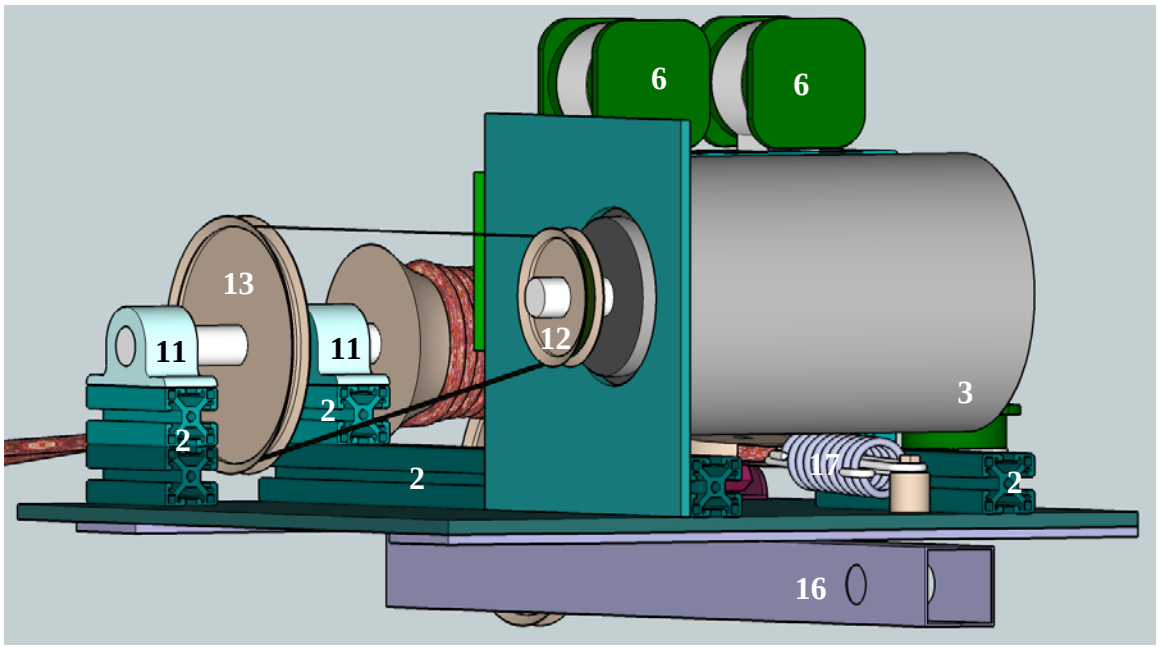

Figure 12: Rear View of the Target Tow System

G.3.1 Motor Controller

The motor controller is an off-the-shelf controller for series-wound DC motors. This controller was chosen because it is currently in mass production and had been previously used to control the motor used in our design. The controller is capable of slowing and/or reversing the DC motor while in the forward mode, which enables this system to be used in the LVD scenarios.

G.3.2 Series-Wound DC Motor

The electric motor provides the torque that drives the capstan drum pulling the target system. This motor was chosen because it is an off-the-shelf product used in the electric golf cart industry. It also meets the torque and controllability requirements and operates on 48V DC.

G.3.3 Capstan Drum, Drive Belt, Pulleys

The capstan drum is connected to the DC motor via the drive belt. The capstan drum uses friction and a specific geometry to pull the rope which is connected to the target system. The maximum speed of the target system can be increased by changing the drive ratio between the motor and pulley shafts.

G.3.4 Encoder Wheel

The encoder is used as a feedback device for controlling the speed and position of the target. The sensor sends a square wave pulse to the control unit which reads and decodes the current position of the target system and makes any necessary adjustment to the motor speed settings.

G.3.5 Main Contactor and Reversing Contactors

The main contactor allows the current from the 48V battery pack to be used by the motor controller setup and provides a safety disconnect (since it can be opened via the emergency stop button on in the control unit). The reversing contactors provide directional flow for the motor as well as "braking." This braking is enabled by shorting out the armature through the plugging diode, which prevents the feedback loop from creating a strong electromagnetic field in the motor. The motor controller can modulate the field current to control the braking torque.

G.4 Control Unit (Part 2)

The control unit is the main interface between the user and the towing system. The control unit houses the signal conditioning system for the speed control input to the motor controller and for the signal from the shaft encoder. The control unit allows the operator to switch between the manual mode and the automatic mode. When in the manual mode, the user can select forward or reverse directions as well as speed control position. When in the automatic mode, the control of the motor system is transferred to a personal computer (PC). Through use of the PC, the operator is able to control and record the tests. The flow chart below (see Figure 13) shows a typical test in automatic mode. The control software must be set by the user prior to starting a test. The variables that may change for each test, which are typically run in a series, are:

- Target Speeds
- Test Vehicle Speed
- Initial Position of the Target
- Trigger Distance

The trigger distance for a given test scenario is the calculated distance between target system and test vehicle at the point when the target system must start moving. Starting the motion of the target at this point in time enables the target and test vehicle to reach a set "zero" point at nearly the same time.

G.5 Test Procedure

A typical CIB test begins with set up of the test vehicle and target system in their starting positions. The operator of the target tow system makes sure that the data acquisition and control software systems are running properly. Upon receiving a signal from the tow system operator, the test vehicle driver accelerates to the defined test vehicle speed. The target tow system begins moving the target when the preset trigger distance is reached. If all parameters (speeds, distances, accelerations) stay within their prescribed limits, the test results are valid. If for any reason target tow system does not start pulling the target system at the proper point in time, the run has to be aborted. During a successful test run, the test vehicle will hit the target or brake prior to striking the target (or come to a full stop before striking the target). After a successful test run, the data acquisition and control software systems have to be stopped. The target system and the test vehicle than need to be reset to their starting positions for the next run (see Figure 13).

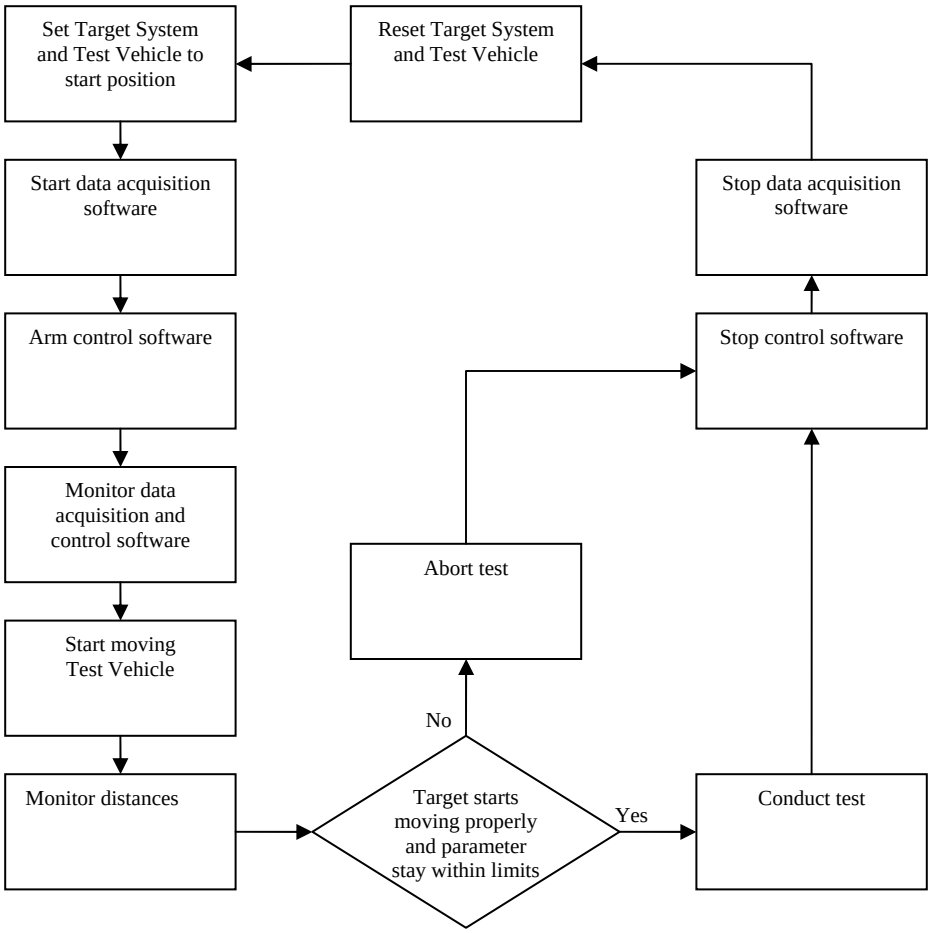

Figure 13: Simplified Test Flow Chart

G.6 Typical Setup

The following pictures and graphics (see Figure 14 through Figure 21) illustrate a typical setup on the test track for Vehicle-to-Vehicle Rear-End test cases, such as Lead Vehicle Moving (LVM), Lead Vehicle Decelerating (LVD) or Lead Vehicle Stopped (LVS) scenarios.

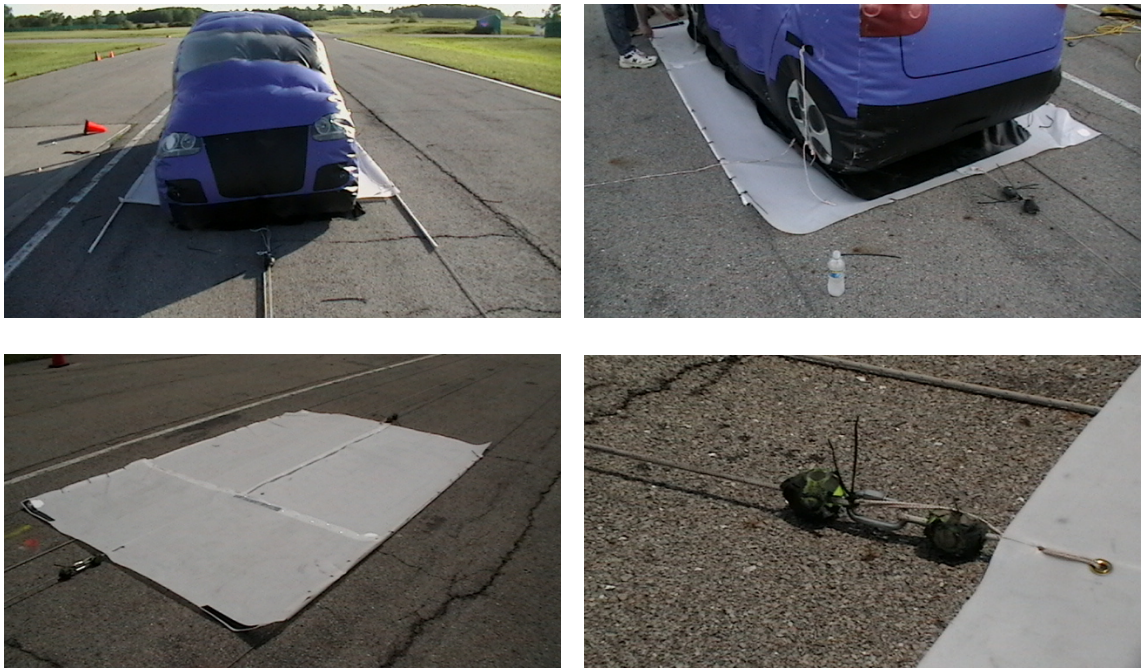

Figure 14: Balloon Car on Ground Sheet with Rope, PVC Guide Pipes, Steel Cables, Zip Ties and Cords

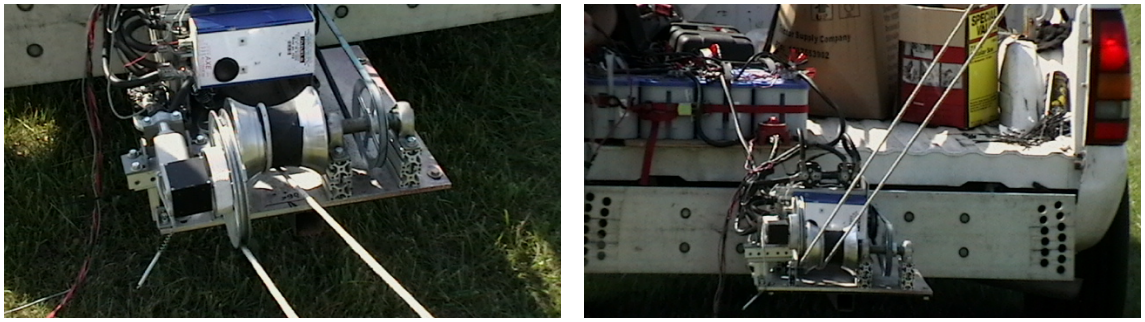

Figure 15: Target Tow Setup on Truck Rear Hitch (Pedestrian Scenario)

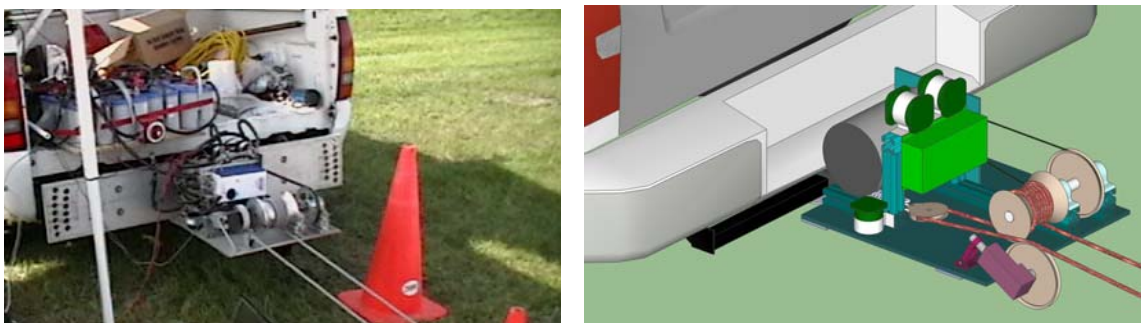

Figure 16: Target Tow Setup on Truck Rear Hitch (LVM Scenario)

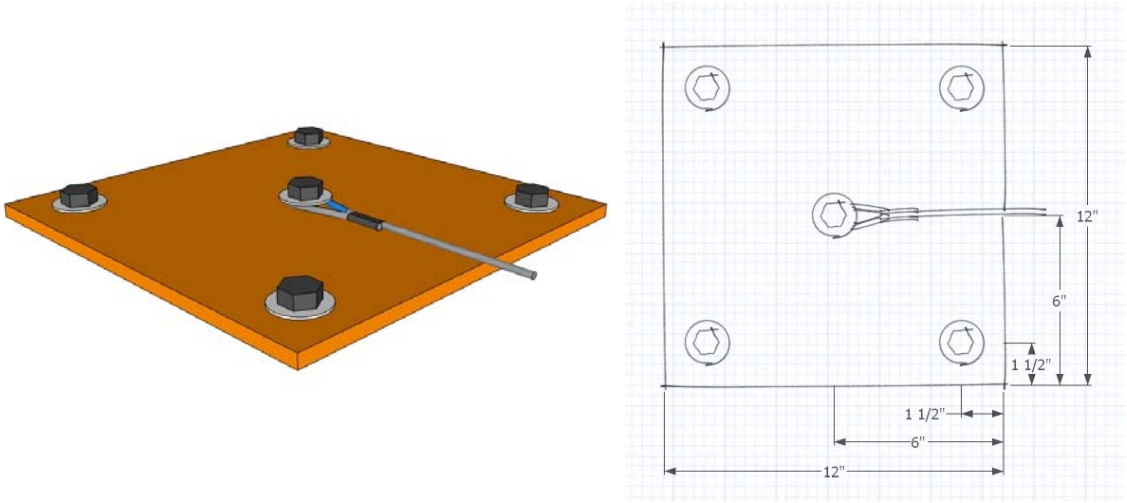

Figure 17: Anchored Base Plate for Steel Cables

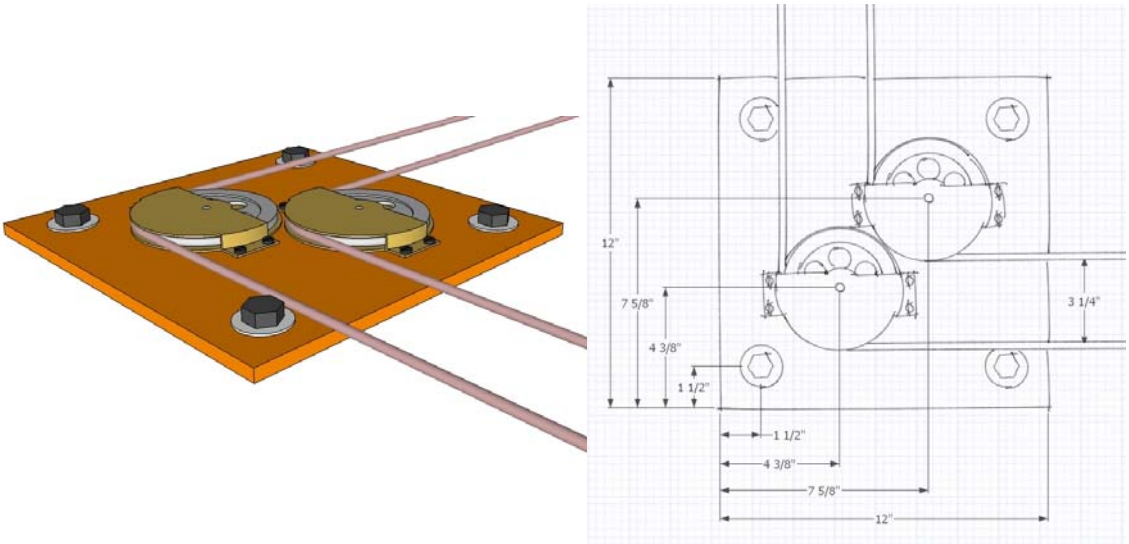

Figure 18: Anchored Base Plate for 90 Degree Rope Pulleys

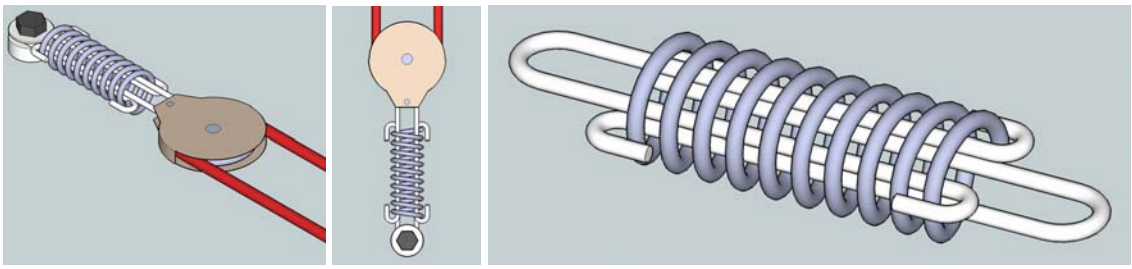

Figure 19: End Pulley with Safety Spring

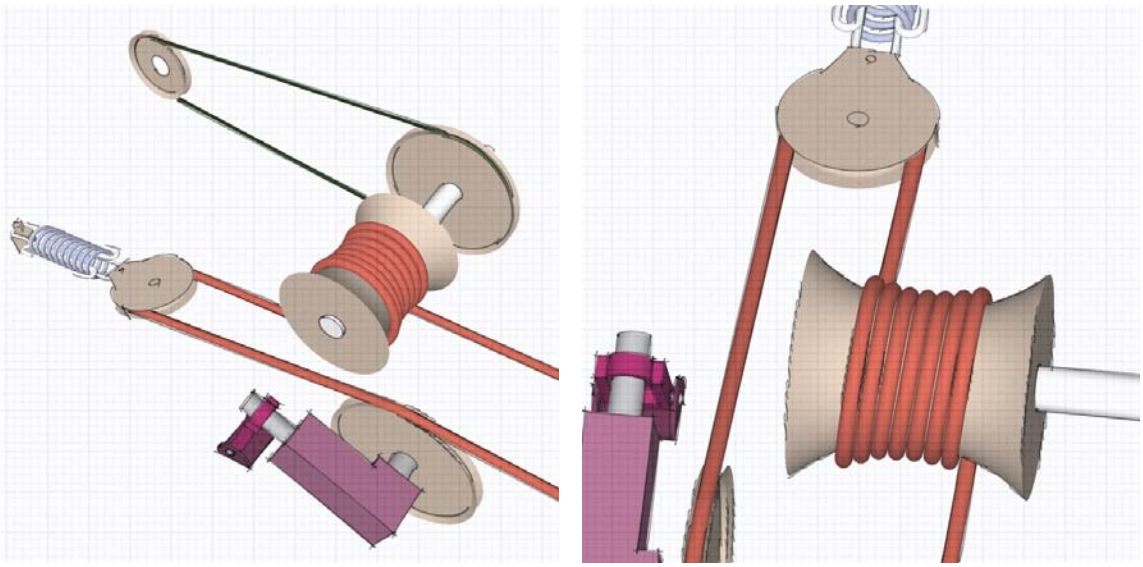

Figure 20: Capstan Drum Assembly with Tow Rope, End Pulley, Safety Spring and Encoder Wheel

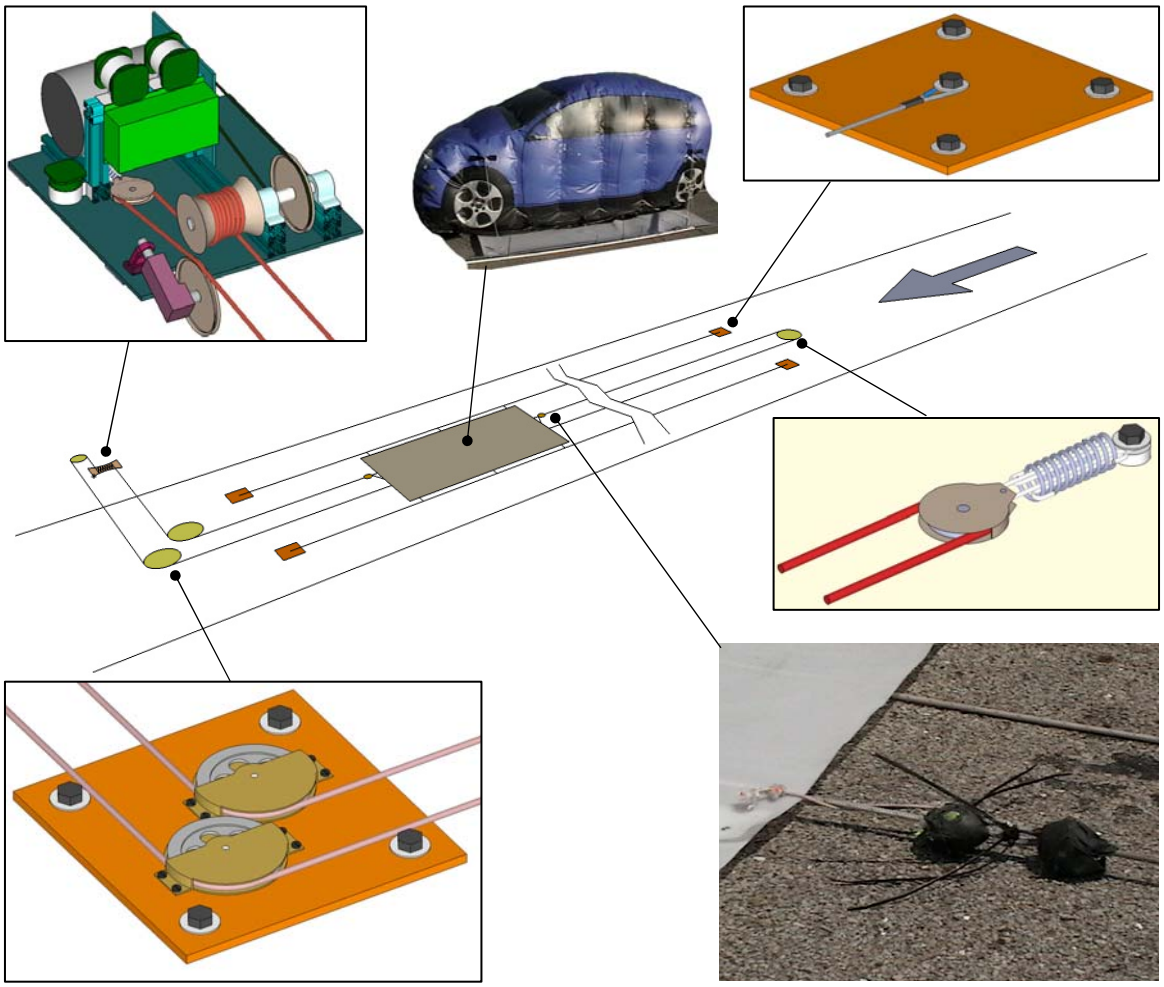

Figure 21: Complete Setup of Target Tow System for LVM Scenario

Appendix H Pedestrian Mannequin Testing Report

This appendix presents a report provided to the CIB Consortium by HRL Laboratories, LLC (HRL). This report discusses results obtained during testing of the adult pedestrian mannequins used in the CIB Project. This report is reproduced here with permission from HRL.

Crash Imminent Braking Project
Adult Pedestrian Test Mannequin Development
Final Report

Submitted by:

HRL Laboratories, LLC
3011 Malibu Canyon Road
Malibu, CA 90265
www.hrl.com

Submitted to:
Crash Avoidance Metrics Partnership (CAMP) on behalf of
Crash Imminent Braking Consortium (CIBC)
39255 Country Club Dr.
Suite B-40
Farmington Hills, MI 48331
(248) 848-9595 ext. 328

Technical Contact:

Mike Carpenter
(586) 986-0917
michael.g.carpenter@gm.com

HRL Points of Contact:

H.P. Hsu
310-317-5992
hhsu@hrl.com

Kevin Geary
310-317-5271
kgeary@hrl.com

Robert Nagele
310-317-5157
rgnagele@hrl.com

Arthur Bekaryan
310-317-5399
abekaryan@hrl.com

July 14, 2009

1. Executive Summary

This document describes the automotive radar measurements at HRL Laboratories, LLC, to test and modify COTS adult mannequins representing 50th percentile adult humans. Under this project, HRL compared the sensors' return data collected from mannequins against results received from real adult humans. The test procedure and radar characterization results of the real adult human and COTS mannequins are described in detail below. Three separate radar systems were used to develop and modify test mannequins which were shown to be a good radar representation at both 24 and 76 GHz. Also, an analysis of the Delphi vision system response and a study determining the effect of street clothing on the delivered COTS mannequins are included. A preliminary test mannequin was delivered to CAMP-CIB on May 7, 2009, and towards the end of the project two final developed mannequins (e.g. #1 and #2) were delivered to CAMP-CIB for the CIB system testing on June 12, 2009.

Background

The Crash Avoidance Metrics Partnership (CAMP), on behalf of the Crash Imminent Braking Consortium (CIBC), consisting of Continental, Delphi, Ford, General Motors, and Mercedes, are conducting a three year cooperative research program with the National Highway Traffic Safety Administration (NHTSA). The focus of this program is to develop minimum performance requirements, objective test procedures, and methods for estimating the potential safety benefits of autonomous Crash Imminent Braking (CIB) Systems. The development of test methods assessing CIB system performance in crashes between vehicles and pedestrians will be required as part of the project. Herein, there is a need to search, acquire, test, and modify Commercial Off-the-Shelf (COTS) mannequins that could reasonably represent typical adult pedestrians with correct physical attributes to serve as human adult-shaped test objects in the evaluation of CIB systems in automobiles. Such a test mannequin is needed to properly develop test methods for the evaluation of CIB systems in simulated vehicle-to-pedestrian impact scenarios. The CIB systems used for the development of the project test procedures include various combinations of 24 GHz UWB short-range radar, 76 GHz mid/long-range radar, mono-camera vision, and stereo-camera vision systems.

2. Project Description & Deliverables

HRL Laboratories collaborated with CAMP-CIB to search, acquire, test, and modify COTS adult mannequins representing 50th percentile adult humans which can be struck by a test vehicle without damaging the test vehicle or posing a safety concern for the testers. A preliminary test mannequin was delivered to CAMP-CIBC on May 7, 2009, and towards the end of the project two final developed mannequins (e.g. #1 and #2) were delivered to CAMP-CIBC for the CIB system testing on June 12, 2009. HRL used the set of sensors, listed in Table 1, to test these mannequins and collect data with the mannequin emulating an adult human in two standing positions, including backward and side orientations. HRL compared the sensor return data collected from the COTS mannequin against data collected from real adult humans, and then selected the adult mannequin models that offer the closest sensor return to that of real adult humans.

Table 1: Sensor Types Required for Pedestrian Mannequin Testing

Sensing System	Supplied By:
Delphi Vision System	CAMP-CIBC
24 GHz UWB short-range radar	HRL
76 GHz mid/long-range radar (Delphi unit)	CAMP-CIBC
76 GHz mid/long-range radar (Continental Unit)	CAMP-CIBC

Specifically, HRL was responsible the following tasks:

- Search for and acquire COTS mannequins with the size and surface texture of a 50th percentile adult human which can be struck by test vehicles between 20 mph and 30 mph without damage to the test vehicle or posing a safety concern to the testers. Alternatively, if such strike-able mannequins are not available, other options may be considered which allow the use of test apparatus that can motivate the mannequin out of the vehicle path just before impact.
- Collect sensor returns with mannequins in standing backward and side oriented positions. Compare this collected sensor return data with similar data collected from real adult humans in the same positions. If necessary, the HRL will make modifications to the mannequins to improve correlation between the sensor return data from the mannequins and real adult humans.
- Select the mannequin with the sensor return data that most closely matches that of the real adult humans for the test procedure development for assessing CIB systems and maintain the appropriate documentation.

3. Measurement Setup

HRL used the series of automotive radar sensors outlined in Table 1 to develop test mannequins that adequately represent adult pedestrians. Only static testing was incorporated into the development process of the adult test mannequins. Radar characterization of the mannequins and actual human adults consisted of positioning them on a testing grid in multiple orientations. Once positioned, data collection began using one of the mentioned radar sensors. CAMP-CIBC provided two 76GHz mid/long-range radar sensors (Continental and Delphi ESR), in addition to a 24GHz UWB M/A-COM short-range radar sensor belonging to HRL Laboratories.

The grid is defined on the pavement of an empty outdoor parking lot at HRL's campus. Figure 1 displays the current testing grid at HRL Laboratories, LLC. For this work, the distance from the ground to the center of the sensor was 83cm.

Figure 1: Outdoor Radar Testing Facility

A series of reference measurements were performed with small and medium sized corner reflectors on several occasions, usually before conducting experiments with mannequins or human test subjects. These reference measurement results were used to confirm that data sets from different days and different measurement campaigns are repeatable and can be directly compared to each another.

Figure 2 is a schematic of the measurement grid used for adult mannequin and human radar characterization. The solid black line from the radar sensor represents boresight of the sensor. Each yellow circle represents a position relative to the radar sensor where a test subject was measured. At each location, the subject was measured in two configurations: backward and side

(turned 90 degrees) facing orientations. Early in the study, we observed a similar radar signature for forward and backward facing test subjects. An additional forward facing orientation was not needed. In all the studied cases, the test subject was standing straight. Off-axis measurements occurred at 5, 7, 10, 15, and 20m for the backward and side profile orientations in 3m increments.

Figure 2: Measurement Grid.

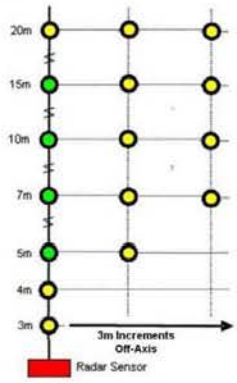

Due to the time sensitive nature of the project and the excessively long processing time of the radar data, a limited collection of data points became the focus for comparison. The test positions represented by a green circle at 5, 7, 10, and 15 m were the testing configurations used during the mannequin development effort.

4. Summary of Results

The M/A-COM, Delphi ESR, and Continental automotive radar sensors were used to perform radar measurements of the adult human adults and COTS mannequin. In order to make a direct comparison, HRL compared each sensor's return data from the real adult humans against data collected from real adult humans. For each sensor, the data was collected and post-processed to extract the SNR or radar return level over the capture time. Ultimately, the recorded measurement window provided the necessary statistics (mean and standard deviation) to effectively compare the adult mannequins and human radar cross sections. Selection of the most promising mannequins was determined in terms of SNR over the entire measurement grid.

4.1 Human Test Subject Measurements

Within this project, the radar characterization of actual human adults was collected in order to use as the benchmark in the development process of the test mannequins. An IRB approval was received before any radar measurements were taken on any individuals.

The participants were asked to remain stationary for approximately 10 seconds at a time, in the standing position. A data capture software program was used to log the performance of the radar sensors over an approximately 10 second time period. In particular, the SNR or RCS amplitude values of the assigned tracks of the radar sensor were recorded over the measurement window and averaged. These mean SNR values, along with standard deviation (SD) and total number of samples in which the target was actually detected were recorded.

At any distance from the sensor, the upper bound is defined as the largest radar return value plus one standard deviation of the set real adult humans analyzed with a particular sensor. Whereas, the lower bound is defined as the smallest radar return value minus one standard deviation of the set real adult humans analyzed with a particular sensor. These upper and lower bounds mark the acceptable range of radar return values the specific radar sensor will typically return for adults in the 50th percentile.

The Figures 3, 4, and 5 represent the adult human radar return on-axis to the sensor, at each of the following separation distances:, 5, 7, 10, and 15 meters. As discussed earlier, the measurements were performed in the backward and side facing configurations.

Figure 3: M/A-COM Radar Return of Human Adults

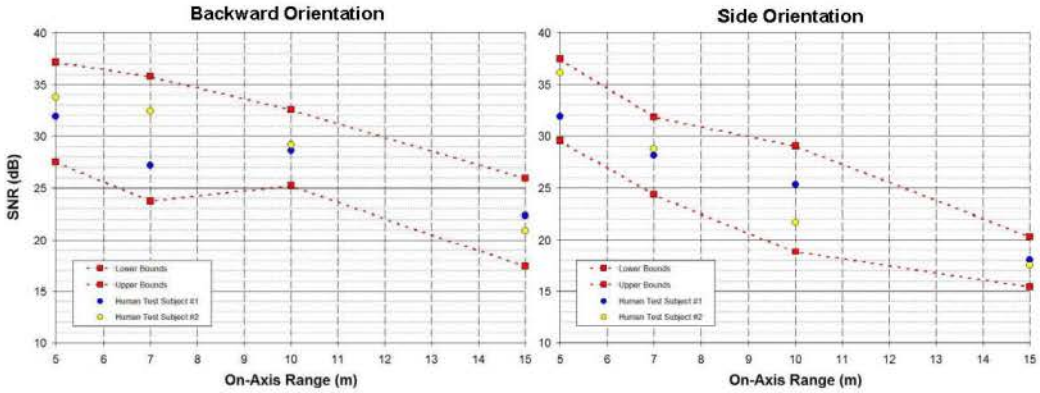

Figure 4: Continental Radar Return of Human Adults

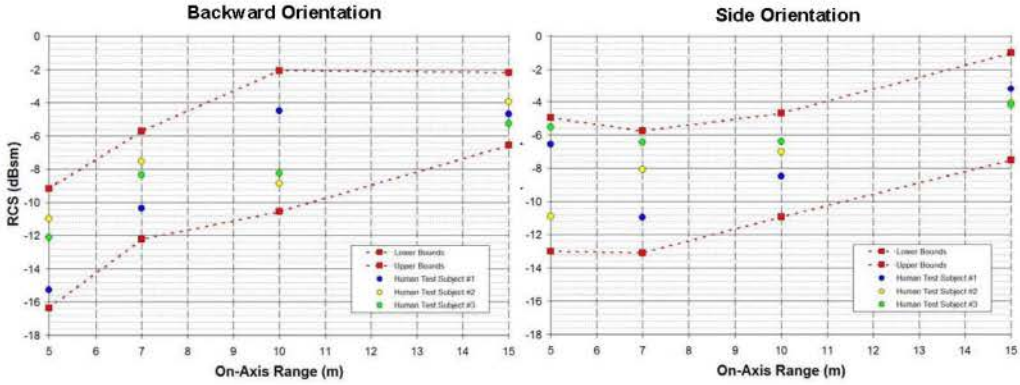

Figure 5: Delphi ESR Radar Return of Human Adults

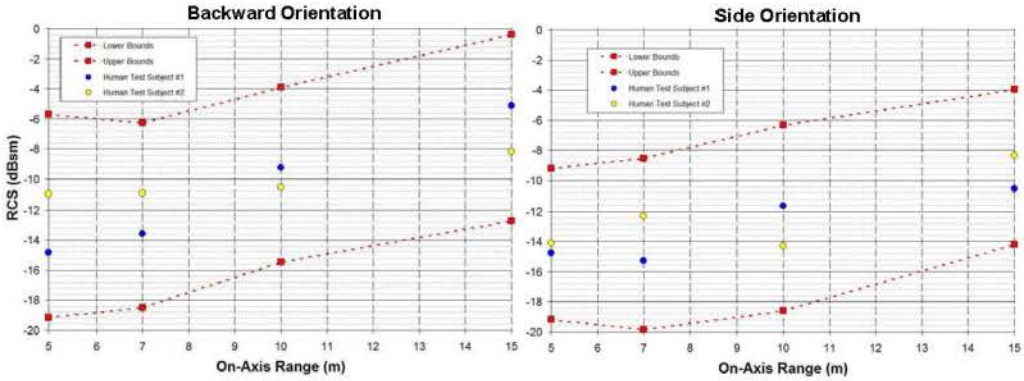

In processing the Delphi sensor, the different dwell types could be utilized. The amplitude data coresponding to the long range dwell types 1 and 2 were averaged together. The long range data was acceptable because of the restricted field of view during testing. In theory, if everything is calibrated and compensated properly, the amplitudes of each dwell type should be the same. This processing technique was used through the entire program.

4.2 Test Mannequin Measurements

Under the specifications provided by CAMP-CIBC, HRL Laboratories acquired several COTS adult mannequins that physically resemble an adult male human. For all the radar measurements, a single polystyrene cube was used to fix the test mannequins in an upright standing position. The mannequins were 5, 7, 10, and 15 meters at backward and side facing configurations. All the test mannequins acquired by HRL Laboratories, LLC, were inflatable to ensure zero damage to the vehicle in the event of a collision.

Figure 6: Unmodified Mannequin Testing

With preliminary measurements from the M/A-COM sensor, an unmodified inflatable mannequin appeared to exhibit a much lower radar return than an adult human. The comparison was made using the previously defined human upper and lower bounds. Therefore, modifications to the test mannequins were needed. The mannequins were outfitted with sections of copper tape, aluminum foil, or both, so that the radar return value recorded by the sensors were within the measured upper and lower bounds of the measured adult humans presented in Section 4.1. With each modification, the mannequin's new RCS would have to be determined. After several design iterations, the test mannequins shown in Figure 8 were shown to be good representations of adult pedestrians at both 24 and 76 GHz.

Figure 7: RCS Modification Schemes

These final iterations were delivered per CAMP's instruction for the CIB system testing before the project completion. Both delivered mannequins (i.e. #1 and #2) are wearing a silver-lined long sleeved shirt. The delivered mannequin #1 has a 2 inch wide by 12 inch long strip of copper tape adhered to each of its outer thigh regions. This was necessary to peak of the signal return of the mannequin, particularly for the M/A-COM 24 GHz system in the side orientation.

Mannequin #2 does not have any copper tape attached to it. In addition to the silver-lined long sleeved metallic shirt, a pair of silver mesh shorts was required. The shorts were placed such that the top of the short's waistband is several inches below the mannequin's waistline. If the shorts were pulled up all the way, the long shirt would conceal most of the shorts material and its effect would be limited.

Figure 8: Delivered Test Mannequins Representing Adult Pedestrians

Delivered Mannequin #1

Delivered Mannequin #2

As suspected, it was not trivial to identify a single modified mannequin with an appropriate radar signal return over all ranges at both 24 GHz and 77 GHz. To summarize the results, plots are shown in figures 9, 10, and 11 of the radar return of the delivered test mannequins at 5, 7, 10 and 15 meters. In each graph, a "lower bound" and "upper bound" is exhibited relating to our human measurements which was the empirically derived data described in Section 4.1.

Over the large majority of the 5 to 15 meter range, both mannequin #1 (yellow data points) and mannequin #2 (purple data points) had an average RCS or SNR return that fell within the upper and lower bounds. In only few cases, the average values fall just outside of our upper and lower bounds, but when we consider the standard deviation of each of those measurements, the standard deviation / error bars extend well into the desired bounds. We therefore concluded that both delivered mannequin #1 and mannequin #2 are reasonable representations of adult pedestrians in terms of radar sensor returns at 24 GHz and 77 GHz.

Figure 9: M/A-COM ESR Radar Return of Delivered Test Mannequins Compared to empirically derived upper & lower human bounds.

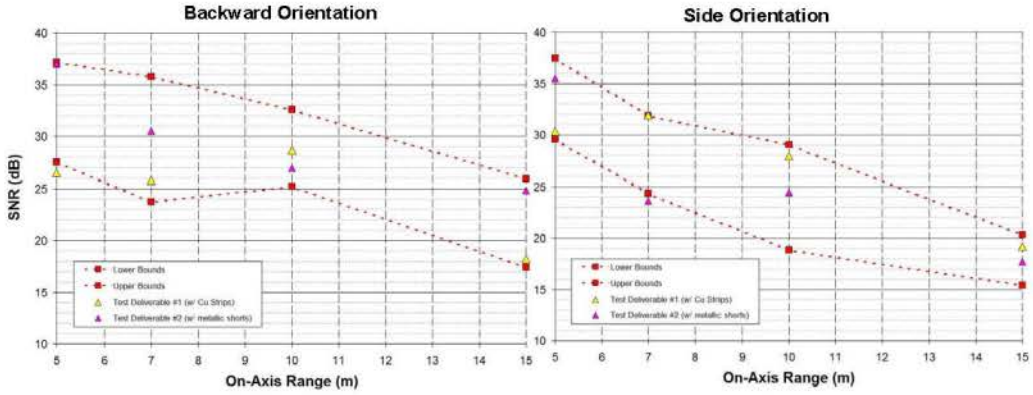

Figure 10: Continental Radar Return of Delivered Test Mannequins Compared to empirically derived upper & lower human bounds.

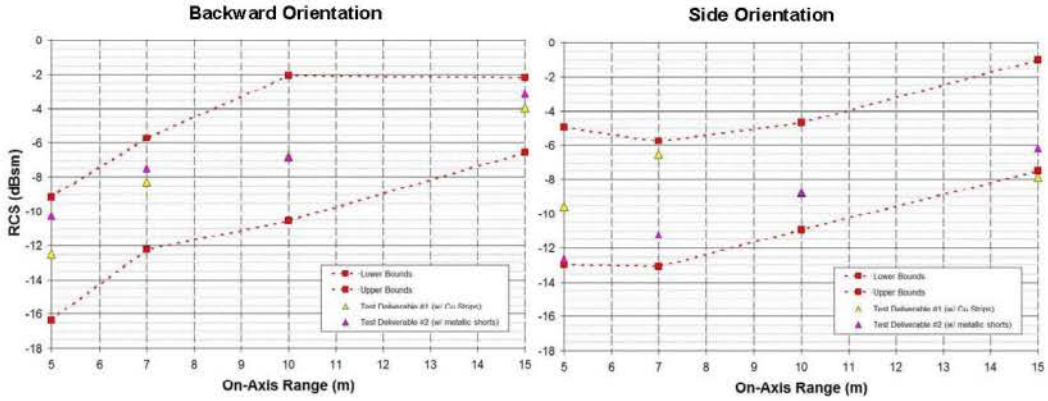

Figure 11: Delphi ESR Radar Return of Delivered Test Mannequins Compared to empirically derived upper & lower human bounds.

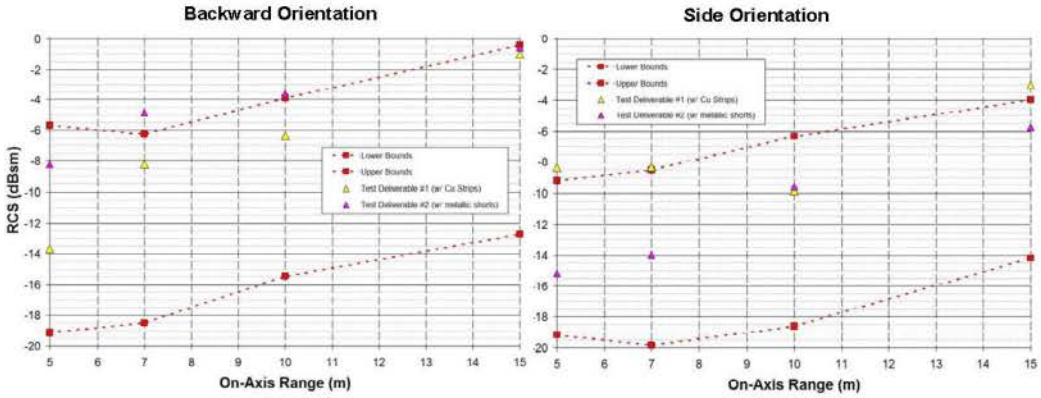

4.3 Vision System Identification of Test Mannequins

A series of tests were conducted with Delphi, Malibu CA using their Volvo XC 90, outfit with a 77 GHz sensor and vision sensor. Mannequins were placed on-axis at about 7 meters and about 14 meters in front of the vehicle. We looked at both mannequin #1 and mannequin #2 at various angles of rotation when secured to our foam mounting block. Alternatively, we studied the performance of the vision system when the mannequins were mounted on their original metal stands.

Figure 12: Delphi Vision System Test Vehicle (left) and Visual Display (right)

The following conclusions were made:

When the mannequins were mounted on their metal stand, the Delphi vision system identified both of them as pedestrians at nearly all angles of orientation. Occasionally when the mannequins were perfectly sideways, (i.e. one leg was hidden behind the second leg), it would have trouble identifying it as pedestrian. We believe this is because the algorithm relies heavily on a pedestrian's two-leg signature for detection, and that this problem also occurs for any human standing sideways perfectly stationary. (Note also that the radar return would not be accurate in the cases with the metal stand unless the metal stand was covered with some type of radar absorbing material. This test was only performed to evaluate the vision characteristics of the mannequins.)

When the mannequins were masking taped to the mounting foam block, the vision algorithm identified the mannequins as pedestrians only when the lower half of the mannequins was in front of the block and visible to the sensor. In

other words, when the legs were visibly hidden by the foam block, the algorithm had a very difficult time identifying the mannequin as a pedestrian.

When the mannequin was facing forward with the foam block directly behind it, occasionally the sensor would have a difficult time seeing the two legs of the mannequin in front of the white foam background. In a few cases, the algorithm would not recognize the mannequin as a pedestrian. When we introduced color contrast with a large black sheet behind the legs but in front of the foam block (see figure), the vision sensor was then able to clearly identify the mannequin as a pedestrian.

4.4 Test Mannequin RCS Variability

Once the test mannequins were developed to represent the radar equivalent of human adults, the COTS mannequin variability and repeatability were examined. Radar measurements were conducted on two mannequins of the same model # but in different colors, as shown below in figure 13. By themselves (without the addition of metallic garments to increase their RCS), the mannequins exhibited low radar return but still different from one another.

Figure 13: Same Model Mannequin purchased in different colors.

The different colored mannequins were tested again in the same manner as the delivered test mannequin #2 with the long sleeved shirt and shorts. In figure 14, the RCS as measured from the Continental radar unit were very similar between the two different colors. The test mannequin RCS seems to be dominated by the addition of the metal-lined garments and applied copper strips as well as how they rest on the figure. Therefore, the color of the mannequin can be chosen to optimize the pedestrian response from the automotive vision system.

Figure 14: Test Mannequin RCS Variation vs Color.

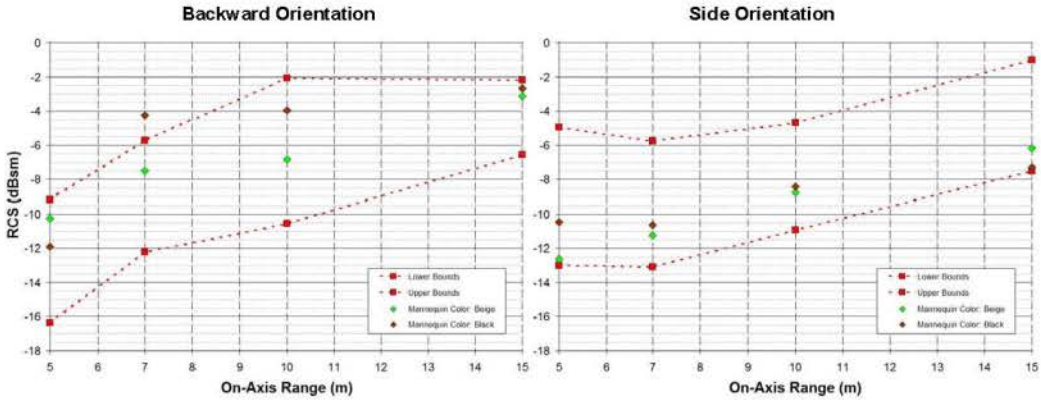

In addition to the influence mannequin color has of RCS, the repeatability or consistency of the radar measurements provides a good indication of that the designed radar return can be trustworthy from day to day. In between the measurements sets, the Continental radar system was powered down. Figure 15 shows the measurement consistency of mannequins of the delivered type #1 (with the copper strips). The standard deviation of each measurement window is labeled on the plots next to there corresponding test location. There was very

Figure 15: RCS Measurement Consistency

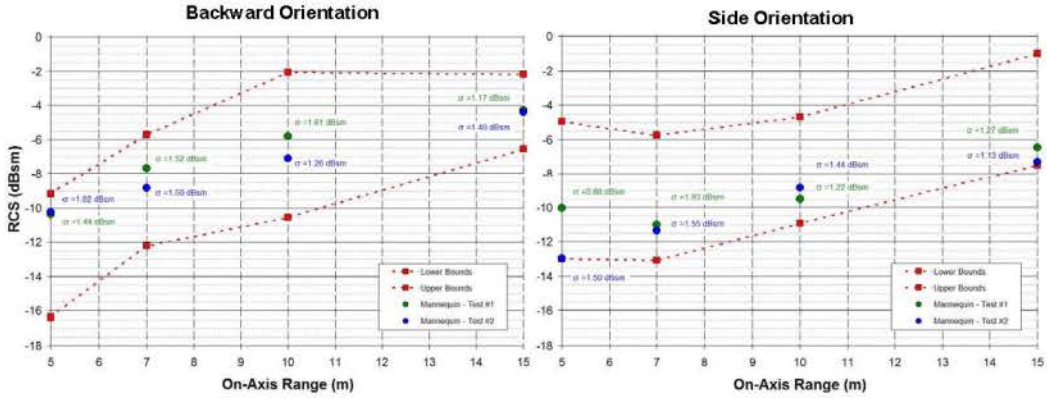

little change in spread of the measurement distribution as indicated by the likeness of the standard deviation values.

4.5 Street Clothing Study

In the past, HRL had the opportunity to perform a brief study on the influence clothes had upon the return measurements of the child mannequins. For our testing, we placed a white cotton T-shirt over the test subject at a fixed distance of 5 meters from the M/A-COM SRR sensor. The measured difference in return was hardly noticeable. It is expected that such an effect would be negligible compared to the standard deviation the mannequin.

However, all this was valid only for the frequency band associated with the M/A-COM sensor (24GHz). Additional testing was required to ensure that at 77GHz, the addition of clothes would not alter the designed RCS of the test mannequins to fall outside the empirically determined human bounds. The Continental radar sensor was used to measure the delivered test mannequin #2 with a T-shirt and pair of basketball shorts over top of the metallic garments in both the backward and side orientations at a fixed distance of 7 meters. An average change in SNR, $|\Delta SNR_{avg}|$, was measured to 4.2 dB in the back facing configuration. While a slightly lower average change in SNR, $|\Delta SNR_{avg}|$, was measured to 2.0 dB in the side facing configuration. In short, the addition clothes may have a negligible effect on the test mannequins at 24 GHz, but at 76 GHz their potential deviation will remove the test mannequins RCS to outside the human bounds.

5. Suggestions for Future Work

To extend the application of the test mannequins as well as their robustness, HRL Laboratories have identified a few limitations and corresponding suggestions for future work. Dynamic testing, implementing a more robust mannequin composition, representing a wider spectrum of the human population, investigating multiple orientations, and studying the impact of the supporting fixture used in the CIB system testing will enable the test mannequins to become a more valuable tool regarding pedestrian safety.

5.1. Different Mannequin Composition

Under the short life of the program, all the possible approaches to developing a test mannequin with a designed RCS representing an adult pedestrian could not be attempted. Alternative mannequin compositions could be developed that are filled partially or completely with water, foam, or some other dielectric materials to ensure a more consistent and robust testing tool. Ideally, a material can be inserted into a human shell that closely resembles the dielectric constants of human skin, tissue, and fat. For example, specific absorption rate (SAR) tests for monitoring the affects of cell phone radiation on humans utilize specific anthropomorphic mannequin (SAM) phantom models. With the emergence of a number a comprehensive EM modeling tools for biological applications, a large part of the design effort can be performed through simulation. Figure 16, represents a SAM phantom that represents a human head typically consists of a shell made from low permittivity and low loss microwave material that is filled with a liquid, such as a glycol mixture, whose dielectric properties match that of human brain tissue. A similar approach could be used to construct full-sized SAM phantom models valid for automotive radar frequency bands.

Figure 16: SAM Phantom.

5.2. Test mannequins only represent an adult male pedestrian

To effectively test CIB systems, different test mannequins need to be designed to represent a larger population of people. The radar measurements of the other human (female and adolescents) can provide valuable information to determine whether the current mannequins can be tailored with minimal effort.

5.3. All measurements were static
Only static measurements of the adult human and test mannequins were performed during this measurement effort. Radar sensors are known to utilize Doppler information and apply other movement tracking techniques to improve performance in dynamic situations. Therefore, dynamic measurements would add confidence and reliability to the static results acquired during this measurement effort.

5.4. Majority of the measurements were on-axis
Most of the measurements were conducted on-axis to the radar sensor in this program. Off-axis measurements at various angles and distances would add confidence and reliability to the on-axis results acquired during this measurement effort. Not only could a comprehensive off-axis measurement study be included in future work, but the mid and long range modes within a sensor isolated to individually validate the test mannequins representation.

5.5. Test Mannequin Supporting Fixture
Any on-going work should make certain that the fixture supporting the test mannequin at CAMP does not interfere with its ability to represent the RCS of a human adult. Through a series of measurements either an alternative fixture or calibration may be determined necessary.

5.6. Validation of the adult test mannequins with other radar sensors
The test mannequins developed in this effort have only been identified as accurate representations of male adults as seen by a single 24 GHz UWB radar sensor and two sensors at 77 GHz. Other versions of radar sensors exist that utilize alternative waveforms and post-processing detection and clustering algorithms. Validating the performance of the test mannequins with other 24 GHz radar sensors (UWB vs. non-UWB) and alternate 77 GHz radar sensors would add confidence and reliability to the results acquired during this measurement effort.

6. Conclusion

Two test mannequins representing the RCS of adult pedestrians were designed, tested, and delivered to CAMP-CIBC for the CIB system testing on June 12, 2009. The test mannequin RCS seems to be dominated by the addition of the metal-lined garments and applied copper strips as well as how they rest on the figure. The color of the mannequin can be chosen to optimize the pedestrian response from the automotive vision system, if necessary. Both the delivered test mannequin #1 and mannequin #2 serve reasonable representations of male adults in terms of radar sensor returns at both 24 GHz and 77 GHz. The repeatability or the consistency of RCS data from repeated radar measurements suggests that the delivered mannequins can be trustworthy for day-to-day use.

Tests with a vision system provided by Delphi, Malibu CA indicated that the mannequins could be identified as a pedestrian provided both legs of the mannequin were visible and sufficient color contrast was presented in a given mounting configuration. As a result, we recommend to use either a black colored mannequin to enhance vision contrast, or alternatively, to clothe the mannequins with a tight, form-fitting pair of bright-colored pants. We also recommend placing the vision-contrast enhancing clothing underneath the metallic mesh shorts of mannequin #2 to improve the vision system performance in the CIB system testing, if necessary.

Appendix I Balloon Car Radar and Visual Properties

The vehicle target requirements used throughout the project are identified below:

- Vehicle target well-correlated to radar profile of a real motor vehicle
- Visual, life-like properties of a real vehicle such that a machine vision system recognizes the target as a vehicle
- Vehicle target with low enough mass such that it is capable of being moved by a tow system
- Vehicle target must be durable and thus capable of maintaining radar or visual profiles after being hit repeatedly by a test vehicle, such that the need for replacement targets are minimized. In addition, target must not damage the test vehicle.
- Vehicle target must have a reasonable cost such that a suitable number of replacement spare targets can be acquired

As noted in the body of the report, the CIB vehicle target was developed over the course of the project through several stages. The 2nd-generation balloon car was used during early stages of this development process (see Figure 22).

Figure 22: 2nd-Generation Balloon Car Front, Side and Rear Views

With the help of the NHTSA Vehicle Research and Test Center (VRTC) representatives, proving ground development work on a 3rd-generation, balloon car vehicle target was conducted over the course of several months in Spring 2009. The 3rd-generation balloon car target (see Figure 23) was used extensively during test method development and final method validation testing.

Figure 23: 3rd-Generation Balloon Car Front, Side and Rear Views
(Figure courtesy of Inflatable Images)

A fundamental requirement for the balloon car target is to enable the CIB sensing systems (e.g., radar- or machine-vision-based) to recognize the target (in this case, a passenger vehicle). In order for the simulated vehicle to be recognized by a machine vision system, the physical configuration of the balloon car must be realistic-looking. The 3rd-generation balloon car exhibited these properties, as shown in the manner in which the machine vision identified the balloon car in the video snapshot shown in Figure 24. Although the vision properties of the balloon car were examined during the project, this area merits future work as these characteristics were not extensively investigated.

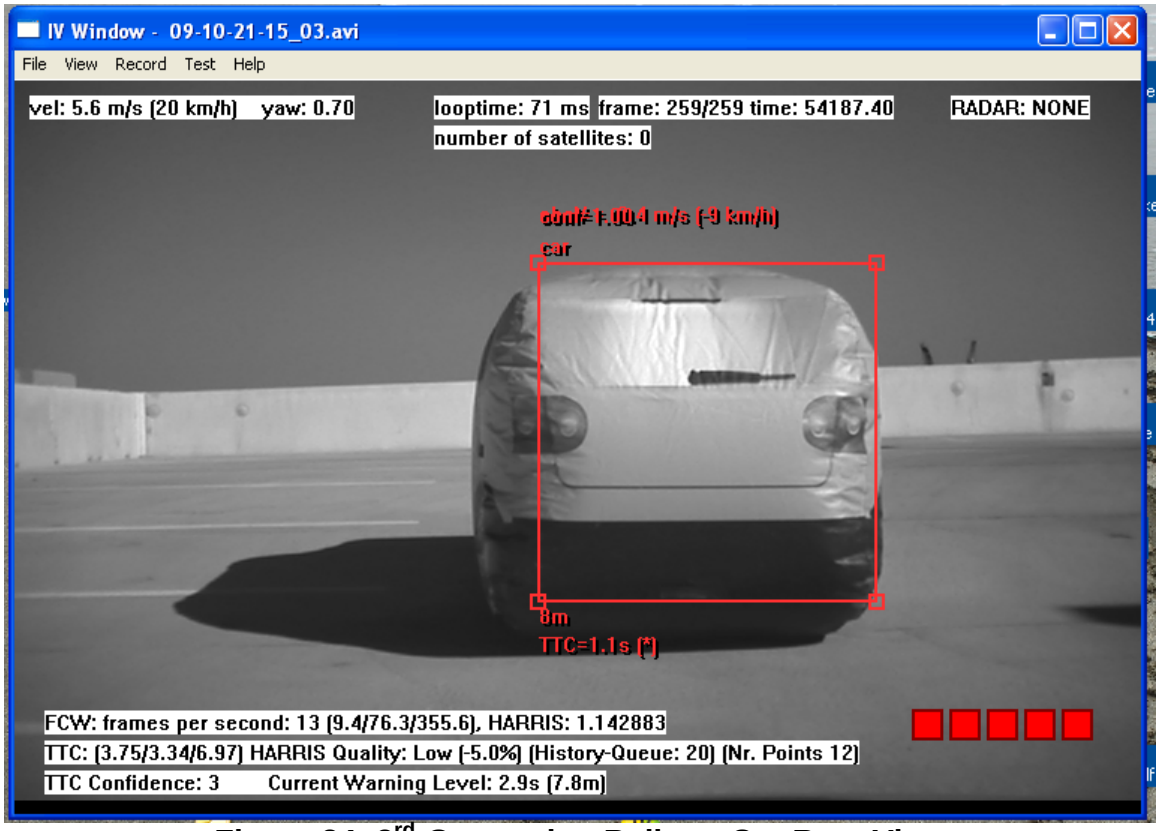

Figure 24: 3rd-Generation Balloon Car Rear View

Similarly, for radar CIB systems, the radar return from the balloon car is critical to enable the Radar sensing system to recognize the balloon car target as a real vehicle. This means that the radar return signature needs to be similar to the corresponding signature received from a passenger vehicle. To address this requirement, radar reflective material was added to the 3rd-generation balloon car for the validation testing. This material was attached to the inside of the balloon car such that it increased the radar reflectivity of the balloon car without changing the exterior visual properties. The interested reader is referred to Appendix J for additional information on this topic.

Appendix J Correlation of Radar Return Characteristics of 3rd - Generation Balloon Car to Real-World Passenger Car

In order to get a more complete picture of the characteristics for the 3rd-generation balloon car, an evaluation of the radar characteristics of this vehicle target was conducted. The 3rd-generation balloon car represents a typical small passenger car. A high-level comparison of the dimensions indicates that this vehicle target surrogate is somewhat smaller than a typical small passenger car in width and length (see Table 3).

Table 3: Dimensions of Balloon Car Compared to an Actual Small Passenger Car

	Height [m]	Width [m]	Length [m]
Balloon Car	1.50	1.50	3.60
Small Passenger Car	1.48	1.79	4.20

J.1 Method

Radar return testing was conducted at rear-end, front-end, side and 45 degree orientations relative to the stationary balloon car following a three-step process (see Figure 25).

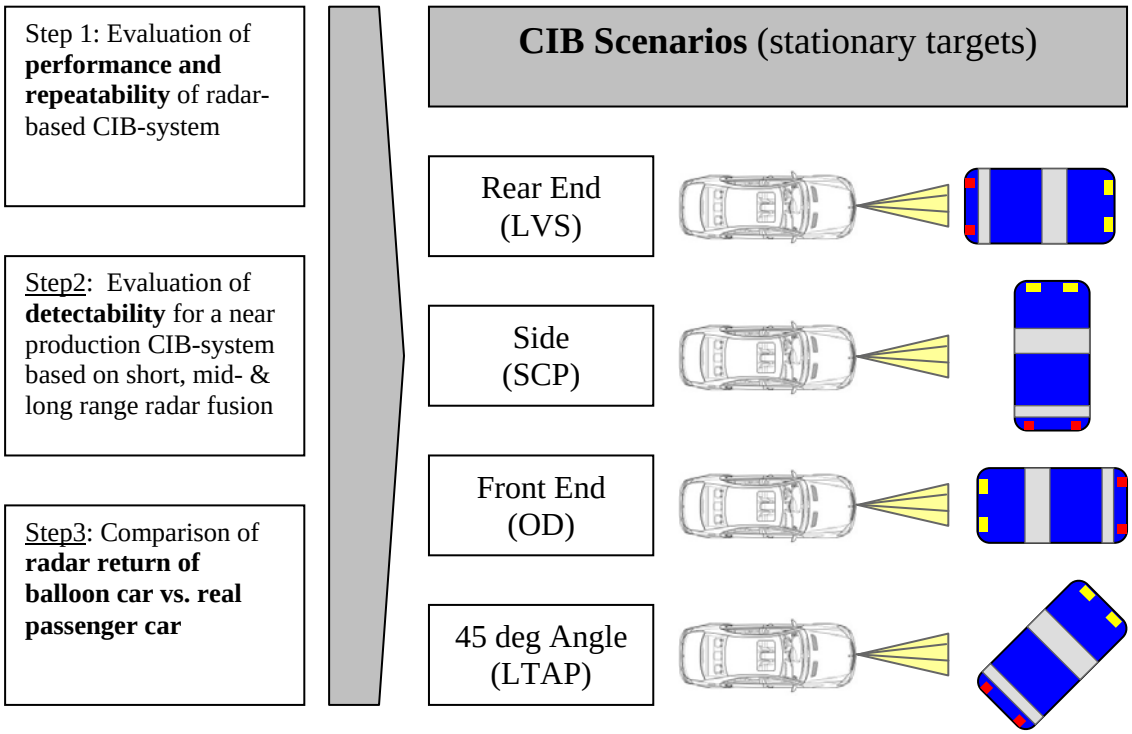

Figure 25: Methodology for Balloon Car Evaluation

Steps 1 and 2 were conducted on a test track using the balloon car as a target. In all four orientations evaluated (i.e., rear-end, front-end, side and 45 degree angle), the test was conducted with a stationary vehicle target while the test vehicle approached at constant speed of 35 mph. The test vehicle was equipped with a data acquisition system and a short/mid/long range Fusion Radar CIB System (similar to the one used in Vehicle F as described in Chapter 3, Section 3.5). Five runs were conducted for each scenario, and the resulting speed reduction was recorded. Additionally, object detection and classification results were evaluated and rated. The comparison of balloon car to radar returns from Step 3 above was conducted in a radar return measurement facility using the balloon car and a full-size passenger car. Since a proprietary measuring method was used in this testing, a detailed description of this method is not provided in this report. The measurement device was configured in a way to ensure high-resolution results. It is important to notice that the results discussed below are based on tests conducted with one CIB sensing system.

J.2 Results of Evaluation

The results of Steps 1 and 2 of this evaluation are summarized in Table 4 and detailed results are provided in Figure 26.

Table 4: Summary of Step 1 and 2 Results

Scenario	Performance and Repeatability	Detection
Rear End (LVS)	• Consistent performance • Excellent repeatability	• Good detection by short-, mid- and long-range radar • Good object classification as a car
Side (SCP)	• High variation in system performance • poor repeatability	• Object classification as a car is not guaranteed • long-range radar loses object
Front End (OD)	• Only 1 system activation with an inadequate performance • Repeatability not given	• Object classification as a car is inadequate • Short range-radar does not detect balloon-car
45 deg Angle (LTAP)	• No system activation	• Object classification as a car is not given

For the rear-end case, the CIB Sensing System appeared to provide good and reliable performance for the balloon car. The testing results indicated five very consistently timed brake activations with significant speed reduction and a good object classification (recognized as a passenger car) within the CIB systems algorithm. Driving toward the balloon car from the side also resulted in five brake activations. However, repeatability of the braking activation timing and the consistency of speed reduction were not as good as the rear-end case. In these side orientations, the object classification algorithms did not consistently detect/classify the balloon car as a passenger car in all cases. Both front-end and 45-degree angle cases delivered poorest results of the scenarios examined. The

brakes only activated in one of the ten runs in these two cases (see Figure 26). In the front-end and 45-degree angle orientations, the short-range radar did not recognize the balloon car properly.

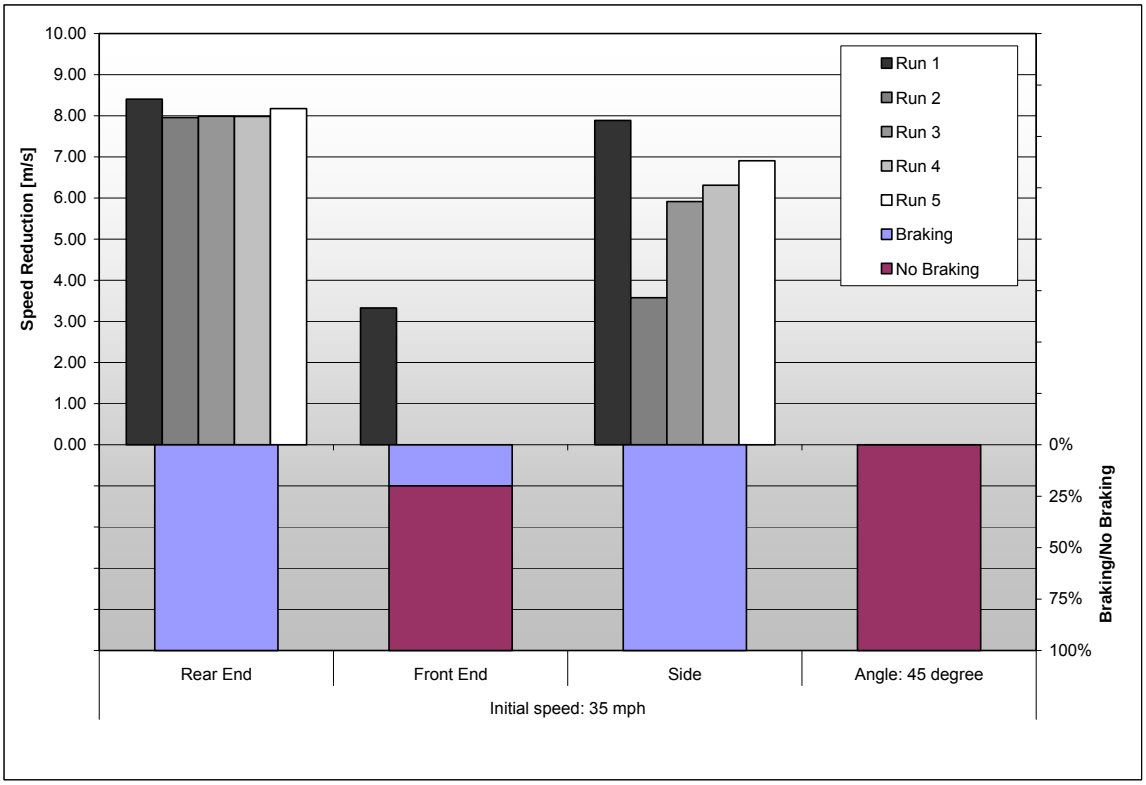

Figure 26: Speed Reductions and Braking/No Braking Distribution

During Step 3 of this research, the radar signature of the balloon car was measured in all the four orientations described earlier and compared to a real passenger car. The same 24 GHz radar sensor was used for all measurements. The measurement of radar signature/return can be represented in a percent-based scale, where 100% represents the maximum detection capability of the radar sensor and 0% equals the noise ratio of the sensor.

As was found in the rear-end orientation in Steps 1 and 2, the corresponding radar signature of the balloon car found in Step 3 corresponded well to the rear-end of a real vehicle (see Figure 27). It was observed that the radar return intensity of the balloon car is slightly higher than the real vehicle in the middle of the vehicle and that the radar signature is also smaller in width.

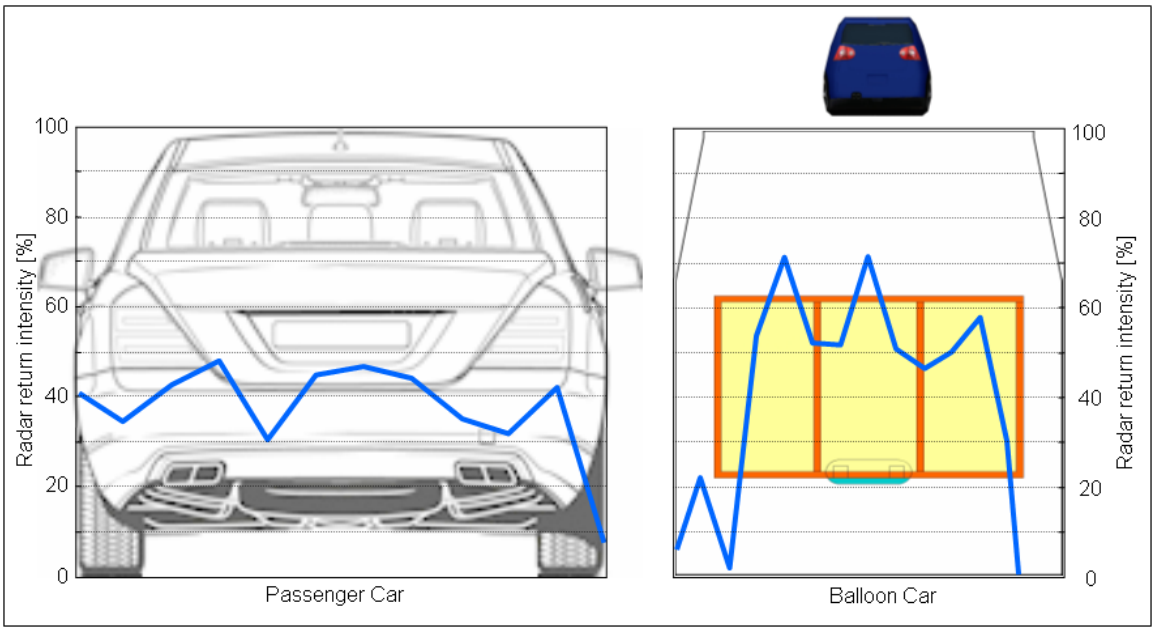

Figure 27: Rear-End Radar Signature of Real Car / Balloon Car
(Figure courtesy of Inflatable Images)

The results of the side-view radar return tests provided an explanation of the reduced performance of the CIB system in a Straight-Crossing Path (SCP) Scenario. A real vehicle shows a medium-high and very constant radar return. The reflecting foils implemented in the balloon car have approximately 2 inches of space between each foil. This condition causes high peaks reflection intensity separated by gap areas where radar returns are absent (see Figure 28).

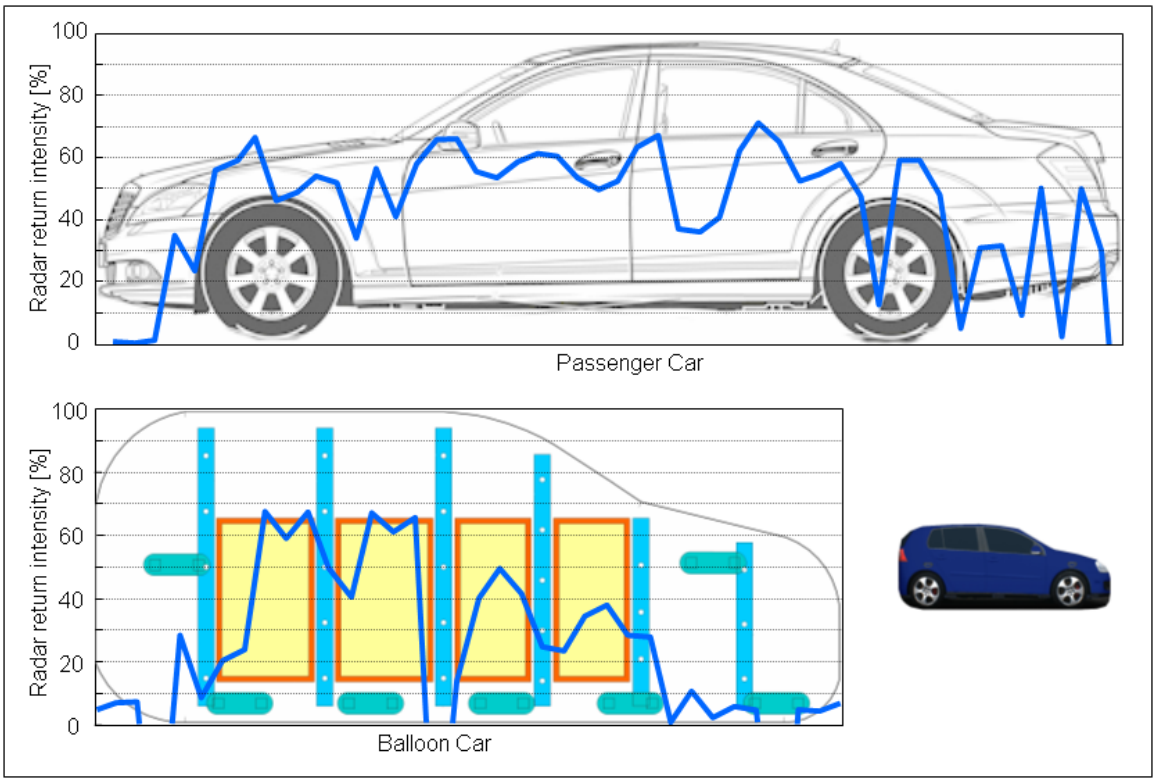

Figure 28: Side Radar Signature of Real Car / Balloon Car
(Figure courtesy of Inflatable Images)

The front-end orientation test results indicate a different pattern of radar returns for a real-passenger vehicle versus balloon car (see Figure 29). The real-passenger vehicle has one peak radar return signature area at the center of the vehicle where the engine is located. On both sides of this area, the radar return is very low due to the tapered shapes of the hood and fenders. These tapered body panels might shield and/or scatter the radar signal rather than returning it to the radar receiver. In sharp contrast to what was observed with the real vehicle, the balloon car shows two peaks in radar return signature at the left and right side and a reduced return in the middle.

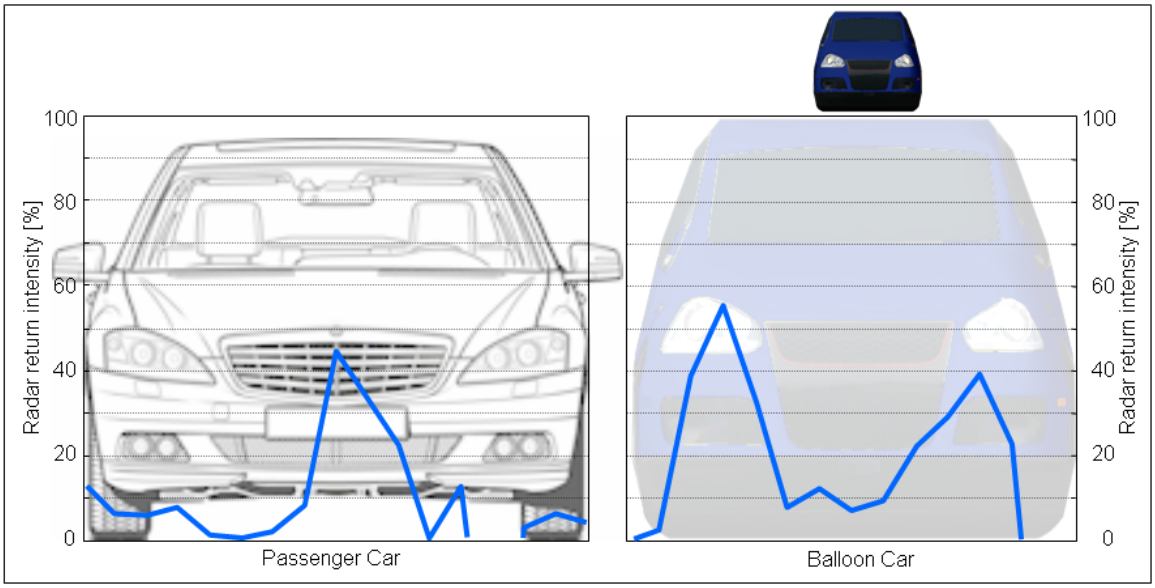

Figure 29: Front End Radar Signature of Passenger Car / Balloon Car
(Figure courtesy of Inflatable Images)

In order to get a better understanding of the balloon car radar return during the Left Turn Across Path (LTAP) Scenario, a comparison of the radar returns for the balloon car and real car were made for nine different angles (see Figure 30). The radar return for the real car shows a nearly constant radar return intensity throughout the various orientations of the car, whereas the balloon car results indicate a particularly significant lack of return intensity between 22 and 45 degrees. This appears to explain the reduced number of CIB system activations during the 45 degree angle orientation tests performed in Step 1 and Step 2.

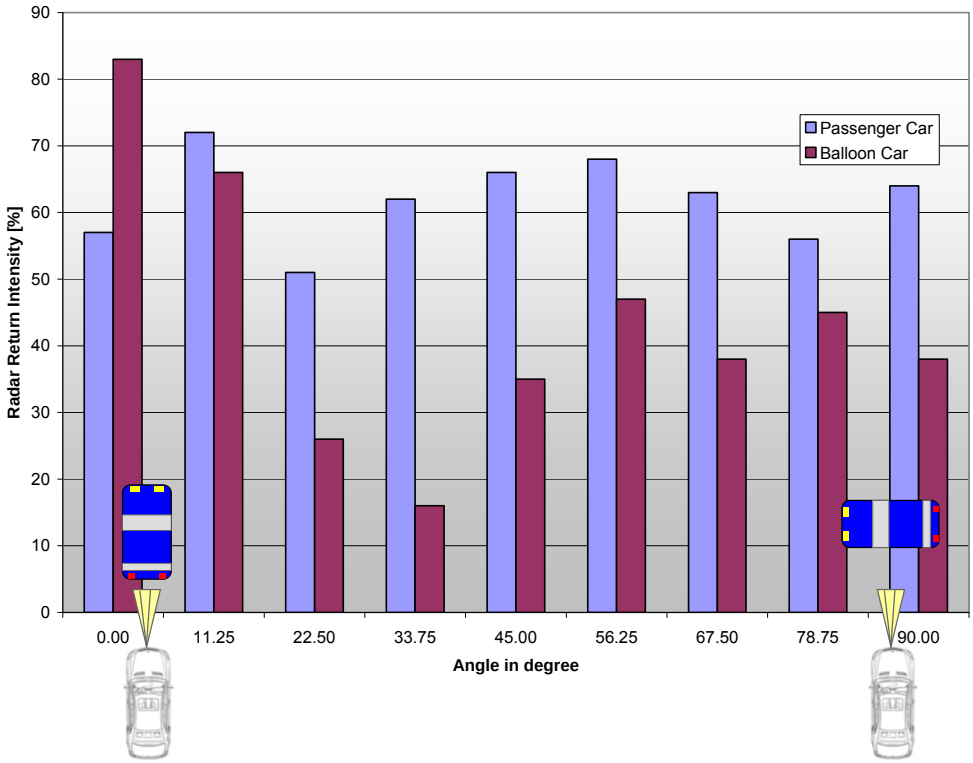

Figure 30: Radar Return Intensity with Angle Deviation

J.3 Summary

In the Lead Vehicle Stopped - LVS rear-end scenario evaluated, the radar returns from the balloon car provided a good match relative to those obtained with a real vehicle. Although the "approach from the side" scenario (similar to SCP) resulted in brake activations, an issue was identified involving the lack of reflecting foils in the front and rear fender areas. In addition, the gaps between the reflective foils could cause the CIB system to improperly characterize the balloon car and miss opportunities for brake activations. However, with relatively minor balloon car changes, it appears these side-orientation issues could be sufficiently addressed to improve the radar-based CIB performance and repeatability.

In the frontal approach scenario (Opposite Direction - OD) and at approach angles approximating 45 degrees (similar to LTAP), the radar return performance was less repeatable than desired. These results might be explained by the curved reflective foils in the front of the balloon car, which may scatter the radar return and/or act as a radar shield. For the angular approach cases, the flat reflecting foils on the side of the balloon car can reflect the radar return away from the radar receiver, which can adversely impact accurate balloon car detection and classification in these frontal angular approach scenarios. Overall, this evaluation suggests that significant improvements of the balloon car radar return are needed for OD and LTAP tests.

Additionally, these test series indicate that proper air pressure must be maintained in the balloon car while performing CIB tests. Changes in air pressure cause changes in the shape of the balloon car and, therefore, the reflective foil which can lead to differences in the radar return of the balloon car.

In summary, this evaluation shows that the balloon car does not accurately represent real car radar returns in all of the CIB crash scenarios that were evaluated. Thus, further balloon car development is needed if the intent is to use a single balloon car in a robust fashion across a wide range of CIB crash scenarios. Future work is recommended to develop a target object with improved real passenger car radar characteristics that includes conducting additional radar return and performance evaluation using a broader range of real vehicle types and sensing systems.

Appendix K Standard Testing Conditions and Equipment

The material in this appendix was adapted from NHTSA's Forward Collision Warning (FCW) System Confirmation Test Procedure for CIB testing purposes. This test procedure ("Forward Collision Warning System NCAP Confirmation Test March 2010") is available as Docket Number - Docket NHTSA-2006-26555.

K.1 Standard Conditions for Testing of CIB Systems

K.1.1 Test Surface Conditions

- The road surface should be straight and flat.
- The road surface should be constructed from concrete or asphalt materials and in a good condition.
- The road surface should be free of significant bumps, potholes, and cracks that could cause the test vehicle to pitch excessively.
- The road surface should be free of manholes, reflectors, or other objects that might be sensed by the CIB systems and adversely affect the test results.
- The surface of the test area should be dry (without visible moisture on the surface) and clean (free of significant dirt, stones, and other debris).
- Unless otherwise specified, both sides of the test lane (15 meters from the test lane center) must be free of any obstacles such as other vehicles, guardrails, poles, trees, signs, bridges, structures, etc. For all scenarios where the target system is moving perpendicular to the test vehicle, it must be unobstructed within a corridor of at least 75 meters.
- Unless otherwise specified, the test lane shall be free of any roadway markings.

K.1.2 Ambient Conditions

- The tests should be conducted during daylight with good visibility, which is defined as an absence of fog and the ability to see clearly for more than 5000 meters.
- The test shall not be conducted with the test vehicle oriented into the sun during conditions when the sun angle is 15 degrees or less above the horizon.
- Ambient temperature must be between 32º F (0º C) and 100º F (38º C).
- Wind speed is limited to 10 m/s (22.4 mph) maximum.
- Tests should not be performed during periods of inclement weather. This includes, but is not limited to, rain, snow, hail, fog, smoke, or ash.

K.2 Equipment for Testing of CIB Systems

K.2.1 Test Vehicle Requirements

- The offset distance between the test vehicle and the lane center must not be higher than +/-0.25 meters.
- Steering input should be limited and very smooth.
- Initial test vehicle speeds should vary no more than +/- 1.0 mph from the indicated test speed.
- The test vehicle tires shall be inflated to the recommended cold inflation pressure as specified on the vehicle placard or optional tire inflation pressure label.
- All non-consumable fluids must be at 100 percent capacity. Fuel must be maintained at least 75 percent capacity during the testing.
- The test vehicle shall be loaded with one driver and all required equipment during the testing. Where possible, the equipment shall be placed on the passenger side of the vehicle.
- The centerline of the test vehicle shall be determined and the lateral, longitudinal, and vertical position of the measurement system GPS antenna shall be measured and recorded.
- The longitudinal distance from the GPS antenna to the front-most position of the test vehicle front bumper shall be measured and recorded.
- Test vehicle CIB systems shall be calibrated/reset as defined by the manufacturer between test runs.

K.2.2 Target Requirements

- Target must be a surrogate that can be struck or have a mechanism that securely avoids contact with the test vehicle immediately prior to anticipated impact and have physical characteristics and radar profile representative of a Pole /Pedestrian or mid-sized, passenger vehicle as determined by the specific test scenario (see Appendix F).
- In scenarios where movement of the target is required, devices for applying movement to the target should not interfere with the vehicles CIB sensor systems.
- The target speed should vary no more than +/-5% from the indicated target speed.
- The offset distance between the target and the lane center must not be higher than +/-0.25 meters except during periods when the target is required to deviate from a straight path (i.e., LTAP scenario).

K.2.3 Instrumentation Requirements

- All test instrumentation must be setup in an orderly manner consistent with good engineering practices.

- Portable tire pressure gage with an operating pressure of at least 700kPa (100 psi), graduated increments of 1 kPa (0.1 psi) and an accuracy of at least + 2.0% of the applied pressure is required.
- Instrumentation used shall meet defined measurement accuracy and data collection rate requirements (see Table 5).

Table 5: Required Instrumentation Accuracies / Collection Rates

Measurement	**Vehicle / Target**	**Accuracy**	**Required Onboard Data Rate**	**Comments**
Longitudinal Position	Test Vehicle	0.10 m	100 Hz	
	Moving Target System	0.10 m	100 Hz	
	Stationary Target System	0.10 m	NA	
Lateral Position	Test Vehicle	0.10 m	100 Hz	
	Moving Target System	0.10 m	100 Hz	
	Stationary Target System	0.10 m	NA	
Longitudinal Speed	Test Vehicle	0.07 m/s	100 Hz	0.25% of full scale (100kph)
	Moving Target System	0.07 m/s	100 Hz	0.25% of full scale (100kph)
Longitudinal Acceleration	System Vehicle	0.10 m/s²	100 Hz	Inertial Measurement Signals to be filtered with a first order 10Hz Butterworth Low-Pass Filter
	Moving Target System	0.10 m/s²	100 Hz	
Lateral Acceleration	System Vehicle	0.10 m/s²	100 Hz	
	Moving Target System	0.10 m/s²	100 Hz	
Yaw Rate	System Vehicle	0.10 deg/s	100 Hz	
	Moving Target System	0.10 deg/s	100 Hz	
Pitch Angle	System Vehicle	0.10 deg	100 Hz	
	Moving Target System	0.10 deg	100 Hz	
Start/Stop CIB Brake actuation	Test Vehicle	0.010 sec	100 Hz	Controller Area Network (CAN) data acceptable. Output response better than 10 ms

K.2.4 Calibration Requirements

- Before the test program is initiated, a test instrumentation calibration system must be implemented and maintained in accordance with established calibration practices. The calibration system shall be set up and maintained as follows:

  A. Measuring and test equipment will be stored and used under appropriate environmental conditions to assure their accuracy and stability.

  B. All measuring instruments and standards shall be calibrated against a higher order standard at periodic intervals not exceeding twelve (12) months. Records showing calibration traceability to the National Institute of Standards and Technology (NIST) shall be maintained for all measuring and test equipment. The calibration frequency can be increased if deemed necessary.

  C. All measuring and test equipment and measuring standards will be labeled with the following information:

     - Date of calibration
     - Date of next scheduled calibration
     - Name of the organization and the technician who calibrated the equipment

  D. A written calibration procedure shall be prepared that includes a minimum of the following information for all measurement and test equipment:

     - Type of equipment, manufacturer model number, etc.
     - Measurement range
     - Accuracy
     - Calibration interval
     - Type of standard used to calibrate the equipment (calibration traceability of the standard must be evident)
     - The actual procedures and forms used to perform the calibrations

  E. Records of calibration for all test instrumentation shall be kept in a manner that assures the maintenance of established calibration schedules. All such records shall be readily available for inspection when requested and shall be included in the final test report.

  F. Test equipment shall receive a pre- and post-test zero and calibration check. This check shall be recorded by the test technician(s) and submitted with the final report.

Appendix L Functional Test Methods

L.1 Rear-End – Lead Vehicle Stopped (LVS)

L.1.1 Test Method

The following procedure was used for testing with both the baseline production vehicles and the PIP vehicles.

First, the target system was placed in the center of a lane with the longitudinal axis orientated parallel to the lane. The rear of the target was positioned to face the front of the test vehicle. The total length of the track should be 450 m to 500 m. The minimum starting distance between the test vehicle and the target was 250 m. The test vehicle was then driven straight to the target system with its initial test speed stabilized prior to reaching 100 m before the target. As shown in Table 6, various test speeds were used for this scenario. Changes in acceleration pedal position were avoided on the last 100 m before hitting the target system. Steering corrections within that range should also be limited and smooth before hitting the target system centrally. The distance between the middle of the vehicle and the centerline was kept lower than 0.5 m. The test ended 5 m after the target vehicle struck the target system. The brake pedal was not applied by the driver until the target system was passed. For exact measurements of speed, distance and angle of the test vehicle to the target system, a differential GPS system with base station was used.

Table 6: Velocities for Lead Vehicle Stopped Scenarios

Velocities	In mph	In km/h
System Vehicle	20	32.2
	30	48.3
	35	56.3
	40	64.4
Target Speed	Stationary	

For baseline testing, this test scenario was conducted with seven different target systems (see Table 7). For each velocity and each target system, 5 runs were conducted to have a representative quantity of results. For some target systems, the maximum speed and number of runs were reduced to avoid damage to the test vehicle or to the target system. The number of runs was also reduced when the tested vehicles CIB system did not react in anyway (audible or visual warning, belt pretension or braking) in three consecutive tests at the first test speed. Under these conditions, only three tests were conducted at each remaining test speed.

Table 7: Target Systems for Lead Vehicle Stopped Scenario

Short Name	LVS1	LVS2	LVS2a	LVS3	LVS4	LVS5	LVS6
Target System	Flip Down	Balloon Car 1	Balloon Car 2	Foam Block	Hanging Target	Balloon Car 1 + Flip Down	Crash Simulator
Picture							

L.1.2 Detailed Results from Baseline Test Phase

Analyses of Time to Collision (TTC) and Range at Brake Initiation were used to get further information of variations within the different tests to find the targets with the most promising performance for further testing. Time-to-collision refers to the time it would take for a collision to occur at the prevailing speeds, distances, and trajectories associated with the driver's vehicle and the closest lead vehicle.* Figure 31 shows the distance at brake initiation for different target systems at 20 and 30 mph. Combining the tested radar-only target (LVS1) with a balloon car that provides visual information and additionally radar depth information (LVS5) results in earlier brake activation of the systems at both test speeds.

* van der Horst, A.R.A., (1990). A time-based analysis of road user behavior in normal and critical encounters, Doctoral Dissertation, Delft University of Technology, Delft, The Netherlands. (Available from the TNO Human Factors Research Institute, PO Box 23, 3769 Soesterberg, The Netherlands).

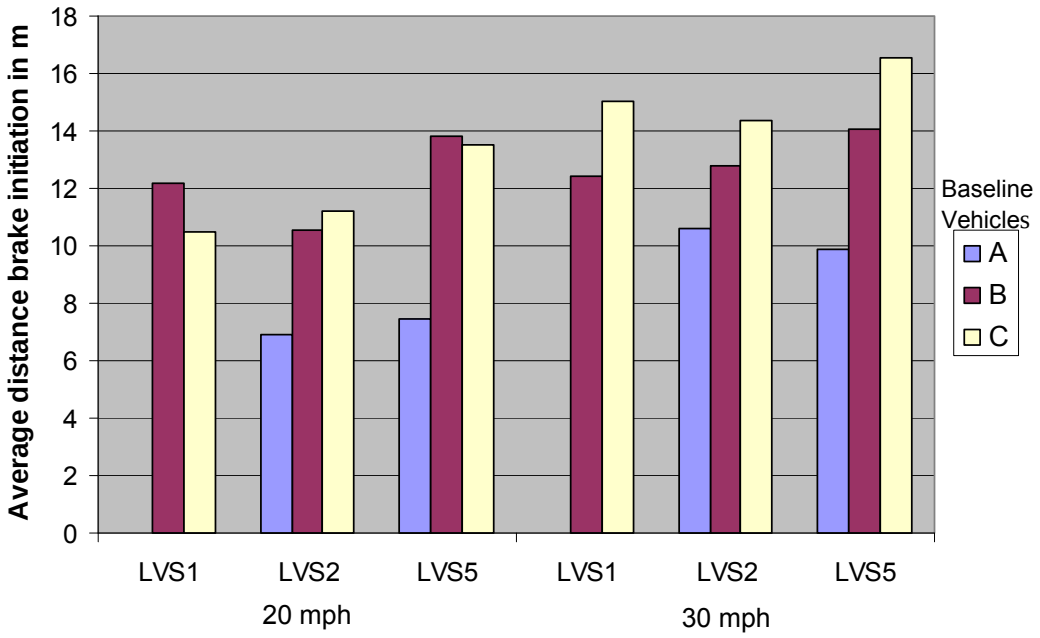

Figure 31: Distance at Brake Initiation for Three Different Targets and Baseline Vehicles A, B, C at 20 and 30 mph

Analysis of this data was broken into two parts. After comparison of the number of test runs with and without brake activations, reductions in impact speed were first assessed as input data for the preliminary CIB benefits estimation analysis and a high-level assessment of overall system performance. Next, TTC (as defined by van der Horst, 1990) and "Range at Brake Initiation" provided an analysis of variation within the tests. These data points provided an assessment of the variation within each individual target type, a comparison of variation between target options, and variation in the performance of each CIB system tested.

The most repeatable results across all three test vehicles occurred with targets that provided visual and radar information. Adding metallic areas such as aluminum paint or other reflective material to balloon cars seems to improve the performance of the target to better represent real-world vehicles. Vehicle A has a similar speed reduction for all initial test velocities, implying that the range at brake initiation increases with higher test speeds. It appears to react to stationary obstacles only when the vision system confirms that an obstacle is a vehicle. No braking occurred for radar-only targets, such as the flip-down or hanging targets. Vehicles B and C reacted differently than Vehicle A across different test speeds in that with higher test speeds the speed reduction decreases. Also the range at brake initiation decreases at higher speeds.

The results of the Lead Vehicle Stopped runs with the production vehicles suggest that targets have to provide information for vision and radar system in a representative way to best match that of a real vehicle. A goal for the next test phases with the PIP vehicles is to improve balloon cars to provide better radar reflectivity and optical performance.

L.1.3 Detailed Results from PIP Test Phase

Both Vehicle E and Vehicle G were built with re-configurable CIB systems. This provided the ability to select different sensor set combinations, TTC settings and requested CIB braking deceleration settings. For the results discussed below for these two vehicles data was collected using radar-only, camera-only and radar/camera fusion. Vehicle F includes only one system configuration, but includes 2-stage braking capability.

TTC and requested deceleration settings on the adjustable systems were selected based upon a high/medium/low priority, dependent upon the available time to complete the total number of tests. “High” priority designation was selected based on the fixed system configuration installed in Vehicle F, plus setting one adjustable system with a low deceleration level (0.3 g) and high TTC setting (1 sec) while setting the other adjustable system with a high deceleration level (0.9 g) and low TTC setting (0.6 sec). “Medium” priority tests included settings which were expected to deliver the maximum speed reduction prior to impact without fully stopping the vehicle, resulting in the maximum theoretical benefit for crash mitigation. These settings included high TTC (1 sec) and high deceleration (0.9 g). Lower priority was given to intermediate system settings between “high” and “medium” priority tests.

L.1.3.1 Vehicle E

Vehicle E was tested with two different TTC settings (i.e., 0.6 and 1.0 seconds and a constant deceleration rate of 0.9 g). Several tests were conducted at 20 mph and 30 mph with two different targets. For the initial speed of 40 mph only one test was done, because the Orange Balloon Car would not withstand multiple impacts using only high-speed impacts.

The sensor settings in the Vehicle E were switched to brake using only radar information for all runs. In a post-processing step, the additional data collected for assessing the performance of the camera and fusion settings was reviewed. Table 8 shows the actual speed reduction for radar-triggered system and for each run if camera and Fusion system would have sent the brake command.

As expected, a higher TTC setting results in higher speed reductions. Table 10 also indicates that the vehicle had higher speed reductions with the orange balloon car. The foam block did not work as a reliable target for this vehicle.

Table 8: Results of LVS Test Runs with Vehicle E using a Deceleration Setting of 0.9g and different TTC Settings

Vehicle E						Speed reduction in mph							
Test scenario	**Host Speed (mph)**	**Target**	**TTC setting**	**Decel setting**	**System**	**Run 1**	**Run 2**	**Run 3**	**Run 4**	**Run 5**	**Run 6**	**Average**	**StdDev in mph**
LVS	20	Orange Balloon Car	0.6	0.9	Radar only	0.43	0.54	0.47	0.45	0.45		0.47	0.04
					Camera only	true	true	true	true	true			
					Fusion	true	true	true	true	true			
		Orange Balloon Car	1.0	0.9	Radar only	7.16	7.18	6.76	8.19	6.98		7.25	0.55
					Camera only	true	true	true	true	true			
					Fusion	true	true	true	true	true			
		Foam Block	1.0	0.9	Radar only	0.78	0.87	0.89				0.85	0.06
					Camera only	false	false	false					
					Fusion	false	false	false					
	30	Orange Balloon Car	0.6	0.9	Radar only	0.83	*	0.63	1.03	0.87	0.63	0.84	0.17
					Camera only	true	false	true	true	false	false		
					Fusion	true	false	true	true	false	false		
		Orange Balloon Car	1.0	0.9	Radar only	7.29	9.53	7.16	7.52			7.87	1.11
					Camera only	true	true	true	true				
					Fusion	true	true	true	true				
		Foam Block	1.0	0.9	Radar only	0.40	1.01	0.58				0.66	0.31
					Camera only	false	false	false					
					Fusion	false	false	false					
	40	Orange Balloon Car	1.0	0.9	Radar only	*						-	
					Camera only	false							
					Fusion	false							

grey, empty cell = no run
* = no braking
True = Camera/Fusion sent brake signal
False = Camera/Fusion didn't send brake signal

L.1.3.2 Vehicle F

Vehicle F was used to verify the approach used in developing and improving the balloon car. The foam block target used for this comparison is a target with a known radar return by one of the project members which provides an internally documented system performance. As shown in Table 9, the speed reductions for the two different targets are comparable.

Table 9: Results of LVS Test Runs with Vehicle F

Vehicle F			Speed reduction in mph						
Test scenario	**Target**	**Host Speed (mph)**	**Run 1**	**Run 2**	**Run 3**	**Run 4**	**Run 5**	**Average**	**StdDev in mph**
LVS	Foam Block	20	11.60	12.97	12.34	13.17	12.70	12.56	0.61
		30	12.21	11.20	11.88	10.73	11.52	11.51	0.57
	Orange Balloon Car	20	11.52	10.73	13.15	13.01	12.81	12.24	1.07
		30	12.83	13.64	13.71	12.90	13.98	13.41	0.51

L.1.3.3 Vehicle G

Vehicle G (see Table 10) was tested with a constant TTC and different deceleration settings. As expected, the highest speed reductions occurred with the highest deceleration level (0.8 g). However, not all runs with this brake level showed improved speed reductions than the lower deceleration levels 0.3 g and 0.6 g. There is a noticeably high variation in the results shown in Table 10.

Table 10 shows the speed reduction of each LVS run made with the Vehicle G as a function of initial speed and deceleration rate. Speed reduction was at its maximum with the high deceleration rate of 0.8 g. One reason for the variance in speed reductions of different runs could be the loss of air changing the shape of the balloon car.

Table 10: Results of LVS Test Runs with Vehicle G using a TTC Setting of 1 S

Scenario: LVS; Target System: Orange Balloon Car; Vehicle G												
					Speed reduction in m/s							Standard Dev in m/s
Test Vehicle Speed	TTC Setting	Decel Settings	Track/ Simulation	Sensor Config	Run 1	Run 2	Run 3	Run 4	Run 5	Run 6	Average	
20mph	1.0sec	0.3g	TRK	Fusion	2.43	2.39	1.81				2.21	0.35
		0.6g	TRK	Fusion	4.12	4.17	4.01	4.21	2.57		3.82	0.70
		0.8g	TRK	Fusion	1.75	4.47	6.86	*	2.78	5.31	4.23	2.02
30mph	1.0sec	0.3g	TRK	Fusion	1.24	1.12	2.35	1.84	2.91	2.83	2.05	0.77
		0.6g	TRK	Fusion	3.84	4.99	2.69	4.60	2.88		3.80	1.02
		0.8g	TRK	Fusion	5.21	4.43	*	7.31	3.66		5.15	1.57

Average and Standard Deviation based on runs which had brake activation
* = no brake activation
grey cell = no run

L.1.4 Evaluation of Method, Targets and Equipment for LVS Scenario Testing

Overall, the LVS results of the PIP vehicles showed a good potential for the orange balloon car as a vehicle surrogate. However, durability became an issue with this type target at higher test speeds and after multiple tests with a car. Also, having to add reflective material to the targets, such as radar-reflective paint to the rear windows and tailored reflective sheets to the bumper (Figure 32), present potential future issues in test repeatability when switching between balloon car samples or test facilities. This added material also modifies the exterior appearance of the target, potentially influencing the results of camera-based or fusion-based CIB system tests. The flexibility to add or modify the radar-reflective characteristics of the target did provide benefit in understanding the necessary target characteristics. Ideally, final characteristic set should be incorporated into the internal structure of future balloon car targets for a repeatable off-the-shelf solution.

Figure 32: Rear View of Orange Balloon Car with Additional Reflective Material

L.1.5 Validation Test Phase

L.1.5.1 Test Method

The Lead Vehicle Stationary (LVS) test setup developed in the baseline testing and PIP 1 testing phases required no further development. One lane of the test track and a balloon car target, as shown in Figure 33 and Figure 34, respectively, was used in the LVS test scenario. The balloon car was stationary and placed on a protective ground sheet. To prevent the balloon car from moving under windy conditions during the test, anchor lines were attached to the four corners of the target in a manner that would not influence the radar reflectivity of the target during a test. This arrangement kept the balloon car target stationary in its prescribed location during the test vehicle approach but allowed it to move freely after impact with the test vehicle (and thus preventing damage to the balloon car).

During a LVS test run, the driver of the test vehicle waited at the starting position at the far end of a test track. Once the balloon car was properly positioned, the test vehicle accelerated to the defined test speed and maintained that speed until striking the balloon car. Note that this strike could occur with or without brake activation.

Most LVS tests used the 3rd-generation balloon car (blue balloon car). However, some earlier tests were conducted with the 2nd-generation balloon car (orange balloon car) before the 3rd-generation balloon car became available. The test results presented below reflect the target used with each LVS test scenario.

Figure 33: 2nd-Generation Balloon Car, Front, Side and Rear Views

Figure 34: 3rd-Generation Balloon Car; Front, Side and Rear Views
(Figure courtesy of Inflatable Images)

L.1.5.2 Detailed Results from Validation Test Phase

Each vehicle was tested at three different initial approach speeds (20, 30, and 40 mph). For each initial approach speed, the tests were repeated on the test track a minimum of 10 times in order to assess the repeatability of the system performance. (Note that some sensor sets were evaluated based on simulated runs conducted post-hoc.) The collected data was structured such that it could be replayed through a software simulation of the sensing system. This allowed the system performance to be analyzed for different sensor combinations without the added time and expense of running additional track tests. For example, two sets of test track data for Vehicle E were used to simulate the data for two additional sensor combinations, resulting in a total of four sensor combination. A summary of the track test results from the LVS scenario is provided in Figure 35.

For each set of runs, this diagram shows the average speed reduction in m/s and the corresponding standard deviations. The speed reduction scale is located on the left. The lower part of the diagram also displays the percent of brake / no brake activations. The x-axis provides information about the test vehicle used for the tests, the test vehicle and target system initial test speeds, the sensing system tested, TTC and system deceleration settings. This explanation applies to all track and simulation result diagrams remaining in Appendix L.

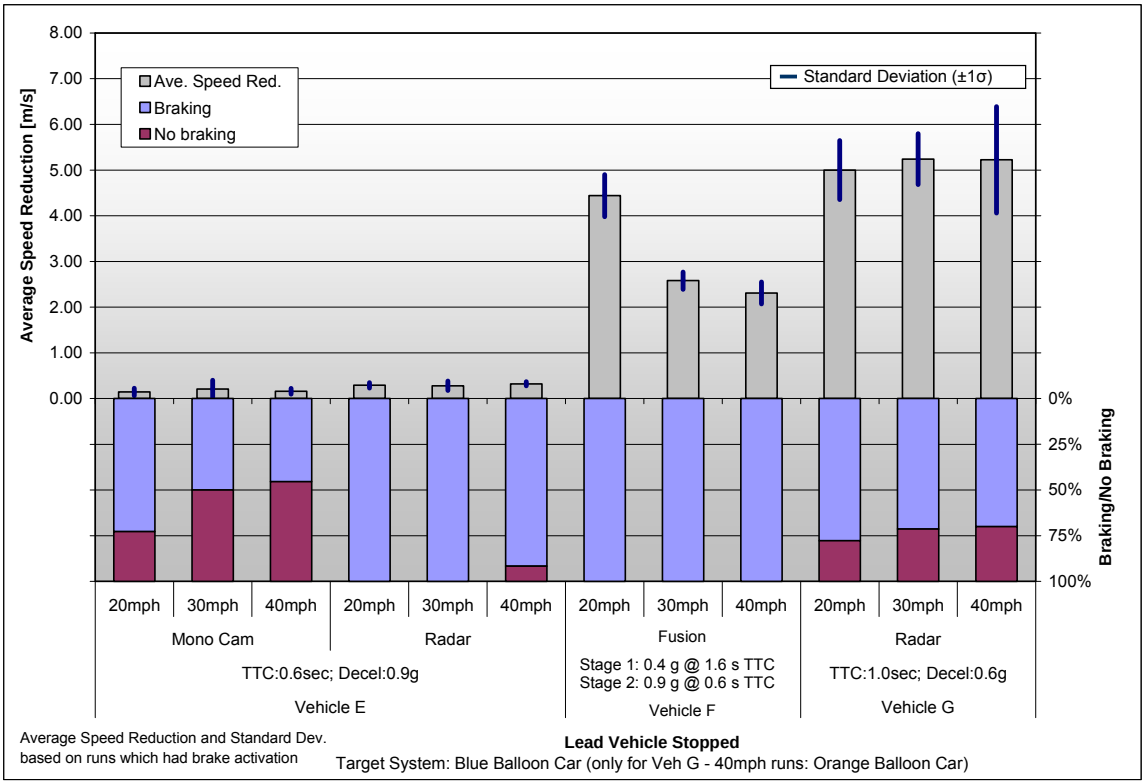

Figure 35: All Test Track Results for LVS Scenario

As shown in Figure 35, all three vehicles achieved brake activations in the LVS scenario. Vehicle F, equipped with the Fusion system, exhibited brake activations in all runs and less significant speed reduction measurements for higher initial speed approach scenarios. Vehicles E and G exhibited some runs without braking system activations. When compared to the other vehicles, Vehicle E achieved very low levels of speed reduction, which is expected due to the low TTC setting (which did not allow an early and strong brake application). This was also the case for both the Radar and the Mono-Vision systems on Vehicle E, but the Vision system had less CIB activations. The Radar system in Vehicle G delivered the highest speed reductions but the CIB system did not activate in approximately 25% of the runs.

L.1.5.2.1 Vehicle E

More detailed representations of the Vehicle E test performance is provided below in Table 11. Each row in the table displays the speed reduction value across each of the individual tests (or runs). The asterisks (*) appearing in the table are used to display CIB non-activations and a grey highlighted cell means there was no such run conducted. It should be stressed that average and standard deviation speed reductions calculations are based on runs which exhibited CIB system brake activations.

Table 11: Detailed Lists of Results for Vehicle E in LVS Scenario

Scenario: LVS; Target System: Blue Balloon Car; Vehicle E; Settings: TTC: 0.6sec; Decel: 0.9g																
			Speed reduction in m/s													Standard Dev in m/s
Test Vehicle Speed	Track/ Simulation	Sensor Config	Run 1	Run 2	Run 3	Run 4	Run 5	Run 6	Run 7	Run 8	Run 9	Run 10	Run 11	Run 12	Average	
20mph	TRK	Mono Cam	0.25	0.19	*	0.07	0.09	0.13	*	0.04	0.13	0.26	*		0.14	0.08
		Radar	0.42	0.30	0.24	0.36	0.26	0.23	0.29	0.30	0.24	0.27			0.29	0.06
	SIM	Fusion	*	0.30	0.24	0.36	0.26	0.23	0.29	0.30	0.24	0.27			0.28	0.04
30mph	TRK	Mono Cam	0.16	0.59	0.09	*	*	*	*	*	*	0.18	0.14	0.10	0.21	0.19
		Radar	0.20	0.27	0.20	0.26	0.24	0.24	0.47	0.43	0.35	0.16			0.28	0.10
	SIM	Fusion	0.20	0.27	0.20	0.26	0.24	0.24	0.47	0.43	0.35	0.16			0.28	0.10
40mph	TRK	Mono Cam	*	*	0.17	0.06	0.15	0.22	*	*	0.20	*	*		0.16	0.06
		Radar	0.37	0.25	*	0.32	0.32	0.33	0.29	0.41	0.28	0.33	0.29	0.36	0.32	0.05
	SIM	Fusion	0.37	0.25	*	0.32	0.32	0.33	0.29	0.41	0.28	0.33	0.29	0.36	0.32	0.05

Average and Standard Deviation based on runs which had brake activation
* = no brake activation
grey cell = no run

The Mono-Vision and Radar runs were tested on the track, whereas the Fusion results were later simulated based on these runs. As mentioned above, the "aggressive" TTC and deceleration settings associated with Vehicle E limited overall CIB system performance. As shown in Figure 36, approximately 44% of the runs with Mono-Vision system exhibited brake activations while approximately 97% of the Radar runs yielded brake activation. The radar sensor detected, typically tracked and analyzed the target before the Vision system. This resulted in more brake activations and higher speed reductions. Furthermore, comparison of the results from runs of different initial speeds displays a decreasing percentage of brake activations with increased initial speeds for the Mono-Vision system evaluated.

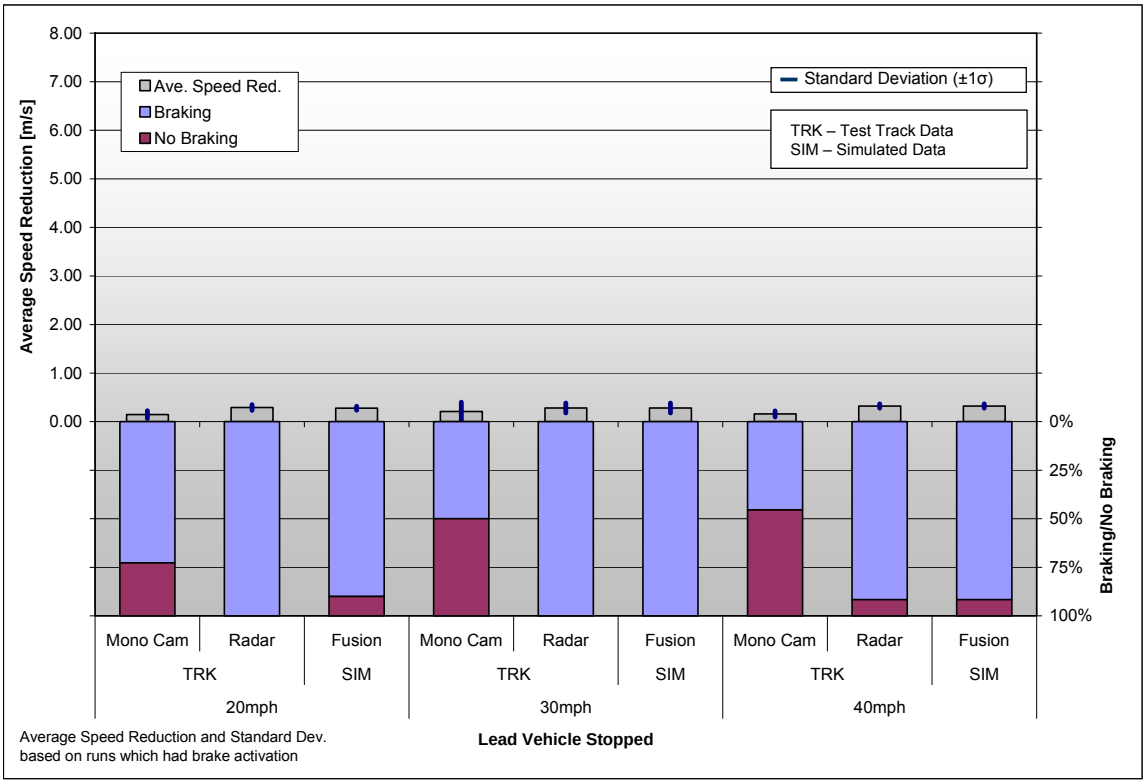

Figure 36: All Speed Reductions for LVS Runs for Vehicle E

L.1.5.2.2 Vehicle F

Unlike like the other vehicles tested that post-processed the Fusion system results, Vehicle F was tested with a fusion algorithm running during the test track runs. Additionally, unlike like the other vehicles tested, this test vehicle is equipped with a two-stage braking system. The two-stage braking system refers to a system with a 0.4 g deceleration applied at 1.6 second TTC followed by a 0.9 g deceleration applied at 0.6 second TTC, depending on the duration of the event. This test series resulted in Stage 1 activations for all 20 mph runs; Stage 2 activations for all 30 mph runs; and a mix of both braking stages at the 40 mph initial test speed conditions (see Figure 37).

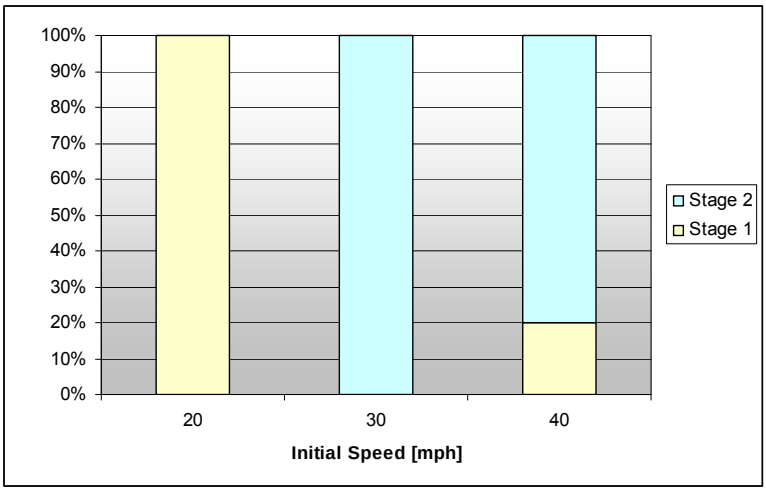

Figure 37: Stage 1 vs. Stage 2 Braking of Vehicle F in LVS Scenario

Hence, all vehicle test runs resulted in CIB activations. As shown in Figure 38, the largest speed reductions occurred at the lowest test speed. Overall, as shown in Table 12, results were very consistent across runs at a given test speed as indicated by the small standard deviation.

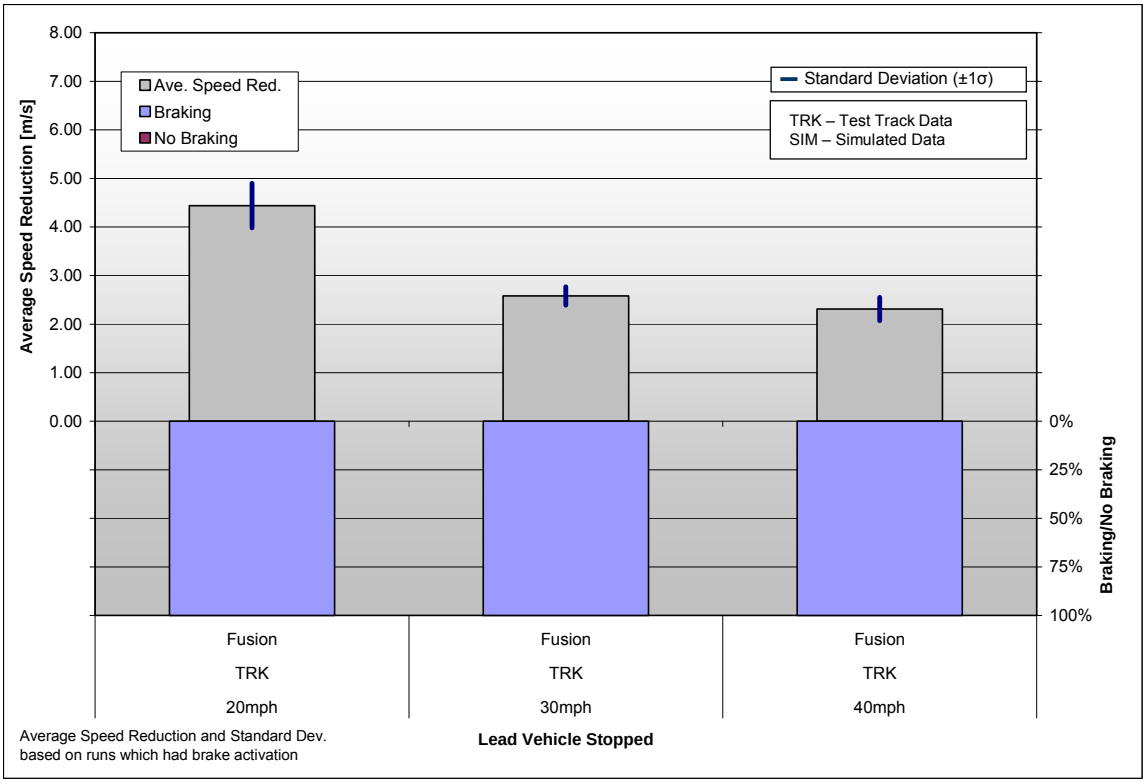

Figure 38: Vehicle F Speed Reductions and Distribution of Braking vs. No Braking for LVS

Table 12: Detailed Lists of Results for Vehicle F in LVS Scenario

Scenario: LVS; Target System: Blue Balloon Car; Vehicle F; Settings: TTC: 1.6sec; Decel: 0.4/0.9g														
			Speed reduction in m/s											Standard Dev in m/s
Test Vehicle Speed	Track/ Simulation	Sensor Config	Run 1	Run 2	Run 3	Run 4	Run 5	Run 6	Run 7	Run 8	Run 9	Run 10	Average	
20mph	TRK	Fusion	4.36	5.02	4.21	4.92	4.08	4.77	3.89	3.71	4.57	4.83	4.44	0.46
30mph	TRK	Fusion	2.56	2.63	2.76	2.63	2.41	2.41	2.62	2.98	2.31	2.49	2.58	0.19
40mph	TRK	Fusion	2.40	2.22	2.73	2.40	2.47	1.93	2.31	2.46	2.16	1.97	2.31	0.24

Average and Standard Deviation based on runs which had brake activation

L.1.5.2.3 Vehicle G

For the track tests conducted with Vehicle G in the LVS scenarios, the braking activations were based on radar sensor information. CIB Performance on the "vision only" and the Fusion systems were simulated via post-processing.

As shown in Figure 39, across all CIB system configurations and test speed conditions, the Vehicle G CIB system provided very similar average speed reductions (about 5 m/s) and CIB activation performance (about 75% activation). The speed reductions shown for the simulated Mono-Vision and Fusion cases (labeled "TRK" in Table 13) are solely based on performance observed on the radar runs.

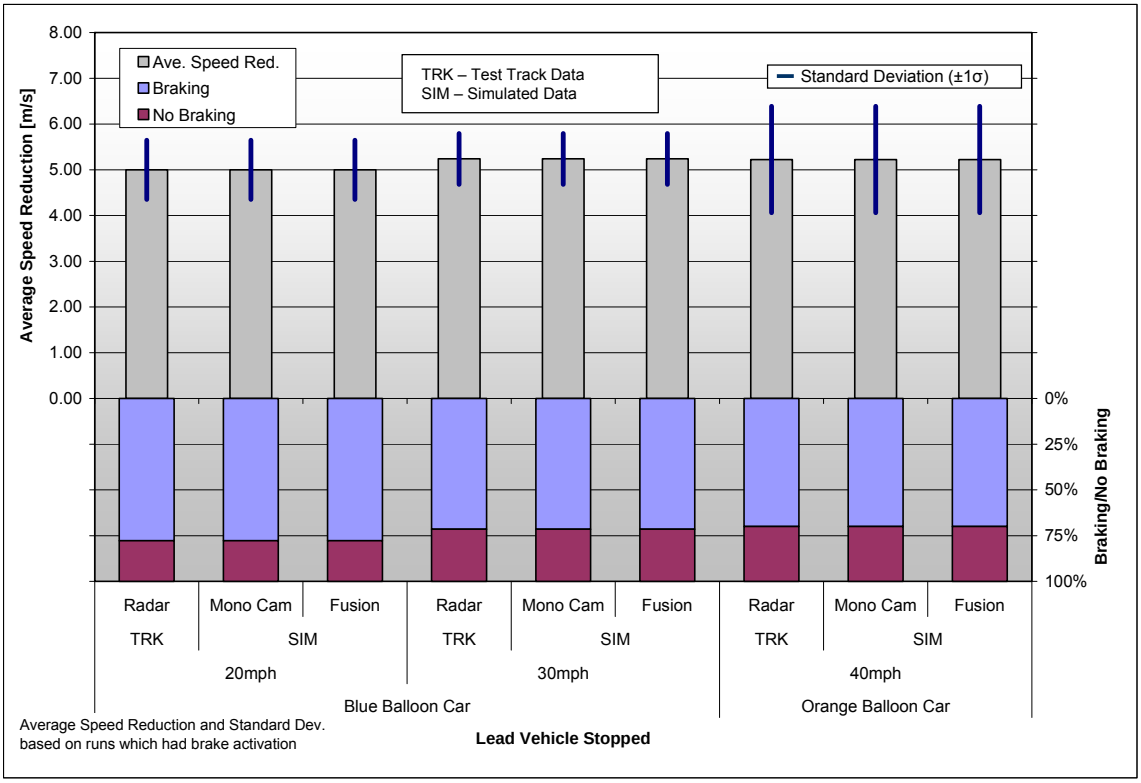

Figure 39: Vehicle G Speed Reductions for LVS Runs

Table 13: Detailed Lists of Results for Vehicle G in LVS Scenario

Scenario: LVS; Vehicle G; Settings: TTC: 1.0sec; Decel: 0.6g

				Speed reduction in m/s											Standard Dev in m/s
Target System	Test Vehicle Speed	Track/ Simulation	Sensor Config	Run 1	Run 2	Run 3	Run 4	Run 5	Run 6	Run 7	Run 8	Run 9	Run 10	Average	
Blue Balloon Car	20mph	TRK	Radar	4.57	5.13	5.07	5.06	6.06	*	3.93	5.18	*		5.00	0.65
		SIM	Mono Cam	4.57	5.13	5.07	5.06	6.06	*	3.93	5.18	*		5.00	0.65
			Fusion	4.57	5.13	5.07	5.06	6.06	*	3.93	5.18	*		5.00	0.65
	30mph	TRK	Radar	6.06	4.88	4.75	*	5.56	4.94	*				5.24	0.56
		SIM	Mono Cam	6.06	4.88	4.75	*	5.56	4.94	*				5.24	0.56
			Fusion	6.06	4.88	4.75	*	5.56	4.94	*				5.24	0.56
Orange Balloon Car	40mph	TRK	Radar	4.32	*	5.88	6.00	4.87	5.56	6.69	*	*	3.25	5.22	1.16
		SIM	Mono Cam	4.32	*	5.88	6.00	4.87	5.56	6.69	*	*	3.25	5.22	1.16
			Fusion	4.32	*	5.88	6.00	4.87	5.56	6.69	*	*	3.25	5.22	1.16

Average and Standard Deviation based on runs which had brake activation
* = no brake activation
grey cell = no run

L.2 Rear-End – Lead Vehicle Moving (LVM)

L.2.1 Test Method

Depending on the target system used, the target must be driven, pulled by a tow vehicle or pulled with a winch with a constant speed of 20 mph. The total length of the track should be 450 m to 500 m. The starting distance between the target system and subject vehicle depends on the initial test speed of the test vehicle (see Table 14). The target system should be kept in the center of lane while it is moving. The distance between the middle of the obstacle and the center of the lane should not exceed 0.5 m. The test vehicle and target system should reach and stabilize their speeds before the distance between them is smaller than 100 m. The system vehicle is driven at different test speeds (Table 14) straight to the target system with constant speed. Changes in accelerator pedal position should be avoided in the last 100 m before hitting the target system to reduce test speed variation. Steering corrections should be limited and smooth in order to hit the target system centrally. The distance between the middle of the vehicle and the center of the target system should not be higher than 0.5 m. The test ends 5 m after the test vehicle strikes the target system. For a successful test, the brake pedal should not be applied by the driver until the target system is passed. The operator/driver of the target system must maintain a constant target speed until the impact has occurred.

Table 14: Velocities for Lead Vehicle Moving Scenarios

Velocities	In mph	In km/h
System Vehicle	40	64.4
	45	72.4
	50	80.5
	60	96.6
Target Speed	20	32.2

L.2.2 Detailed Results from Baseline Test Phase

In this scenario four target systems were used, as shown in Table 15. Five test runs were conducted at each of three different initial vehicle speeds for all four target systems. Initial speeds for the test vehicles included 40, 50 and 60 mph. In all cases, the target system was moved with 20 mph, resulting in relative speed differences of 20, 30 and 40 mph, respectively.

Table 15: Target Systems for Lead Vehicle Moving Scenario

Short name	LVM1	LVM2	LVM3	LVM4
Target System	Hanging Target	Crash Simulator	Balloon Car Carrier	Towed Balloon Car
Picture				

The system performance of the three test vehicles was comparable in this scenario. All three vehicles showed fairly constant TTC at brake activations over increasing initial test speeds. That means the range to the target at which brake activation begins increases with higher test speeds in order to maintain the evaluated constant TTC approach. The difference in the achieved speed reductions is caused by the different system parameters of each CIB system. The activation rate of all CIB systems was higher than the results obtained in the LVS runs with the same target systems (see Table 16). This indicates that moving obstacles are easier to verify for these CIB systems.

Table 16: Comparison of Brake Activations for LVM and LVS of Hanging Target

Target	Scenario	Vehicle	Runs with braking	Runs without braking	Total
Hanging Target	LVM	A	11	1	12
		B	5	0	5
		C	10	2	12
	LVM Total		26	3	29
	LVS	A	0	7	7
		B	11	0	11
		C	9	2	11
	LVS Total		20	9	29

As shown in Figure 40, target systems LVM2 and LVM3 worked well for the CIB systems. Compared to target LVM1, they delivered much higher speed reductions on a constant level (lower standard deviations). Especially at higher initial test speeds, the brake performances of the vehicles decreased with target LVM1, as shown in Figure 40. This is caused by a later recognition of the target with LVM1 compared to LVM2 and LVM3.

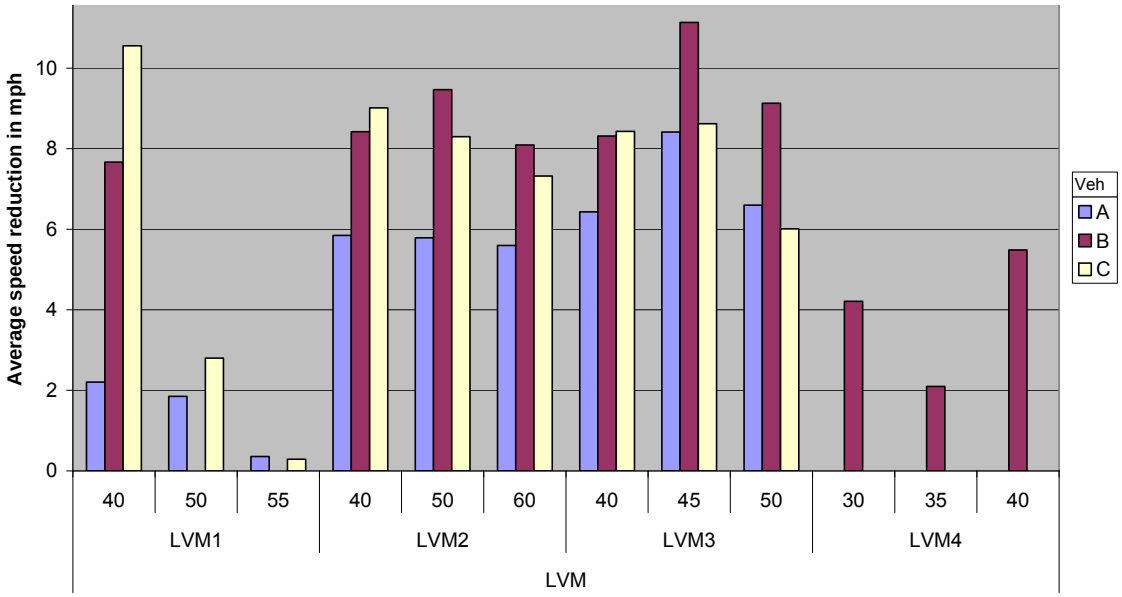

Initial speeds of target vehicle in mph for different targets. Lead target system travelled at 20 mph.

Figure 40: Comparison of Speed Reductions for All Vehicles and Initial Test Speeds with Different Target Systems

LVM4, a towed balloon car, was only used for tests with one vehicle in this test phase. This preliminary data was collected for further development of this test scenario with a target conveyance system. This pulled balloon car showed comparable results for TTC with LVM1, LVM2 and LVM3. However, speed reduction and range at brake initiation were lower than LVM2 and LVM3 levels.

L.2.3 Detailed Results from PIP Vehicle Test Phase

LVM testing was conducted with only one target for the PIP series of testing. For these tests, the LVM3 target (balloon car carrier) was employed. This target was also used for the baseline testing. The newly developed target tow system was unavailable for the PIP testing because it was not yet sufficiently developed at the time of these tests. PIP Vehicle E was also not available for these tests due to a data acquisition system component failure. Equipment availability limitations prevented a re-scheduling of these tests with Vehicle E once repairs were completed. Therefore, tests were conducted only with the Vehicle F and G.

Overall, both PIP vehicles had some issues recognizing the balloon target below the carrier boom. This was apparently caused by the lower radar reflection from the balloon target compared to the carrier vehicle and boom from which the target was suspended. To improve the radar reflectivity, a reflective tarp was added to the Balloon, as shown in Figure 41. For Vehicle F testing, an additional paper corner reflector was added in the lower area of the balloon target.

Figure 41: Balloon Car Carrier with Additional Radar Reflective Parts

L.2.3.1 Vehicle E

Vehicle E not available for these tests due to a data acquisition system component failure. Equipment availability limitations prevented a re-scheduling of these tests with Vehicle E once repairs were completed.

L.2.3.2 Vehicle F

The Vehicle F was able to brake in a consistent way with the Balloon Car Carrier as a target after adding additional radar reflective material to the rear end of the balloon car. As shown in Table 17, the speed reduction is in a narrow band. Also, the TTC at initiation of braking was very consistent at about 1.1 seconds as an overall average.

Table 17: Vehicle F Results for Lead Vehicle Moving

Scenario: LVM; Target System: Balloon Car Carrier; Vehicle F; Settings: TTC: 1.6sec; Decel: 0.4/0.9g										
				Speed reduction in m/s						Standard Dev in m/s
Target speed	Test Vehicle Speed	Track/ Simulation	Sensor Config	Run 1	Run 2	Run 3	Run 4	Run 5	Average	
20mph	40mph	TRK	Fusion	4.16	4.26	4.48	4.94	4.85	4.54	0.35
	50mph	TRK	Fusion	4.77	5.18	4.83	4.77	4.29	4.77	0.32

Average and Standard Deviation based on runs which had brake activation

L.2.3.3 Vehicle G

Vehicle G was tested with constant TTC setting of 1 second while vehicle deceleration settings of 0.3 g and 0.8 g were used. The results are summarized in Table 18. Tests with an initial speed of 40 mph (closing speed of 20 mph) resulted in lower speed reductions than runs with the higher speed of 50 mph (closing speed of 30 mph). A deceleration setting of 0.8 g had consistently higher speed reductions at the 50 mph runs.

Table 18: Vehicle G Results for Lead Vehicle Moving

Scenario: LVM; Target System: Balloon Car Carrier; Vehicle G												
						Speed reduction in m/s						Standard Dev in m/s
Target speed	Test Vehicle Speed	TTC Setting	Decel Settings	Track/ Simulation	Sensor Config	Run 1	Run 2	Run 3	Run 4	Run 5	Average	
20mph	40mph	1.0sec	0.3g	TRK	Fusion	*	2.58	1.83	2.89	1.75	2.26	0.56
			0.8g	TRK	Fusion	*	0.18				0.18	-
	50mph	1.0sec	0.3g	TRK	Fusion	2.04	2.28	3.08	2.71	2.14	2.45	0.44
			0.8g	TRK	Fusion	8.99	6.03	5.00	3.77	5.59	5.88	1.94

Average and Standard Deviation based on runs which had brake activation
* = no brake activation
grey cell = no run

L.2.3.4 Assessment/Evaluation of Vehicle Test Method, Targets and/or Equipment

This test scenario overall was well understood by the test participants based on past CIB system development. Further development was needed for the tow system intended for use in the validation tests, which will use common balloon car targets that are well correlated to surrogate vehicles. As with the LVS test methodology, it is desirable to incorporate the radar reflective material characteristics added to these targets into the internal structure of future balloon cars to ensure a repeatable off-the-shelf target solution.

L.2.4 Validation Test Phase

L.2.4.1 Test Method

For the Lead Vehicle Moving (LVM) scenario, a target tow system was developed to provide controlled target movement (see Appendix G). Detailed test procedures and specific target tow system adaptations for the LVM Scenario were also developed.

The LVM tests were performed using one lane of the test track and the same balloon cars used in the LVS test scenario (see Figure 33 and Figure 34). The balloon car was accelerated and moved on a stable ground sheet (see Figure 42). This ground sheet was connected to a rope which was connected to the target towing system. The rope was looped through the pulleys and tensioned such that the target could be pulled by the motor head during each test run and then easily reset to the original position after each test. A steel cable was tensioned between two anchored base plates on each side of the test lane. The balloon car was placed on the ground sheet which was connected to cables via polyvinyl chloride (PVC) plastic guidance pipes (see Figure 43). Each steel cable was threaded through the center of a pipe so that the straight movement of the target was possible even under substantial cross-wind situations.

To conduct a LVM test run, the driver of the test vehicle waits at the starting position at the far end of a test track. When the operator of the towing system is ready to initiate a test, the test driver accelerates to the defined initial test speed. After the test vehicle

passes a specified point on the track, the towing system begins accelerating the balloon car target to its initial test speed. Both the test vehicle and the balloon car move at their defined test speeds until the test vehicle strikes the balloon car, which may or may not be preceded by a brake activation.

To prevent balloon car and test vehicle damage, the balloon car must be able to break away from the towing system at the moment of impact. This is achieved by attaching the balloon car to the ground sheet and the tow ropes via breakable mechanical "fuses."

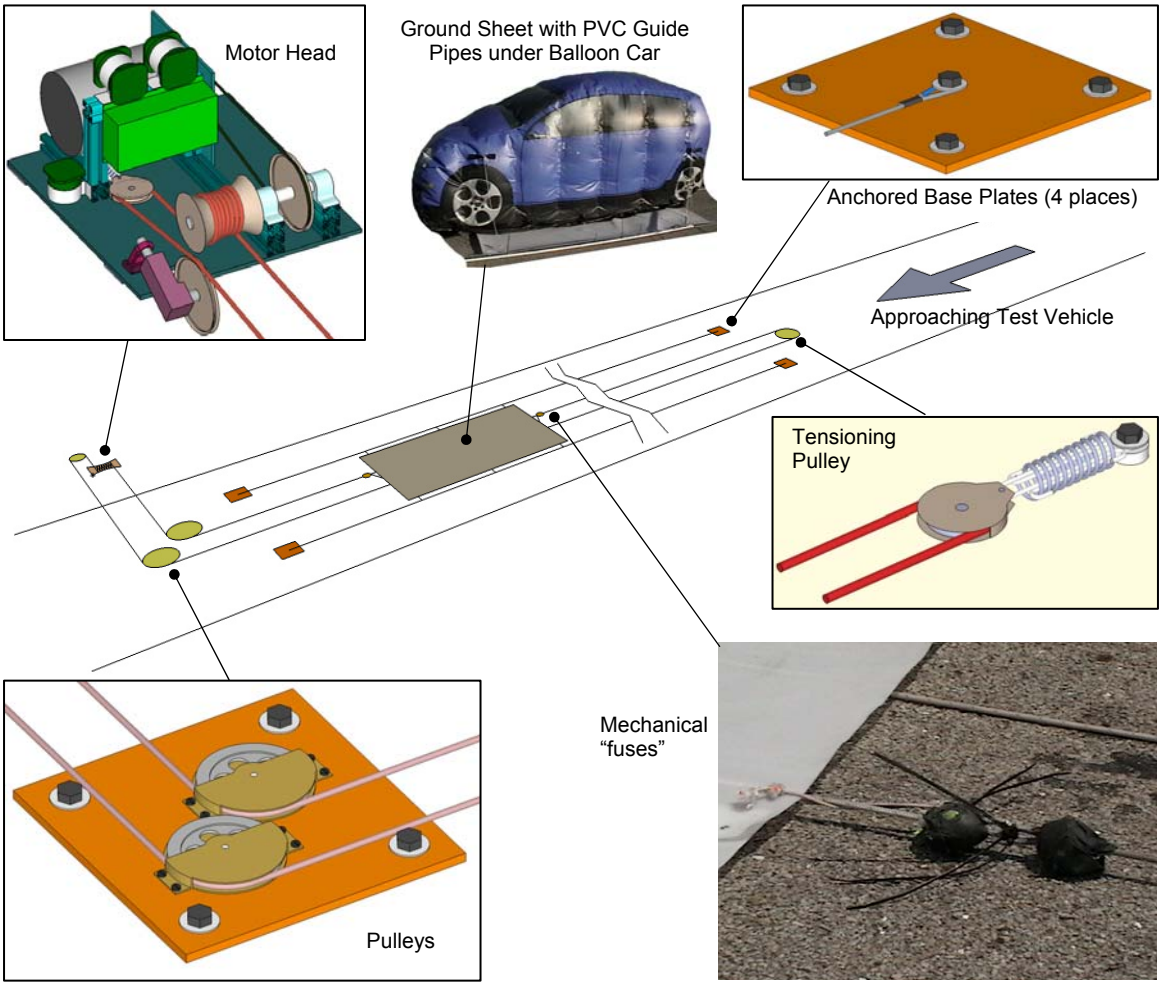

Figure 42: Lead Vehicle Moving Setup

Figure 43: 3rd-Generation Balloon Car with PVC Guide Tubes and Ground Sheet

L.2.4.2 Detailed Results from Validation Test Phase

The results from the LVM scenario (see Figure 44) are comparable to those found with the LVS scenario. Once again, due to the "aggressive" TTC and deceleration settings, Vehicle E showed very small speed reduction values in this test scenario and in the Mono-Vision only condition, braking activations often did not occur. Relative to the LVS results, Vehicle F and Vehicle G had similar speed reduction values. Vehicle F had about a 6 m/s speed reduction across all tests, whereas Vehicle G provided the single highest speed reduction in a test where a 40 mph vehicle approached the target moving at 20 mph. Relative to the LVS scenario, results were more variable in the LVM scenario owing to the additional variation caused by the movement of the balloon car and the sensing of this movement. For all vehicles, this resulted in a wider variance of the measured speed reductions for a given test run set.

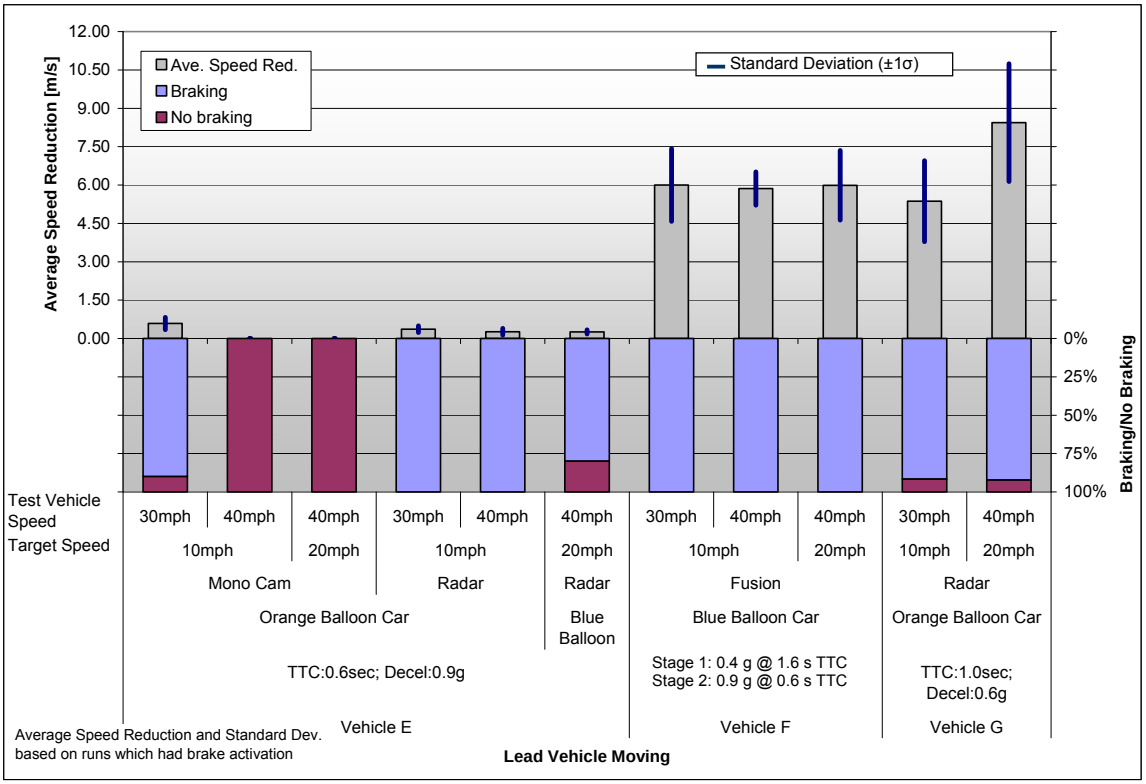

Figure 44: All Track Test Results for LVM Scenario

L.2.4.3 Vehicle E

For Vehicle E, the earlier LVM tests used the 2nd-generation balloon car. When the 3rd-generation balloon car became available, this target was used exclusively due to the improvements in target durability. The breakdown of which target was used across each test is shown in Table 19. Results from these vehicle tests (see Figure 45 and Table 19) again show that using an "aggressive" TTC and decelerations setting (0.6 sec and 0.9 g, respectively) does not allow sufficient time for substantive speed reductions. In addition, many Mono-Vision system runs ended without brake activations even when the systems triggered a brake activation. Only in the 30 mph test vehicle / 10 mph target speed combination was this system able to provide a brake signal in sufficient time to achieve speed reductions.

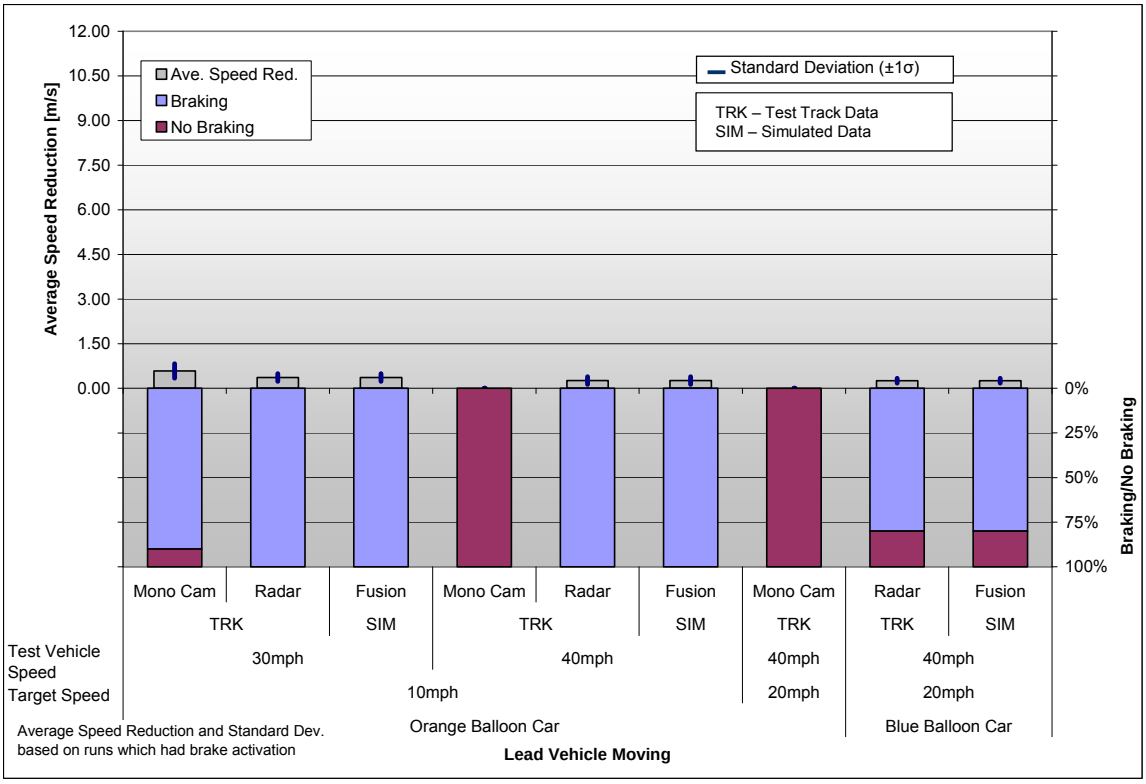

Figure 45: All Speed Reductions for Vehicle E LVM Runs, including Simulation Results

Table 19: Detailed Lists of Results for Vehicle E in LVM Scenario

Scenario: LVM; Target Systems: Blue/Orange Balloon Car; Vehicle E; Settings: TTC: 0.6sec; Decel: 0.9g																	
					Speed reduction in m/s												Standard Dev in m/s
Target System	Target speed	Test Vehicle Speed	Track/ Simulation	Sensor Config	Run 1	Run 2	Run 3	Run 4	Run 5	Run 6	Run 7	Run 8	Run 9	Run 10	Run 11	Average	
Orange Balloon Car	10mph	30mph	TRK	Mono Cam	0.68	*	0.48	0.51	0.58	0.28	0.86	0.59	1.01	0.28		0.59	0.24
				Radar	0.48	0.45	0.53	0.40	0.45	0.38	0.13	0.23	0.18	0.31	0.45	0.36	0.13
			SIM	Fusion	0.48	0.45	0.53	0.40	0.45	0.38	0.13	0.23	0.18	0.31	0.45	0.36	0.13
		40mph	TRK	Mono Cam	*	*	*	*	*	*	*	*	*	*	*	-	-
				Radar	0.21	0.14	0.58	0.26	0.29	0.15	0.27	0.26	0.19			0.26	0.13
			SIM	Fusion	0.21	0.14	0.58	0.26	0.29	0.15	0.27	0.26	0.19			0.26	0.13
	20mph	40mph	TRK	Mono Cam	*	*	*	*	*	*	*	*	*	*		-	-
Blue Balloon Car	20mph	40mph	TRK	Radar	0.27	0.31	0.31	0.14	*							0.26	0.08
			SIM	Fusion	0.27	0.31	0.31	0.14	*							0.26	0.08

Average and Standard Deviation based on runs which had brake activation
* = no brake activation
grey cell = no run

L.2.4.4 Vehicle F

Average speed reductions for the Vehicle F Radar Fusion system (about 6 m/sec) are comparable across test sets (see Table 20 and Figure 46). As mentioned earlier, the variance in the target movement in this scenario may have contributed to standard deviations which were higher than in the corresponding LVS runs for Vehicle F. The distributions of Vehicle F Stage 1 and Stage 2 braking activations that occurred during LVM test runs are provided in Figure 47, which indicates Stage 1 activations only occurred in the 30/10 mph test vehicle/target speed combination.

Table 20: Detailed Lists of Results for Vehicle F in LVM Scenario

Scenario: LVM; Target System: Blue Balloon Car; Vehicle F; Settings: TTC: 1.6sec; Decel: 0.4/0.9g															
				Speed reduction in m/s											Standard Dev in m/s
Target speed	Test Vehicle Speed	Track/ Simulation	Sensor Config	Run 1	Run 2	Run 3	Run 4	Run 5	Run 6	Run 7	Run 8	Run 9	Run 10	Average	
10mph	30mph	TRK	Fusion	5.45	5.70	5.51	4.24	7.00	5.19	5.60	4.98	7.15	9.21	6.00	1.42
	40mph	TRK	Fusion	4.61	5.06	6.65	6.08	5.69	6.04	6.19	5.86	6.71	5.75	5.86	0.65
20mph	40mph	TRK	Fusion	5.95	5.62	3.92	3.25	6.84	7.21	6.61	6.75	6.92	6.85	5.99	1.36

Average and Standard Deviation based on runs which had brake activation

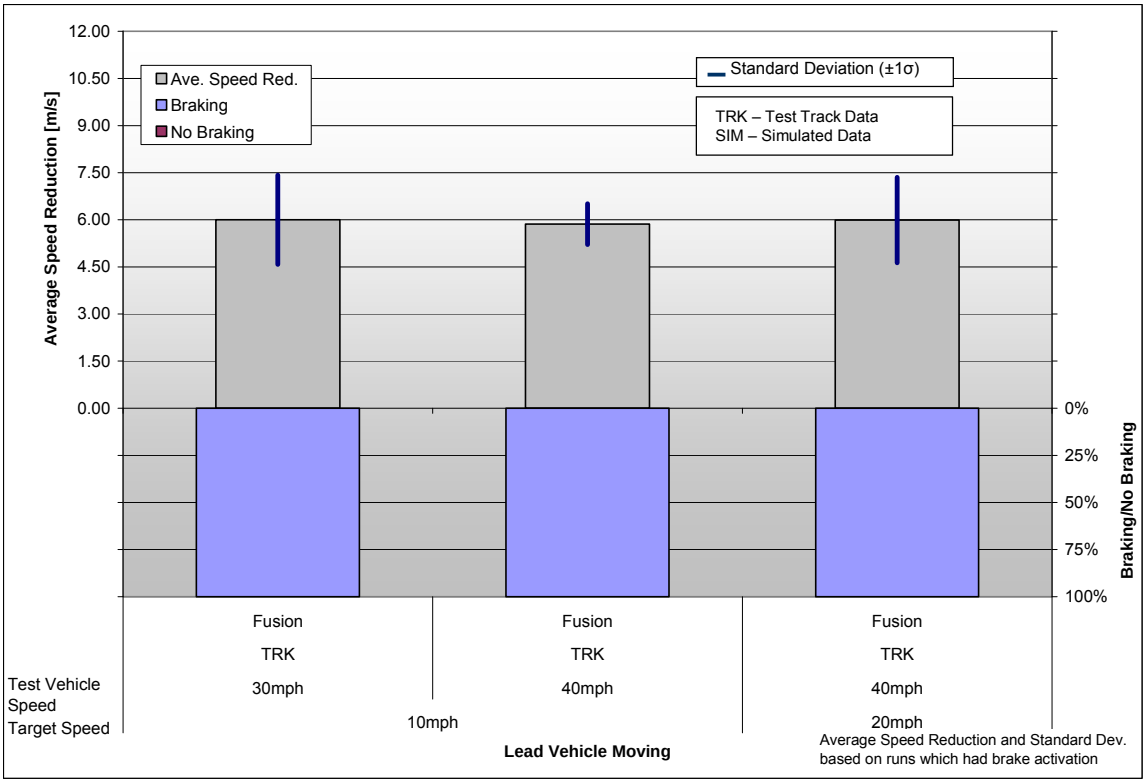

Figure 46: Speed Reductions for Vehicle F in LVM Runs

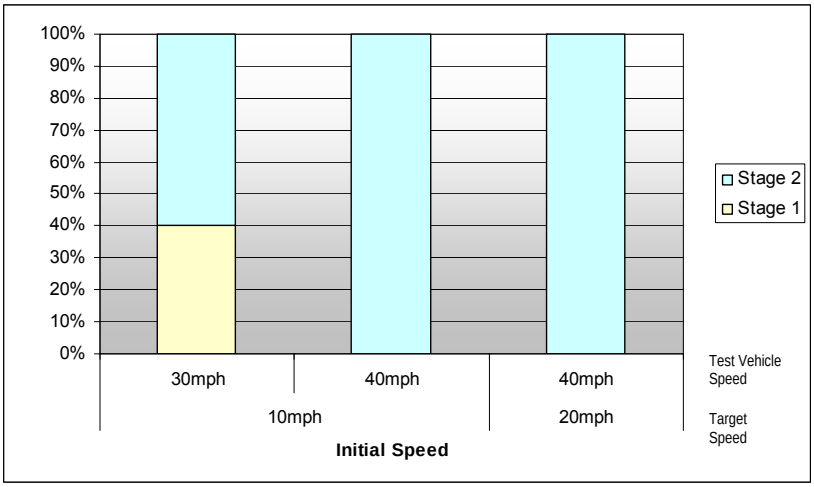

Figure 47: Stage 1 vs. Stage 2 Braking in Vehicle F LVM Scenario Runs

L.2.4.5 Vehicle G

Both of the LVM tests were conducted at an initial 20 mph speed difference between the target and the test vehicle. Overall, results indicated low variability within a test condition and overall 92% brake activations (see Table 21). Speed reduction values were also higher in the 40/20 mph relative to the 30/10 mph condition (see Figure 48). The simulated Fusion (65% activations) and Mono-Vision (85% activations) results showed fewer brake activations than the Radar runs (92% activations).

Table 21: Vehicle G in LVM Scenario Detailed Lists of Results

Scenario: LVM; Target System: Orange Balloon Car; Vehicle G; Settings: TTC: 1.0sec; Decel: 0.6g																		
				Speed reduction in m/s														Standard Dev in m/s
Target speed	Test Vehicle Speed	Track/ Simulation	Sensor Config	Run 1	Run 2	Run 3	Run 4	Run 5	Run 6	Run 7	Run 8	Run 9	Run 10	Run 11	Run 12	Run 13	Average	
10mph	30mph	TRK	Radar	*	3.06	6.94	3.56	6.25	5.13	6.13	7.00	6.12	2.56	6.43	5.87		5.37	1.58
		SIM	Mono Cam	*	3.06	6.94	3.56	6.25	5.13	6.13	7.00	6.12	2.56	6.43	5.87		5.37	1.58
			Fusion	*	3.06	6.94	3.56	6.25	5.13	6.13	*	*	*	*	*		5.18	1.57
20mph	40mph	TRK	Radar	5.55	6.13	7.56	6.81	*	7.62	9.00	9.81	7.25	7.19	9.15	12.82	12.38	8.44	2.30
		SIM	Mono Cam	*	6.13	7.56	6.81	*	7.62	9.00	9.81	7.25	7.19	*	12.82	12.38	8.66	2.33
			Fusion	*	6.13	7.56	6.81	*	7.62	9.00	9.81	7.25	7.19	*	12.82	12.38	8.66	2.33

Average and Standard Deviation based on runs which had brake activation
* = no brake activation
grey cell = no run

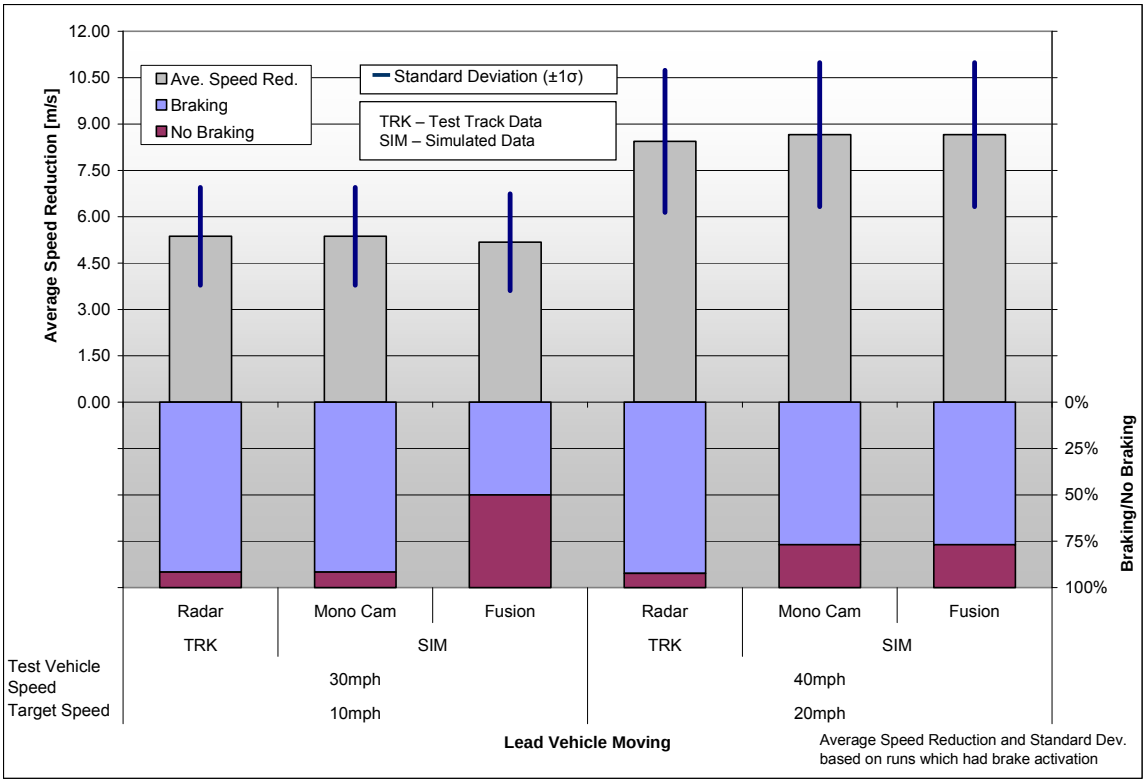

Figure 48: All Speed Reductions for LVM Runs, including Simulation Results, for Vehicle G

L.3 Rear-End – Lead Vehicle Decelerating (LVD)

L.3.1 Test Method

For development of Lead Vehicle Deceleration (LVD) scenario, a straight and flat test track with two lanes is needed. The total length of the track should be 450 m to 500 m. No obstacles should be present on either side of the lane used and in a distance within 15 m from the center of the lane, including vehicles, guardrails, poles, trees, man holes, etc. The track should be paved with concrete or asphalt to ensure repeatability of the conducted tests. The target system has to move with a constant speed in this scenario (until braking).

It is helpful to implement a procedure that allows the impact point with the target in the same area of the test track for every test. Using fixed starting points for the test vehicle and target system improves the test repeatability relative to the position of the impact point. New starting points are needed for the different test speeds to accommodate the changes in timing between target and test vehicle during the test.

To maintain a similar location for each impact the operator of the target system has to activate the brakes at a fixed point to achieve the deceleration of the target system.

The test vehicle and target system are each driven with a constant test speed, as indicated in Table 22 and Figure 49. The selection of the test speeds was based on a joint agreement with NHTSA to limit the test parameters for the LVD method after consideration of the capabilities of the employed testing set-up/approach, repeatablility and safety considerations. The selection of the test speeds is not critical as prior to the deceleration of the target, the relative speed between the test vehicle and the target is zero regardless of the initial speeds selected for testing. The driver of the test vehicle must maintain the initial lead distance between the vehicles at a defined range (Table 23). The target system should be kept in the center of lane while moving. The distance between middle of the obstacle and the center of the lane should not exceed 0.5 m. The test vehicle and target system should reach and stabilize their speeds as well as the distance between each other before the target system begins to decelerate (Table 24). Changes in accelerator pedal position should be avoided in the last 100 m before hitting the target system. Steering corrections should be limited and smooth in order to hit the target system centrally. The distance between the middle of the vehicle and the center of the target system should not be higher than 0.5 m. The test ends 5 m after the test vehicle strikes the target system. For a successful test, the brake pedal should not be applied by the driver until the target system is passed. The operator/driver of the target system must maintain a constant target speed until the impact has occurred.

Table 22: Velocities for Lead Vehicle Decelerating Scenarios

Velocities	In mph	In km/h
System vehicle	20	32.2
Target system	20	32.2

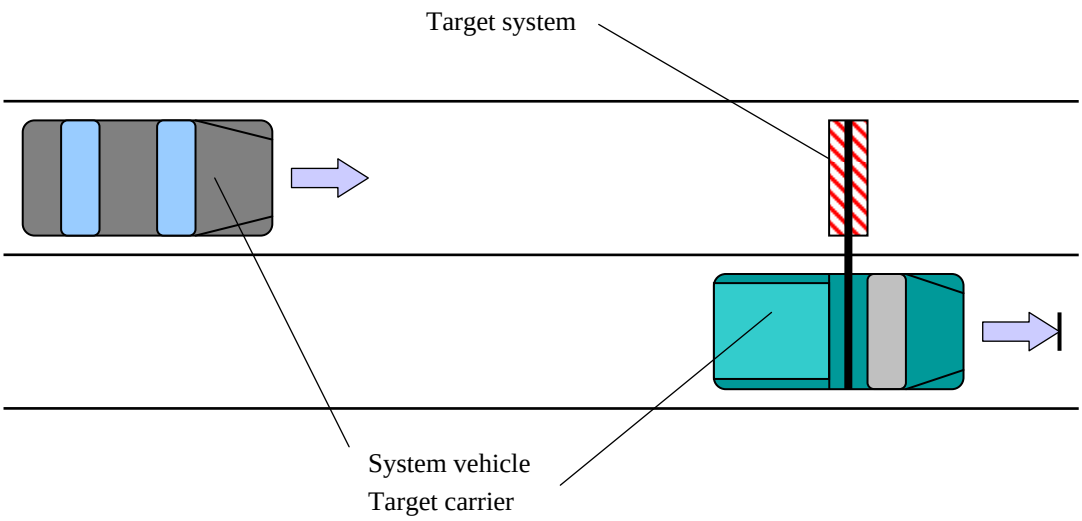

Figure 49: System Vehicle with an Additional Target Carrier Vehicle

Table 23: Following Distance between System Vehicle and Target System

Initial Range	In m	In sec
Distance 1	8.9	1.0
Distance 2	17.9	2.0

Table 24: Deceleration Rate for Target System

Desired Deceleration Levels m/s^2
3.0
6.0

As shown in Table 25, three target systems were used for this test scenario. These included the crash simulator, hanging target and balloon car carrier.

Table 25: Target Systems for Lead Vehicle Deceleration Scenario

Short name	LVD1	LVD2	LVD3
Target System	Hanging Target	Crash Simulator	Balloon Car Carrier
Picture			

L.3.2 Detailed Results from Baseline Vehicle Testing

Figure 50 shows a sample Lead Vehicle Deceleration run. The target vehicle begins to brake at 1.3 sec. The target system operator attempted to maintain the deceleration level to around 0.3 g. At 3.7 seconds, the test vehicle begins to brake. At the point of impact, around 4.9 seconds, the test vehicle has reduced its speed by 11.7 km/h.

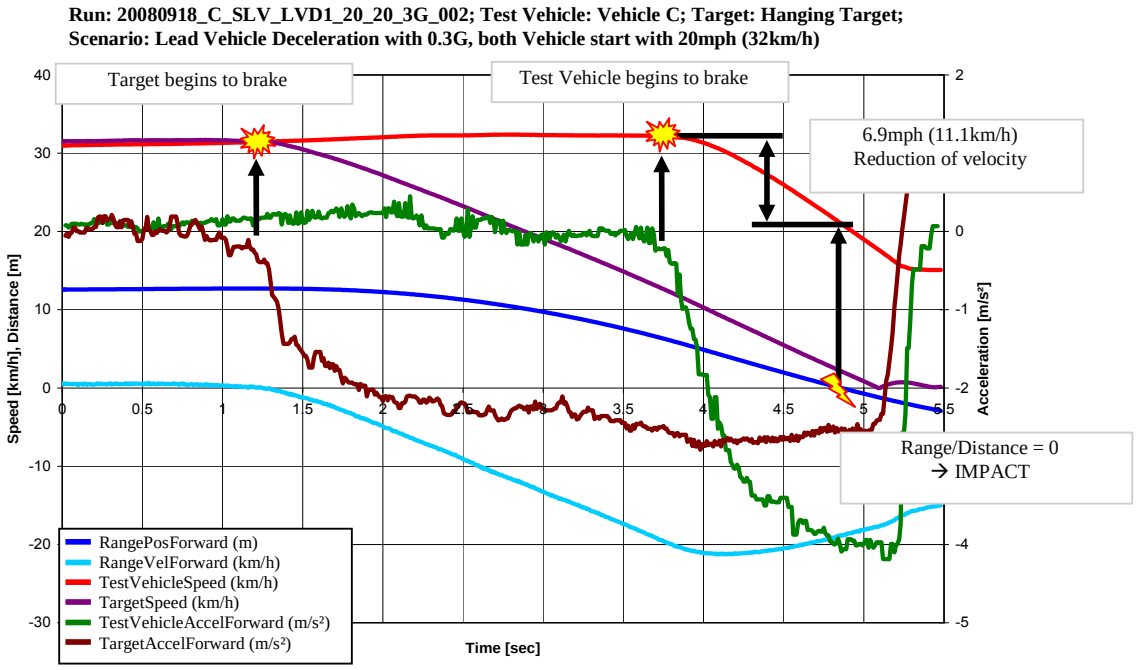

Figure 50: Sample Test Data from Lead Vehicle Deceleration Scenario

Overall, the results of the LVD runs show a higher standard deviation than the LVM and LVS runs. This is due to the following two reasons. First, the test parameters involved in of the lead vehicle decelerating test were challenging to control. Second, the vehicles' CIB systems need time to verify targets before activating the brakes. Lower following distance and higher deceleration rates of the lead vehicle make it harder for the systems to react in a timely manner. Based only on runs in which CIB activation resulted, as

shown in Figure 51, Vehicles A and C showed increased speed reductions with longer following distance.

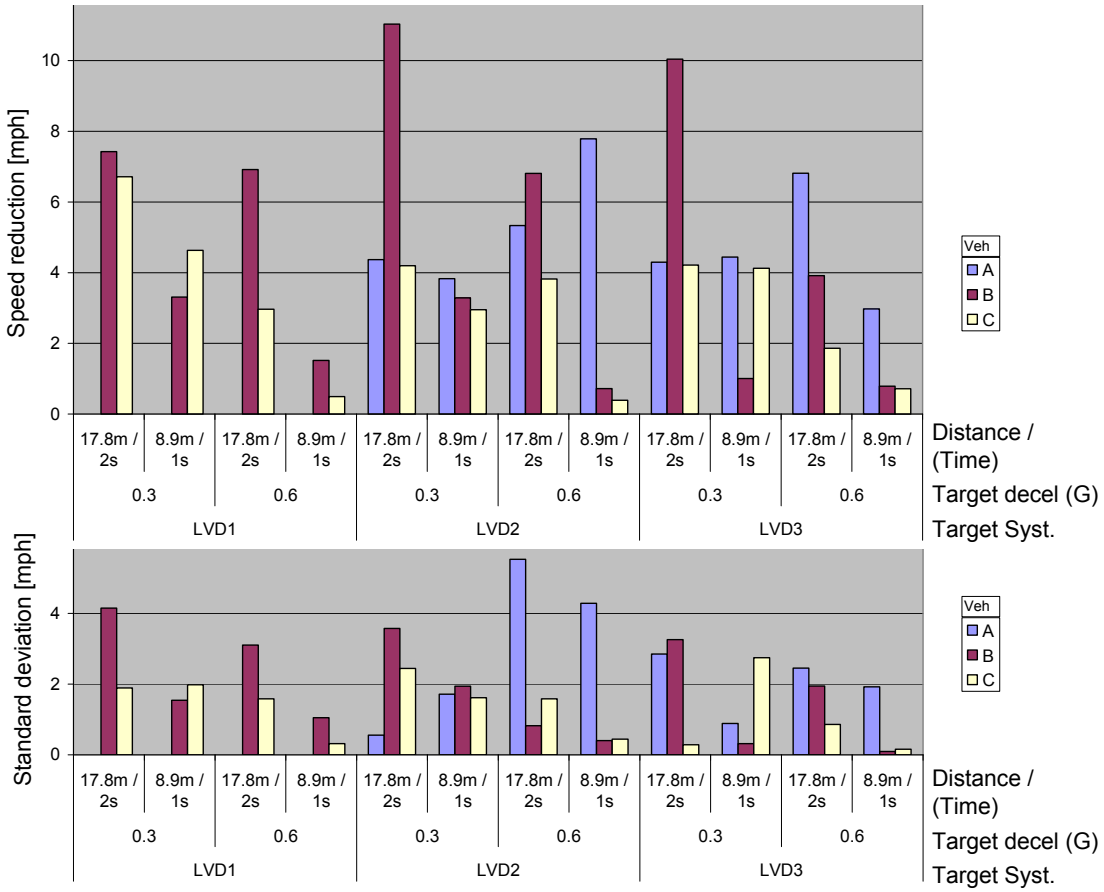

Figure 51: LVD Speed Reductions and Standard Deviations for All Test Vehicles

As shown in Figure 52, the most non activations were noted for runs with the lower lead time of 1 s.

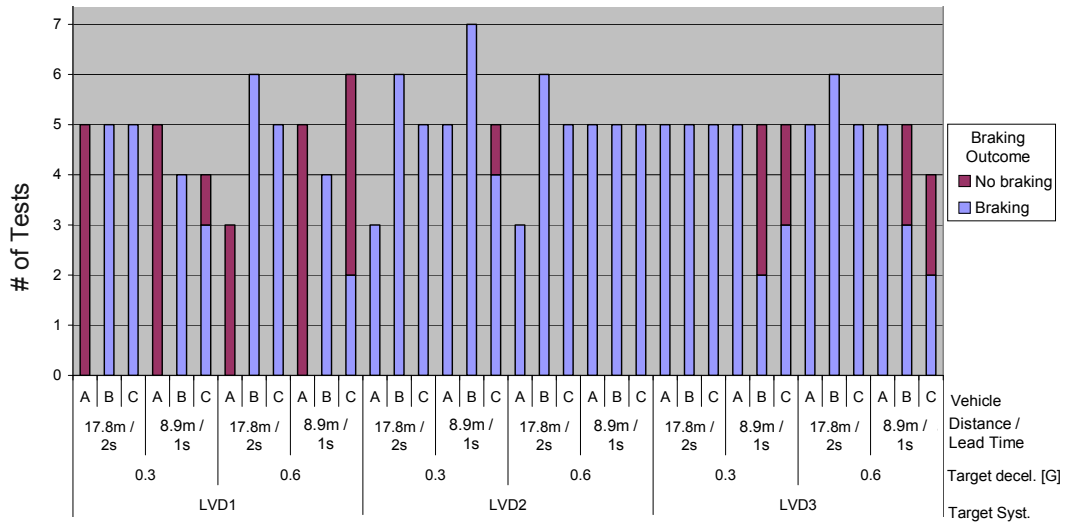

Figure 52: LVD Runs with and without Brake Activations

L.3.3 Detailed Results from PIP Vehicle Testing

LVD testing was conducted with the same balloon car carrier LVD3 used for the baseline testing since the tow system intended for this testing was not yet developed sufficiently at the time of these tests. The same radar-reflective components included in the LVM PIP vehicle tests were incorporated for the LVD tests. As with the LVM tests, Vehicle E was not available for these tests due to a data acquisition system component failure. Equipment availability limitations prevented a re-scheduling of these tests with Vehicle E once repairs were completed. Therefore, tests were conducted only with Vehicle F and G.

L.3.3.1 Vehicle F

Vehicle F test data (Table 26) shows lower speed reductions and three non-activations with a combination of the 1-second (8.9 m) following distance and 0.6 g target deceleration levels. When the initial following distance is extended from 8.9 meters to 17.8 meters, higher test vehicle speed reductions result. When the target system deceleration level is reduced from 0.6 g to 0.3 g, a higher speed reduction is achieved with both following distances. This condition also results in smaller standard deviations within the test data. Overall, however, the results for the Vehicle F vary significantly in all four combinations of LVD tests.

Table 26: Results for Vehicle F Lead Vehicle Deceleration Runs

Vehicle F		Host & Target Speed (mph)	Distance in m	Target decel in G	Speed reduction in mph						StdDev in mph
Test scenario	Target				Run 1	Run 2	Run 3	Run 4	Run 5	Average	
LVD	Balloon Car Carrier	20	8.9	0.3	3.15	1.19	5.19	2.91	4.76	3.44	1.60
				0.6	0.16	*	*	0.43	*	0.29	0.19
			17.8	0.3	6.58	5.19	9.80	7.40	7.36	7.27	1.68
				0.6	1.61	1.43	6.91	2.95	1.88	2.96	2.29

* = no braking

L.3.3.2 Vehicle G

The results shown in Table 27 indicate a high degree of variation in all four test sets. Higher speed reduction is noticeable in tests with the longer 2-second (17.8 m) lead time between the test vehicle and target system.

Table 27: LVD Speed Reductions and Standard Deviations for All Test Vehicles

Vehicle G					Host & Target Speed (mph)	Distance in m	Target decel in G	Speed reduction in mph						StdDev in mph
Test scenario	Target	TTC setting in sec	Decel setting in G	System				Run 1	Run 2	Run 3	Run 4	Run 5	Average	
LVD	Balloon Car Carrier	1	0.8	Fusion	20	8.9	0.3	2.06	2.59	2.91	3.04	2.51	2.62	0.38
							0.6	2.06	3.47	0.92	1.16	2.01	1.92	1.00
						17.8	0.3	6.33	6.69	4.50	0.63	4.14	4.46	2.41
							0.6	4.34	6.08	3.83	2.82	5.57	4.53	1.32

L.3.3.3 Assessment/Evaluation of Vehicle Test Method, Targets and/or Equipment

Overall, there were high variations in the results of all conducted tests (i.e., for both the production and PIP vehicles). With less distance and higher deceleration rates, there is not much time left for the CIB systems to verify the target and activate the brakes. By using a test setup that requires two drivers, additional issues are introduced regarding maintaining constant test parameters (initial speeds, initial distance and deceleration level of target system). These parameters become more controllable with the use of an automated target conveyance system in the validation tests.

L.3.4 Validation Test Phase

L.3.4.1 LVD Testing Method

The test setup for the Lead Vehicle Deceleration (LVD) scenario is identical to the arrangement used for the LVM scenario, except for one important difference. The tow system controller program had to be extended so that the balloon car would decelerate at a defined rate once it had been accelerated to the required initial target speed. For this set of tests, a time headway (or following time) of 2 seconds between the vehicle and the balloon car was chosen which equates to 17.8 m of separation for the initial test speed of 20 mph. After the defined separation distance and initial speeds were stabilized, the tow system decelerated the balloon car at a specified rate.

L.3.4.2 Detailed Results from Validation Test Phase

In these LVD tests, Vehicle F and Vehicle G exhibited high numbers of brake activations and higher speed reduction values than Vehicle E (see Figure 53).

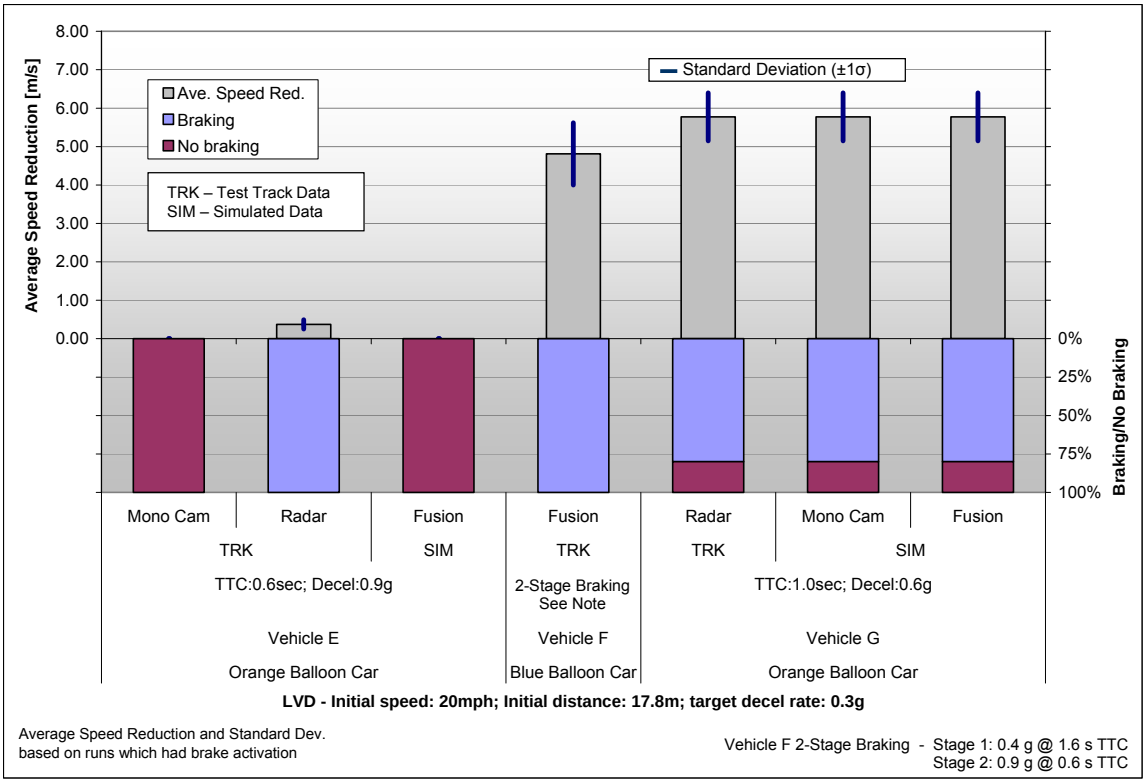

Figure 53: All Track Test and Simulation Results for LVD Scenario

L.3.4.3 Vehicle E

As shown in Table 28, for Vehicle E (employing the low TTC and high deceleration settings), no brake activations in either the Mono-Vision or Fusion runs were observed. Note the Fusion simulation does not have brake activations since the Vision system did not detect, track and analyze the target. In contrast, the Radar system triggered brake activations during all test runs and yielded consistently low speed reductions.

Table 28: Detailed Lists of Results for Vehicle E in LVD Scenario

Scenario: LVD; Target System: Orange Balloon Car; Vehicle E; Settings: TTC: 0.6sec; Decel: 0.9g																		
						Speed reduction in m/s												Standard Dev in m/s
Target speed	Test Vehicle Speed	Target decel	Distance	Track/ Simulation	Sensor Config	Run 1	Run 2	Run 3	Run 4	Run 5	Run 6	Run 7	Run 8	Run 9	Run 10	Run 11	Average	
20mph	20mph	0.3g	17.8m	TRK	Mono Cam	*	*	*	*	*	*	*	*	*	*	*	-	-
					Radar	0.42	0.33	0.51	0.23	0.54	0.23	0.28	0.52	0.29	0.38		0.37	0.12
				SIM	Fusion	*	*	*	*	*	*	*	*	*	*		-	-

Average and Standard Deviation based on runs which had brake activation
* = no brake activation
grey cell = no run

L.3.4.4 Vehicle F

As shown in Table 29, the Vehicle F Fusion-based system provided braking in all test runs. Only Stage 1 braking (of 0.4 g) was achieved in all of the tests run for the LVD scenario. In addition, the speed reduction values were consistent across these runs.

Table 29: Detailed Lists of Results for Vehicle F in LVD Scenario

Scenario: LVD; Target System: Blue Balloon Car; Vehicle F; Settings: TTC: 1.6sec; Decel: 0.4/0.9g																	
						Speed reduction in m/s											Standard Dev in m/s
Target speed	Test Vehicle Speed	Target decel	Distance	Track/ Simulation	Sensor Config	Run 1	Run 2	Run 3	Run 4	Run 5	Run 6	Run 7	Run 8	Run 9	Run 10	Average	
20mph	20mph	0.3g	17.8m	TRK	Fusion	5.44	3.86	5.75	5.43	4.92	4.46	4.76	4.54	3.26	5.67	4.81	0.81

Average and Standard Deviation based on runs which had brake activation

L.3.4.5 Vehicle G

For Vehicle G, as indicated in Table 30, the Radar only tests were performed on the track while the Mono-Vision and Fusion were simulated based on Radar run. Since the brake trigger signals for the Mono-Vision and Fusion systems are identical to that of the Radar, the simulations of these systems yield identical performance to that of the Radar (as can be seen in Table 30). Vehicle G provided the highest average speed reductions and provided brake activation during 80% of the trials.

Table 30: Detailed Lists of Results for Vehicle G in LVD Scenario

Scenario: LVD; Target System: Orange Balloon Car; Vehicle G; Settings: TTC: 1.0sec; Decel: 0.6g																	
						Speed reduction in m/s											Standard Dev in m/s
Target speed	Test Vehicle Speed	Target decel	Distance	Track/ Simulation	Sensor Config	Run 1	Run 2	Run 3	Run 4	Run 5	Run 6	Run 7	Run 8	Run 9	Run 10	Average	
20mph	20mph	0.3g	17.8m	TRK	Radar	*	6.44	6.12	6.63	6.14	5.31	*	5.25	5.31	5.00	5.78	0.62
				SIM	Mono Cam	*	6.44	6.12	6.63	6.14	5.31	*	5.25	5.31	5.00	5.78	0.62
					Fusion	*	6.44	6.12	6.63	6.14	5.31	*	5.25	5.31	5.00	5.78	0.62

Average and Standard Deviation based on runs which had brake activation

* = no brake activation

L.4 Pedestrian Scenarios

The two primary situations identified involving pedestrian impacts included pedestrians crossing the impacting vehicle's path and pedestrians walking along the side of the road in-path with the striking vehicle. Most of the cases identified involved urban driving conditions with the impacting vehicle estimated to be traveling at relatively slow speeds, typically less than 25 mph.

At the time of the testing for the initial method development, an acceptable test mannequin target was not available with adequate CIB sensor response correlation relative to human subjects. Therefore, testing with the baseline production systems was not conducted. The test method development conducted during the PIP vehicle test phase focused on the design of potential support structures and mannequin movement techniques. During this time, a mannequin correlation development project was scoped with an independent research lab to determine appropriate test target mannequins. See Appendix H.

L.4.1 Test Procedure Assumptions

These tests involved suspending a surrogate target representing a human pedestrian in the path of the test vehicle. The target must be suspended in a manner which isolates the target as much as practicable from the surrounding environment as well as from the suspension structure. The target and support structure must also perform in a manner which prevents damage to the test vehicle when impacting the target. The support structure must also be capable of moving the mannequin target across the path of the test vehicle and/or in-path of the test vehicle at speeds representative of a walking pedestrian. Once the target is suspended, it will be positioned at a reference position at the expected impact point. The test vehicle is then positioned with the center of the front bumper contacting the target and the position recorded as a fixed point on the differential global positioning system (DGPS) for use in recording the ground-truth data between the test vehicle and the target, including range and range rate to the target. This reference point also allows the transmission of range and range rate CAN data from the test vehicle to the tow system for use in triggering and controlling the motion of the pedestrian target. Once the fixed point is established, the test vehicle will be moved to a sufficient distance from the target to allow the driver to accelerate to a steady-state test speed. From the crash data research analysis conducted early in the project, pedestrian impacts typically occur in urban environments with relatively low vehicle speeds and walking pedestrians. Therefore, the structure and tow system was designed to accommodate 20 mph vehicle test speeds and 2 – 3 mph mannequin travel speeds. Consistent with the other test methods, the vehicle dynamics and ground-truth data will be collected through the DGPS system. The documented test results included the percentage of autonomous braking events recorded during the test series, as well as the speed reduction achieved between the time braking is initiated and impact with the target.

L.4.2 Mannequin Development

The mannequin development project was scoped with an independent research laboratory with the capabilities of conducting controlled radar response testing using both human test subjects and potential mannequin targets. The goal was to identify and select

commercial off-the-shelf mannequins which are strike-able by the test vehicle and can be correlated to 50th percentile adult humans with limited modifications. The CIB sensors used in this work included a 24 GHz ultra-wide band short range radar, provided by the research facility, two 76 GHz mid-/long-range radars provided by the CIB Consortium, and a data logging camera. Visual characteristics of the proposed mannequins were verified by the CIB Consortium using the pedestrian classification algorithms contained within the mono- and stereo-camera vision sensors built into the PIP vehicles.

L.4.3 Support Structure and Target Motion Control Development

During the PIP vehicle test phase, the development of the support structure and target motion control focused on the pedestrian crossing-path condition. This was partially to make use of the support structure previously developed for the poles and trees test scenarios and due to testing time limitations and the lack of representative mannequin targets. Figure 54 shows the application of the pole/tree support structure to use in pedestrian impact tests.

Figure 54: Support Structure Proposal for Pedestrian Cross-Path Testing

In addition to the support posts and upper tension cable used in the pole/tree target applications, a towline and routing pulleys were added in order to enable moving the pedestrian mannequin along the desired path. Figure 54 includes a foam cut out of a pedestrian shape used to assist in developing the mannequin support configuration. Figure 55 shows the upper support bracket used to attach and stabilize a harness supporting the mannequin. This bracket includes pulleys at each end that travel along the upper tension cable to prevent sagging of the tow line. The upper loop of the towline is then attached to the bracket in order to drive the bracket and harness assembly.

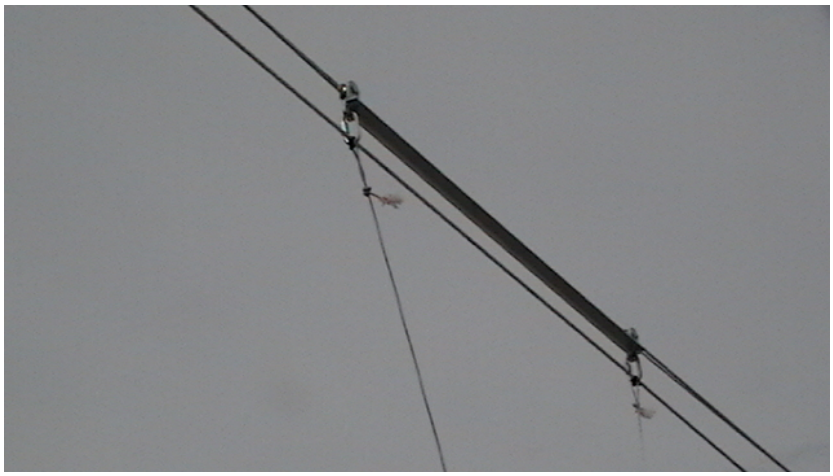

Figure 55: Upper Support Bracket Assembly

The routing of the tow line is shown in Figure 56. This routing allows bi-directional control of the mannequin target. In the event that the mannequin support harness or tow line become tangled, the tow line is looped around a lower pulley, allowing the operators to easily loosen and lower the tow line for repair. Figure 57 through Figure 59 include photos of this application. Once the tow line is routed as shown, it is then connected to the same tow motor system used for towing the moving balloon car targets, as shown in Figure 60.

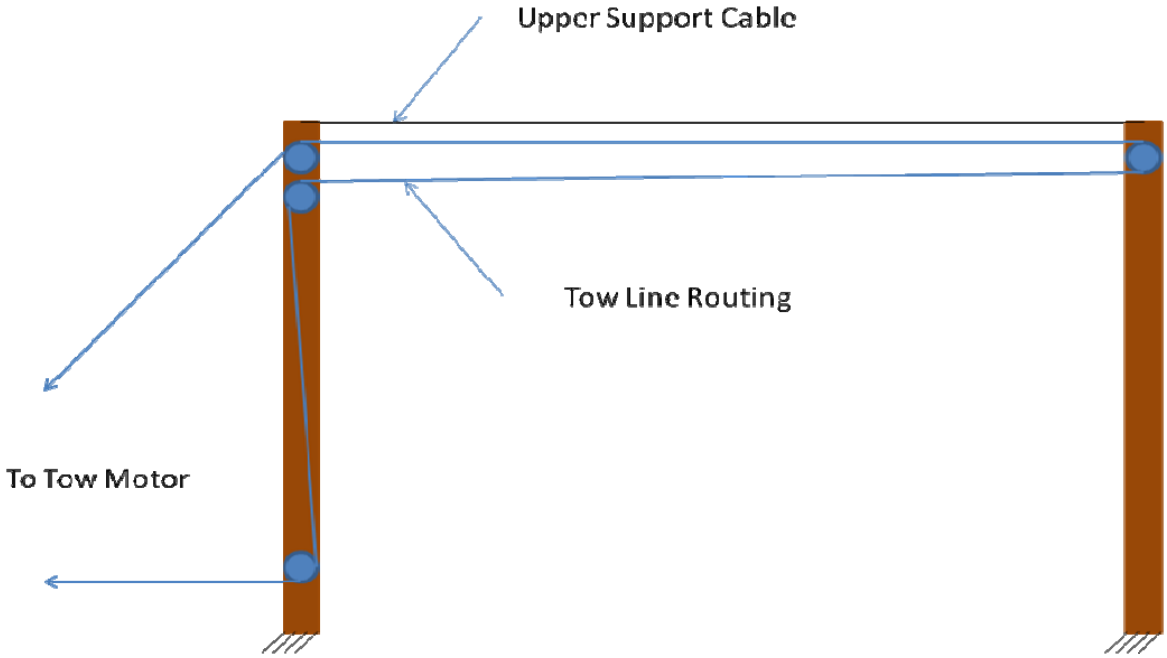

Figure 56: Tow Line Routing for Pedestrian Support Structure

Figure 57: Tow-Motor Side of the Tow Line Routing

Figure 58: Lower Pulley on Tow Motor Side of Tow Line Routing

Figure 59: Return Side of Tow Line Routing

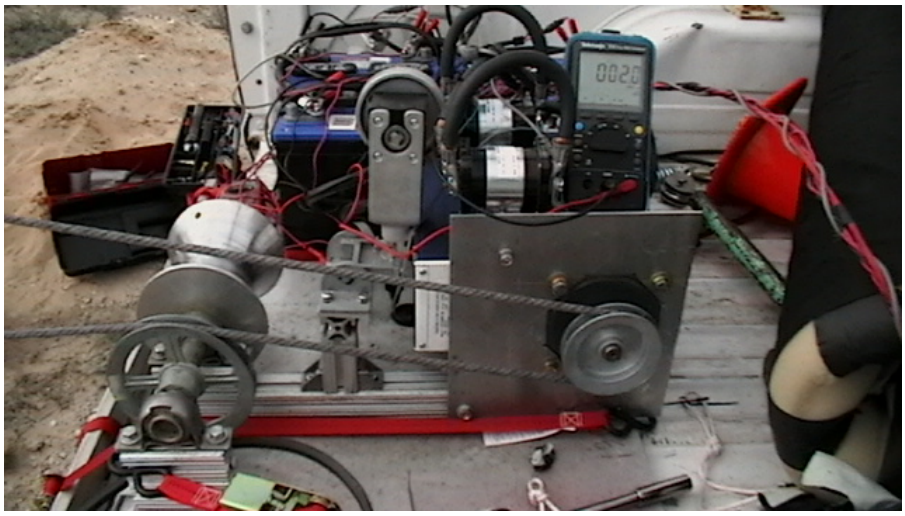

Figure 60: Application of Tow Motor Assembly for Pedestrian Testing

As previously stated, no formal CIB pedestrian impact testing was conducted with this configuration. Preliminary evaluations were conducted strictly to verify that the system was capable of moving a mannequin target across the desired test path and timing of the mannequin target motion could be coordinated with the test vehicle. Further development and validation of this configuration was expected to occur in the validation testing phase of the project.

L.4.4 Validation Test Phase

L.4.4.1 Pedestrian Testing Method

In this section, the results for the Pedestrian Scenario tests are reviewed. In this scenario, the simulated pedestrian was moved at 3 mph (4.8 km/h) in Cross-Path (perpendicular) and In-Path (parallel) directions relative to the approaching test vehicle. The correlation between an actual 50th percentile male and the pedestrian target employed in this testing is described in Appendix H.

This test method used the target towing system for moving the pedestrian mannequins. Unlike the balloon cars, a pedestrian mannequin was supported from a high anchorage point utilizing two boom cranes to maintain proper movement (see Figure 61 and Figure 62). This allowed for faster set up than the approach used during tests conducted for the method development phase of the project.

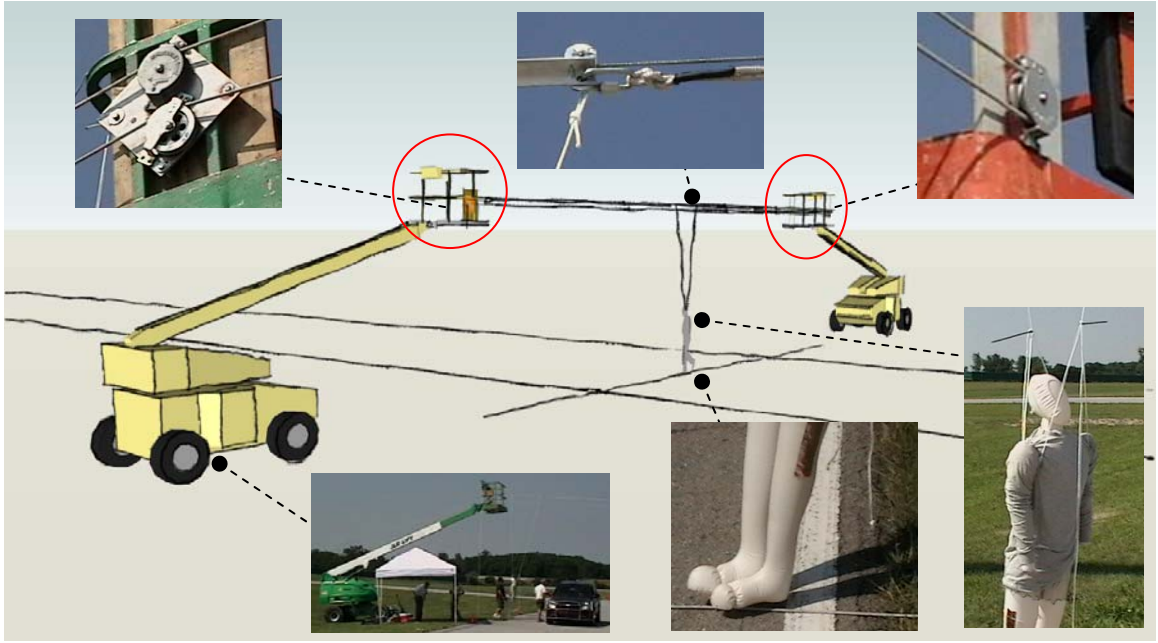

Figure 61: Test Equipment and Setup for Pedestrian Crossing Path Testing

Note: The towing system is not shown in this figure. The towing system was positioned along the track and connected with a looped rope through the pulleys attached to the booms.

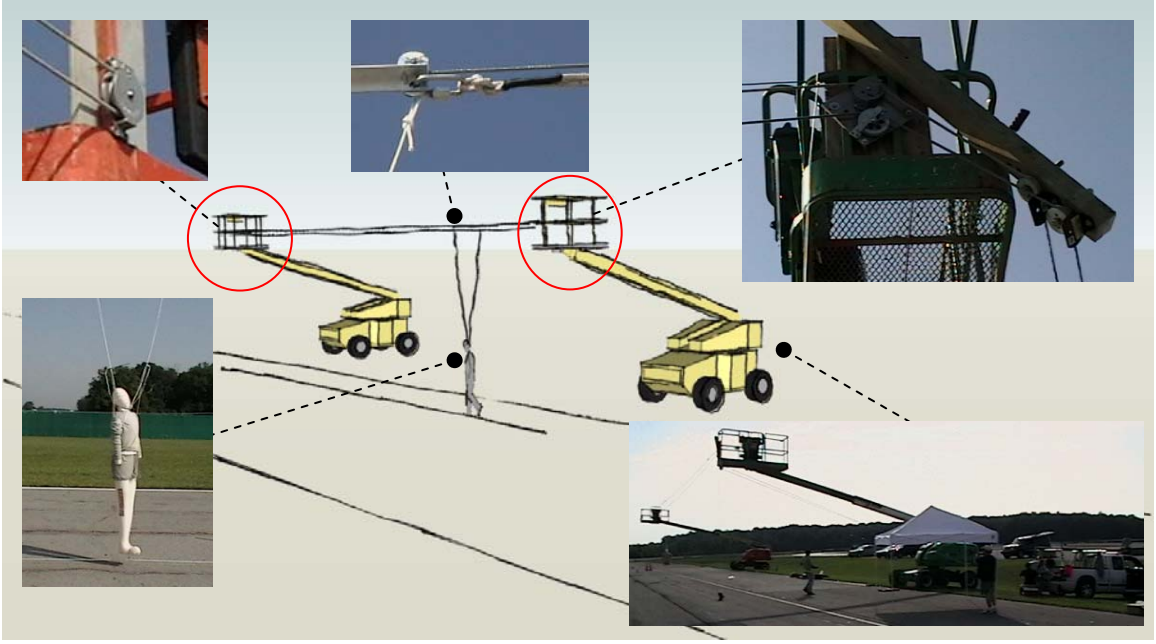

Figure 62: Test Equipment and Setup for Pedestrian In-Path Testing

Note: In the scenario shown in this figure, the towing system is located on the rear hitch of the white truck in the lower right photo.

L.4.4.2 Pedestrian Test Results

As shown in Figure 63 and Table 31, no brake activations (and hence, speed reductions) occurred in the Pedestrian Cross-Path scenario. In addition for the Pedestrian In-Path runs, only Vehicle G exhibited brake activations. Note that Mono-Camera and Fusion results are fully dependent on (and identical to) the Radar results.

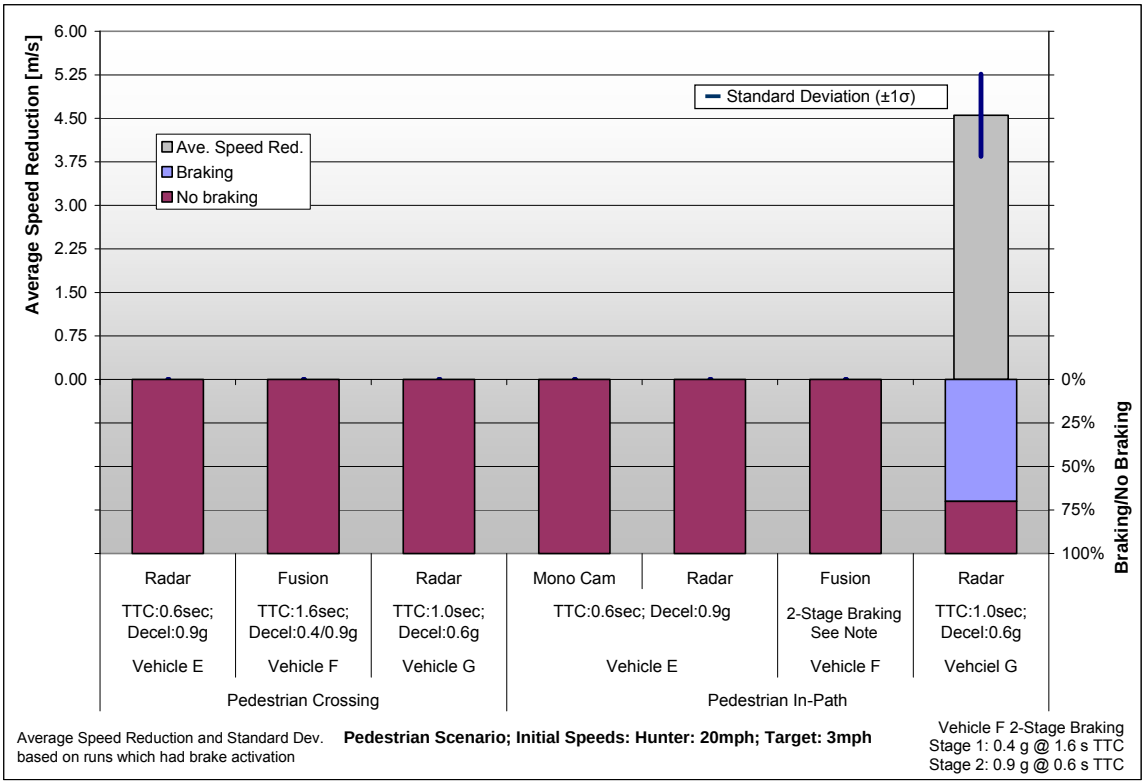

Figure 63: All Track Results for Pedestrian Cross-Path and Pedestrian In-Path Testing

Table 31: Vehicle G Results for Pedestrian Cross-Path and In-Path Tests

Scenario: Pedestrians; Target System: Pedestrian Dummy; Vehicle G; Settings: TTC: 1.0sec; Decel: 0.6g																
					Speed reduction in m/s											Standard Dev in m/s
Scenario	Target speed	Test Vehicle Speed	Track/ Simulation	Sensor Config	Run 1	Run 2	Run 3	Run 4	Run 5	Run 6	Run 7	Run 8	Run 9	Run 10	Average	
Pedestrian Crossing	3mph	20mph	TRK	Radar	*	*	*	*	*	*	*	*	*	*	-	-
			SIM	Mono Cam	*	*	*	*	*	*	*	*	*	*	-	-
				Fusion	*	*	*	*	*	*	*	*	*	*	-	-
Pedestrian In-Path	3mph	20mph	TRK	Radar	4.38	*	*	*	3.88	4.75	3.50	5.62	5.00	4.75	4.55	0.71
			SIM	Mono Cam	4.38	*	*	*	3.88	4.75	3.50	5.62	5.00	4.75	4.55	0.71
				Fusion	4.38	*	*	*	3.88	4.75	3.50	5.62	5.00	4.75	4.55	0.71

Average and Standard Deviation based on runs which had brake activation
* = no brake activation

L.5 Straight Crossing Path (SCP)

L.5.1 Test Method

The straight crossing path (SCP) test method simulates an intersection collision, front-to-side-crash scenario. This test method recreates conditions of crash scenario cases identified and examined in the CDS/National Automotive Sampling System (NASS) database as SCP where two vehicles collide at 90 degrees. To support testing in this project, two different test methods were reviewed for applicability and then track tested during the "baseline vehicle test" phase.

For this type of intersection test, a long stretch of flat test track was used that included a section that crossed the main length of track perpendicular at 90 degrees. Total length of the track should be between 300 m and 350 m with a crossing section of track at 150 m in length. The width of the test track or lane should be at least two lanes (3.5 m per lane width) to allow for test vehicles and test targets to be positioned properly when conducting the tests. Because vehicles are using forward-looking sensing systems for detecting and tracking oncoming vehicles or targets, obstacles like vehicles, guardrails, poles, trees, man holes, etc. should be kept away from the test lanes. Adjacent to the test lanes on both sides of the lane and beyond a distance of 15 m from the center of the lane there should not be any of the obstacles listed above that could affect the testing. The track should be made of concrete or asphalt to allow for measuring the braking capabilities of the CIB systems being tested.

The test vehicle containing the CIB system is placed in the center of one lane. The "target" vehicle is placed in the lane perpendicular to the test vehicle at a 90 degree angle. For the baseline testing phase, the balloon car was towed behind a tow vehicle using a long rope. The tow vehicle was located in the perpendicular lane adjacent to the lane used by the test vehicle. The side face of the target balloon car faces the front of the test vehicle with the CIB system. The minimum starting distance for the test method is 150 m for the test vehicle from the point of impact. This distance depends upon the maximum speed of the test. Approximately 100 m before the impact point, the test vehicle and the oncoming target should each have reached the predefined test speed. The CIB system test vehicle is driven straight to the target system, which is driven or pulled (balloon car) to the different test speeds (see Table 32). The test speeds must be kept constant and changes in speed have to be avoided especially on the last 100 m before hitting the target system. In addition, there should be minimal steering input along the path to the target to reduce test variation. The test ends approximately 5 m after the CIB-equipped test vehicle strikes the target system. For a successful test, the brake shall not be applied by the test vehicle driver until after the impact with the target system (Figure 64).

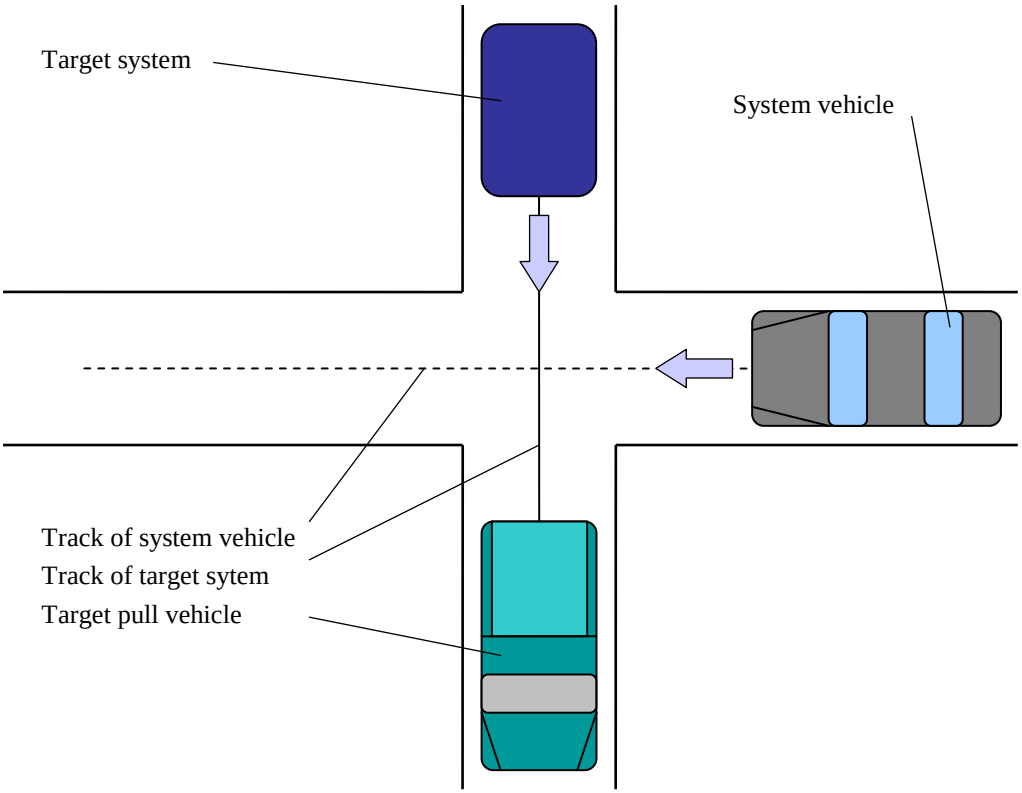

Figure 64: CIB System Test Vehicle with a Mobile Target

For baseline vehicle testing, Table 32 shows the speeds for the target (towed balloon car) and the test vehicle that were conducted.

Table 32: Longitudinal Velocities for Straight Crossing Path Crash Scenario Test Method

	Test Vehicle	Target speed (target)	Closing Speed
Longitudinal Velocities	**Mph (km/h)**	**Mph (km/h)**	**Mph (km/h)**
Test Speed Combinations	20 (32.2) 25 (40.2) 30 (48.2)	10 (15.6) 10 (15.6) 10 (15.6)	20 (32.2) 25 (40.2) 30 (48.2)

The SCP test scenario used the balloon car pulled by a tow vehicle. The towing vehicle was driven up to the designed test speed and driven at a constant speed until the target balloon car reached the impact point in the middle of the intersection. Timing of the scenario to ensure the test vehicle would impact the target at the correct impact point was accomplished by calculating distance and times to the impact point for given test speeds.

Radio communication was used between a spotter, the driver of the test vehicle, and the driver of the target to cadence the test to help insure that the two vehicles arrive at the impact point at the correct time. This method was used only for the baseline vehicles and was an open loop "trial and error" method of completing the SCP test scenario.

L.5.1.1 Other Instrumentation Requirements

For the ground truthing of this scenario, a differential GPS system was used to capture vehicle-to-vehicle ranging data. This system provides functionality for measurements of moving targets and measurements of test vehicle to target relative motion. Both vehicles (vehicle with the CIB system and the balloon car tow vehicle) were equipped with DGPS systems to provide vehicle dynamics. In addition, a DGPS "target box" and "test vehicle box" were used to capture vehicle relative motions during the testing with each target. This position information is saved to the storage drive on the instrumentation laptop containing DGPS software. This includes GPS data (longitude, latitude and altitude). In the case of the balloon car tow vehicle, the impact point is projected from the towing vehicle's GPS unit to the balloon car side door surface. This translation of the target impact point from the GPS unit to the side door allows range to be calculated from the front bumper of the test vehicle to the side door center point of the target balloon car. Thus accurate ranging data can be taken with the DGPS. Since vehicle CAN data was unavailable for this round of testing only the DGPS ground truth data was needed to record and document the pertinent CIB characteristics for each test vehicle.

L.5.1.2 Test Targets Used

The target system used for the SCP crash scenario tests is briefly described in Table 33.

Table 33: Target System Used for Straight-Crossing Path Testing with Production Vehicles

Target system short name	Target system	Brief Explanation	View
SCP1	Towed blue balloon car	Balloon car with reflective paint towed behind a tow vehicle	

L.5.2 Detailed Results from Baseline Vehicle Testing

The only test system used for this scenario is shown in Table 33. For each velocity and each test vehicle, runs were conducted at test vehicle speeds of 20 mph, 25 mph, and 30 mph and target speeds of 10 mph in the lateral direction to the test vehicle's direction of travel. This resulted in closing speeds of 20, 25 and 30 mph. These closing speeds kept balloon car damage to a minimum given that the blue balloon cars are durable at closing speeds up to 40 mph. The cable mechanism which guided the balloon car while it was being towed was damaged several times. This was due to the test vehicle braking (driver braking and not autonomous braking) over the cable and causing a side load on the cable which damaged the mounting mechanism and mounting points. Also, testing was stopped

at higher test speeds when a test vehicle's CIB system did not respond by braking over multiple sequential runs at a lower test speed.

Table 34 shows the results of the baseline testing for the SCP scenario using target SCP1, a towed balloon car. There were no braking events for all tests that were run for the SCP scenario for any of the vehicles and only one test run in which a warning occurred. The sole collision warning was for Vehicle C at 20 mph. It is believed in this case the balloon car entered the intersection prematurely and was detected due to its long time in the intersection before being impacted. It was impacted in the rear corner and was almost missed during the test. Based on these testing results and the field of view of the sensors tested, further testing for three vehicles was considered of limited value. The expectation for Vehicles A, B and C was that given the characteristics and geometry of the crash scenario, these vehicles with narrow field of view sensors would have difficulty in detecting a target coming in to the intersection from a lateral angle.

Table 34: Straight-Crossing Path Tests Results for Baseline Production Vehicles Target SCP1 – Towed Balloon Car with Tow Vehicle

Target: SCP1 - Towed Balloon Car with Tow Vehicle			
Set 1			
Speeds	**Test Vehicle**	**20 mph**	
	Target System	**10 mph lateral**	
Test Vehicle	**No of runs**	**Warnings**	**CIB Brake**
Vehicle A	2	0	0
Vehicle B	5	0	0
Vehicle C	3	1	0
Set 2			
Speeds	**Test Vehicle**	**25 mph**	
	Target System	**20 mph lateral**	
Test Vehicle	**No of runs**	**Warnings**	**CIB Brake**
Vehicle A	2	0	0
Vehicle B	2	0	0
Vehicle C	1	0	0
Set 3			
Speeds	**Test Vehicle**	**30 mph**	
	Target System	**10 mph lateral**	
Test Vehicle	**No of runs**	**Warnings**	**CIB Brake**
Vehicle A	1	0	0
Vehicle B	3	0	0
Vehicle C	1	0	0

L.5.3 PIP Test Phase

The test procedure for the SCP scenario was changed from the baseline vehicle testing by using a different tow system. The same SCP1 balloon car target was used. For the PIP phase of testing, the automated motorized tow system was used to eliminate the affect of having a vehicle towing or holding a target in near proximity to the actual target (see Figure 65).

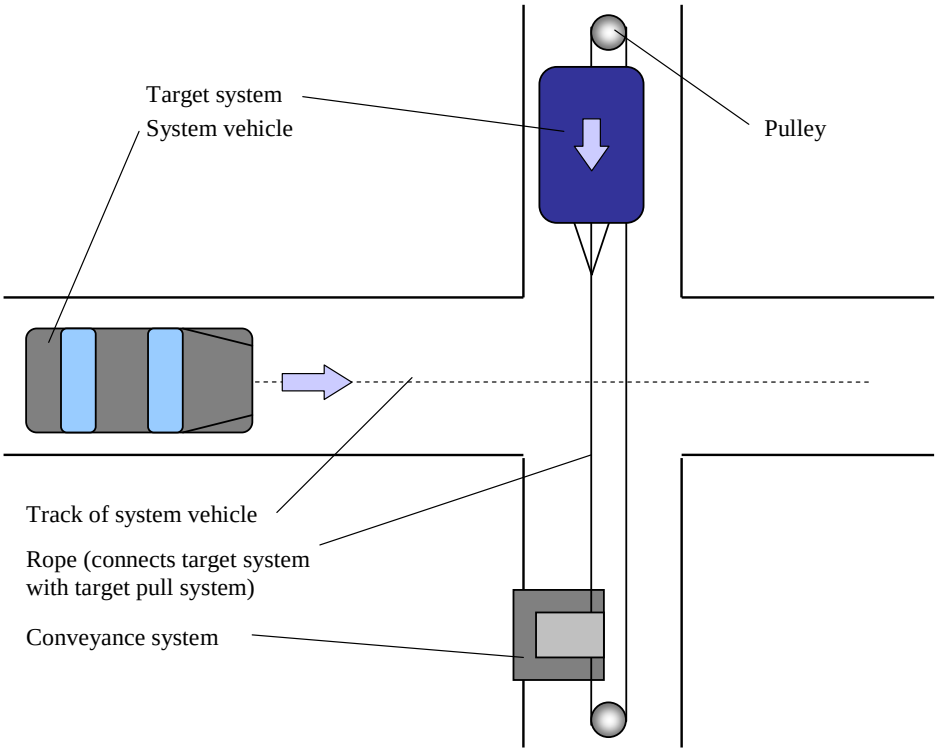

Figure 65: Balloon Car with Tow System for Straight-Crossing Path Testing of PIP Vehicles

For the PIP vehicle testing the following table (Table 35) shows the speeds for the target and the test vehicle that were employed during this phase of testing. Note that the longitudinal speeds for the target vehicle are perpendicular to the test vehicles. The closing speeds are based upon the longitudinal velocity of the test vehicle as it moves to the target, which essentially has zero speed relative to the test vehicle in the test vehicle's longitudinal direction.

Table 35: Longitudinal Velocities for Straight-Crossing Path Crash Scenario

	Test Vehicle	Target speed	Closing Speed
Longitudinal Velocities	**Mph (km/h)**	**Mph (km/h)**	**Mph (km/h)**
Test Speed Combinations	20 (32.2) 20 (32.2) 30 (48.2)	10 (15.6) 20 (32.2) 10 (15.6)	20 (32.2) 20 (32.2) 30 (48.2)

L.5.3.1 Targets Used for PIP Vehicle Testing

The target system used for the SCP testing is listed and briefly described in Table 36.

Table 36: Target Systems used for Straight-Crossing Path Testing with PIP Vehicles

Target System Short Name	Target System	Brief Explanation	View
SCP1	Towed blue balloon car	Balloon car with radar reflective material and poor visual properties with a vision system – very robust to high speed impacts	

The balloon car was attached to the drive rope via wire ties or zip ties to allow a breakaway attachment when the balloon car was impacted. The balloon car is also attached at each side to the attachment cables that run the length of the test lane(s). The cables keep the balloon car from moving side to side in windy conditions and hold the balloon car in line after it is struck by the impacting vehicle. Tarp material was used as a consumable cover at the bottom of the balloon cars to protect from damage at the abrasive roadway to balloon interface.

L.5.4 Detailed Results from PIP Vehicle Test Phase

All three PIP vehicles were used for the SCP (Vehicles E, F and G), but with different CIB sensor settings as described previously in Section 3.5 of the report.

The SCP test scenario was conducted using a custom developed motorized tow system. For each vehicle, and while using the target system SCP1, test runs were conducted at the speeds shown in Table 35. Also, testing was stopped at higher test speeds when a test vehicle's CIB system did not respond by braking over multiple sequential runs at a lower test speed.

The results of the PIP vehicle testing for the SCP scenario using the target SCP1 indicated no vehicle had any warnings and no CIB brake activations for the chosen test speeds. The lateral or perpendicular relative motion makes it difficult for the sensing systems to detect and classify these events. Although it should be noted that it may be

feasible for the target to be detected and tracked by any of the three given systems, the target is potentially disregarded due to a deliberate threat-assessment strategy implementation.

The SCP testing for the PIP vehicles has shown that none of the vehicles responded to the target and test process. This result is not unexpected since many of these systems were designed to disregard targets coming in a perpendicular or lateral direction.

The test method developed is applicable to simulating the crash scenario of a SCP as would occur at an intersection. A target was developed which is radar and vision system "realistic" and capable of being impacted repeatedly with minor damage at relatively low speeds in the SCP crash scenario. A motorized tow system was also developed to provide the proper trajectory to the target relative to the test vehicle equipped with a CIB system to simulate the SCP scenario. Thus, the foundation for this test method was completed and used in the test method validation testing sequence. Using a motorized tow system to transport a balloon car perpendicular to the test vehicle was shown to simulate the trajectories and relative motions of this crash scenario at low closing speeds and do so in a non-destructive fashion.

The SCP method evolved from a tow vehicle carrying the balloon car to the intersection to an automated motorized balloon car tow system that transported the target to the intersection. In both cases, the control of the target system was open loop and timing was done manually by coordination between the driver and a spotter monitoring the target to test vehicle clearance. In the future, a closed loop control method is needed to allow more precise positioning of the target relative to the test vehicle. In addition, the balloon car was the only target capable of enabling this maneuver, although SCP1 was difficult for the vision to classify as a vehicle.

Overall, coordination and timing of the SCP scenario was very dependent on human interface to coordinate and setup the test in the correct sequence of time required. Hence, the advantages to using an automated motorized balloon car tow system for this scenario are as follows:

- Better speed and acceleration control occur with the motorized tow system (the tow vehicle velocity and acceleration were not very well controlled due to human error which was expected based on earlier testing)
- The balloon car that is towed with the developed drive system has no metal parts near the balloon car that can reflect RF signal back to the test vehicle's radar to cause false activations
- The drive system is more repeatable from trial run to trial run in towing versus the balloon car using a tow vehicle driven by a human

The main disadvantage to this test method is primarily the cost of a custom-built tow system to hold and transport the balloon car.

L.5.5 Validation Test Phase

The SCP scenario developed in prior testing during the baseline and PIP vehicle testing was further refined in this phase of development and validation testing. This development focused primarily on the manner in which the balloon car target was towed.

Since the 3rd-generation balloon car target was not yet available, only the 2nd-generation balloon car was used for the final SCP test method validation testing (see Figure 66). As demonstrated during the test method development phase of the project, only the Stereo-Vision sensing system integrated into Vehicle E enabled brake activations under this test scenario. Therefore, Vehicle E was the only vehicle used in this testing.

Figure 66: 2nd-Generation Balloon Car Front, Side and Rear Views

As shown in Figure 67, the precise timing required for the SCP test is challenging for a CIB sensing system. This is due to the lateral motion between the two test vehicles just before the impact point, as the sensing system must immediately recognize and respond to the target. The limited time the target is in the field of view prior to impact challenges the system's ability to perform threat assessment and apply the CIB system. A target is usually recognized very late or not at all prior to impact. The tests, conducted with Vehicle F, also used the target tow system developed during this project and exercised closed loop control between the towed target and the test vehicle.

Figure 67: Test Method Sequence of Events for the SCP Test Scenario

At the beginning of the SCP test, the test vehicle is located at one end of the test track lane and the balloon car is positioned at the end of the intersecting track. This test set up uses the target tow system (tow rope, steel braided guide cables, balloon car carrier, anchor plates, tow motor, and drive rope). The drive system towed the balloon car carrier along the braided guide cables toward the intersection and at the predetermined target speed.

As mentioned above, carefully controlled timing between the test vehicle and the target is critical for the SCP scenario. If the timing is not correct, the test vehicle and the target will not impact. Consequently, a closed-loop control target tow system was necessary to

ensure that the balloon car and the test vehicle arrived at the defined impact point at the same time (see Appendix G). The closed-loop control enabled proper position and speed of the balloon car relative to the test vehicle. Position sensing systems for the balloon car and the test vehicle were used to control the speed and distance between the target and the test vehicle.

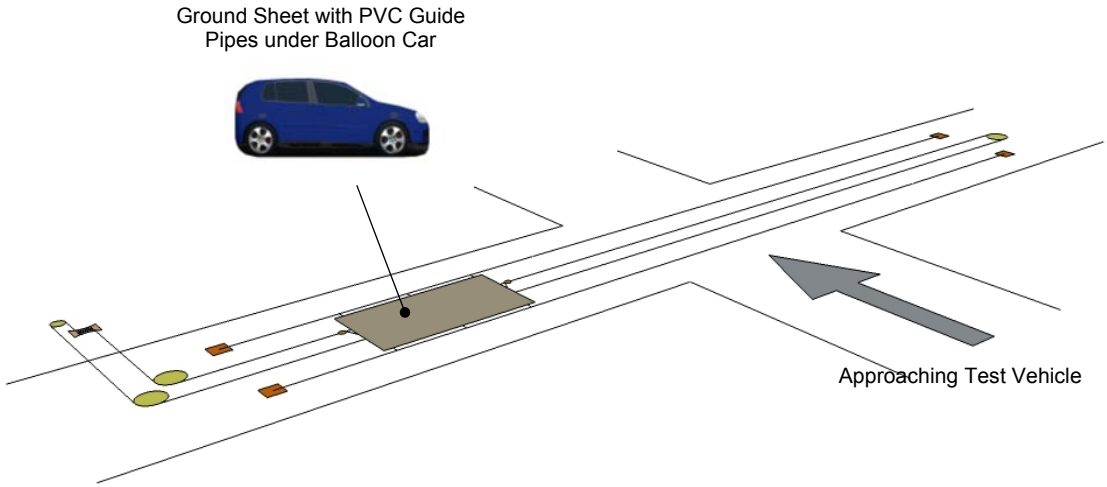

(Balloon Car photo courtesy of Inflatable Images)

Figure 68: Test Method System Components for the SCP Test Scenario

Vehicle E was evaluated with both the Radar and Stereo-Vision systems active over a set of 31 runs at three different host vehicle and target (balloon car) speed scenarios (20 mph test vehicle and 10 mph target, 30 mph test vehicle and 10 mph target, and 20 mph test vehicle and 20 mph target). The corresponding Mono-Vision and Fusion data sets were simulated. A summary of the results for Radar, Mono-Vision and Fusion are provided in Figure 69, with more detailed results provided in Table 37. In this test scenario there were very few brake activations and, thus, very little speed reduction data available.

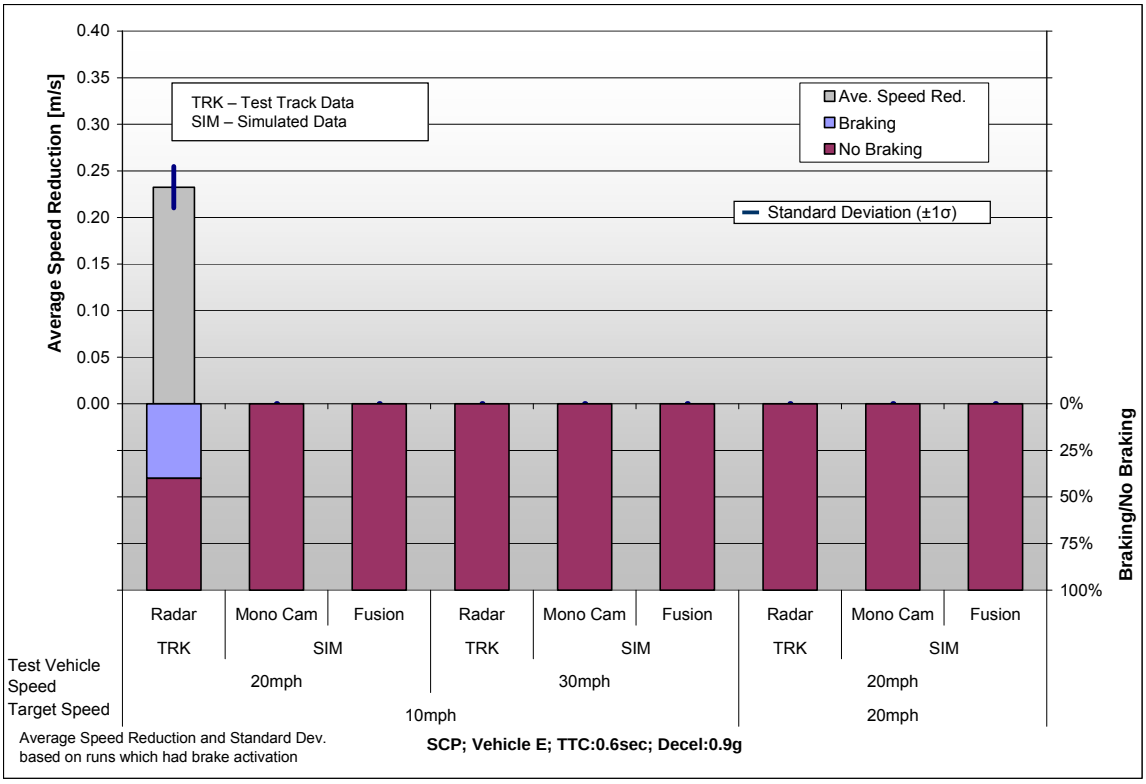

Figure 69: Track Test Results for SCP Scenario

Only 4 of the 31 runs resulted in brake activations, all of which occurred during the 20 mph test vehicle and 10 mph target test scenario.

Table 37: Detailed Lists of Results for Vehicle E in SCP Scenario

Scenario: SCP; Target System: Orange Balloon Car; Vehicle E; Settings: TTC: 0.6sec; Decel: 0.9g																	
				Speed reduction in m/s													Standard Dev in m/s
Target speed	Test Vehicle Speed	Track/ Simulation	Sensor Config	Run 1	Run 2	Run 3	Run 4	Run 5	Run 6	Run 7	Run 8	Run 9	Run 10	Run 11	Run 12	Average	
10mph	20mph	TRK	Radar	0.24	0.25	*	0.24	*	*	*	*	0.20	*			0.23	0.02
		SIM	Mono Cam	*	*	*	*	*	*	*	*	*	*			-	-
			Fusion	*	*	*	*	*	*	*	*	*	*			-	-
	30mph	TRK	Radar	*	*	*	*	*	*	*	*	*				-	-
		SIM	Mono Cam	*	*	*	*	*	*	*	*	*				-	-
			Fusion	*	*	*	*	*	*	*	*	*				-	-
20mph	20mph	TRK	Radar	*	*	*	*	*	*	*	*	*	*	*	*	-	-
		SIM	Mono Cam	*	*	*	*	*	*	*	*	*	*	*		-	-
			Fusion	*	*	*	*	*	*	*	*	*	*	*		-	-

Average and Standard Deviation based on runs which had brake activation
* = no brake activation
grey cell = no run

L.6 Left Turn Across Path – Opposite Direction (LTAP-OD)

L.6.1 Test Method

As previously described in Section 2 of the report, LTAP-OD represented the only test scenario examined involving turning targets struck by the test vehicle and, hence, required significant development. For that reason, simulations were conducted as part of a bottom-up analysis of representative NASS/CDS crash cases to establish the initial test conditions. These consisted of lateral velocities ranging between 8 – 32 km/h (5 – 20 mph) and up to 90 degrees impact trajectory. The maximum closing speeds for the LTAP-OD turning case was initially defined to be 80 km/h (50 mph).

Figure 70, below, shows the preliminary scenario graphic for the LTAP-OD test scenario.

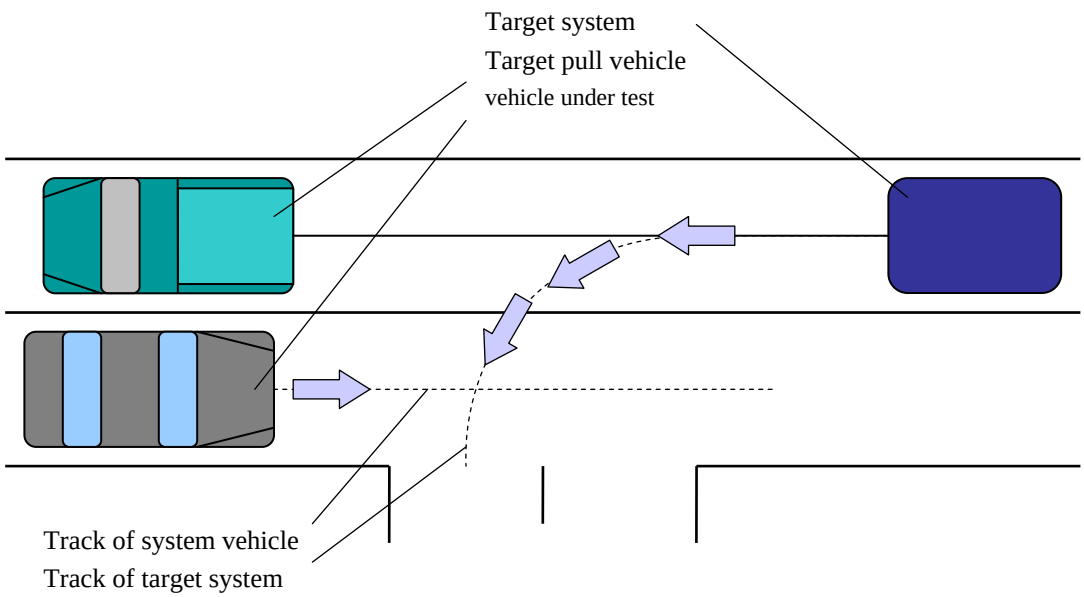

Figure 70: System Vehicle with a Towed Balloon Car as the Target. A Special Mechanism Forces the Balloon Car into a Circular Path

The test speeds were defined to have the target vehicle turn left with a velocity of either 10 mph or 15 mph with the test vehicle speed defined at 20 mph and 30 mph. These four combinations were repeated five times to ensure repeatability and consistency in the test data.

The balloon car was placed on a carrier system that was guided by two steel cables. Initially this carrier system was pulled at the required steady state test speeds by another vehicle. This was eventually replaced by the new automated tow system developed for use in all moving target test scenarios. After the towed balloon vehicle reaches steady state test speed it hits the stationary pivot point at the end of a third cable, which is parallel and one lane width (15 feet) away as shown in Figure 71. The tow mechanism

breaks away from the balloon vehicle and carrier and continues to move in an arc in front of the test vehicle.

This test method requires extensive track set up in order to properly guide the test target. Additionally, only moving balloon cars were identified as being capable of duplicating the desired dynamics of the struck vehicle without interfering or damaging the test vehicle. Three steel cables were secured and stretched across the test track to guide the balloon carrier and pivot rope.

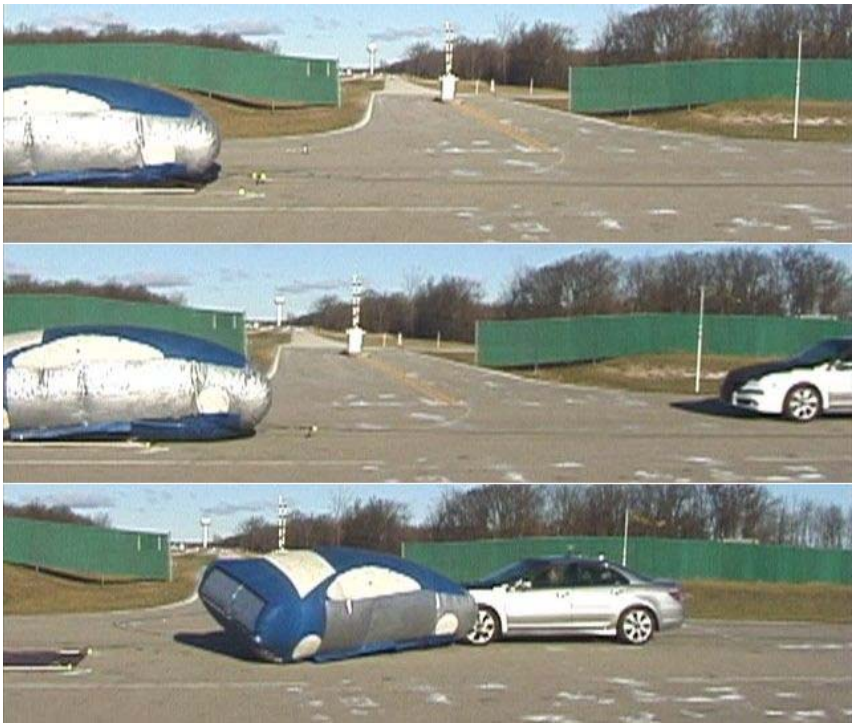

Figure 71: Baseline LTAP OD Test Sequences: Balloon Car Pulled by Rope (Top); Rope Brakes Away, Balloon Car Begins Turning (Center); Balloon Car Follows Arc and Hits Test Vehicle (Bottom)

Baseline testing was mainly conducted in two ways as shown in Figure 72 and Figure 73. In both scenarios, the balloon car is pulled by a second vehicle. A major issue was identified using this approach with respect to controlling the timing of the impact between the test vehicle and target at the right point along the target's turning arc. Also, repeatability was inherently difficult given the trajectories of the two vehicles. Figure 74 shows an alternative method to conduct this test. The balloon car is pulled directly by the test vehicle itself. The advantage of this method is that impact always occurs at the same point once some initial test runs are conducted to establish the proper length of the towing rope. However, a disadvantage of towing the target with the test vehicle is that the balloon car always moves with the same speed as the test vehicle. This reduces the test matrix to only a few speed combinations, such as 15 mph or 20 mph for both vehicles.

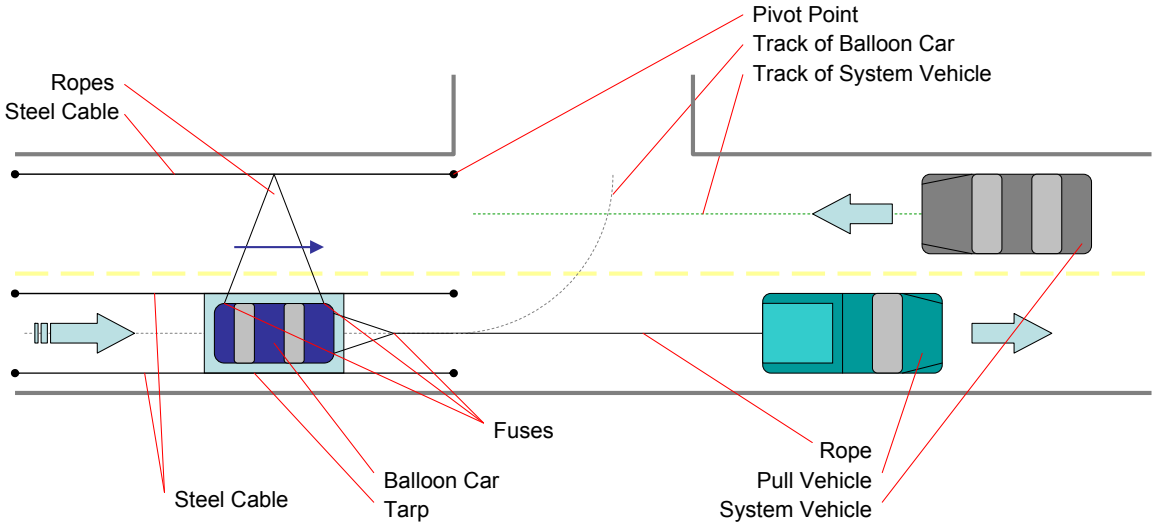

Figure 72: Balloon Car is Pulled by Pull Vehicle, Scene 1 - Short Time Before Impact, Straight Pulling along Steel Cables

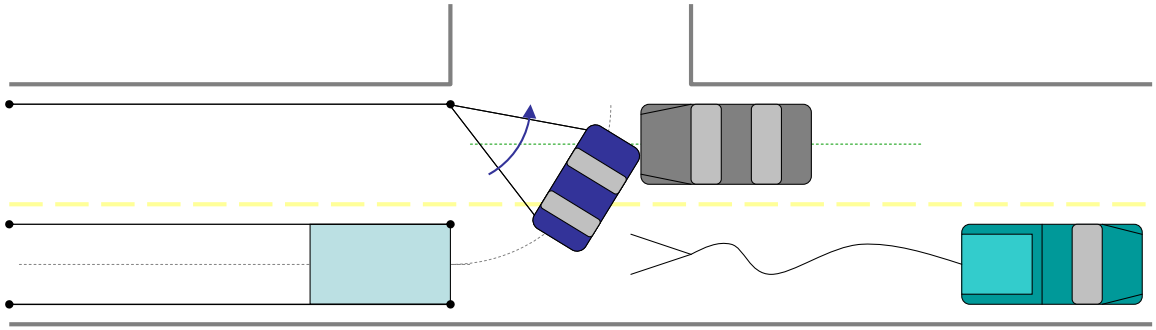

Figure 73: Balloon Car is Pulled by Pull Vehicle, Scene 2 - At the Time of Impact, Balloon Car Rotates Around Pivot Point

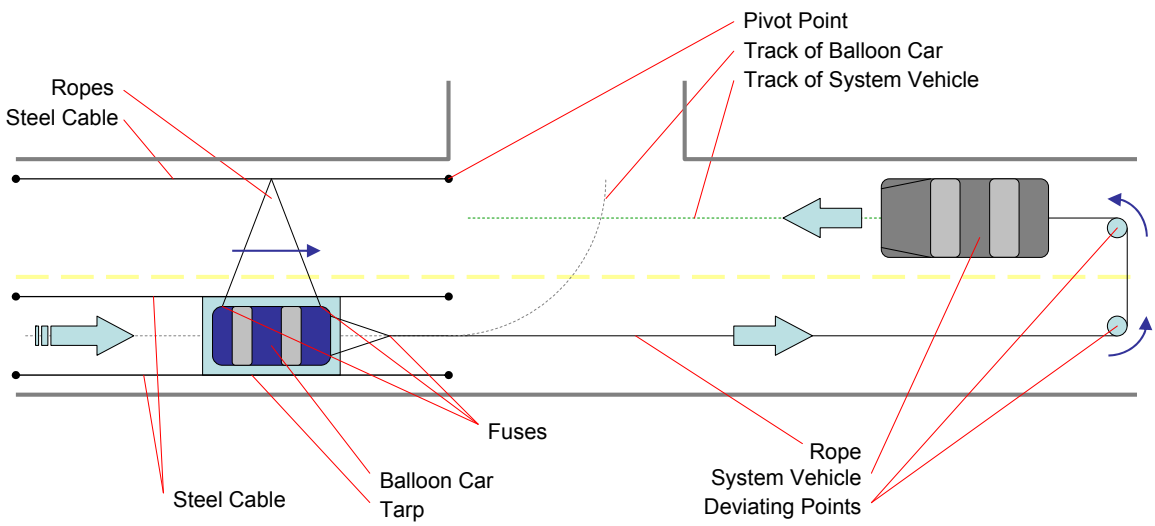

Figure 74: Balloon Car Pulled by System Vehicle Just Prior to Impact

L.6.2 Detailed Results from Baseline Test Phase

From the baseline vehicles tested, a total of seven runs were completed using the balloon car at the required test speeds. None of the three vehicles reacted to the LTAP-OD test scenario. Vehicle A was tested two times, Vehicle B was tested three times and Vehicle C was tested two times.

L.6.3 Detailed Results from PIP Vehicle Test Phase

For the PIP vehicle tests, the automated balloon car tow system was available. That made it possible to conduct several test series with different test speeds and all three PIP vehicles. Tested speed combinations used were 20 mph for the test vehicle versus 10 mph for the target, 30 mph for the test vehicle versus 10 mph for the target, and 20 mph for both. None of the vehicles' systems reacted with any braking in this scenario regardless of which sensor combinations and TTC/deceleration settings were used. Overall, 32 runs were conducted and data was collected. Vehicle E was tested for 18 runs, Vehicle G was tested for six runs and Vehicle F was tested for eight runs.

This LTAP-OD test scenario was difficult to perform on the test track.

L.6.4 Validation Test Phase

The LTAP-OD scenario developed in prior testing during the baseline and PIP vehicle testing was further refined in this phase of development and validation testing, primarily in the manner in which the balloon car target was towed.

L.6.4.1 Testing Method

The LTAP-OD test was further refined in this phase of development and validation in several areas including towing of the balloon car target, balloon car target correlation with a real vehicle and closed loop control of the tow sled and balloon car. Since the 3rd-generation balloon car (see Figure 75) development was completed prior to this LTAP-OD testing, this was the only target used in validation testing. In addition, for

reasons further described below, Vehicle E was the only vehicle tested for this scenario in validation testing (since the remaining two vehicles had demonstrated in earlier testing that they would not brake for this test condition).

Figure 75: 3rd-Generation Balloon Car Front, Side and Rear Views
(Figure courtesy of Inflatable Images)

As stated earlier, given the CIB sensing challenge (similar to that described for the SCP scenario) and the lack of prior CIB activations during earlier rounds of LTAP-OD testing with two of the three test vehicles, the demonstration and validation of this test method was completed by running one vehicle (Vehicle E) multiple times at the predetermined test speeds. These tests also allowed exercising the target tow system developed during this project in the LTAP-OD test scenario and allowed exercising the closed loop control between the towed target and the test vehicle.

The LTAP-OD test is a longitudinal-type crash scenario where the test vehicle and a towed balloon car target approach each other in adjacent lanes (see Figure 78). At the start of the test, the test vehicle was located at one end of the test track lane and balloon car target was located at the other end of the test track in a lane adjacent to the test vehicle lane. This test method used the same set of equipment used in the OD and SCP Path testing. As previously discussed, the closed loop target tow control system (see Appendix G) was used in this scenario to control the balloon car positioning relative to the test vehicle. As with the SCP test scenario, precise control of the balloon car is critical so that the balloon car arrives at the impact point at the same time as the test vehicle to enable the LTAP-OD scenario impact. If the timing is off significantly, the vehicles will not impact as desired.

As with the SCP test scenario, a method needed to be developed to enable the balloon car to impact the test vehicle in the desired fashion. The system developed used a “pivot point” at the end of a steel cable located next to the two guide cables for the balloon car. The balloon car, while resting on the carrier material, is towed down the test track to the impact point and is guided by two steel cables next to each side of the balloon car. The balloon car remains in the adjacent lane to the test vehicle until just before the test vehicle arrives at the impact point. As the test vehicle enters the intersection, the balloon car is pulled into the test vehicle path via a third steel cable (see Figure 76). As the rope from the third steel cable pulls the balloon car laterally and breaks the “fuses” attaching the balloon car to the carrier, the balloon car is released from the carrier. The carrier remains attached to the steel guide cables. The balloon car is then guided by the rope and pivots in

a path similar to a vehicle making a left turn in an intersection and into the path of the oncoming test vehicle. The length of the rope allows the balloon car turning radius to be adjusted to the predetermined radius for the test scenario (see Figure 77 and Figure 78). A turning radius of 5 meters (approx 15ft) was used.

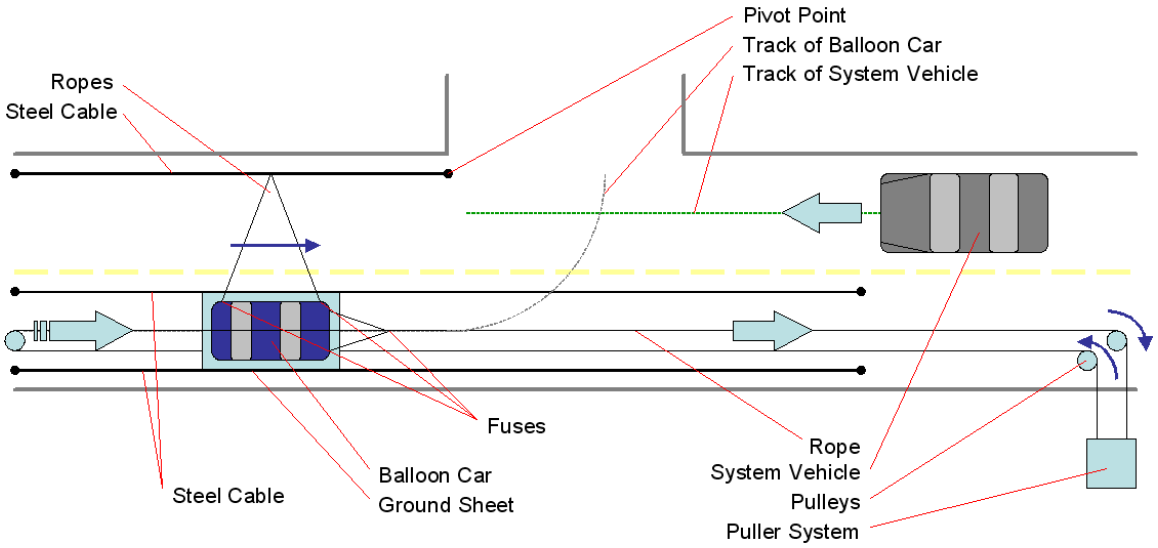

Figure 76: Test Method System Components for the LTAP-OD Test Scenario

Figure 77: Test Sequence of Events for the LTAP-OD Test Scenario – Wide View

Figure 78: Test Sequence of Events for the LTAP-OD Test Scenario – Close View

As mentioned earlier for the LTAP-OD testing, Vehicle E (including Mono-Vision, Stereo-Vision and a Radar systems) was used to conduct a set of 11 runs for two different initial speed combinations (20 mph test vehicle / 10 mph target and 30 mph test vehicle / 15 mph target). During this testing, the vehicle actuated the CIB system based only on inputs from the Mono-Vision systems. The Radar was inactive during this testing and results indicated the Radar system did not detect the target in this condition. The Stereo-Vision system was active during this testing.

Results indicated that no brake activations occurred during the 11 test runs with Vehicle E. As mentioned earlier, this is likely due to the “last-second” lateral motion of the target relative to the test vehicle prior to impact. Recall, this same result also occurred during earlier testing. The 45 to 90 degree approach angle in the intersection during the target turn makes it difficult for the system to predict an impending impact given the brief time available before the impact occurs. The main issue here is not sensing of the target vehicle, but the predictability of the target’s path. This is illustrated in the series of photos provided in Figure 77 and Figure 78.

The reader is reminded that Vehicles F and G were not used in this testing because earlier data indicated that they would not have significant brake activations for this test scenario. The 11 runs conducted here with Vehicle E allowed the tested system to demonstrate the test method, and in particular, the precisely timed nature of the movement of the balloon car relative to the test vehicle immediately prior to impact.

L.7 Opposite Direction (OD)

L.7.1 Test Method

The opposite direction (OD) test method simulates a head on crash scenario. This test method recreates conditions of crash scenario cases identified in the CDS/NASS database analysis categorized as opposite direction.

For this type of test a long stretch of flat test track was used with a total length between 300 m and 350 m. The width of the test track or lane should be at least two lanes (3.5 m) to allow for test vehicles and test targets to be positioned properly when conducting the tests. Because CIB vehicles are using radar and vision systems for sensing oncoming vehicles or targets, obstacles like vehicles, guardrails, poles, trees, man holes, etc. should be kept away from the test lanes. Adjacent to the test lanes on both sides of the lane and beyond a distance of 15 m from the center of the lane, there should not be any of the obstacles listed above that could affect the testing. The track should be made of concrete or asphalt to allow for measuring the braking capabilities of the CIB systems being tested.

The test vehicle containing the CIB system is placed in the center of one lane. The "target" vehicle is placed in the adjacent lane facing the test vehicle if it is using a boom to carry the target. In some cases, a towed balloon car was placed in the same lane as the test vehicle. The face of the target faces the front of the test vehicle with the CIB system. The minimum starting distance is 250 m. Approximately 100 m before the impact point, the test vehicle and the oncoming target should have reached and stabilized to the initial test speeds. The CIB system test vehicle is driven at different test speeds (see Table 38) straight to the target system with constant speed. The target system is also driven or pulled (balloon car) to the different test speeds (Table 38). The test speeds must be kept constant and changes in speed have to be avoided especially on the last 100 m before hitting the target system. In addition, there should be minimal steering input along the path to the target to reduce test variation. The distance between the centerline of the test vehicle and the centerline of the target vehicle should not be greater than 0.5 m. The test ends approximately 5 m after the test vehicle strikes the target system. For a successful test, the test vehicle's brake shall not be applied by the driver until after the impact with the target system (see Figure 79).

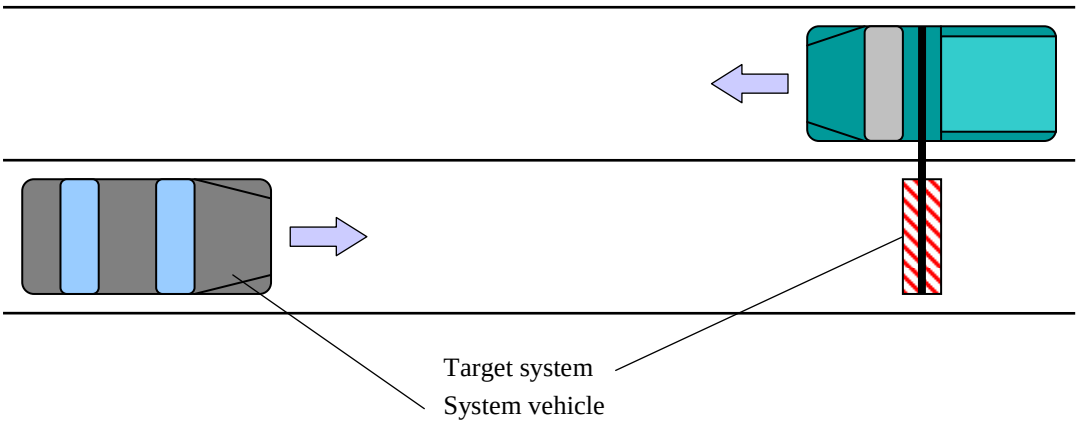

Figure 79: CIB System Test Vehicle with a Mobile Target

For baseline vehicle testing, Table 38 shows the speeds for the target and the test vehicle that were conducted. Low speeds were chosen because the target and test vehicle speeds are additive and consistent closing speeds were desired across test scenarios. A secondary consideration was the impact speed with the target and the potential for damage to test equipment. Note that the longitudinal speeds for the target vehicle are negative since it is an oncoming speed.

Table 38: Longitudinal Velocities for Opposite Direction Crash Scenario

	Test Vehicle Speed	**Target Speed**	**Closing Speed**
Longitudinal Velocities	**Mph (km/h)**	**Mph (km/h)**	**Mph (km/h)**
Test Speed Combinations	20 (32.2) 20 (32.2) 25 (40.2)	-10 (-15.6) -15 (-24.1) -15 (-24.1)	30 (48.2) 35 (56.3) 40 (64.3)

Note: The negative values for the target speeds shown in the table reflect that the target is traveling in the opposite direction from the test vehicle.

L.7.1.1 Targets Used

Each of the target systems used for the OD tests are briefly described in Table 39.

Table 39: Target Systems used for Opposite Direction Testing with Production Vehicles

Target System Short Name	Target System	Brief Explanation	View
OD1	Hanging corner reflector target attached to pickup truck with Boom	Corner reflector which provides concentrated radar feedback. Target fixture flips up after impact	
OD2	Towed Balloon Car	Radar and Camera systems, moving target that is struck. Balloon representation of a vehicle	
OD3	Balloon Car Carrier	Radar and Camera systems, moving target to allow proper closing speeds that is struck. Balloon representation of a vehicle	

L.7.2 Detailed Results from Baseline Testing

This test scenario was conducted with the three target systems shown in Table 39. For each velocity and each target system test, runs were conducted at test vehicle speeds of 20 mph and 25 mph and target speeds of 10 mph and 15 mph in the opposite direction along the longitudinal axis. This resulted in closing speeds of 30 mph, 35 mph and 40 mph, respectively. Thus, maximum closing speeds for these three target systems were near 40 mph or less. (At higher speeds either the target systems were damaged and/or resulting vehicle damage occurred.) The front end of the production vehicles were covered with either gaffers tape, foam insulating material, polymer tape, bubble wrap or a combination of these materials to reduce front end damage. In some cases, the number of test runs was reduced when damage was evident. This occurred when the tested vehicles CIB system did not react in any manner (audible or visual warning, belt pretension or braking) three times in a row at the lowest speed. In such cases, only three tests for each test speed were conducted instead of the 10 runs made during the later PIP testing.

Table 40 below shows the results of the baseline OD testing with Target OD1, a hanging corner reflector. In the case of the Vehicle B, Vehicle B had collision warning alarms and CIB braking at each test speed. The remaining two vehicles had no warnings or brake activations. Furthermore, the testing for Vehicles A and C was reduced since vehicle and target damage was occurring due to a lack of any CIB braking. Results with Target OD2, the balloon car carrier, are shown in Table 41. Again Vehicle B showed warnings and braking at all three speeds and Vehicles A and C did not have any warnings or braking at the speeds where they were tested. The results for target OD3, towed balloon car are shown in Table 42. Results showed that only Vehicle B had one warning and brake activation for this target. Vehicles A and C only completed a few of the tests with this

target (with no warning activation) due to the fact that at closing speeds greater than 35 mph the front end of the vehicle could have been damaged.

Table 40: Opposite Direction Tests Results for Baseline Production Vehicles Target OD1 – Hanging Corner Reflector

Target: OD1 - Hanging Corner Reflector			
Set 1			
Speeds	**Test Vehicle** **Target System**	**20 mph** **10 mph oncoming**	
Test Vehicle	**No of runs**	**Warnings**	**CIB Brake**
Vehicle A	2	0	0
Vehicle B	5	5	5
Vehicle C	2	0	0
Set 2			
Speeds	**Test Vehicle** **Target System**	**25 mph** **10 mph oncoming**	
Test Vehicle	**No of runs**	**Warnings**	**CIB Brake**
Vehicle A	1	0	0
Vehicle B	5	5	5
Vehicle C	1	0	0
Set 3			
Speeds	**Test Vehicle** **Target System**	**25 mph** **15 mph oncoming**	
Test Vehicle	**No of runs**	**Warnings**	**CIB Brake**
Vehicle A	0	0	0
Vehicle B	5	3	3
Vehicle C	0	0	0

Table 41: Opposite Direction Tests Results for Baseline Production Vehicles – Target OD2 Balloon Car Carrier

Target: OD2 - Balloon Car Carrier			
Set 1			
Speeds	**Test Vehicle**	**20 mph**	
	Target System	**10 mph oncoming**	
Test Vehicle	**No of runs**	**Warnings**	**CIB Brake**
Vehicle A	3	0	0
Vehicle B	5	3	3
Vehicle C	3	0	0
Set 2			
Speeds	**Test Vehicle**	**25 mph**	
	Target System	**10 mph oncoming**	
Test Vehicle	**No of runs**	**Warnings**	**CIB Brake**
Vehicle A	2	0	0
Vehicle B	5	5	5
Vehicle C	2	0	0
Set 3			
Speeds	**Test Vehicle**	**25 mph**	
	Target System	**15 mph oncoming**	
Test Vehicle	**No of runs**	**Warnings**	**CIB Brake**
Vehicle A	0	0	0
Vehicle B	5	5	5
Vehicle C	0	0	0

Table 42: Opposite Direction Tests Results for Baseline Production Vehicles – Target OD3 Towed Balloon Car

Target: OD3 - Towed Balloon Car			
Set 1			
Speeds	**Test Vehicle**	**20 mph**	
	Target System	**10 mph oncoming**	
Test Vehicle	**No of runs**	**Warnings**	**CIB Brake**
Vehicle A	4	0	0
Vehicle B	5	1	1
Vehicle C	0	0	0
Set 2			
Speeds	**Test Vehicle**	**25 mph**	
	Target System	**10 mph oncoming**	
Test Vehicle	**No of runs**	**Warnings**	**CIB Brake**
Vehicle A	0	0	0
Vehicle B	1	0	0
Vehicle C	0	0	0

Table 43 shows the average speed reduction (based only on trials where activations occurred) for all vehicles tested A, B, and C and the Target system OD1, OD2 and OD3.

Table 43: Speed Reduction for the Three OD Cases (OD1, OD2, and OD3)

			Average Speed Reduction (in km/h) Across the Three Trials Run		
Target no	**Target name**	**Initial speed**	**Vehicle A**	**Vehicle B**	**Vehicle C**
OD1	Hanging Corner Reflector	20 mph / -10 mph	no braking	2.73	no braking
		25 mph / -10 mph	no braking	3.21	no braking
		25 mph / -15 mph	not tested	0.41	not tested
			Average Speed Reduction in km/h		
Target no	**Target name**	**Initial speed**	**Vehicle A**	**Vehicle B**	**Vehicle C**
OD2	Balloon Car Carrier	20 mph / -10 mph	no braking	2.7	no braking
		25 mph / -10 mph	no braking	2.78	no braking
		25 mph / -15 mph	not tested	1.75	not tested
			Average Speed Reduction in km/h		
Target no	**Target name**	**Initial speed**	**Vehicle A**	**Vehicle B**	**Vehicle C**
OD3	Towed Balloon Car	20 mph / -10 mph	no braking	1.37	not tested
		25 mph / -10 mph	not tested	0	not tested
		25 mph / -15 mph	not tested	not tested	not tested

Results indicated that braking was only evident in Vehicle B. The speed reduction for the opposite direction case for Vehicle B showed higher speed reduction at the lower closing velocity.

L.7.3 PIP Vehicle Test Phase

The OD test procedure was changed from the production vehicle testing by using a different target and tow system. The new method is depicted in Figure 80. In the testing for the production phase, three target types were used and are identified as OD1, OD2 and OD3. In each case, the target was moved to its required speed, either 10 mph or 15 mph, in the opposite direction to the travel of the vehicle under test containing the CIB braking system. For the PIP phase of testing, a tow system was designed and built to eliminate the affect of having a vehicle towing or holding a target in near proximity to the actual target.

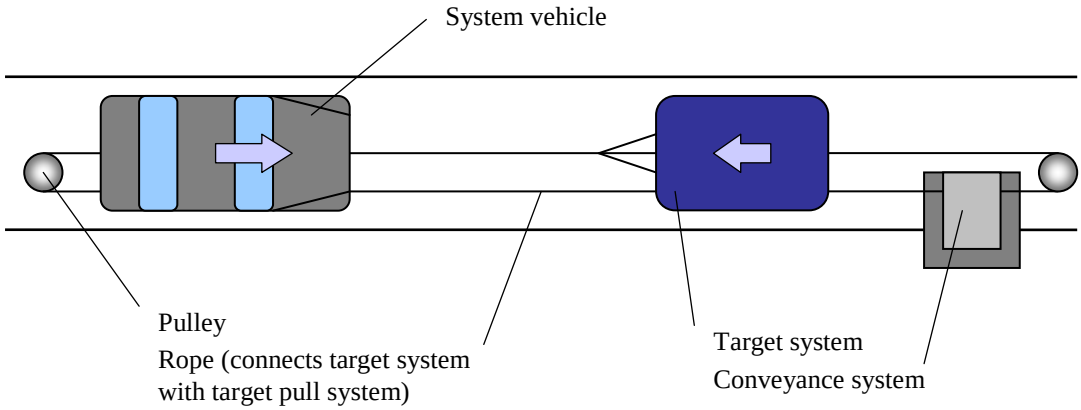

Figure 80: Balloon car with Tow System for Opposite Direction Testing of PIP Vehicles

For the PIP vehicle testing Table 44 shows the speeds for the target and the test vehicle that were conducted during testing. Note that the longitudinal speeds for the target vehicle are negative since it is an oncoming speed.

Table 44: Longitudinal Velocities for Opposite Direction Crash Scenario

	Test Vehicle Speed	Target Speed	Closing Speed
Longitudinal Velocities	**Mph (km/h)**	**Mph (km/h)**	**Mph (km/h)**
Test Speed Combinations	20 (32.2) 30 (48.2) 20 (32.2)	-10 (-15.6) -10 (-15.6) -20 (-32.2)	30 (48.2) 40 (64.3) 40 (64.3)

The test scenarios included one target type, a balloon car towed with a custom built tow system. Two different balloon cars were used during the testing. The blue balloon car identified in the target type section was used for 90% of the testing. Near the end of the testing, a newer, more visually representative orange balloon car was used. However, very few runs were made with the orange balloon car due to its weakness in being hit multiple times at closing speeds greater than 30 mph.

L.7.3.1 Detailed Results from PIP Vehicle Testing

For the OD testing with the prototype vehicles, all three PIP vehicles were used, but with different sensor settings (as described in Section 3.5 of the report). This test scenario was conducted with two different target systems: the orange balloon car and the blue balloon car. For each velocity and each target system, test runs were conducted at test vehicle speeds of 20 mph and 30 mph and target speeds of 10 mph and 20 mph in the opposite direction along the longitudinal axis. This resulted in closing speeds of 30 mph and

40 mph. Whereas the maximum closing speeds for the blue balloon car target systems was near 40 mph or less, the maximum closing speed for the orange balloon car was 30 mph or less. At higher speeds, the target systems were damaged or vehicle damage occurred. The front end of the production vehicles were covered with either gaffers tape, foam insulating material, polymer tape, bubble wrap or a combination of these materials to reduce front end damage. Also, specially fabricated steel tubing bumper guards were installed on Vehicle E and Vehicle G as a precaution to prevent front-end damage. In some cases, the number of test runs was reduced when damage was evident. This occurred when the tested vehicles CIB system did not react in any way (i.e., audible or visual warning, belt pretension or braking) several times in a row at the lowest speed. The orange balloon cars, in particular, were easily damaged.

Table 45 below shows the results of the PIP vehicle testing for OD with the target LVS2A (i.e., Towed Blue Balloon Car). Results indicated that no vehicle had any warnings or CIB brake activations for the chosen test speeds. Target OBC (i.e., towed orange balloon car) results are shown in Table 46. Again, none of the PIP vehicles had any warning or CIB braking activations at the speeds tested. The three PIP test vehicles ran very few of the tests with the OBC target. This was due to the fact that at closing speeds greater than 30 mph damage to this balloon car would occur. In fact through repeated testing, the life of the OBC balloon car at 30 mph is about nine impacts before extensive damage would occur.

Table 45: Opposite Direction Tests Results for PIP Vehicles – Target LVS2A Towed Blue Balloon Car

Target: Towed Blue Balloon Car						
Set 1						
Speeds	**Test Vehicle**	**20 mph**				
	Target System	**10 mph**				
Test Vehicle	**System**	**TTC [sec]**	**Decel [G's]**	**No of runs**	**Warnings**	**CIB Brake**
Vehicle E	Radar + Stereo Vision	1.0	0.9	5	0	0
Vehicle F	Radar Fusion	N/A	N/A	5	0	0
Vehicle G	Fusion: Radar + Vision	1.0	0.6	5	0	0
Set 2						
Speeds	**Test Vehicle**	**30 mph**				
	Target System	**10 mph**				
Test Vehicle	**System**	**TTC [sec]**	**Decel [G's]**	**No of runs**	**Warnings**	**CIB Brake**
Vehicle E	Radar + Stereo Vision	1.0	0.9	3	0	0
Vehicle F	Radar Fusion	N/A	N/A	3	0	0
Vehicle G	Fusion: Radar + Vision	1.0	0.6	3	0	0
Set 3						
Speeds	**Test Vehicle**	**20 mph**				
	Target System	**20 mph**				
Test Vehicle	**System**	**TTC [sec]**	**Decel [G's]**	**No of runs**	**Warnings**	**CIB Brake**
Vehicle E	Radar + Stereo Vision	1.0	0.9	3	0	0
Vehicle F	Radar Fusion	N/A	N/A	2	0	0
Vehicle G	Fusion: Radar + Vision	1.0	0.6	3	0	0

Table 46: Opposite Direction Tests Results for PIP Vehicles – Target OBC Towed Orange Balloon Car

Target: Towed Orange Balloon Car						
Set 1						
Speeds	**Test Vehicle**	**20 mph**				
	Target System	**10 mph**				
Test Vehicle	**System**	**TTC [sec]**	**Decel [G's]**	**No of runs**	**Warnings**	**CIB Brake**
Vehicle E	Radar + Stereo Vision	1.0	0.9	3	0	0
Vehicle F	Radar Fusion	N/A	N/A	2	0	0
Vehicle G	Fusion: Radar + Vision	1.0	0.6	3	0	0

Hence, the results indicate that the speed reduction for the PIP systems did not respond to the targets in either warning or in CIB system brake activation.

The testing for the PIP vehicles has shown that none of the vehicles responded to the opposite direction targets and test process. This result was not unexpected since many of these systems may have been specifically designed to disregard targets coming in an opposite direction trajectory.

The opposite direction test method evolved from a tow vehicle carrying the balloon car (three tow vehicle methods) to the impact point with the test vehicle to a balloon car drive system that transported the target to the impact point. In both cases, the control of the target system was open loop and timing was done manually by coordination between the driver and a spotter monitoring the target to test vehicle clearance. The impact point

between the balloon car and the test vehicle varied from run to run and did not occur in the exact same point due to the inaccuracy of the current test methods. As was discussed for the SCP method, the next phase of testing required a closed loop control method to allow more precise positioning of the target with respect to test vehicle. In addition, the balloon cars were the only targets capable of enabling this maneuver. The blue balloon car was robust to high speed impacts but difficult for the vision system to classify as a vehicle. The orange balloon car was better visually but of weak durability when impacted at even low speeds. The targets for the baseline and the PIP testing also required painting with aluminum paint to aid in radar reflectivity which can be time-consuming and labor intensive.

Overall, the test method was acceptable to set up the crash scenario by positioning the balloon car in front of the test vehicle. It was possible to move the balloon car longitudinally in the opposite direction to the test vehicle to test an oncoming vehicle to vehicle crash scenario. Coordination and timing was somewhat dependant on the human interface to coordinate and set up the test in the correct sequence of time required.

L.7.4 Validation Test Phase

L.7.4.1 Testing Method

The OD test method developed during the baseline and development testing phases was further refined in this development and validation testing phase, with the primary improvements being made in the towing of the balloon car target. The 2nd-generation balloon car was used for this testing (see Figure 81), since the 3rd-generation balloon car was not available when this testing was conducted. In addition, Vehicle E was the only vehicle tested in the OD scenario during validation, because the results from the earlier method development tests indicated that the other two systems would not apply the brakes in this test condition. Therefore, the demonstration and validation of this test method was completed by running multiple test runs at the predetermined test speeds with Vehicle E. The Stereo-Vision system installed in Vehicle E was also active during this testing.

Figure 81: 2nd-Generation Balloon Car Front, Side and Rear Views

As mentioned earlier, at the start of an OD test run, the test vehicle was positioned at one end of the test track lane, and balloon car target was positioned at the other end of the test track lane. This test method also used the target tow system, steel braided guide cables, the balloon car carrier, anchor plates, the tow motor, and the drive rope (see Figure 82 and Appendix G). Overall, the tow approach was similar to that used with the LVM test method, except in this case the balloon car approached the vehicle head-on.

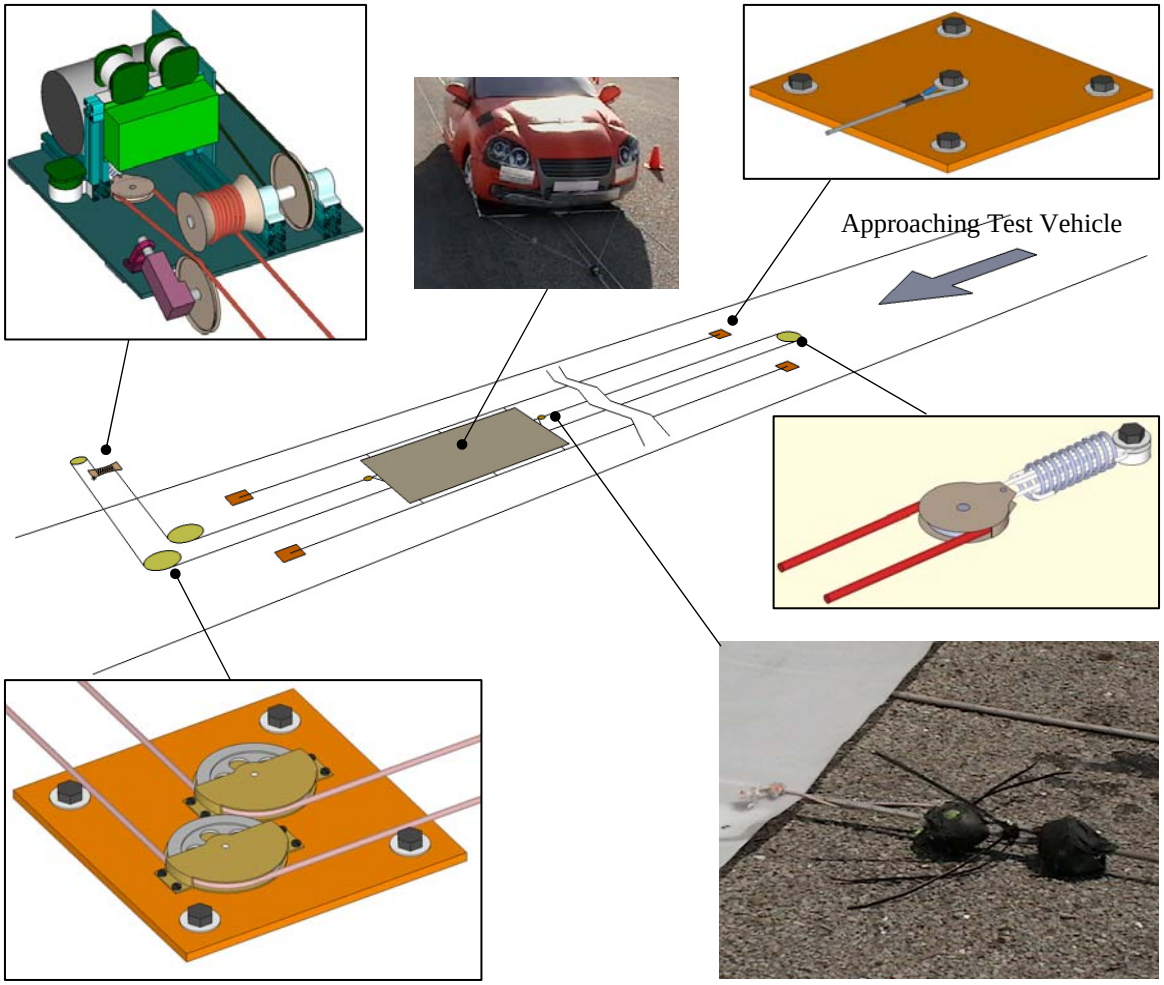

Figure 82: Test Method System Components for the OD Test Scenario

L.7.4.2 Detailed Test Results

Vehicle E, which included Mono-Vision, Stereo-Vision and Radar sensing systems, was used to conduct a set of 10 runs for each of the three different initial/target speed combinations (20 mph test vehicle / 10 mph target, 30 mph test vehicle / 10 mph target, and 20 mph test vehicle / 20 mph target). During these test runs, both the Radar and Stereo-Vision systems were active, whereas the Mono-Vision and Fusion results were later simulated. No braking events were noted in these test runs and, therefore, no speed reductions were observed for either the active or simulated systems evaluated. This is consistent with earlier testing from the baseline and development phases of the project. As indicated above, Vehicles F and G were not used in this OD testing because earlier test data indicated they also would not have brake activations for this test scenario.

L.8 Pole / Tree

L.8.1 Test Method

The research from the data analysis phase of the project highlighted four potential CIB-applicable, vehicle-to-object crash conditions, all of which were preceded by a road departure. These conditions included impacts with poles, trees, roadside structures, and the ground. Autonomous braking systems become significantly less effective as the vehicle departs the roadway due to the reduction in tire traction. Therefore, the field data for these crash conditions was filtered to include only impacts which occurred within one lane-width of the roadway surface. Ground impacts were also eliminated due to the inability of CIB sensing systems to differentiate between the ground beneath the vehicle and a potential impact with a berm or ditch. Additionally, it was assumed that most of the roadside structures in question would provide similar sensor signatures as targets representing stationary vehicles. This would allow benefits estimates for impacts with roadside structures to be calculated based on the Lead Vehicle Stopped test results. Therefore, this section focuses on developing test methods and targets for the remaining pole and tree crash conditions.

Based on the crash data analysis conducted, two pole sizes and configurations were selected for testing in this scenario. These included representations of a 10 cm metal pole and a 30 cm wooden pole/tree. This scenario represented a new test configuration with no established test target options. Therefore, the first iteration of testing using the baseline production vehicles focused mainly on developing the preliminary test methodology, as well as initial target designs. These targets and test methods were then further developed during the PIP vehicle testing.

L.8.1.1 Test Procedure

These tests involve suspending a surrogate target representing a pole or tree in the path of the test vehicle. The target must be suspended in a manner which isolates the target as much as practicable from the surrounding environment as well as from the suspension structure. The target and support structure must also perform in a manner which prevents damage to the test vehicle upon impact with the target. Once the target is in place, the test vehicle is positioned with the center of the front bumper contacting the target. This position is then recorded as a fixed point on the DGPS and used in recording the ground-truth data between the test vehicle and the target, which includes range and range rate to the target. Once the fixed point is established, the test vehicle is moved to a sufficient distance from the target to allow the driver to accelerate to a steady-state test speed. For consistency with the other test methods, speeds ranging from 20 mph to 40 mph were established for the test vehicle, and the vehicle dynamics and ground-truth data were collected through the DGPS. The documented test results include the percentage of autonomous braking events recorded during the test series, as well as the speed reduction achieved between the time braking is initiated and impact with the target.

L.8.1.2 Detailed Results from Baseline Tests

For the baseline test phase, only one test vehicle was used due to the timing of the tests and the expiration of the lease agreement associated with Vehicle C. Since Vehicle B provided braking under certain scenarios which had not triggered responses in the other

two vehicles, it was selected for these tests. The CIB system on that vehicle included radar sensors only. Therefore, the preliminary target development focused on surrogates applicable to that technology.

A simple set of two target sizes was constructed from different foam materials and coated with a layer of metallic foil tape. The amount and position of this foil was adjusted to roughly correlate to similar-sized trees and poles located on the test facility premises. Correlation, in this case, was based upon data from a supplemental test vehicle which contained a development radar unit. This supplemental vehicle included instrumentation that provided an indication of whether an object was detected in-path of the vehicle. Various poles and trees were identified on the test facility premises that were surrounded by as little clutter as possible. The vehicle was then driven up to these objects until the front bumper nearly touched the object and the in-path object indication was activated. The vehicle was then driven slowly rearward until the in-path object indication disappeared. The distance between the vehicle and the object was then measured. Multiple measurements were taken for each object to assess variation in these values. These measurements were then repeated using the preliminary pole and tree targets until the adjustments to the foil resulted in similar results. Each target was then suspended from the boom portion of the hanging target used previously for other vehicle-to-vehicle testing as shown in, Figure 83 and Figure 84. After some initial trial runs, the large pole target was deemed too heavy and stiff, leading to potential damage to the test vehicle. Therefore, further testing with the baseline vehicle was limited to the 10 cm metal pole target with the understanding that further target development would be needed for the next phase of tests.

Figure 83: Baseline Testing with Large Pole/Tree Target

Figure 84: Baseline Testing w/ Target Suspended from Boom of Hanging Apparatus

As shown in Table 47, 15 test runs were completed for this scenario with 13 CIB activations. Test speeds used in this phase included 20 mph, 25 mph, 30 mph, and 40 mph. Most of the tests were conducted with the pole impacting the center of the test vehicle bumper. A small number were conducted with left and right offset impacts. No significant differences, however, were noted in the test results based on target impact point. Of the activations that were recorded, an overall mean speed reduction of 3.36 mph was achieved with an overall standard deviation of 2.10 mph. The speed reductions and percentage of CIB activations are comparable to other test scenarios conducted with this vehicle. The standard deviation, however, was rather high. Based on the manner in which the target was suspended from the boom connected to the support vehicle, it is possible that the support vehicle affected the test results, potentially influencing the number of system activations as well as the variation in speed reductions. With no access to the vehicle's sensor data, this could not be verified until a more refined test method was developed in the next phase.

Table 47: Baseline Vehicle B Test Results for Small Pole Scenarios

Initial Speed [mph]	target Impact	Activation	Speed Reduction [mph]	Mean	Std Dev	Overall Mean	Overall Std Dev
20	central	braking	3.69	3.36	2.28	3.36	2.10
20	central	braking	0.04				
20	central	braking	5.01				
20	central	no braking					
20	central	braking	4.70				
20	right	no braking		4.33	2.39		
20	left	braking	6.02				
20	left	braking	2.64				
25	center	braking	5.59	5.17	0.92		
25	center	braking	4.12				
25	center	braking	5.79				
30	center	braking	0.63	1.95	1.18		
30	center	braking	2.30				
30	center	braking	2.91				
40	center	no braking		0.27			
40	center	braking	0.27				

L.8.1.3 Detailed Results from Prove-out Tests with PIP Vehicles

The prove-out tests using the PIP vehicles focused on developing a more refined test method and generating test data from the various PIP system configurations to determine whether this test method is capable of adequately differentiating system performance levels. For this phase of testing, two main objectives required addressing. First, more representative targets were needed for both the 10 cm metal pole and the 30 cm wooden pole/tree. Second, a support structure was needed which was capable of positioning the target(s) in the proper location and orientation without interfering with the sensor responses from the PIP vehicles. The structure had the added requirement of supporting the targets in a manner which allowed impact between the test vehicle and targets without damaging the test vehicles or causing a hazard to the test personnel. Figure 85 displays the support structure developed for this phase of testing.

Figure 85: Support Structure for Pole/Tree Tests w/ PIP Vehicles

The support structure shown Figure 85 consists of two vertical posts measuring 4”x4”x14’ with a plywood base attached to the bottom of each post. These posts are placed as far apart across the test track as practicable to minimize their potential effect on the CIB sensor readings. A tension cable connects the top ends of the two posts. Two cables from the top end of each post are then each connected through ratcheting cable winches to ground anchors positioned outboard of the posts equidistant from the posts such that each support cable forms an approximate 45° angle with the ground. Once the posts are erected and the guide cables attached to ground stakes, the ratcheting cable winches are tightened equally until the upper tension cable is tight and the support posts are vertically level. If necessary, the bottom position of the support posts were adjusted using a sledge hammer until the posts was vertical along both their planes. Once the post positions were verified and the cables tightened, an anchor stake was driven through a hole in each of the post base plates to ensure that the plates remained fixed in place, as shown in Figure 86. The size and length of the ground anchors was selected based upon the solidity of the soil at the test site. The prove-out tests with the PIP vehicles were conducted at a proving grounds in Texas, which was largely hard-pan desert soil. Stakes of $^{5}/_{8}$” diameter x 3’ were sufficient in this location to prevent the stakes from pulling up during the test.

Figure 86: Staking Method Used for Anchoring the Post Base Plate

Once the support structure was fabricated, a towline was strung through a series of pulleys and attached to the same tow system motor assembly used for the vehicle-to-vehicle tests using towed balloon cars. (This towline was also installed for use in the vehicle-to-pedestrian test scenarios.) However, the towline also provided a convenient means of attaching the pole and tree targets to the support structure, providing the ability to move and lower the targets as needed between tests. To maintain the targets at the appropriate height, a threaded chain link and pulley were used to connect the towline to the upper tension cable at the target attachment point (see Figure 87). The lower end of the target was then attached to a taught lower support line, shown above in Figure 86, which helped minimize any swinging motion from the target. A small-diameter rope was used for this attachment to prevent any potential interference that a cable might pose to CIB radar sensors. Connections between the targets and these upper and lower support lines were made using plastic wire ties. This was done to allow the target to break free of the support structure upon impact, minimizing the potential for damage to the test vehicle and minimizing the forces transmitted through the support structure itself.

Figure 87: Chain Link Attachment Connecting the Towline and Upper Tension Cable

The final step in constructing the support structure was masking the vertical posts and other hardware as much as possible from interfering with the CIB sensors. The preferred choice for accomplishing this is to place the vertical support posts as far apart as possible. The ground surface at this test location, however, became uneven quickly beyond the edge of the test track. Therefore, radar-absorbing foam was added to the leading edge of the support posts, as shown in Figure 88.

Figure 88: Radar-Absorbing Foam Added to Support Posts

With the support structure fabricated, the next step in developing the pole and tree test method involved constructing and correlating representative targets. The PIP vehicles used in this test phase included the capability of recording the sensor data returned from a given target. Therefore, target correlation in this phase could be conducted with a higher level of confidence than the method used with the baseline production vehicles. Similar to the process used for the baseline tests, surrogate poles and trees were identified on the test facility premises which had as little surrounding clutter as possible. These included various trees, telephone poles, flagpoles and sign posts. The test vehicles were driven separately toward each object until the center of the front bumper contacted. Each vehicle was then driven slowly rearward as the data acquisition system recorded the radar power return versus distance measurements as well as the camera image data. After recording a few series in this manner, however, it was noted that undulations in the ground surface were causing irregular sensor return data. Therefore, a more controlled technique was employed. After locating an unused telephone pole and flagpole on the premises, sections of each were cut to approximately 4 feet in length. These samples were then supported within the target support structure in the same location as the intended target position, as shown in Figure 89, Figure 90, Figure 91, and Figure 92. The correlation measurements were then repeated, this time with more consistent data measurements.

Figure 89: Telephone Pole Sample Supported at Target Location

Figure 90: Position of PIP Vehicle at Start of Correlation Data Measurement

Figure 91: Beginning of Correlation Data Measurement of Telephone Pole Sample

Figure 92: Correlation Data Measurement Using Metal Pole

Once the baseline data was collected, targets representing 10 cm metal poles and 30 cm wooden trees/poles were developed and correlated as closely as possible to corresponding real objects. Lightweight and soft target materials were selected based upon lessons learned from the baseline tests with production vehicles. Low-density foam tubes, commonly referred to as "swim noodles," measuring 4 feet in length and 4 inches in diameter were used as the core target structure. To represent the small metal pole, a single foam tube was wrapped in metallic foil tape along its entire length. An overlay of clear packaging tape was then applied to the entire target to help keep the foil in place, maintain the target shape, and prevent any sharp edges from developing along the foil. This target required few development iterations since the exposed foil tape provided the closest correlation achievable with a structure that could be struck by the test vehicles without causing damage. Figure 93 depicts the final small pole target design.

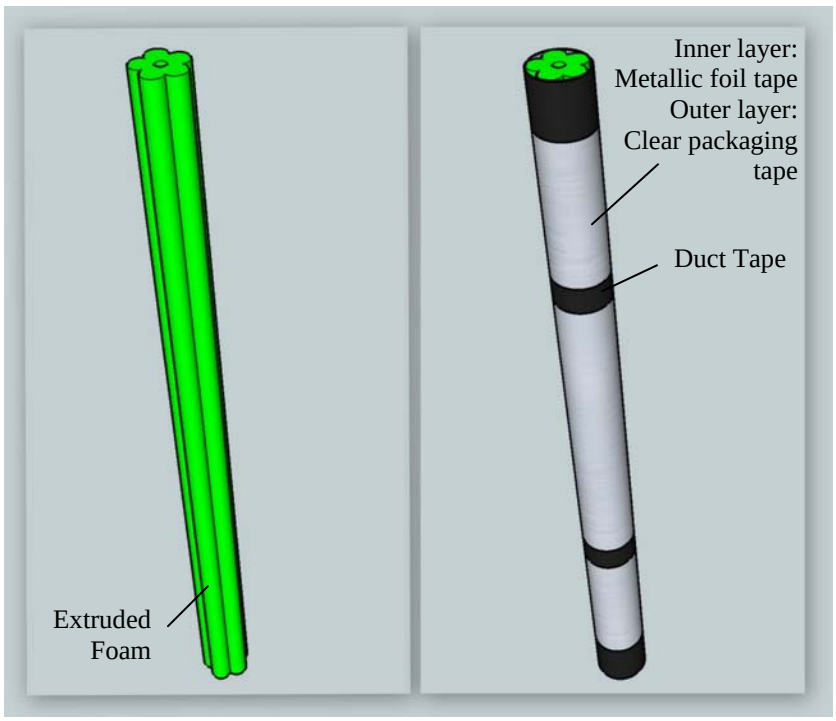

Figure 93: Small Pole Target Design

The graph shown in Figure 94 displays the radar correlation measurements made between the simulated pole target depicted in Figure 93, above, and the sample poles measured earlier. Upper and lower bounds were developed using 4th-order polynomial trend lines of the average sample pole measurements ± 1 standard deviation. These trend lines are highlighted as bold solid black lines. The average values of all of the sample pole measurements are highlighted as a bold solid blue line. The small pole target measurements are shown as a bold solid red line. The results indicated that correlation for the small pole target was generally good. The mean return for this target fell within ±1 standard deviations of the mean return for the sample of real objects.

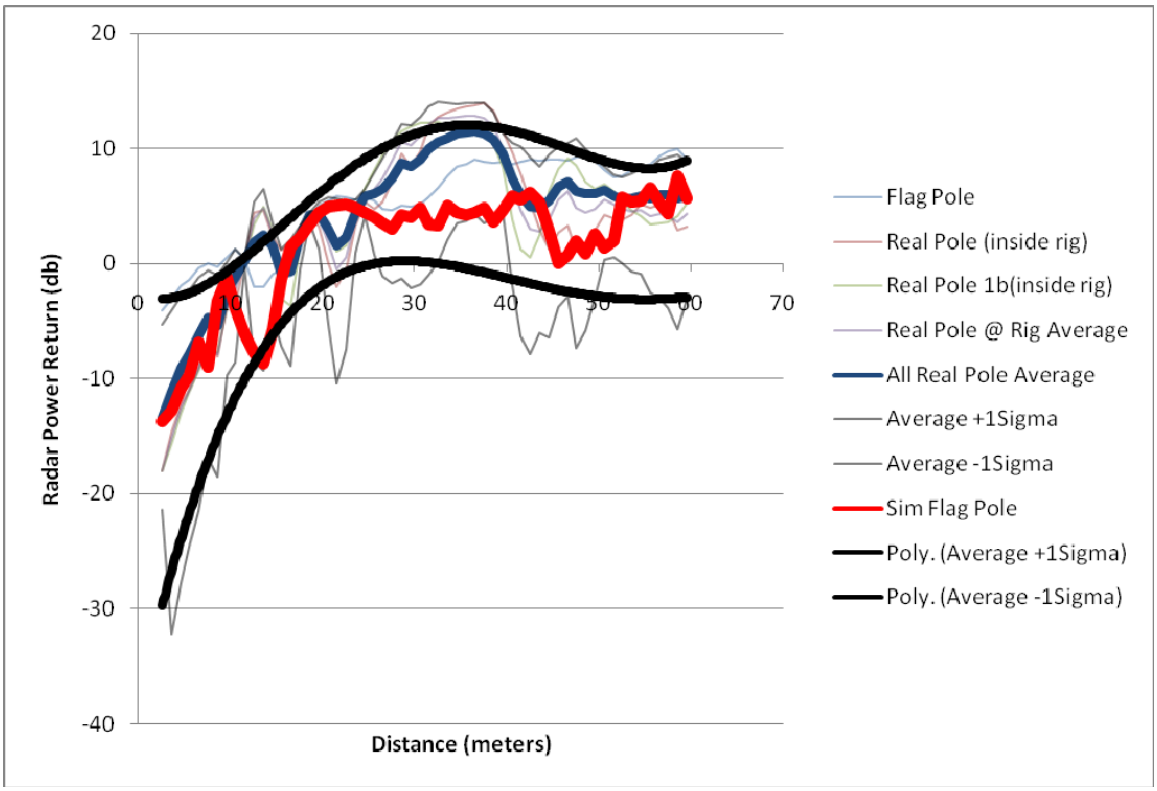

Figure 94: Correlation between Sample Metal Poles and the Small Pole Target

Correlating the larger pole/tree target posed more difficulty due to the very low power returns measured from the telephone pole section. For this target, various materials were tried until a satisfactory combination was developed. Two designs provided reasonable correlation, but with different levels of durability. The first used a 12 inch diameter by 4 foot long cardboard tube as a core. These tubes are typically used as forms for constructing concrete pillars. This core was then layered with metallic foil tape, foam, and a quilted shipping blanket, all held together with high-strength tape. The amount of metallic tape used and the thickness of the foam and quilting were then adjusted until the radar return measurements achieved from this target matched the surrogate object as closely as possible. While this target was reasonably easy to construct and correlate, the cardboard tube forming the internal structure was not sufficiently durable to complete the testing. Therefore, a second target was designed using a bundle of six low-density foam tubes like those selected for the smaller target. These tubes were arranged to achieve the same diameter and length as the previous target. As before, metallic foil tape and a quilted shipping blanket were layered until the radar return measurements achieved from the target matched the surrogate object as closely as possible. Figure 95 and Figure 96, shown below, depict the two large-pole target designs.

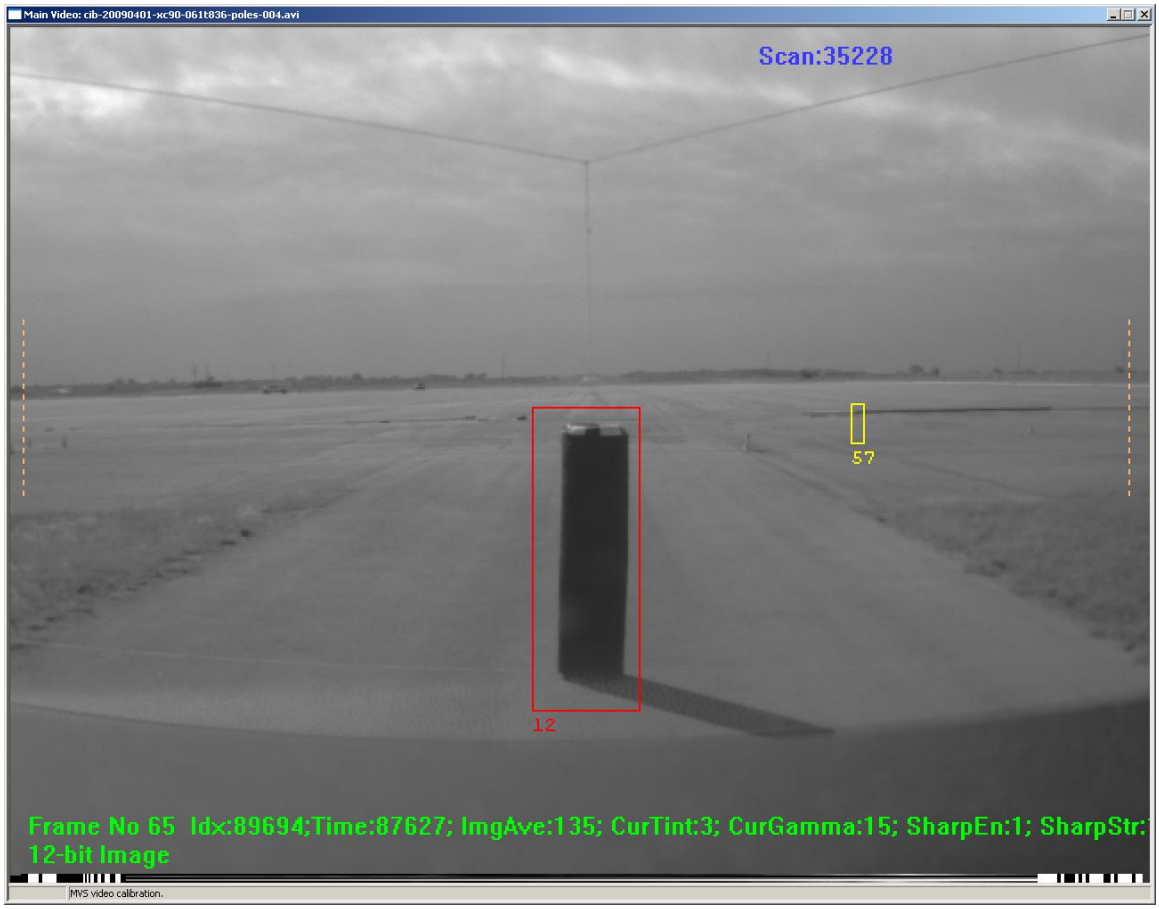

Figure 95: Large-Pole Target 1st Iteration Using Cardboard Cylinder

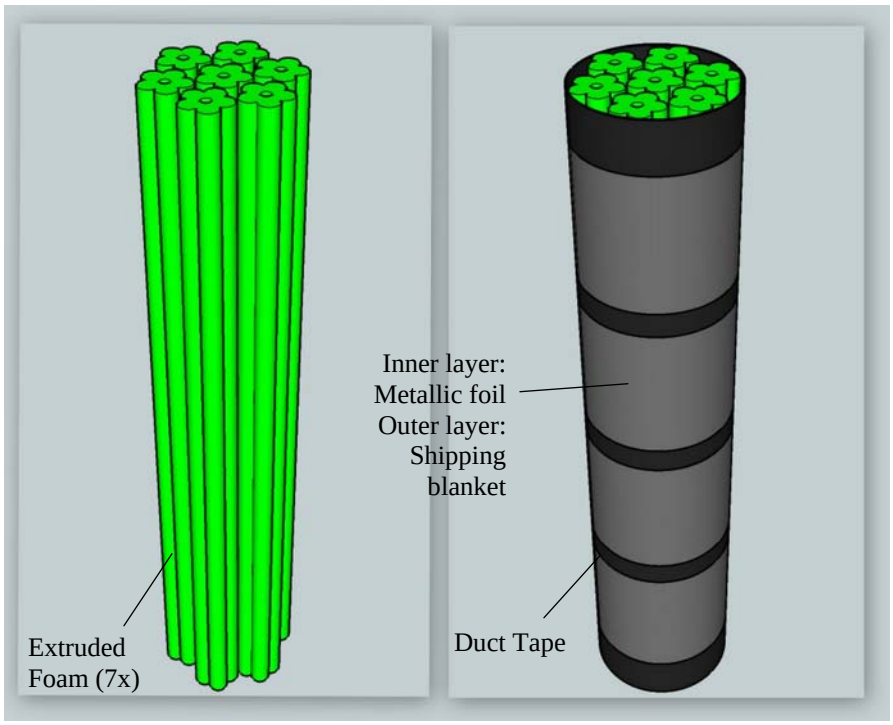

Figure 96: Large-Pole Target 2nd Iteration Using Bundled Foam Tubes

The graph shown in Figure 97 displays the radar correlation measurements made between the simulated wood pole/tree target depicted in Figure 95 and Figure 96, above, and the sample poles measured earlier. Once again, upper and lower bounds were developed using 4th-order polynomial trend lines of the average sample pole measurements ±1 standard deviation. These trend lines are highlighted as dashed red lines. The average values of all of the sample pole measurements are highlighted as a bold solid blue line. The large pole target measurements are shown as a solid red line. The results indicated that correlation for the large pole target was generally good. The mean return for this target fell within ±1 standard deviations of the mean return for the sample of real objects.

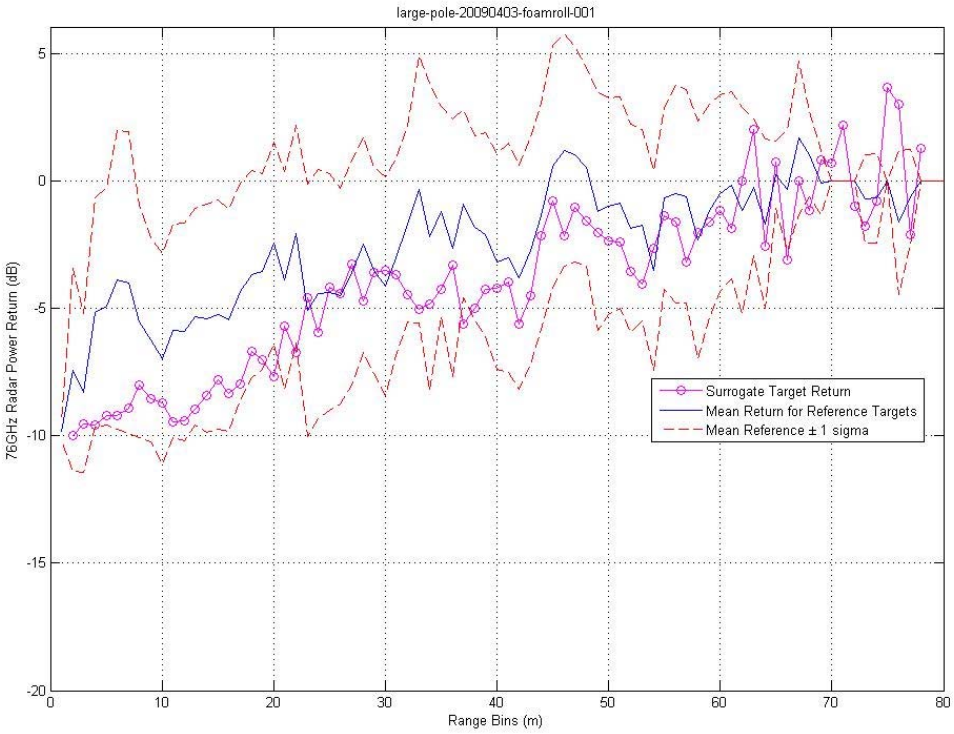

Figure 97: Correlation between Simulated Large Pole/Tree Target and Actual Poles

Table 48 and Table 49 contain test data summaries for the three PIP vehicles under each CIB system configuration evaluated. As these tables indicate, the PIP CIB systems activated in relatively few tests. Of the braking activations that did occur, many of these resulted in less than 1 mph of speed reduction. All of the activations which resulted with the small and large pole targets occurred using radar-only sensor configurations.

Due to the early development stage of the stereo vision system in Vehicle E, data from this system had to be derived from post-processing and was limited to information regarding whether the object was detected. A summary of the stereo vision test results for poles is shown in Table 50 below.

Table 48: PIP Test Results for Small Pole Target

PIP Vehicle	TTC Setting (sec)	Decel Setting (g's)	Sensor Set	Initial Speed [mph]	Speed Reduction [mph]					Mean	Std Dev	Overall Mean	Overall Std Dev
					Run 1	Run 2	Run 3	Run 4	Run 5				
S550	fixed	fixed	fixed	20	**	**	10.60	**	**	10.60	n/a	5.54	7.16
	fixed	fixed	fixed	30	**	0.47	**	**	**	0.47	n/a		
	fixed	fixed	fixed	40	**	**	**	**	**	n/a	n/a		
XC90	1.0	0.3	Radar	20	**	**	**	**	**	n/a	n/a	6.90	n/a
				30	**	**	6.90	**	**	6.90	n/a		
				40	**	**	**	**	**	n/a	n/a		
			Mono Camera	20	**	**	**	**	**	n/a	n/a		
				30	**	**	**	**	**				
				40	**	**	**	**	**				
			Fusion	20	**	**	**	**	**	n/a	n/a		
				30	**	**	**	**	**				
				40	**	**	**	**	**				
	1.0	0.8	Radar	20	**	**	**	**	**	n/a	n/a	n/a	n/a
				30	**	**	**	**	**				
				40	**	**	**	**	**				
			Mono Camera	20	**	**	**	**	**	n/a	n/a		
				30	**	**	**	**	**				
				40	**	**	**	**	**				
			Fusion	20	**	**	**	**	**	n/a	n/a		
				30	**	**	**	**	**				
				40	**	**	**	**	**				
Equinox	0.6	0.9	Radar	20	**	**	**	0.31	0.58	0.45	0.19	0.30	0.28
				30	**	**	**	**	**	n/a	n/a		
				40	**	**	**	0.02	**	0.02	n/a		
			Mono Camera	20	**	**	**	**	**	n/a	n/a		
				30	**	**	**	**	**	n/a	n/a		
				40	**	**	**	**	**	n/a	n/a		
			Fusion	20	**	**	**	**	**	n/a	n/a		
				30	**	**	**	**	**	n/a	n/a		
				40	**	**	**	**	**	n/a	n/a		
	1.0	0.9	Radar	20	**	**	**	**	5.73	5.73	n/a	3.25	2.33
				30	2.98	3.85	**	0.92	1.19	2.24	1.41		
				40	**	**	5.86	5.41	0.04	3.77	3.24		
			Mono Camera	20	**	**	**	**	**	n/a	n/a		
				30	**	**	**	**	**	n/a	n/a		
				40	**	**	**	**	**	n/a	n/a		
			Fusion	20	**	**	**	**	**	n/a	n/a		
				30	**	**	**	**	**	n/a	n/a		
				40	**	**	**	**	**	n/a	n/a		

** - indicates no autonomous braking commanded

Note: Mono Camera and Fusion sensor set configurations were assessed through post-processing of the data collected during testing conducted with the Radar sensor set on both Vehicle E and Vehicle G.

Table 49: PIP Test Results for Large Pole/Tree Target

PIP Vehicle	TTC Setting (sec)	Decel Setting (g's)	Sensor Set	Initial Speed [mph]	Speed Reduction [mph]					Mean	Std Dev	Overall Mean	Overall Std Dev
					Run 1	Run 2	Run 3	Run 4	Run 5				
F	fixed	fixed	fixed	20	9.76	**	**	6.06	10.71	8.84	2.46	6.37	3.96
	fixed	fixed	fixed	30	**	**	**	**	**	n/a	n/a		
	fixed	fixed	fixed	40	1.09	**	**	4.23	**	2.66	2.22		
G	1.0	0.3	Radar	20	**	**	**	**	**	n/a	n/a	2.89	5.55
				30	**	**	**	**	11.21	11.21	n/a		
				40	0.13	0.13	0.09	**	**	0.12	0.02		
			Mono Camera	20	**	**	**	**	**	n/a	n/a		
				30	**	**	**	**	**				
				40	**	**	**	**	**				
			Fusion	20	**	**	**	**	**	n/a	n/a		
				30	**	**	**	**	**				
				40	**	**	**	**	**				
	1.0	0.8	Radar	20	1.36	**	0.34	**	**	0.85	0.72	2.35	5.38
				30	**	0.07	14.50	0.07	**	4.88	8.331164		
				40	**	**	0.09	0.02	**	0.06	0.049497		
			Mono Camera	20	**	**	**	**	**	n/a	n/a		
				30	**	**	**	**	**				
				40	**	**	**	**	**				
			Fusion	20	**	**	**	**	**	n/a	n/a		
				30	**	**	**	**	**				
				40	**	**	**	**	**				
E	0.6	0.9	Radar	20	0.31	0.31	**	0.25	0.25	0.28	0.03	0.28	0.03
				30	**	**	**	**	**	n/a	n/a		
				40	**	**	**	**	**	n/a	n/a		
			Mono Camera	20	**	**	**	**	**	n/a	n/a		
				30	**	**	**	**	**	n/a	n/a		
				40	**	**	**	**	**	n/a	n/a		
			Fusion	20	**	**	**	**	**	n/a	n/a		
				30	**	**	**	**	**	n/a	n/a		
				40	**	**	**	**	**	n/a	n/a		
	1.0	0.9	Radar	20	**	**	**	**	**	n/a	n/a	n/a	n/a
				30	**	**	**	**	**	n/a	n/a		
				40	**	**	**	**	**	n/a	n/a		
			Mono Camera	20	**	**	**	**	**	n/a	n/a		
				30	**	**	**	**	**	n/a	n/a		
				40	**	**	**	**	**	n/a	n/a		
			Fusion	20	**	**	**	**	**	n/a	n/a		
				30	**	**	**	**	**	n/a	n/a		
				40	**	**	**	**	**	n/a	n/a		

** - indicates no autonomous braking commanded

Note: Mono Camera and Fusion sensor set configurations were assessed through post-processing of the data collected during testing conducted with the Radar sensor set on both Vehicle E and Vehicle G.

Table 50: Stereo Vision Test Results for Pole Targets

Test Mode	# Files	Object Detected	TTC - % Detected Objects			Notes
			0.3 sec	0.6 sec	1.0 sec	
Small Pole	29	100%	66%	89%	97%	Subject to ongoing improvement
Large Pole	28	100%	79%	86%	64%	Subject to ongoing improvement

As a result of the limited activations produced during the PIP testing, this test method required further development in the validation testing phase. Although the test methodology has been developed insufficient activation data leaves the potential benefit from this scenario questionable at this point. It was uncertain whether the limited number

of activations is due to variation in the developed targets versus real-world poles and trees or system sensing limitations.

L.8.2 Validation Test Phase

For this vehicle-to-object scenario, the Pole and Tree targets used in earlier PIP vehicle testing were used for the validation test phase. As discussed in Appendix F, the Pole and Tree targets consisted of 4-inch (10 cm) and 12-inch (30 cm) diameter "pole" cylinders, respectively (see Figure 98). These are subsequently referred to as small and large pole targets, respectively. For this test method, the targets were suspended statically from the ropes used in the target tow system. All three test vehicles were used in validating this test method.

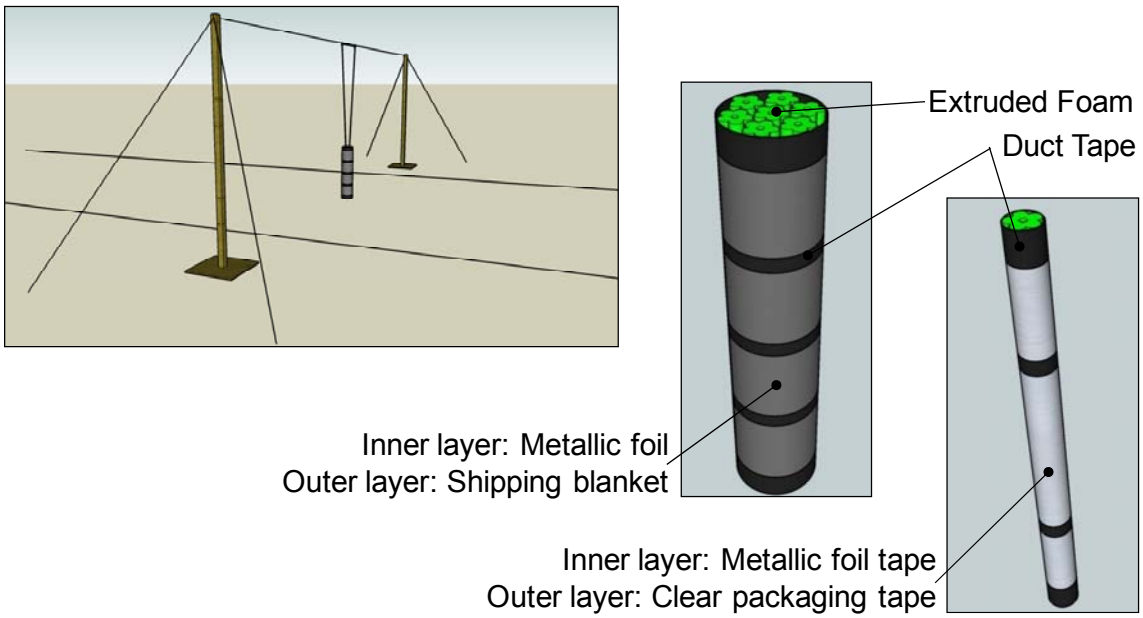

Figure 98: Pole/Tree Target Configurations

L.8.2.1 Pole/Tree Test Results

As shown in Figure 99, results with the small pole target indicated that only Vehicle G exhibited brake activations (and hence, any speed reductions). For this vehicle, the percentage of brake activations and speed reductions were similar across initial test speeds.

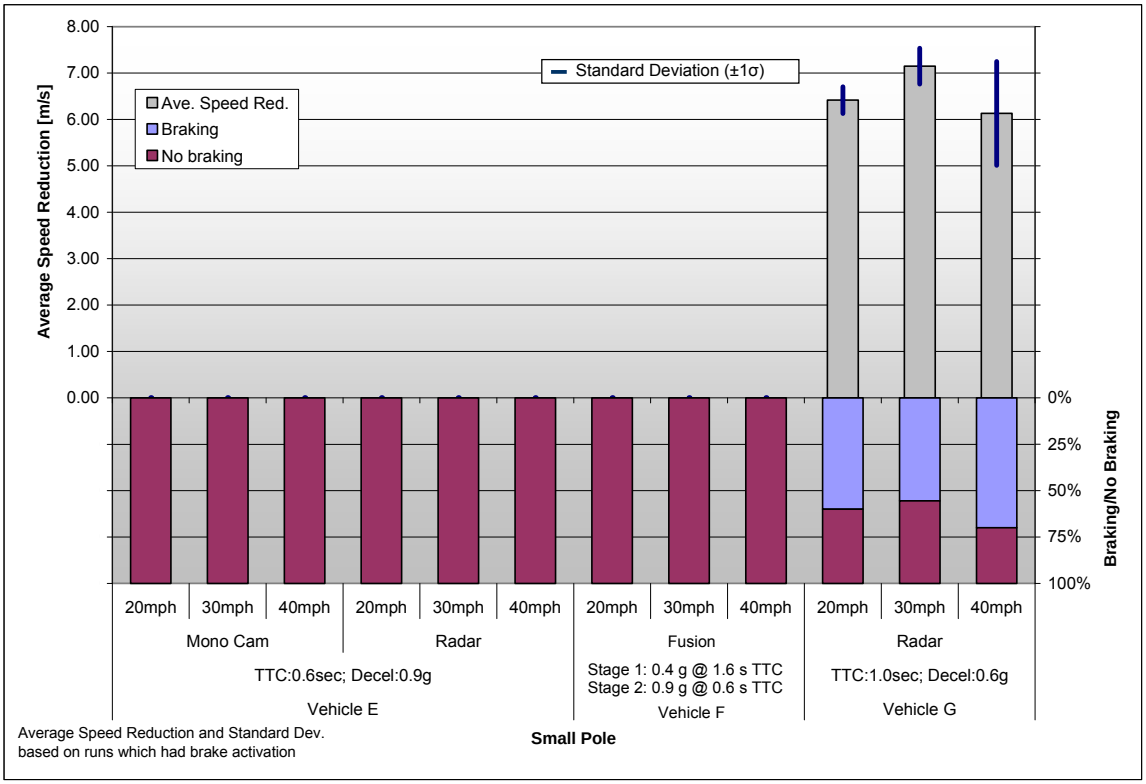

Figure 99: All Track Test Results for Small Pole

As shown in Figure 100, results with the large Pole target indicated that overall, brake activations either did not occur or only occurred rarely with about half of the Vehicle-Sensor Combinations evaluated. Vehicle G had a higher amount of brake activations across all initial speeds. The Vehicle F Fusion system had a few activations at the lower speeds and the Vehicle E Radar system activated more often at higher speeds.

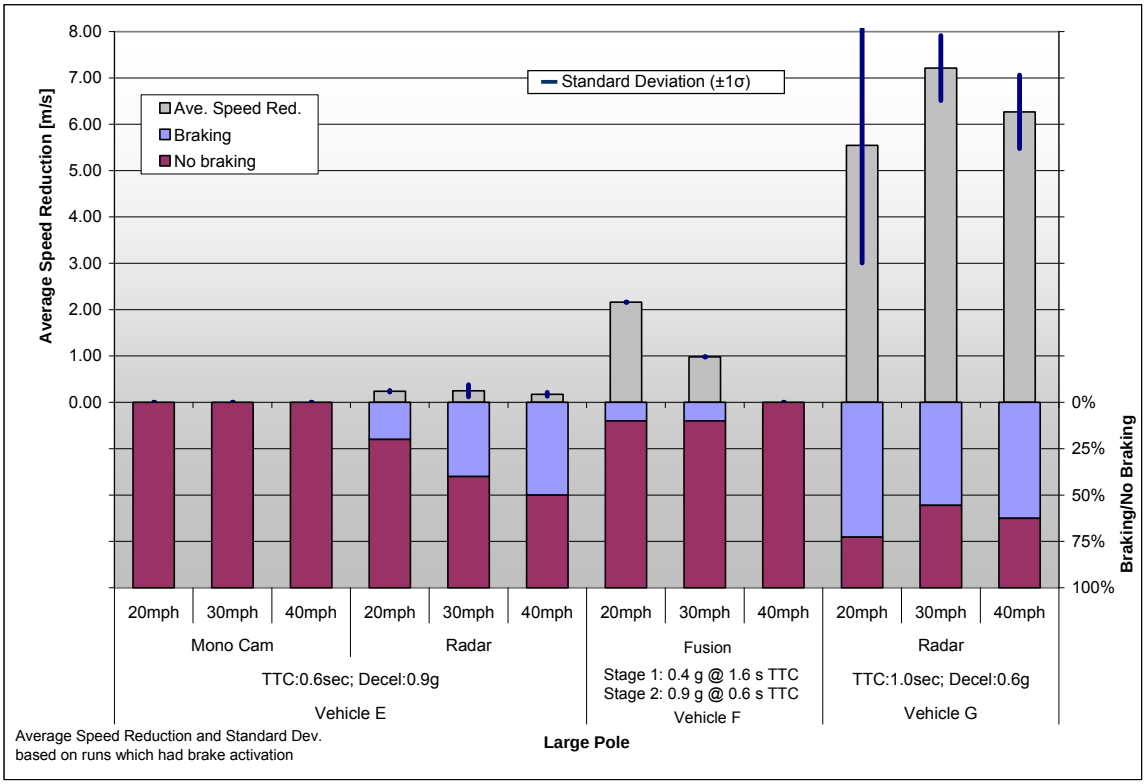

Figure 100: All Track Test Results for Large Pole

L.8.2.1.1 Vehicle E Results

As shown in Table 51 and Figure 101, Vehicle E exhibited few brake activations and these activations only occurred with the Radar system with the large pole target. (Put in another way, the Mono-Vision and Fusion systems did not activate the brakes, and no brake activations were observed with the small pole target.) For this latter Radar large-pole combination case, the percentage of brake activations increased with higher initial test speeds.

Table 51: Small and Large Pole Raw Data Summary for Vehicle E

Scenario: Poles; Target System: Small/Large Pole; Vehicle E; Settings: TTC: 0.6sec; Decel: 0.9g															
				Speed reduction in m/s											Standard Dev in m/s
Target System	Test Vehicle Speed	Track/ Simulation	Sensor Config	Run 1	Run 2	Run 3	Run 4	Run 5	Run 6	Run 7	Run 8	Run 9	Run 10	Average	
Small Pole	20mph	TRK	Mono Cam	*	*	*	*	*	*	*	*	*	*	-	-
			Radar	*	*	*	*	*	*	*	*	*	*	-	-
		SIM	Fusion	*	*	*	*	*	*	*	*	*	*	-	-
	30mph	TRK	Mono Cam	*	*	*	*	*	*	*	*	*	*	-	-
			Radar	*	*	*	*	*	*	*	*	*	*	-	-
		SIM	Fusion	*	*	*	*	*	*	*	*	*	*	-	-
	40mph	TRK	Mono Cam	*	*	*	*	*	*	*	*	*	*	-	-
			Radar	*	*	*	*	*	*	*	*	*	*	-	-
		SIM	Fusion	*	*	*	*	*	*	*	*	*	*	-	-
Large Pole	20mph	TRK	Mono Cam	*	*	*	*	*	*	*	*	*	*	-	-
			Radar	0.23	*	*	*	*	0.25	*	*	*	*	0.24	0.02
		SIM	Fusion	*	*	*	*	*	*	*	*	*	*	-	-
	30mph	TRK	Mono Cam	*	*	*	*	*	*	*	*	*	*	-	-
			Radar	*	0.38	*	0.30	*	*	0.24	0.07	*	*	0.25	0.13
		SIM	Fusion	*	*	*	*	*	*	*	*	*	*	-	-
	40mph	TRK	Mono Cam	*	*	*	*	*	*	*	*	*	*	-	-
			Radar	*	*	0.16	0.16	0.15	*	0.25	*	*	0.15	0.17	0.04
		SIM	Fusion	*	*	*	*	*	*	*	*	*	*	-	-

Average and Standard Deviation based on runs which had brake activation
* = no brake activation

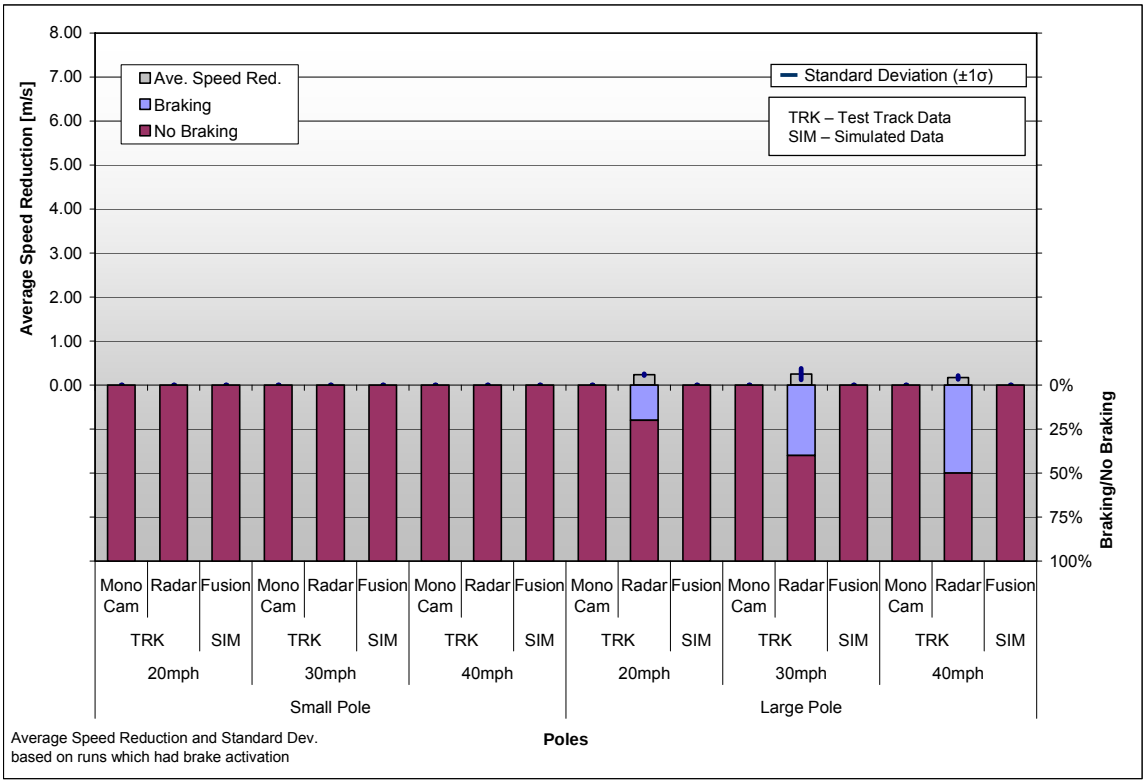

Figure 101: Small and Large Pole Data Chart for Vehicle E

L.8.2.1.2 Vehicle F Results

The Vehicle F Fusion system initiated braking only for the large pole in two cases with low and medium initial speeds (see Table 52 and Figure 102). Thus, this system never activated the brakes in response to the small pole target.

Table 52: Small and Large Pole Raw Data Summary for Vehicle F

Scenario: Poles; Target System: Small/Large Pole; Vehicle F; Settings: TTC: 1.6sec; Decel: 0.4/0.9g															
				Speed reduction in m/s											Standard Dev in m/s
Target System	Test Vehicle Speed	Track/ Simulation	Sensor Config	Run 1	Run 2	Run 3	Run 4	Run 5	Run 6	Run 7	Run 8	Run 9	Run 10	Average	
Small Pole	20mph	TRK	Fusion	*	*	*	*	*	*	*	*	*	*	-	-
	30mph	TRK	Fusion	*	*	*	*	*	*	*	*	*	*	-	-
	40mph	TRK	Fusion	*	*	*	*	*	*	*	*	*	*	-	-
Large Pole	20mph	TRK	Fusion	*	*	*	*	*	2.16	*	*	*	*	2.16	-
	30mph	TRK	Fusion	*	*	0.98	*	*	*	*	*	*	*	0.98	-
	40mph	TRK	Fusion	*	*	*	*	*						-	-

Average and Standard Deviation based on runs which had brake activation
* = no brake activation
grey = no run

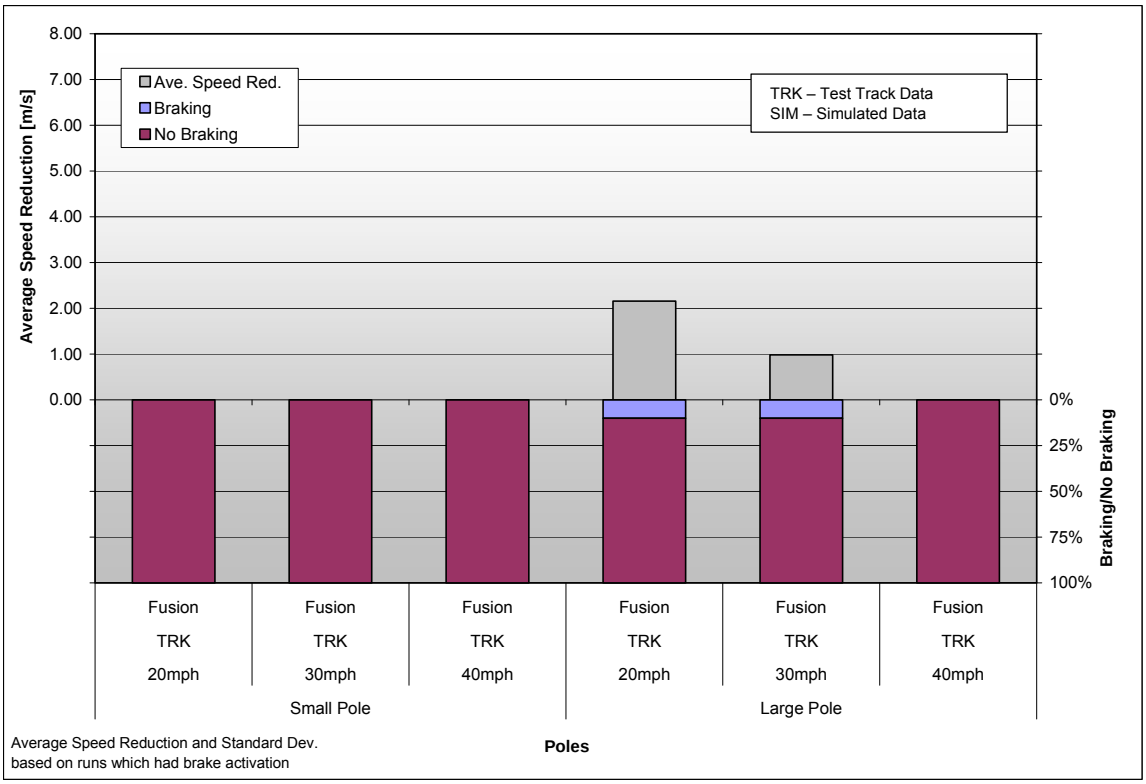

Figure 102: Small and Large Pole Raw Data Chart for Vehicle F

L.8.2.1.3 Vehicle G Results

Braking activations were triggered with Vehicle G Radar system in more than 60% of the runs for both the small and large pole poles (see Table 53 and Figure 103). When the brakes were activated, the speed reductions were high compared to Vehicle E and Vehicle F. The simulated Mono-Vision and Fusion results indicated no brake activations (and hence, speed reductions) occurred.

Table 53: Small and Large Pole Raw Data Summary for Vehicle G

Scenario: Poles; Target System: Small/Large Pole; Vehicle G; Settings: TTC: 1.0sec; Decel: 0.6g

				Speed reduction in m/s												Standard Dev in m/s
Target System	Test Vehicle Speed	Track/ Simulation	Sensor Config	Run 1	Run 2	Run 3	Run 4	Run 5	Run 6	Run 7	Run 8	Run 9	Run 10	Run 11	Average	
Small Pole	20mph	TRK	Radar	*	*	6.50	6.50	6.75	6.43	5.88	*	6.43	*		6.42	0.29
		SIM	Mono Cam	*	*	*	*	*	*	*	*	*	*		-	-
			Fusion	*	*	*	*	*	*	*	*	*	*		-	-
	30mph	TRK	Radar	*	*	*	7.12	*	7.75	6.81	6.81	7.25			7.15	0.39
		SIM	Mono Cam	*	*	*	*	*	*	*	*	*			-	-
			Fusion	*	*	*	*	*	*	*	*	*			-	-
	40mph	TRK	Radar	4.18	6.68	7.19	6.73	5.94	*	7.06	*	5.12	*		6.13	1.12
		SIM	Mono Cam	*	*	*	*	*	*	*	*	*	*		-	-
			Fusion	*	*	*	*	*	*	*	*	*	*		-	-
Large Pole	20mph	TRK	Radar	6.13	5.81	*	*	5.69	*	5.81	0.00	9.25	5.93	5.75	5.55	2.54
		SIM	Mono Cam	*	*	*	*	*	*	*	*	*	*	*	-	-
			Fusion	*	*	*	*	*	*	*	*	*	*	*	-	-
	30mph	TRK	Radar	*	*	7.43	6.56	*	7.38	6.50	8.19	*			7.21	0.70
		SIM	Mono Cam	*	*	*	*	*	*	*	*	*			-	-
			Fusion	*	*	*	*	*	*	*	*	*			-	-
	40mph	TRK	Radar	*	5.77	5.13	6.62	*	6.82	7.00	*				6.27	0.79
		SIM	Mono Cam	*	*	*	*	*	*	*	*				-	-
			Fusion	*	*	*	*	*	*	*	*				-	-

Average and Standard Deviation based on runs which had brake activation
* = no brake activation
grey cell = no run

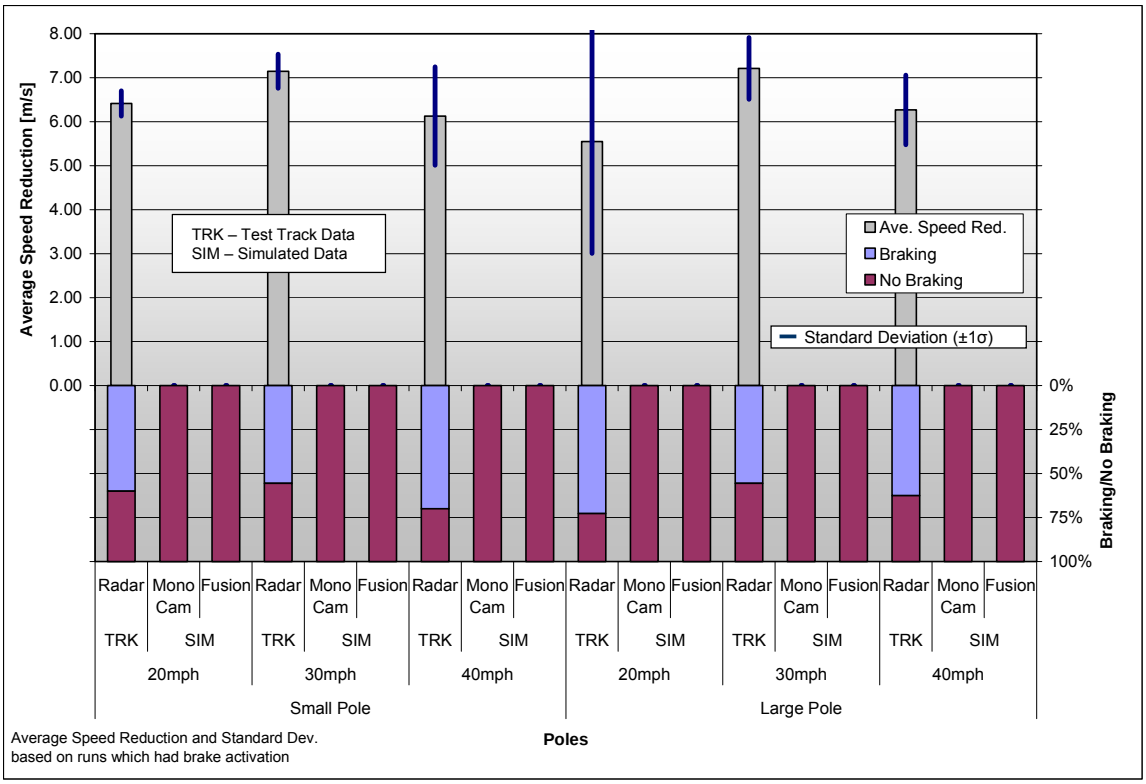

Figure 103: Small and Large Pole Raw Data Chart for Vehicle G

L.9 Rear End – Cut-In

L.9.1 Test Method

For this Rear End – Cut In scenarios, the initial target vehicle speed was 20 mph, the test vehicle speed was varied between 50 and 60 mph and the cut-in distances were varied between 40 m and 70 m. The initial evaluation of these parameters was performed with the production vehicles (Vehicles A, B and C). Various test vehicle speeds and cut-in distances were evaluated and the system reaction was monitored. Test requirements consist of the target vehicle speed at a constant 20 mph and the test vehicle speed at 50 mph and 60 mph (Table 54). The cut-in distances as shown in Table 55 continued to be varied between 40 m and 70 m while limiting the lateral velocity of less than 16 km/h (10 mph) and up to 30 degrees impact offset to the target vehicle. In order to get the test vehicle up to the steady state test speeds and perform the cut-in maneuver safely, a long straight away of at least 400-500 m is required.

Table 54: Velocities for Cut-In Scenarios

Velocities	In mph	In km/h
System vehicle	60	96.6
	50	80.5
Target system	20	32.2

Table 55: Distance between System Vehicle and Target System at Cut-In

Cut-In range	In m
Distances between	40 – 70

L.9.2 Results from Baseline Vehicle Testing

A major issue in the ability to execute and control this test method safely was identified while developing this test scenario. Initial attempts were made during the first test runs to achieve a specific desired cut-in distance and rate while also controlling the other test parameters. This proved virtually impossible, even with a very highly trained test driver. Therefore, focus shifted to gathering large samples of relatively, random, cut-in distances ranging from approximately 40 m to 70 m. It was hoped that by collecting data in this manner, a better understanding of the test parameter issues could be determined in order to develop a more controlled test method. While some conclusions were possible from the data collected, an executable and repeatable test methodology could not be found.

At the longer test vehicle cut-in distances and at all cut-in speeds, (50 mph and 60 mph) the test vehicle had sufficient time to stabilize and react to the target vehicle detected ahead. This produced comparable test results to the LVM test results. For the cases where the test vehicle cut-in distances were shorter, the sensor systems do not have sufficient time to detect, classify and react to the target vehicle (see Figure 104). This figure shows high variation of test results but an obvious trend to higher activation rates with higher cut-in distance.

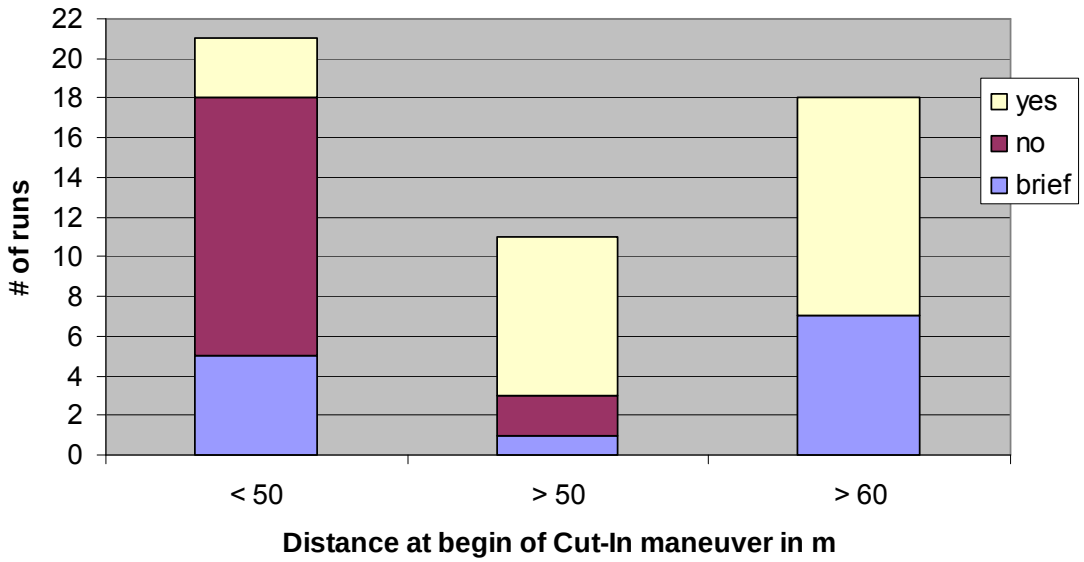

Figure 104: Comparison of Brake Activations of Baseline Vehicles with Early and Late Cut-Ins

L.10 Final Test Procedures for Validated Test Methods

Below are the final test procedures for the LVS, LVM and LVD scenarios. Methods for these three scenarios were validated during the project.

L.10.1 Final LVS Test Procedure

The Lead Vehicle Stopped test procedure is shown below.

L.10.1.1 Test Description

To test the capability of the test vehicle CIB system in a Rear End – Lead Vehicle Stopped Scenario, the test vehicle is driven in a straight and level lane toward a stationary target at a constant forward velocity. The test vehicle brakes must not be manually applied until the target is either struck (with or without autonomous braking) or the test vehicle comes to a full stop prior to striking the target.

L.10.1.2 Instrumentation and Test Conditions

- Instrumentation and general testing conditions are described in Appendix K
- Test Track configuration is comprised of one lane of a straight, flat testing area with a length of 350 meters

L.10.1.3 Test Procedure

- Place the target in the center of the test vehicle lane with the longitudinal axis orientated parallel to the lane. The rear of the target faces the front of the test vehicle (see Figure 105).
- The minimum starting separation distance between the test vehicle and the target is 300 meters (for lower speeds). The test vehicle must reach and maintain the defined test speed (see Table 56) for a distance of at least 100 meters before the target location.
- The test vehicle is driven straight toward the target with constant speed
- The test vehicle brakes must not be manually applied until the target is struck or the test vehicle comes to a complete stop automatically prior to striking the target
- The test will be repeated at the specified speed until a specified number of valid runs are recorded. A valid run is one in which all specified parameters fall within the limits described and all test results mentioned below are recorded.
- This procedure is repeated for all defined test speeds (see Table 56)
- Repeat this procedure for all defined targets

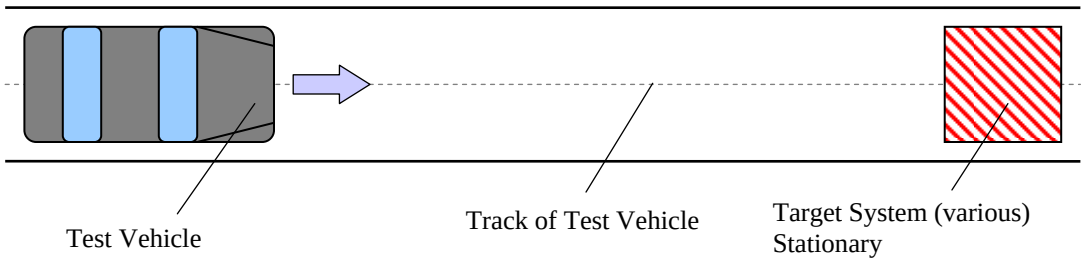

Figure 105: Test Vehicle with Stationary Target

Table 56: Test Speeds for Lead Vehicle Stopped

Velocities	In mph	In km/h
Test Vehicle	20 30 40	32.2 48.3 64.4
Target System	**Stationary**	

L.10.1.4 Expected Test Results

The following data is to be recorded for each valid test run:

- Test vehicle speed versus time
- Test vehicle acceleration versus time
- Test vehicle position versus time
- Test vehicle yaw versus time
- Position of target system, to clarify impact point
- Brake/accelerator pedal, steering wheel actuation versus time
- Test vehicle autonomous braking activated: yes/no
- Target was struck or test vehicle avoided impact completely via braking: yes/no

L.10.2 Final LVM Test Procedure

L.10.2.1 Test Description

To test the capability of the test vehicle CIB System in a Rear End – Lead Vehicle Moving Scenario, the test vehicle is driven in a straight and level lane toward a moving target at a constant forward velocity. Movement of the target must be constant in velocity and parallel to and in the same lane as the test vehicle. The test vehicle brakes must not be manually applied until the target is struck (with or without autonomous braking) or the test vehicle automatically brakes to the same or lower speed than the target system prior to striking the target.

L.10.2.2 Instrumentation and Test Conditions

- Instrumentation and general testing conditions are described in Appendix K
- Test Track configuration is comprised of one lane of a straight, flat testing area with a length of 400 meters

L.10.2.3 Test Procedure

- Place the target in the center of the test vehicle lane with the longitudinal axis orientated parallel to the lane. The rear of the target faces the front of the test vehicle (see Figure 106).
- The test vehicle is driven straight toward the target with constant speed. The target system moves with a constant but lower speed (see Table 57).
- The test vehicle brakes must not be manually applied until the target is struck or the test vehicle automatically brakes to the same speed or a lower speed than the target
- Repeat at the specified speed until a specified number of valid runs are recorded. A valid run is one in which all specified parameters fall within the limits described and all test results mentioned below are recorded.
- This procedure is repeated for all combinations of defined test vehicle and target speeds (see Table 57)
- Repeat this procedure for all defined targets

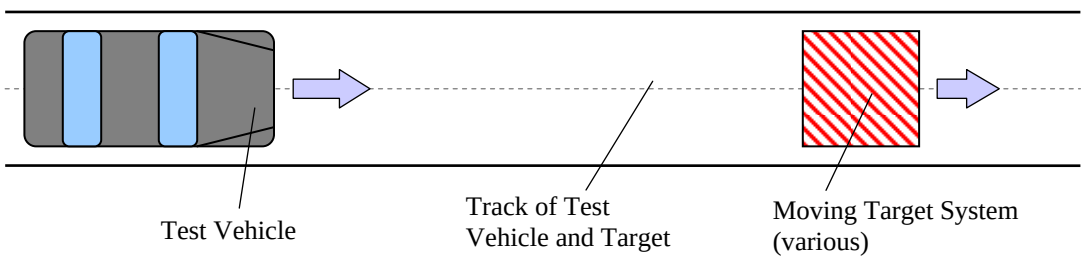

Figure 106: Test Vehicle with Moving Target

Table 57: Test Speeds for Lead Vehicle Moving

		Test vehicle		Target system	
		In mph	In km/h	In mph	In km/h
Velocities	**Set 1**	20	32.2	10	16.6
	Set 2	30	48.3	20	32.2
	Set 3	40	64.4	20	32.2

L.10.2.4 Expected Test Results

The following data is to be recorded for each valid test run:

- Test vehicle speed versus time
- Test vehicle acceleration versus time
- Test vehicle position versus time
- Test vehicle yaw versus time
- Target system speed versus time
- Target system acceleration versus time
- Target system position versus time
- Brake/accelerator pedal, steering wheel actuation versus time
- Test vehicle autonomous braking activated: yes/no
- Target was struck or test vehicle avoided impact completely via braking: yes/no

L.10.3 Final LVD Test Procedure

L.10.3.1 Test Description

To test the capability of the test vehicle CIB System in a Rear End – Lead Vehicle Decelerating Scenario, the test vehicle is driven in a, straight and level lane with constant forward velocity matching the initial forward velocity of the target. The initial separation distance between the test vehicle and the target must be as noted below. After this separation distance and matching velocity have been achieved, the target decelerates at a specified rate to a full stop. The test vehicle brakes must not be manually applied until the target is struck (with or without autonomous braking) or the test vehicle comes to a full stop prior to striking the target.

L.10.3.2 Instrumentation and Test Conditions

- Instrumentation and general testing conditions are described in Appendix K
- Test Track configuration is comprised of one lane of a straight, flat testing area with a length of 400 meters

L.10.3.3 Test Procedure

- Place the target in the center of the test vehicle lane with the longitudinal axis orientated parallel to the lane. The rear of the target faces the front of the test vehicle (see Figure 107).
- The test vehicle is driven straight toward the target system with a constant speed matching the initial forward velocity of the target (see Table 58). The initial separation distance between test vehicle and target must be achieved (see Table 59).
- Maintain this situation for at least two seconds before initializing the deceleration of the target (see Table 59). Decelerate the target system to a full stop. For

guidance and additional requirements for the deceleration of the target see Appendix K, "Standard Testing Conditions and Equipment." The test vehicle brakes must not be manually applied until the target is struck or the test vehicle comes to a complete stop automatically prior to striking the target.

- This procedure is repeated at all defined test speeds (see Table 58) until the specified number of valid runs are recorded. A valid run is one in which all specified parameters fall within the limits described and all test results mentioned below are recorded.
- Repeat this procedure for all defined targets

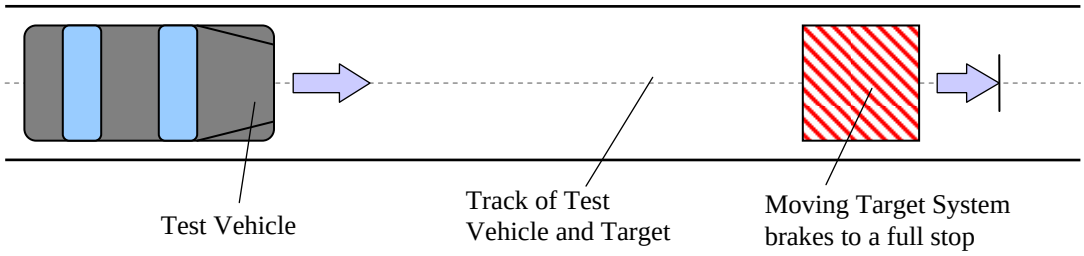

Figure 107: Test Vehicle with Decelerating Target

Table 58: Test Speeds for Lead Vehicle Decelerating

Velocities	In mph	In km/h
Test Vehicle	20	32.2
Target System	20	32.2

Table 59: Additional Test Parameters for Lead Vehicle Decelerating

Parameter	Dimension
Initial Distance	17.8 m
Target System Deceleration Rate	0.3 g

L.10.3.4 Expected Test Results

The following data is to be recorded for each valid test run:

- Test vehicle speed versus time
- Test vehicle acceleration versus time
- Test vehicle position versus time
- Test vehicle yaw versus time
- Target system speed versus time
- Target system acceleration versus time

- Target system position versus time
- Brake/accelerator pedal, steering wheel actuation versus time
- Test vehicle autonomous braking activated: yes/no
- Target was struck or test vehicle avoided impact completely via braking: yes/no

L.11 Stereo-Vision Test Data

The developmental nature of the Stereo Vision system installed in Vehicle E exhibited an operational limitation which affects the level of information available from that system. During PIP vehicle testing, output from the Stereo Vision system did not include a functional autonomous brake command since the vehicle interface system was not yet developed. Therefore, the tests during that phase of the project were limited to assessment of the capability of that system to track various test targets and the accuracy of the sensor measurements. During validation testing, an embedded CIB control algorithm was added to the Stereo Vision system that enabled output of a recordable signal which indicated when the system would have initiated a brake command at various TTC levels (without triggering actual CIB system brake activations). Consequently, this data on braking "trigger point" was used, along with the test results collected from the other CIB functions of the vehicle, to determine expected system performance associated with the Stereo Vision sensors (and algorithm) for each of the test scenarios.

Table 60 provides results across the various test scenarios Stereo-Vision sensors. This table indicates the percentage of tests in which the test target was detected, the percentage of tests in which brake commands were sent at each of three TTC settings, and the percentage of sensor measurements which fell within the accuracy limits of the manufacturer as compared to the ground-truth data. The "Performance Limit" measurements refer to the percentage of tests where sensor range measurements fell within ± 10% of the ground-truth data.

Table 60: Test Data Summary for Stereo-Vision System in Vehicle E

Data Set Name	Valid Sequences	Target Tracked	Braking Command			Performance Limit		
			TTC=1 sec	TTC=0.6 sec	TTC = 0.3 sec	TTC=1 sec	TTC=0.6 sec	TTC = 0.3 sec
Small Pole	30	100%	100%	100%	100%	80.0%	83.3%	96.7%
Large Pole	30	100%	100%	100%	100%	90.0%	90.0%	96.7%
LVM	47	100%	100%	100%	100%	N. A.	N. A.	N. A.
LVS	42	100%	100%	100%	100%	98.0%	100%	100%
LTAP-OD	9	100%	55.6%	77.8%	100%	N. A.	N. A.	N. A.
Pedestrian Crossing	4	100%	50.0%	100%	100%	50.0%	75.0%	100%
Pedestrian In-Path	21	100%	100%	100%	100%	N. A.	N. A.	N. A.
OD	35	100%	100%	100%	100%	N. A.	N. A.	N. A.
SCP	15	93.3%	53.3%	73.3%	93.3%	N. A.	N. A.	N. A.

This data shows that in cases where the targets crossed the path of the test vehicle (i.e., LTAP-OD, Pedestrian Crossing, SCP), CIB system braking commands were issued in less than 100% of the test runs. There appears to a trend for low-activation rates at the higher TTC settings. This may be due to the more limited length of time in which the target is within the sensing system field of view prior to target impact. In the remaining "straight ahead" vehicle-to-vehicle, pole, and pedestrian in-path scenarios, braking commands were always recorded across all TTC settings examined.

Furthermore, performance limits shown in Table 60 indicate that potential measurement errors would likely affect overall CIB performance. Unfortunately, in slightly more than

half of the test conditions, performance limits could not be determined due to insufficient synchronization between the ground truth measurement system and the Stereo-Vision data acquisition system. This synchronization issue became apparent during post-processing of the test data.

Overall, although these results demonstrate the potential capability of the Vehicle E Stereo-Vision system to detect the test targets and trigger a brake command, insufficient data exists to determine CIB system performance with this system. Due to this limitation, test results from this system are not included within the specific test scenario sections detailed earlier in the report.

Appendix M Comparison of Data Acquisition Systems Used in LVD Scenario

An analysis was performed to compare two different ways to measure relevant data for the post-processing of LVD runs. This was useful to examine the accuracy of the target tow system and the measurement methods used in this testing, and for suggesting potential improvements to the towing system. The main issue with the LVD test method is that it is not possible to obtain direct differential GPS data for the balloon car pulled by the target tow system because the GPS hardware is not sufficiently durable to mount directly to the balloon car (when considering impacts will occur).

In this test phase, the target tow system (described in Appendix G) was used in a fully automated mode. In this mode, the target tow system accelerated and decelerated the balloon car automatically based on the speed and distance of the approaching test vehicle. The system was set up such that it was possible to compare speeds and distances of balloon car and test vehicle. The speed and distance of the test vehicle relative to a fixed point was submitted to the target tow system control unit by the GPS measurement system. The speed and distance of the balloon car relative to the same fixed point was collected by an encoder wheel on the target tow system. This made it possible to calculate the speed difference and the distance between the two objects (see Figure 108). Based on this information, the deceleration of the balloon car in the LVS scenario was initiated by the target tow system control unit. This deceleration initiated at a separation distance of 17.8 m, which is 2-second following (headway) time at the 20 mph initial speed.

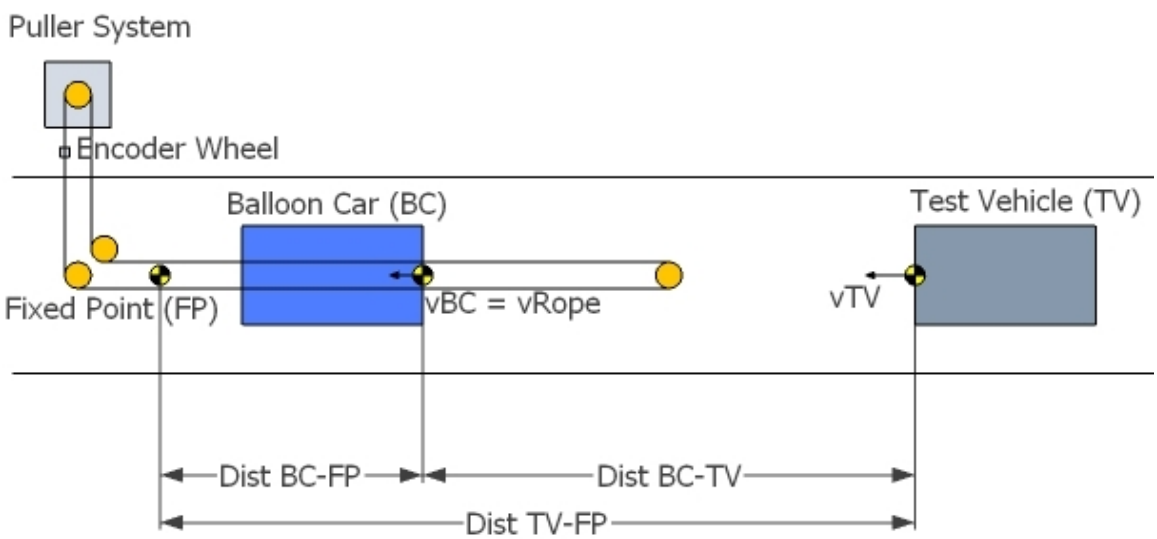

Figure 108: Target Tow System Configuration for Measuring Speed and Position

In the post-processing, this data was used to identify CIB system impact speed reduction values and the distance between the balloon car and test vehicle when the balloon car began to decelerate. In addition, analysis of the balloon car deceleration initiation point and deceleration rates was performed.

In this comparison, two data sets are compared for the same set of 10 runs. The first row of data in Table 61 was recorded by the radar sensor, as part of the Vehicle F CIB system. The second row of data in this table was recorded by an encoder wheel attached to the target tow system. Figure 109 also provide a comparison of the encoder wheel data relative to the radar measurement data.

Table 61: Distance between Balloon Car and Test Vehicle when Balloon Car Starts Decelerating

Scenario: LVD; Target System: Blue Balloon Car; Vehicle F; Initial speeds: 20mph; Initial distance 17.8m													
		Distance [m] between Balloon Car and Vehicle, when Balloon Car starts braking											Standard Dev in m
Test Phase	Data Acquisition System	Run 1	Run 2	Run 3	Run 4	Run 5	Run 6	Run 7	Run 8	Run 9	Run 10	Average	
Task 8 - PIP 2	Radar Sensor	21.93	13.91	17.13	16.66	15.94	13.50	17.46	14.39	19.83	21.42	17.22	3.01
	Encoder Wheel	22.67	12.78	22.30	17.01	16.88	14.80	18.55	16.29	21.77	23.42	18.65	3.69
	Difference	3.27%	-8.82%	23.21%	2.05%	5.55%	8.80%	5.85%	11.65%	8.93%	8.54%	7.67%	

In eight out of 10 runs, the encoder wheel measured a higher distance than the radar sensor (between 2% and 12%). In Run 2, the encoder wheel measured less distance than the radar sensor (-9% lower). In Run 3, the encoder wheel measured a very high distance compared to the radar sensor (+23% higher).

The main differences between the encoder wheel and radar distance measurements appear to be due to the vibrations and stretching of the towing rope. Analysis of the radar measurement of all 10 runs shows that it was not possible to use the encoder wheel measurement to begin the balloon car deceleration within a small error tolerance surrounding the pre-defined 17.8 m separation distance.

In addition, a comparison of the radar sensor data to that obtained with highly accurate differential GPS data was made to support the accuracy of the Radar system used in this analysis. This evaluation indicated that the radar data was within -0.25% to +2.12% of the GPS data. In comparison, the tow system encoder wheel measurements varied between -9% to +23% relative to the radar measurements.

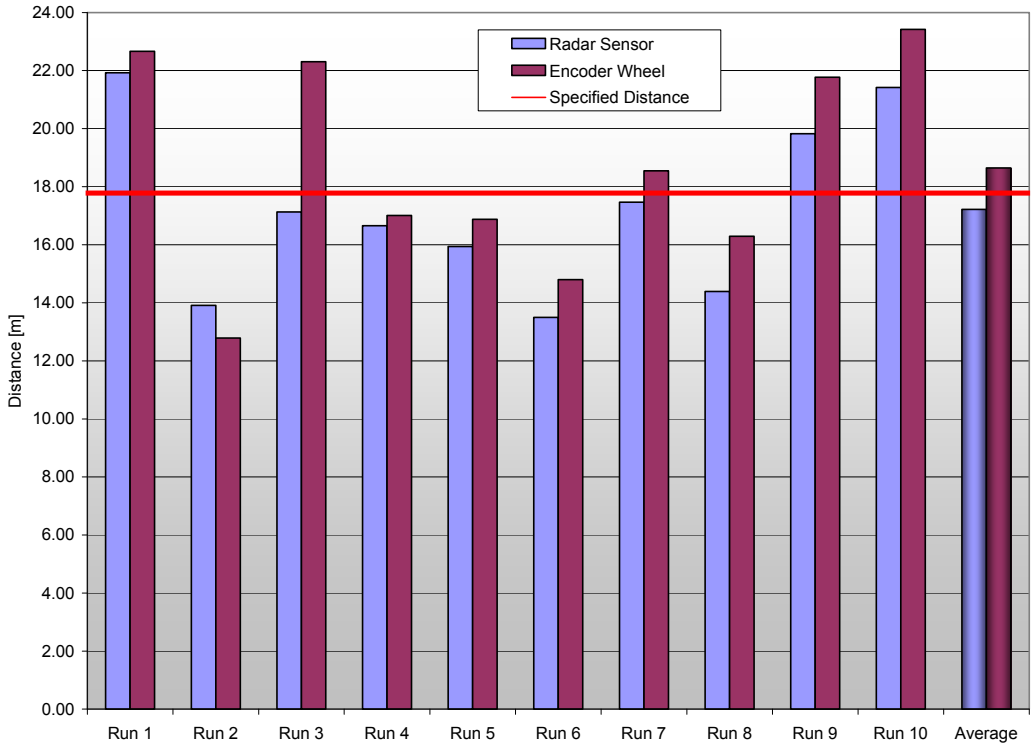

Figure 109: Comparison of Distance between Balloon Car and Test Vehicle when Balloon Car Starts Decelerating

Modifying the test equipment to improve the balloon car position measurement would greatly improve the test repeatability. Possible improvement methods include measuring the position of the balloon car with a non-contact optical device or by setting up a movable differential GPS unit that travels in synch with the balloon car (but which would not be struck by the test vehicle.)

Appendix N Conduct Real-World Operational Assessment Data (ROAD) Trip and Recommend Operational Test Methods

N.1 ROAD Trip Overview

CIB systems need to be able to quickly and accurately sense and analyze emerging crash situations. The following material details the data collected and analyzed from the Real-World Operational Assessment Data (ROAD) Trip that was used to develop CIB operational performance tests. This trip data was used to assess a system's robustness to false CIB system brake activations (i.e., "false positives") and to understand how each sensor type responded to a rich set of realistic driving environments.

N.2 ROAD Trip Data Analysis

The trip was made up of a combination of "city-driving" days and "transit" days. City-driving days were used to collect information on driving conditions in 10 major cities across the United States. This data typically included a mix of driving in downtown business areas, suburban neighborhoods and city freeways. Transit days were used to travel between major cities along the route and consisted of a balance of interstate and secondary highway driving.

Figure 110 and Figure 111 show plots of cumulative speed distributions for city-driving days vs. transit days for the two vehicles (Vehicles E and H) that participated in the ROAD Trip. As can be seen in these figures, transit days had a higher concentration of higher speeds, while city driving days typically showed a bimodal distribution, resulting from the combination of city and freeway driving. Figure 112 shows a comparison of the actual speed distribution for the entire trip as compared to the expected distribution derived from the Real-World User Profile (RWUP). Although there are some differences shown in Figure 112 (e.g., for Vehicle E in the 0-10 mph category), the comparison of actual speeds traveled vs. the predicted speeds is overall quite good.

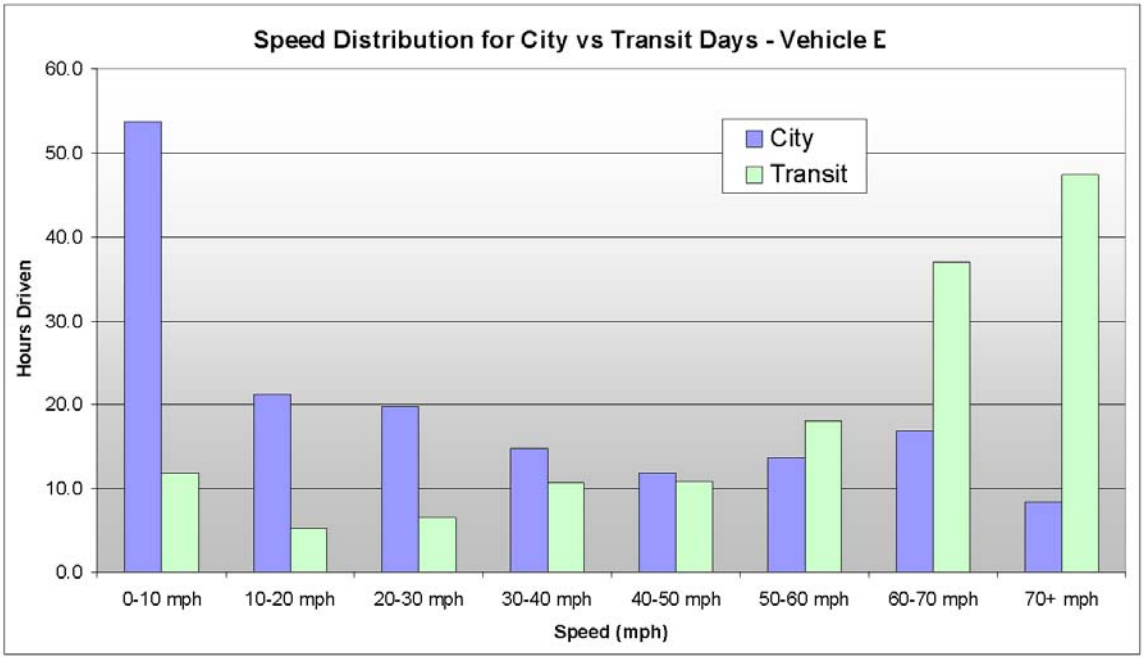

Figure 110: ROAD Trip Speed Distributions for Vehicle E

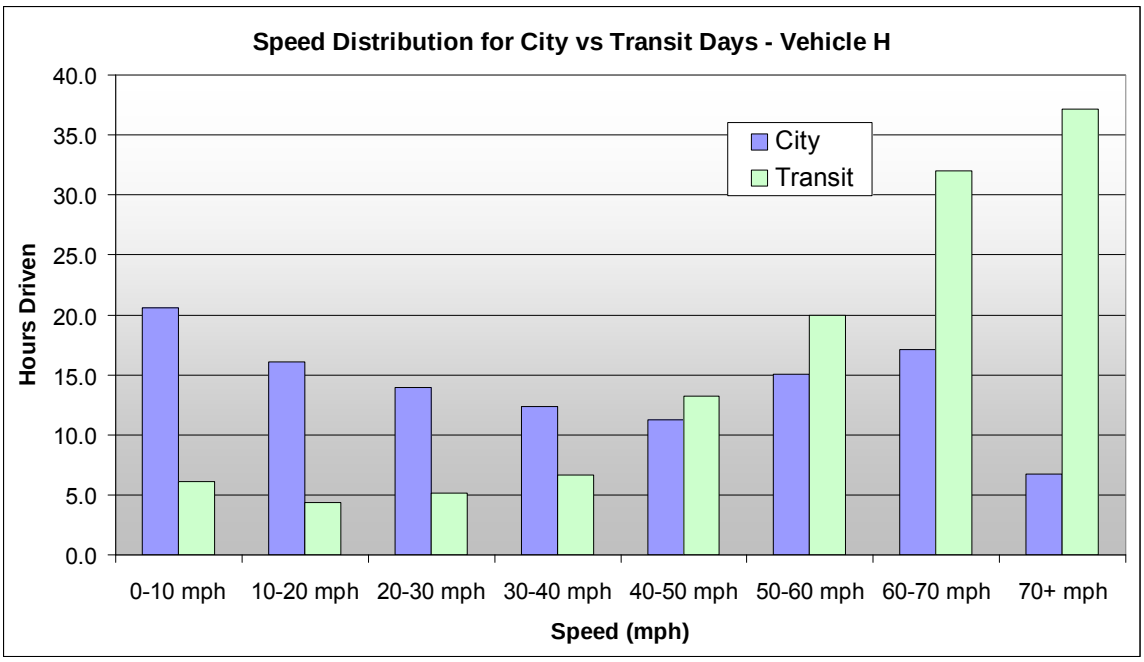

Figure 111: ROAD Trip Speed Distributions for Vehicle H

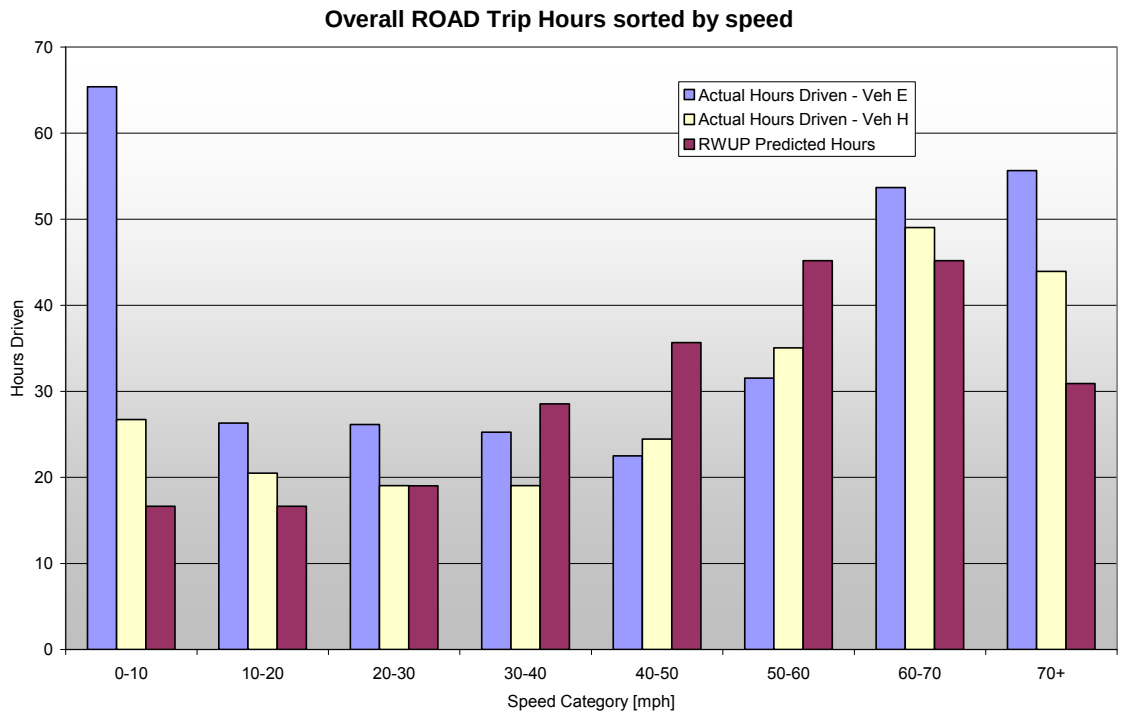

Figure 112: Actual ROAD Trip Speed Distribution vs. RWUP Predicted Distribution

Both vehicles used for the ROAD Trip incorporated sensing systems that included Long/Mid-Range Radar and a Mono-Vision system. Data from these systems was taken continuously for the entire trip and with sufficient detail to allow reprocessing later to isolate the performance of the systems in different configurations – Radar-only, Vision-only and Fused Vision and Radar. Unlike Vehicle H, Vehicle E was also equipped with a stand-alone Stereo-Vision sensing system. Since this system did not have sufficient storage capacity to allow continuous data capture, data "snapshots" were captured for a pre-defined amount of time before and after an event (i.e., when a pre-defined trigger was violated).

N.2.1 Analysis of Stand-alone Long/Mid-Range Radar-Based System

In order to evaluate the ROAD Trip data for a single radar sensor typology, it is necessary to distinguish radar-only targets from fused (radar plus vision) targets. Although a resimulation of the ROAD Trip data provided the ability to distinguish radar-only targets from fusion targets, it should be noted that all CIB alerts recorded on the ROAD Trip were based on the fused (radar plus vision) target output. Therefore, it became necessary to create a rudimentary threat assessment algorithm for the radar-only target data based on the TTC with the closest in-path stationary, moving, or moveable target. (A moveable target is one that was initially observed to be moving and has become stationary.)

Since the ability to directly extract the acceleration of the target (lead) vehicle from the collected radar data did not exist within our dataset, the simple "momentary TTC"

equation associated with stationary targets (range divided by range rate) was used for all targets. Furthermore, whenever a stationary and moving / moveable target were simultaneously reported, the closest target was chosen as the primary target of interest.

The equation used for the TTC calculation when the primary target is stationary is as follows:

$$TTC = \frac{R}{V_o} \quad , \qquad (1)$$

Where

R = Range to the closest, in-path stationary target

V_o = Range Rate to the closest, in-path stationary target

Since the majority of events (over 90%) detected for the Stand-alone Long/Mid-Range Radar-Based System involved stationary targets, the impact of not using the target acceleration in the TTC calculation (as would be desired) is somewhat minimized.

Table 62 presents the three sensitivity settings used in assessing false activation occurrence with the radar-only set up. It should be noted that determination of system sensitivity is generally considered to be a highly proprietary aspect of CIB system design and cannot be described in detail here. Sensitivity is related to simple TTC (i.e., range divided by range rate) but often takes many more variables into consideration in order to increase robustness to false events. Thus, analysis of false events within one sensor set is feasible, while comparison of false events between systems from different sensor combination is not possible. The sensitivity settings used in the analyses in this chapter were selected based on expert judgment and experience with the sensor systems given their current state of development.

Table 62: TTC Settings for Precharge and Intervention Braking

Alert Type	Sensitivity Setting	Time to Collision (TTC) Criteria (seconds)
Precharge	Baseline	0.9
	+25% sensitivity	1.04
	+ 50% sensitivity	1.3
Intervention Braking	Baseline	0.5
	+25% sensitivity	0.6
	+50% sensitivity	0.7

As illustrated in Figure 113, the primary false precharge ("near miss") events were associated with Curve Entry, Curve Exit, and Short Radius Turns driving scenarios. The majority of the event types examined were observed in each of the sensitivity settings. Note that in Figure 113 the Baseline + 25% and Baseline + 50% events were normalized to the total number of Baseline events, making it possible for percentage values to exceed 100%. This can result because as the sensitivity is increased, more events are expected to occur as compared to the baseline setting.

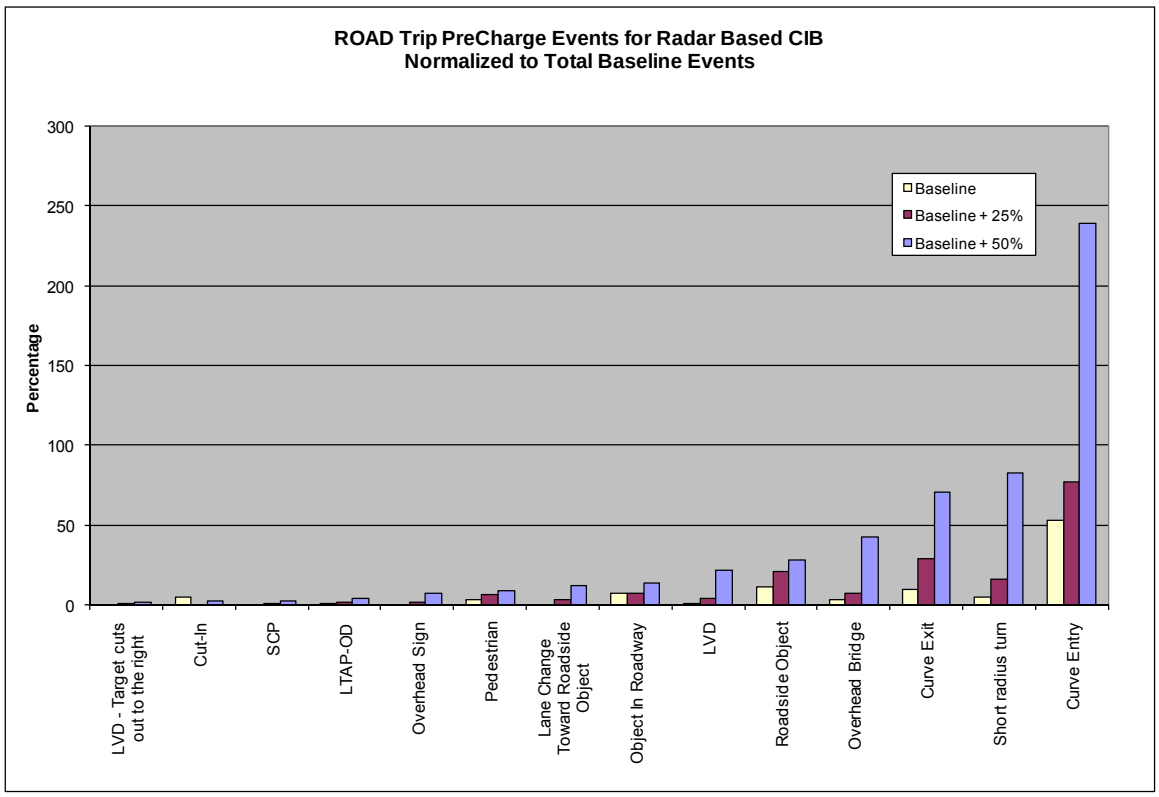

Figure 113: Radar-only Precharge Events (by Scenario)

As illustrated in Figure 114, the primary false intervention events were associated with Objects in Roadway and Curve Entry Scenarios. In addition, Curve Exit, Roadside Object, Overhead Bridge, and Overhead Sign false intervention events were observed at each of the sensitivity settings.

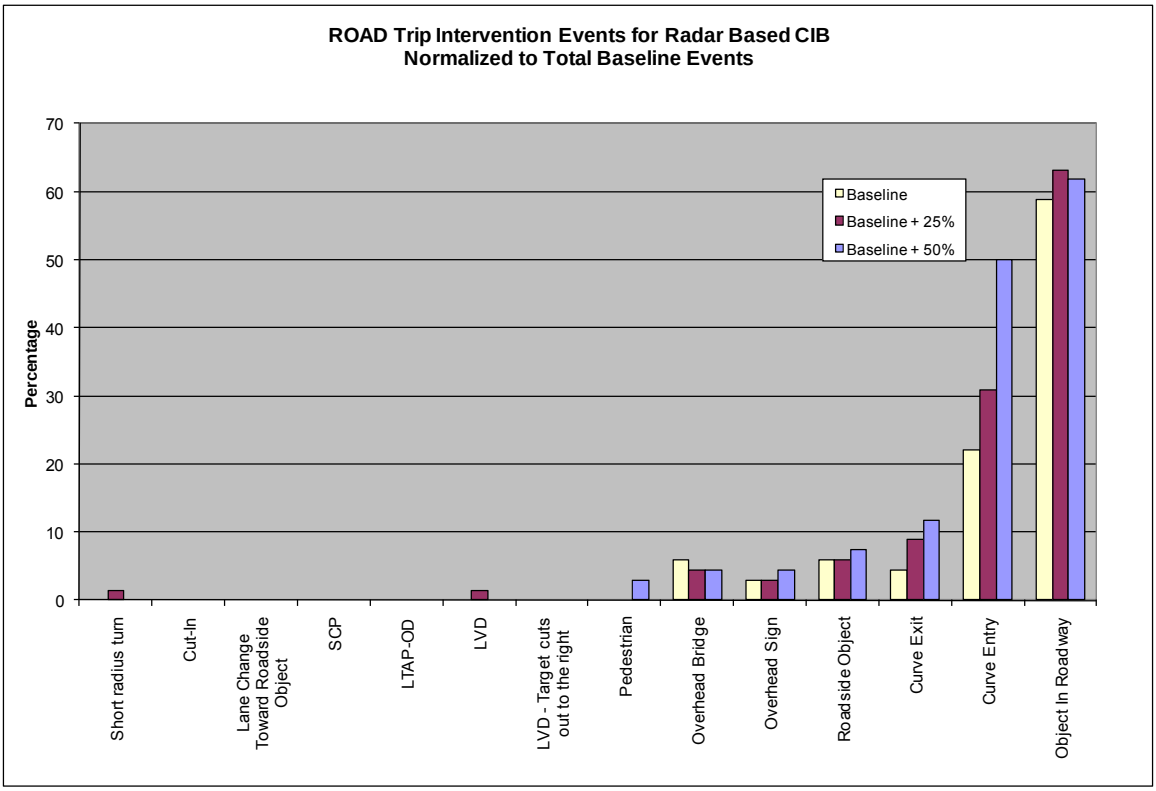

Figure 114: Radar-only Intervention Events (by Scenario)

N.2.1.1 Scenario Descriptions

N.2.1.1.1 Object-in-Roadway False-Event Scenario

An Object-in-Roadway false event can occur when the radar detects reflective objects embedded in the road, such as manhole covers, Bott's Dots, or metal grates. If the detection persists, it may appear to the radar to be a stationary vehicle in the host vehicle's path, which can result in a false intervention event. Figure 115 provides illustrations of this type of scenario. While this event only accounted for a small percentage of Precharge Events, the tendency of this type of false target to persist results in it accounting for approximately 40% of false interventions at all three sensitivity settings.

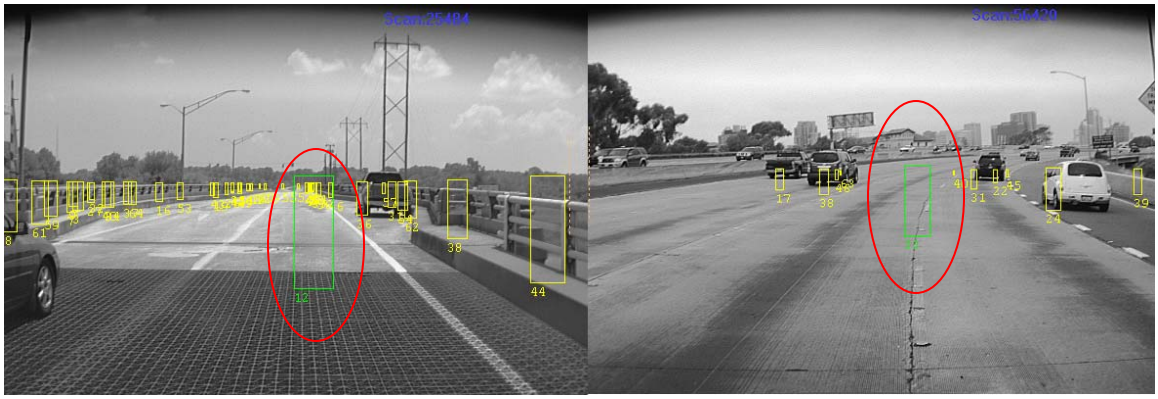

Figure 115: Objects in Roadway Detected as In-Path Targets

N.2.1.1.2 Kinematic Analysis of Object-in-Roadway False-Event Scenario

A kinematic analysis of the Object-in-Roadway False-Event Scenarios illustrated in Figure 116 shows that the speed of the host vehicle during this alert was typically between 20 and 80 mph for all alert sensitivity settings. The vehicle yaw rate at the time of the curve entry alerts was generally below ± 5 deg/s (see Figure 117), further indicating that the Object-in-Roadway false events often occur while changing lanes over the embedded objects.

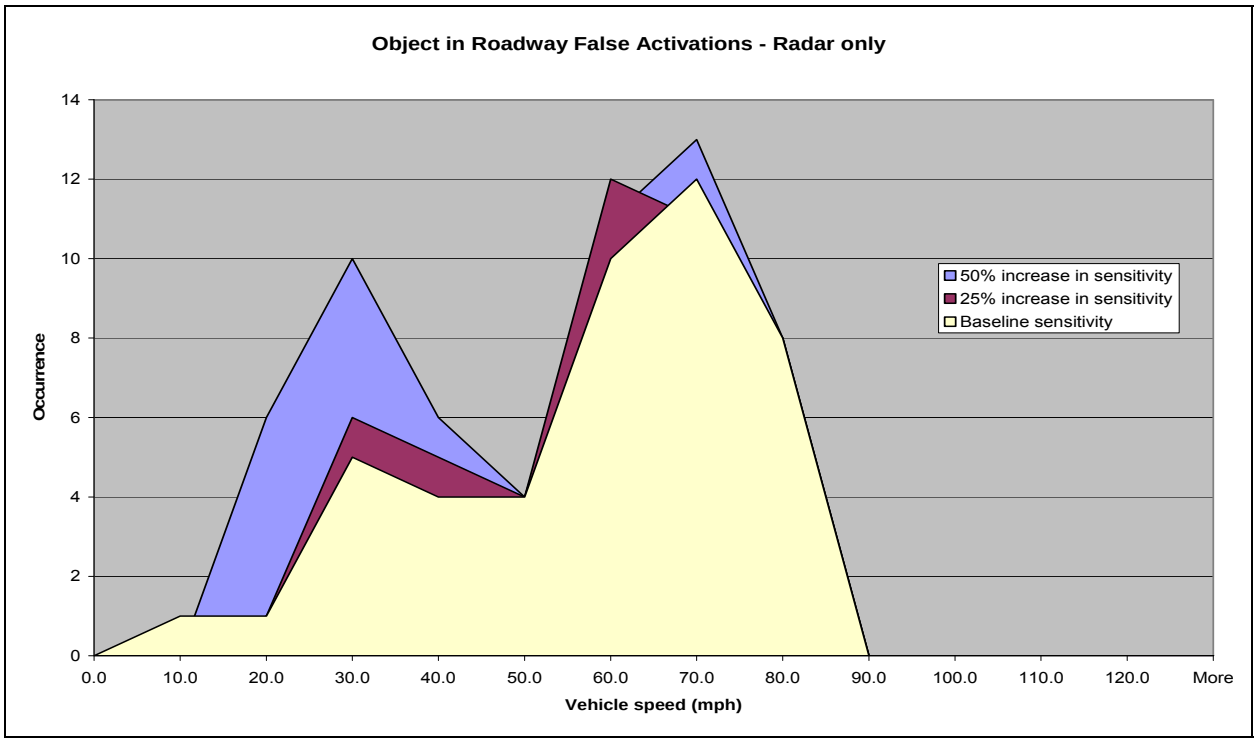

Figure 116: Vehicle Speed Distribution for Objects-in-Roadway

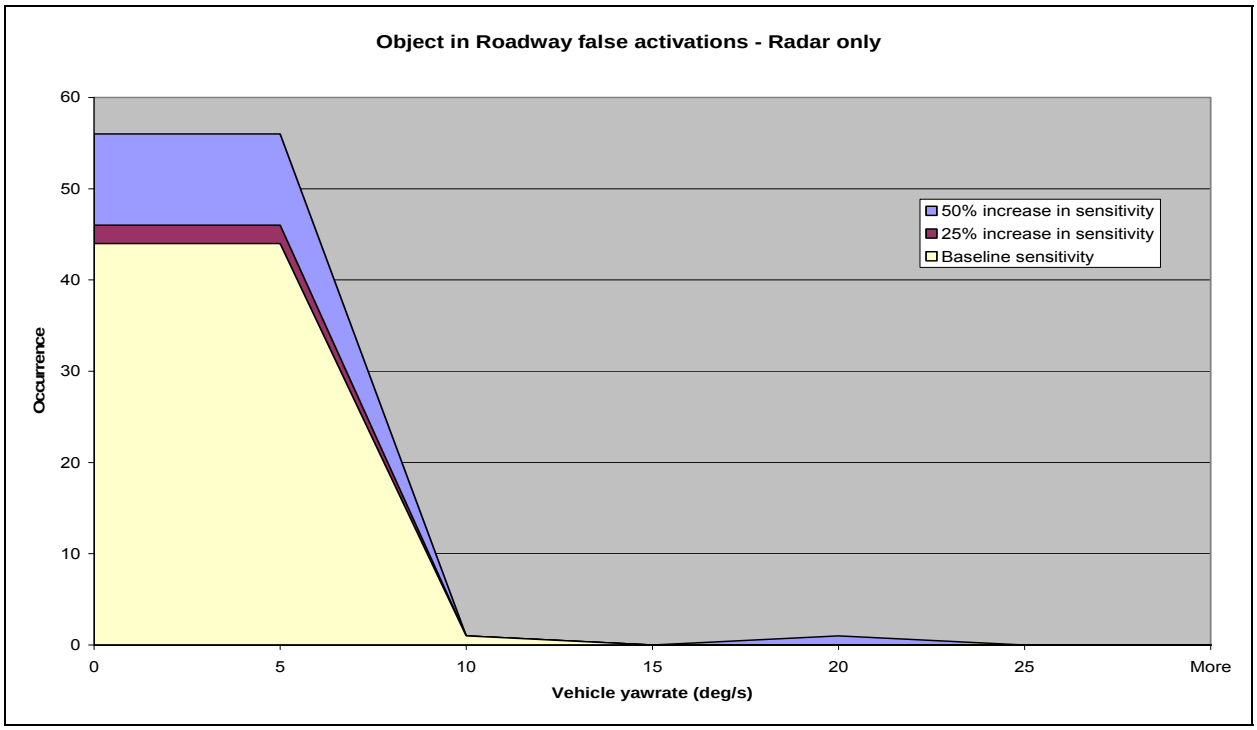

Figure 117: Yaw Rate Distribution for Objects in the Roadway

N.2.1.1.3 Curve-Entry False-Event Scenario

As illustrated in Figure 118, Curve-Entry False-Event Scenario can occur when the radar detects reflective objects on the side of the road at the entrance to a curve (i.e., before the host vehicle has actually entered the curve). This event resulted in approximately 40% of all false activations at each sensitivity setting.

Figure 118: False Activation on Stationary Object during Curve-Entry

(green rectangle indicates primary target identified by radar)

N.2.1.1.4 Kinematic Analysis of Curve-Entry False-Event Scenario

A kinematic analysis of Curve-Entry False-Event Scenarios indicated that the speed of the host vehicle during this alert was typically between 20 and 55 mph for all alert sensitivity settings (see Figure 119). The vehicle yaw rate at the time of the curve-entry alerts was generally below ± 15 deg/s (see Figure 120), which further indicates that the curve-entry alerts largely occur just before the host vehicle starts to turn into the curve. An assessment of the radius of curvature observed during this event further supports this hypothesis, since this type of event largely occurs on curve radii between 200 and 500 meters (see Figure 121).

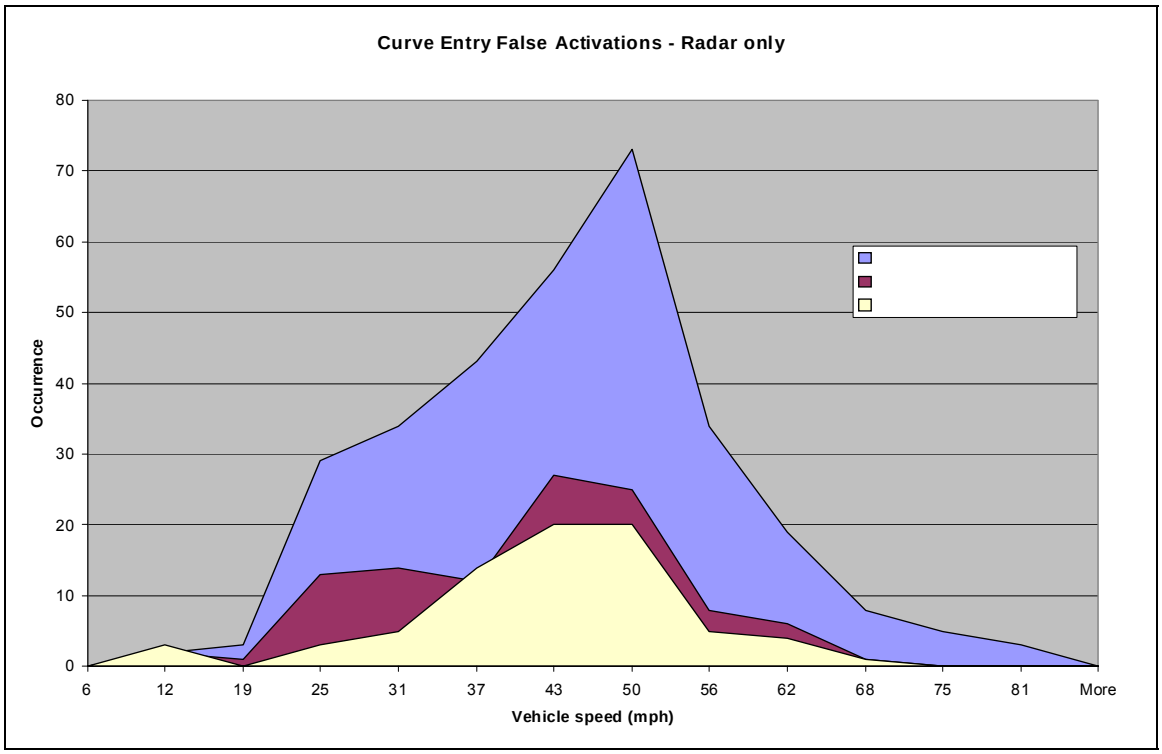

Figure 119: Speed Distribution for Radar-Only-Based, False Activations – Curve-Entry

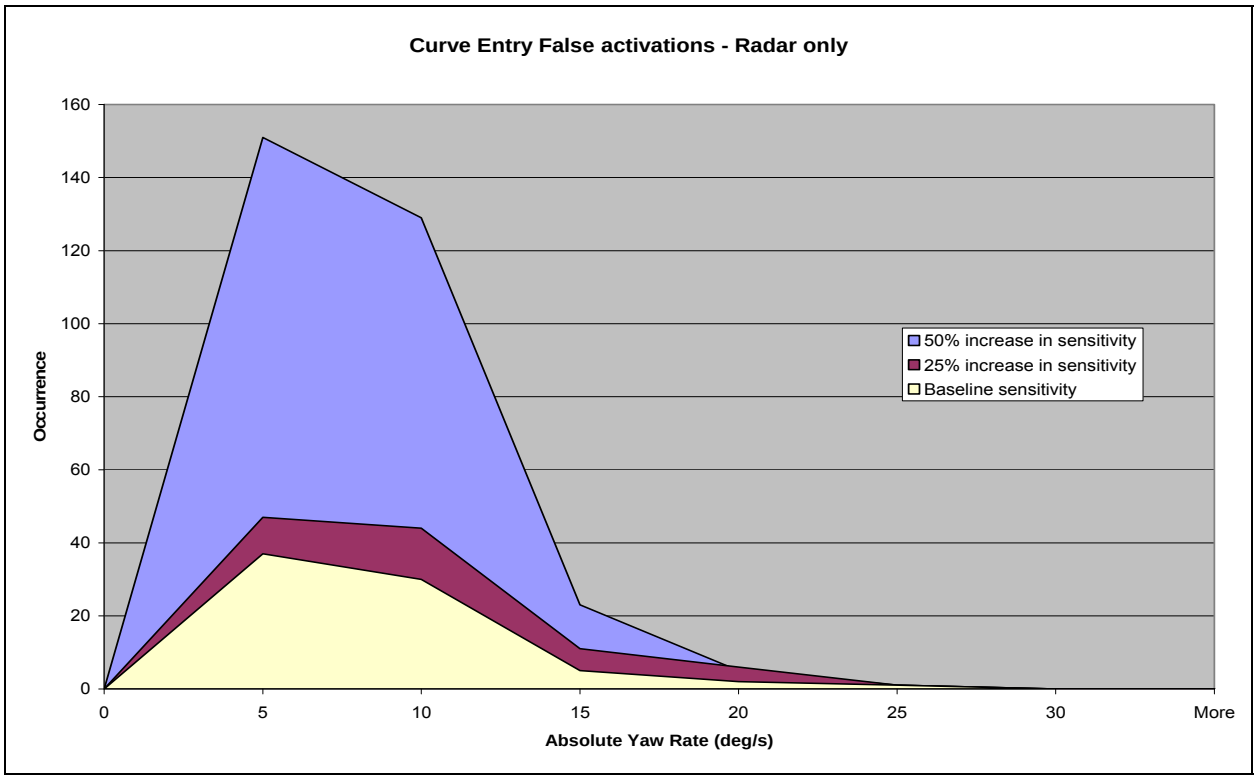

Figure 120: Yaw Rate Distribution for Radar-Only-Based, False Activations – Curve-Entry

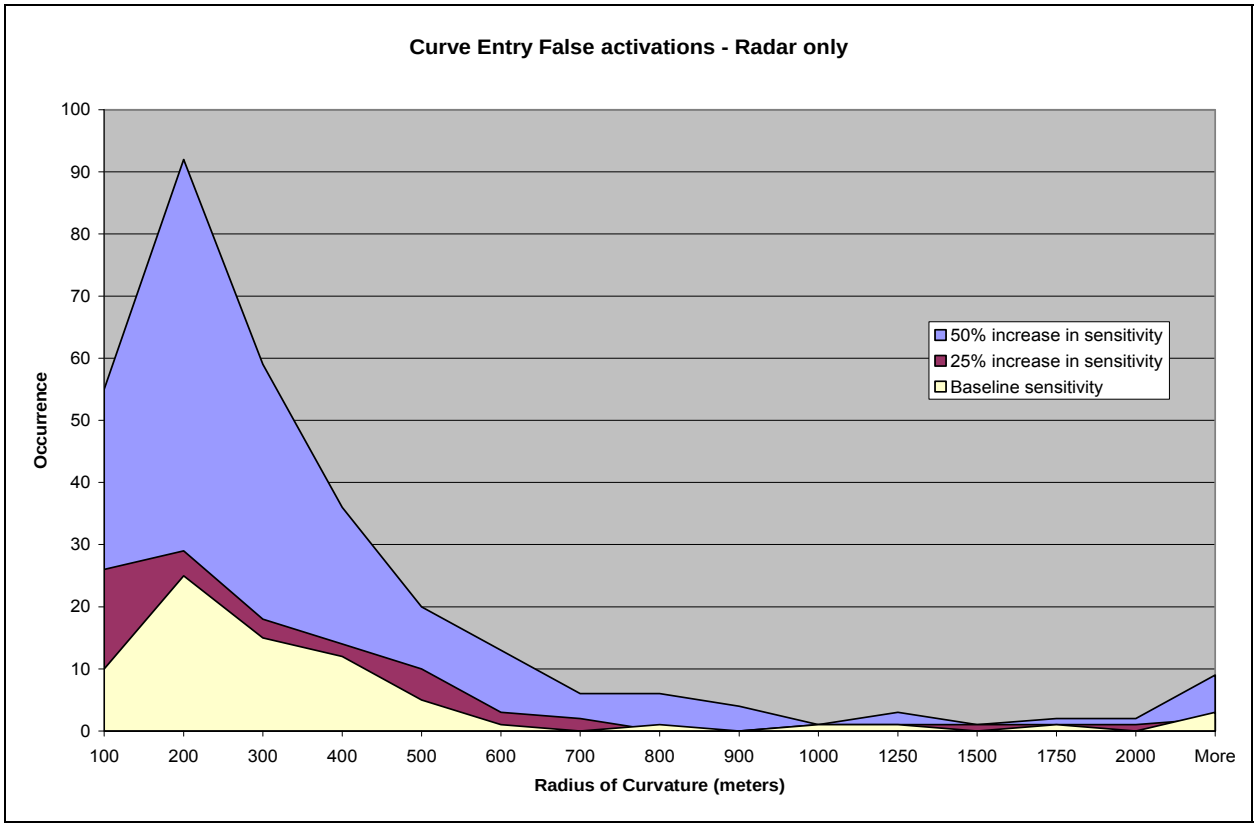

Figure 121: Radius of Curvature Distribution for Radar-Only-Based, False Activations – Curve-Entry

N.2.1.1.5 Curve-Exit Scenario False-Event Scenario

Similar to the Curve-Entry Scenario, a Curve-Exit False-Event Scenario can occur when the radar detects reflective objects on the side of the road while exiting the curve. Figure 122 illustrates this type of false event. This type of event resulted in approximately 8%, 14%, and 13% of all false activations observed with the baseline threat assessment, +25% sensitivity, and +50% sensitivity setting, respectively.

Figure 122: False Activation on Stationary Object during Curve-Exit

(Note: this figure shows the scene exiting the first half of an S-curve)

N.2.1.1.6 Kinematic Analysis of Curve-Exit False-Event Scenario

Similar to that observed with the Curve-Entry Scenario, a kinematic analysis of the Curve-Exit False-Event Scenarios indicate (see Figure 123) that the speed of the host vehicle during this alert was typically between 25 and 60 mph for all alert sensitivity settings. The vehicle yaw rate at the time of the curve entry alerts was generally below ± 10 deg/s, as shown in Figure 124.

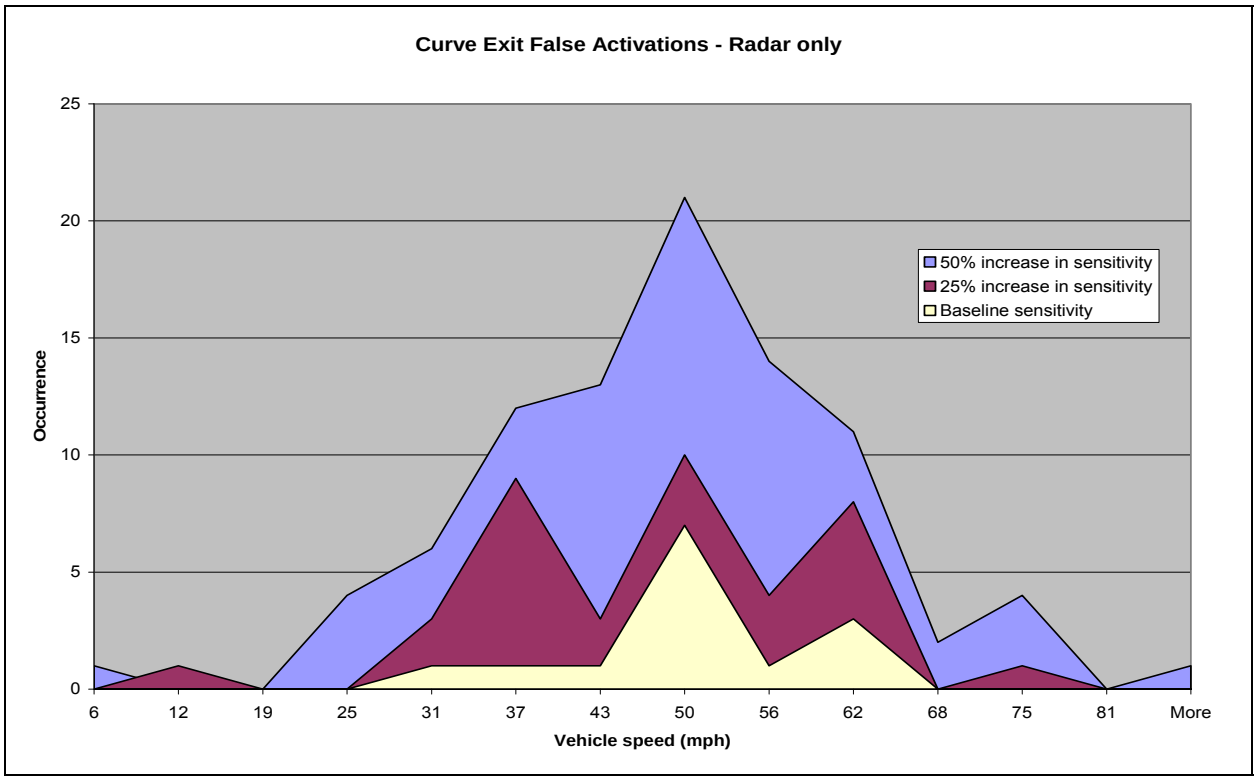

Figure 123: Speed Distribution for Radar-Only-Based, False Activations – Curve-Exit

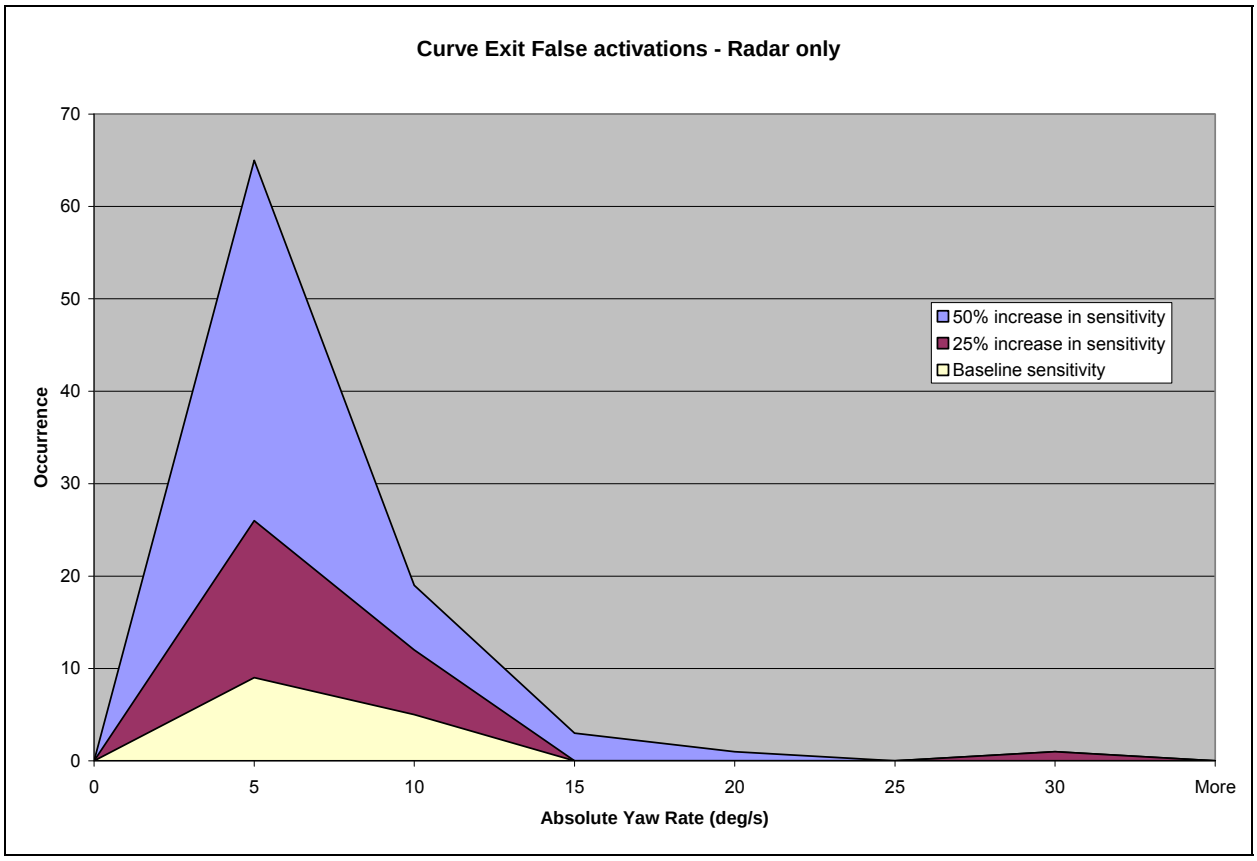

Figure 124: Yaw Rate Distribution for Radar-Only-Based, False Activations – Curve-Exit

N.2.1.1.7 Roadside Objects False-Event Scenario

A Roadside Object event can occur when an object that is on the side of the roadway is detected as being in the host vehicle's path. This is often the result of the host vehicle wandering within its lane or changing lanes toward a roadside object. Figure 125 illustrates this type of false event. This event resulted in approximately 9%, 10%, and 5% of all false activations observed with the baseline threat assessment, +25% sensitivity, and +50% sensitivity setting, respectively.

Figure 125: False Events Caused by Roadside Objects

N.2.1.1.8 Kinematic Analysis of Roadside-Objects False-Event Scenario

A kinematic analysis of the Roadside-Object False-Event Scenarios illustrated in Figure 126 indicates that the speed of the host vehicle during this type of event was typically between 30 and 85 mph with the majority occurring between approximately 35 and 60 mph.

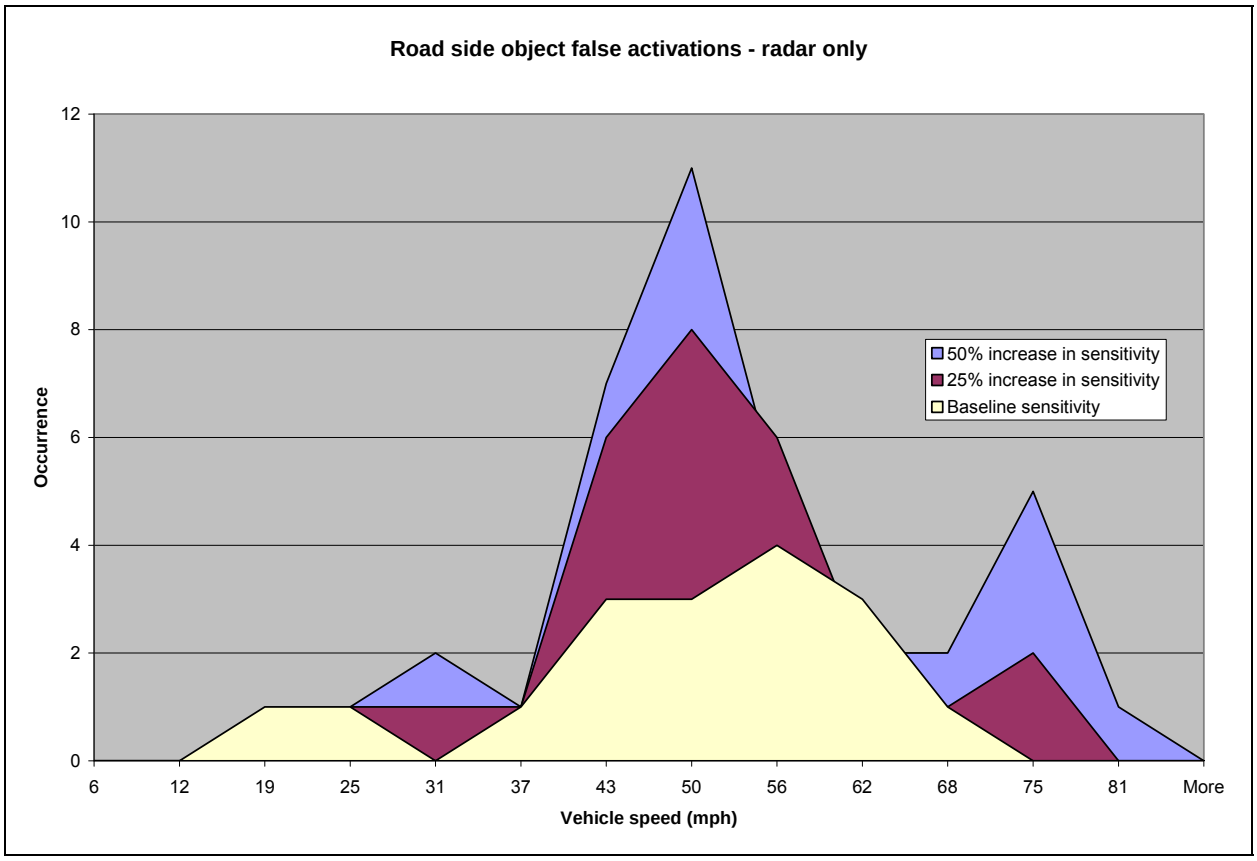

Figure 126: False Activation on Stationary Object Due to Roadside Objects

N.2.1.1.9 Overhead Signs and Bridges False-Event Scenario

The Overhead Signs and Bridges type of false event can occur when the radar detects an overhead object and interprets it as being in the host vehicle's path. Figure 127 provides an illustration of this type of false event. This event resulted in approximately 5.5%, 5.5%, and 9% of all false activations observed with the baseline threat assessment, +25% sensitivity, and +50% sensitivity setting, respectively.

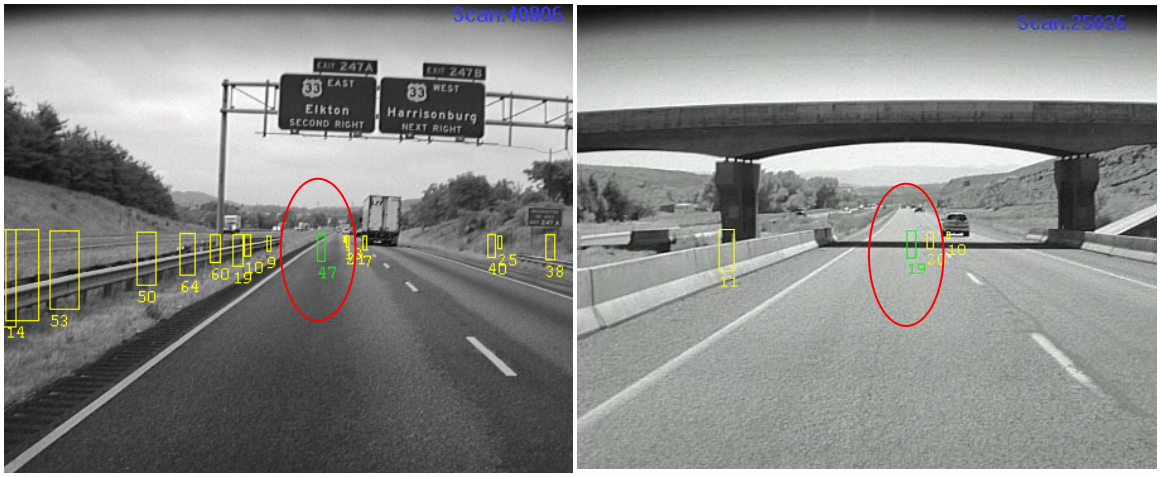

Figure 127: False Activation on Stationary Object Due to Overhead Object

N.2.1.1.10 Kinematic Analysis of Overhead Signs and Bridges False-Event Scenario

A kinematic analysis of Overhead Sign and Bridge False-Event Scenario indicates that the speed of the host vehicle during this type of event was typically between 30 and 85 mph with the majority occurring between 50 and 85 mph as show in Figure 128.

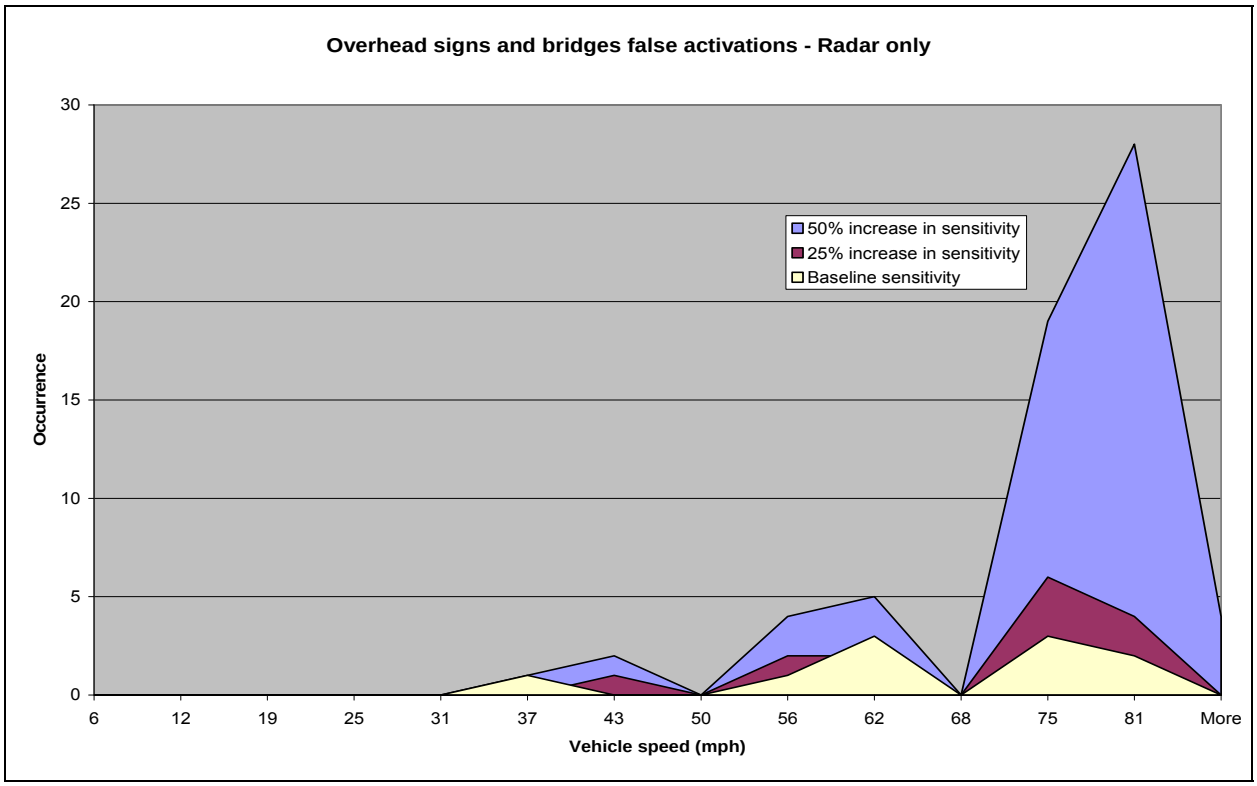

Figure 128: Speed Distribution for Radar-Only-Based, False Activations – Overhead Signs and Bridges

N.2.1.1.11 Short Radius Turns False-Event Scenario

The Short Radius Turns event can occur when the radar detects an object while performing a low-speed turn (see Figure 129). This event resulted in approximately 3%, 7%, and 13% of all false activations observed with the baseline threat assessment, +25% sensitivity, +50% sensitivity setting, respectively.

Figure 129: False Activation during Short Radius Turn

N.2.1.1.12 Kinematic Analysis of Short Radius Turn False-Event Scenario

A kinematic analysis of the Short Radius Turns False-Event Scenario indicates that the speed of the host vehicle during this alert was typically between 5 and 15 mph across all alert sensitivity settings, as shown in Figure 130. Furthermore, the vehicle yaw rate at the time of this event was generally between ± 15 deg/s to ± 35 deg/s (see Figure 131). Because yaw rate is commonly used to predict the host vehicle's path, it is feasible that for brief instances of time the host vehicle will appear to be on a collision course with an object that is clearly not in the intended path. An assessment of the radius of curvature observed during this event (see Figure 132) also reveals turns of a very tight radius, up to 50 meters radius.

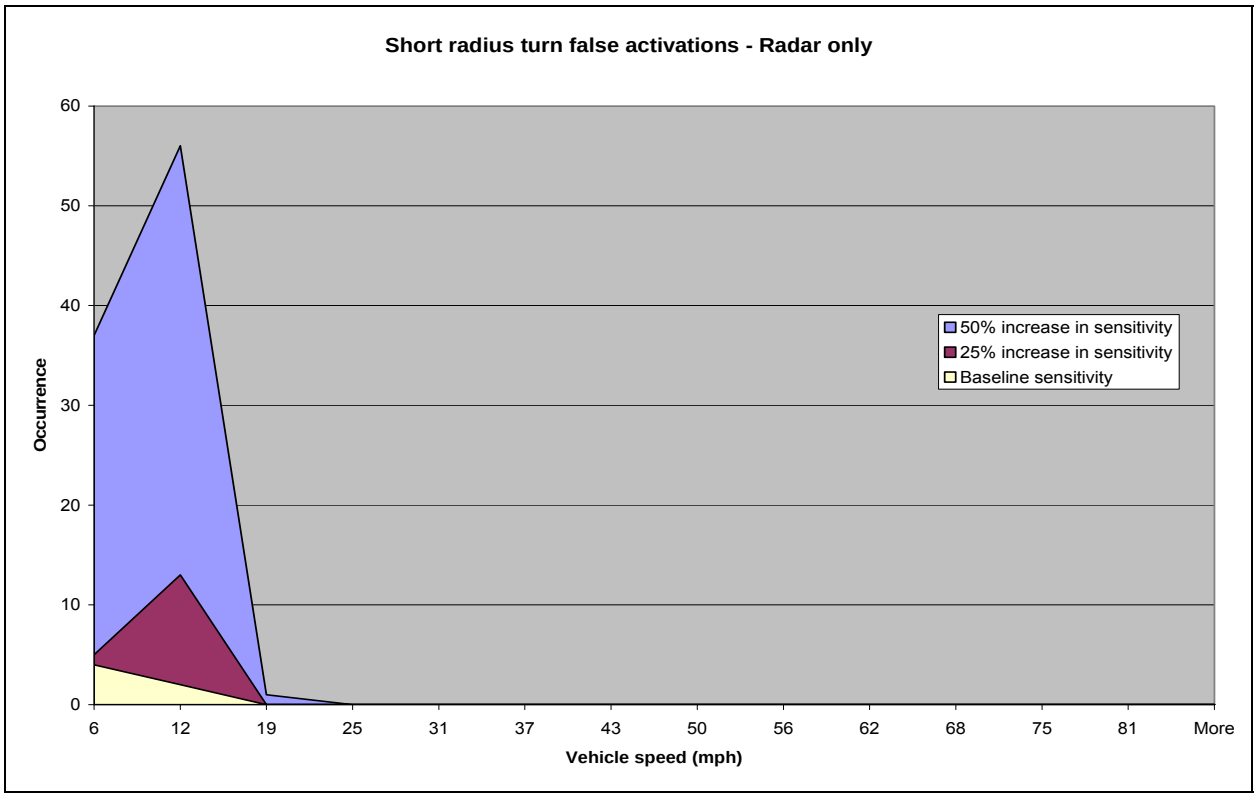

Figure 130: Speed Distribution for Radar-Only-Based, False Activations – Short-Radius Turn

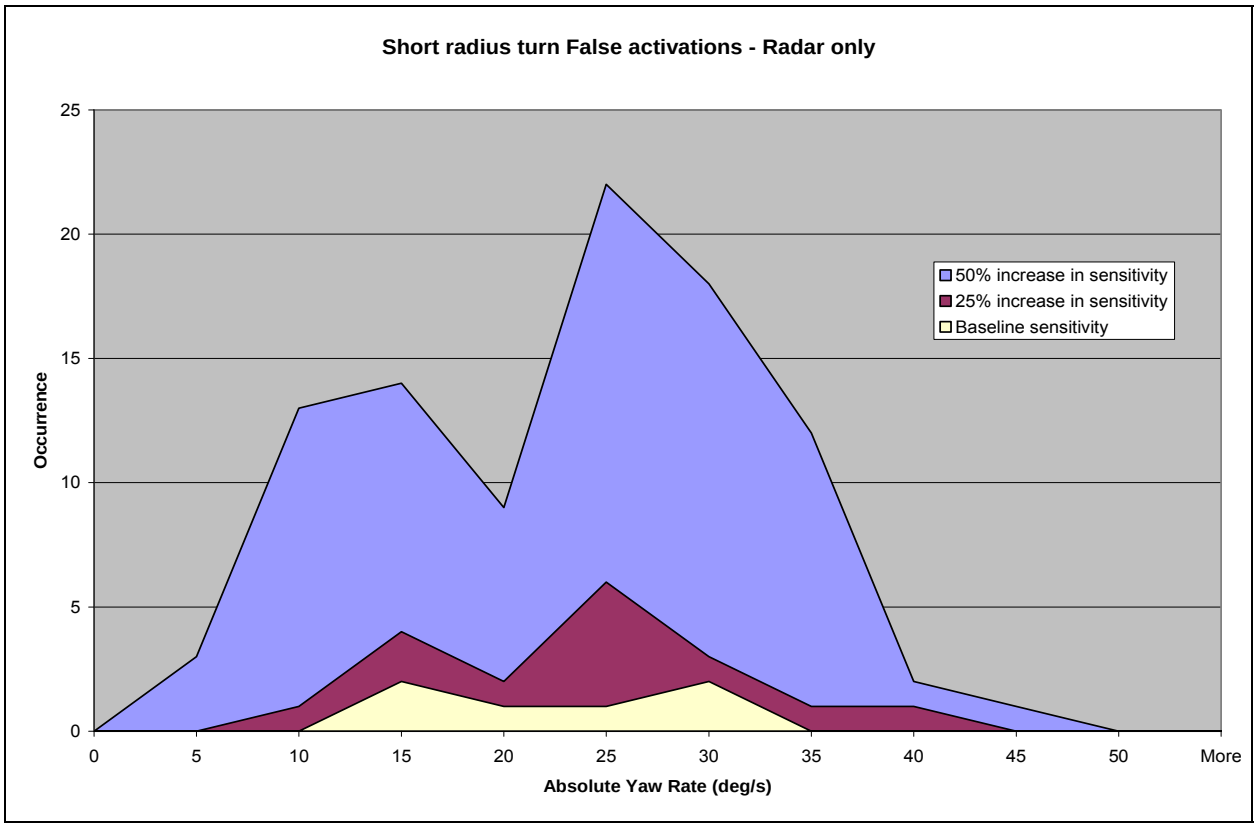

Figure 131: Yaw Rate Distribution for Radar-Only-Based, False Activations – Short-Radius Turn

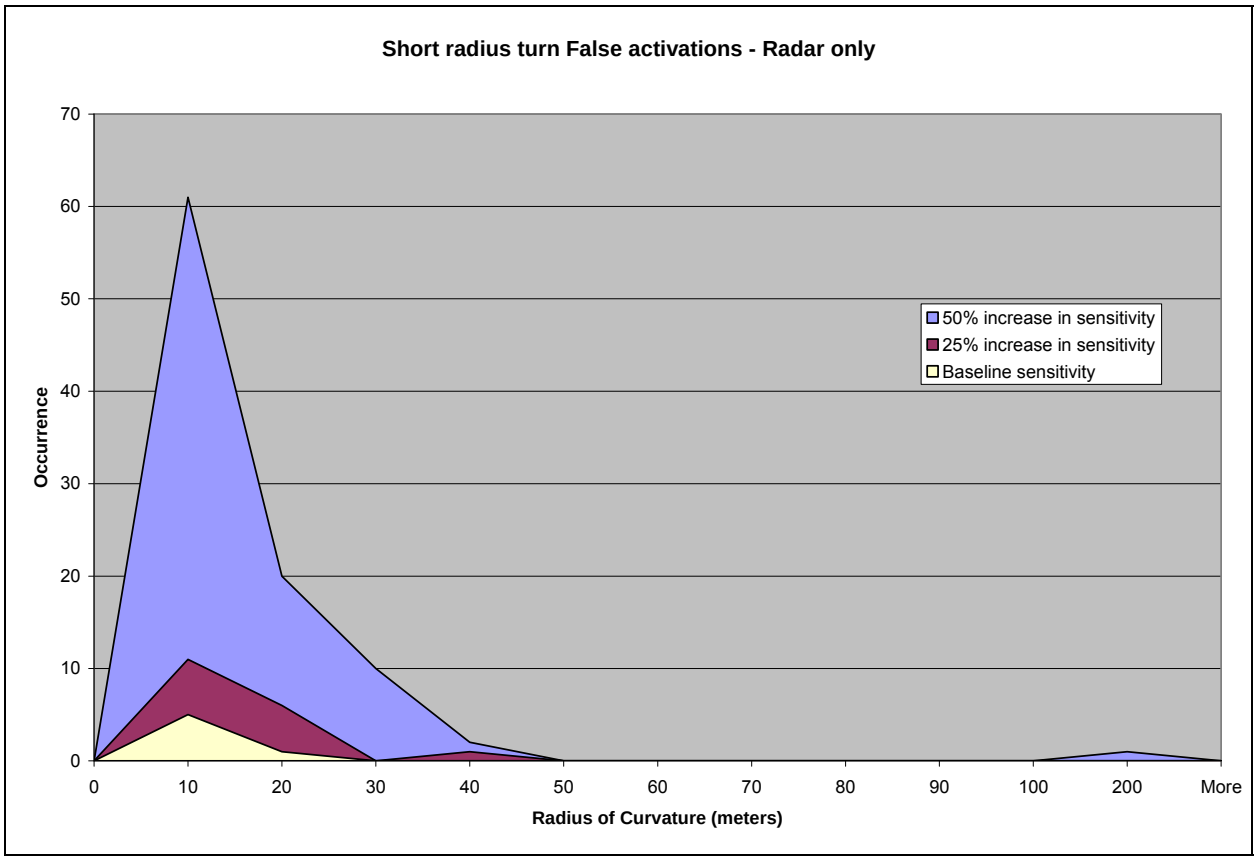

Figure 132: Radius of Curvature Distribution for Radar-Only-Based, False Activations – Short-Radius Turn

N.2.2 Analysis of Stand-alone Mono-Vision System

In order to evaluate the CIB data in a Mono-Vision-only configuration, the entire dataset had to be resimulated (in order to eliminate any radar influence on the performance of the vision detection algorithms) and a new threat assessment module was created. The Baseline sensitivity of the system was set similar to that of the fusion-based system.

Since the threat assessment of the resulting system configuration was not suitably optimized for a "vision-only" sensing input, a larger number of false interventions and near misses occurred than would be anticipated in a production system. Because of the higher number of false events observed, +25% and -25% changes in system sensitivity relative to the baseline were employed (instead of using +25% and +50% as was done for the other sensing combinations). This setting approach was chosen because it was felt to provide a better indication of how false intervention performance might change with changing sensitivities, while still giving a realistic representation of potential false event scenarios.

As expected, investigation of the vision-only false events indicated that a different set of false event classification scenarios had to be defined. Mono-Vision systems do not measure range and range rate directly but instead rely on visual scene cues, such as position of the detected vehicle in the frame and its change in size and motion from frame

to frame. The majority of the observed false events appear to be the result of the perceived size or position of the detected vehicle changing abruptly across frames, usually due to other objects in the scene (e.g., shadow or road markings) being included as part of the perceived vehicle. Figure 133 shows the distribution of false intervention events across sensitivity settings. In order to illustrate how the number of events changed with sensitivity settings, the data in this figure were normalized to the total number of baseline events.

Figure 134 shows the same false intervention information except each scenario is normalized as a percentage of the total number of events for each sensitivity setting. This was done to illustrate how the distribution of event types changed with sensitivity settings.

Figure 135 shows the distribution of false precharge ("near miss") events across sensitivity setting conditions normalized to the total number of baseline events. This was done to illustrate how the number of events changed with sensitivity settings.

Figure 136 shows the same false, precharge information with each scenario normalized as a percentage of the total number of events for each sensitivity setting. This was done to illustrate how the distribution of event types changed with sensitivity settings.

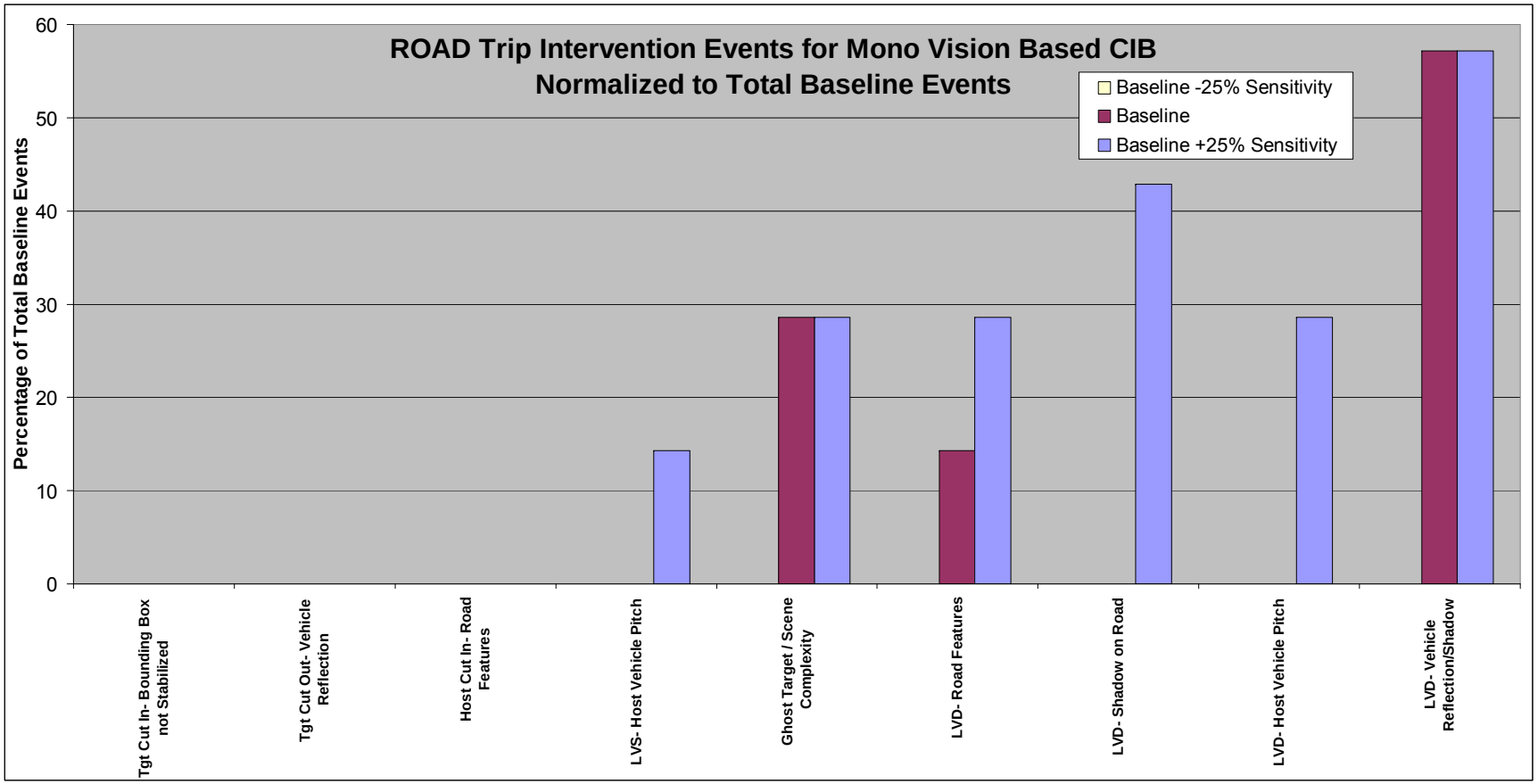

Figure 133: Scenario Classifications for Mono-Vision-Only False Interventions

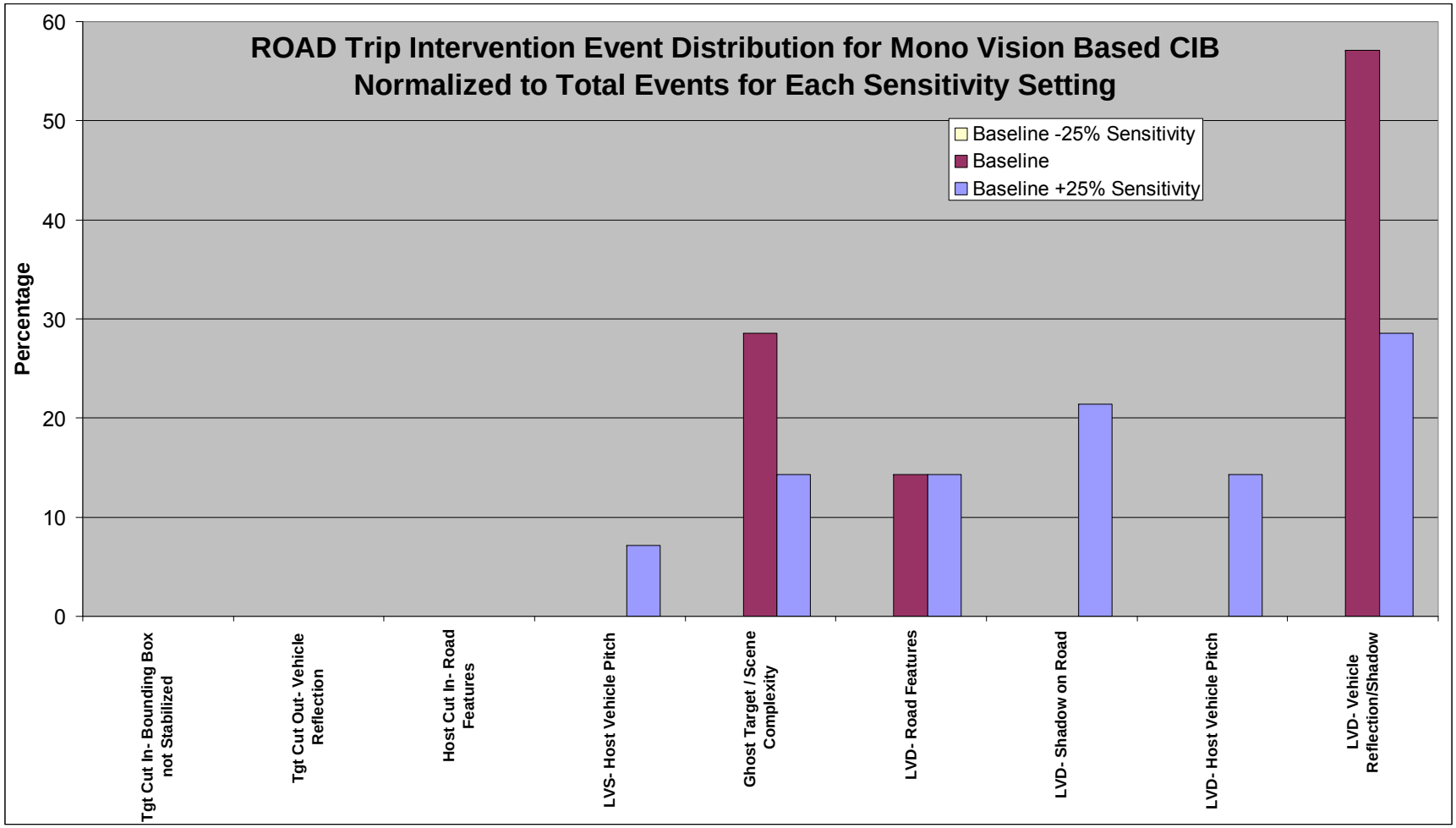

Figure 134: Scenario Distribution for Mono-Vision-Only, False-Intervention Events

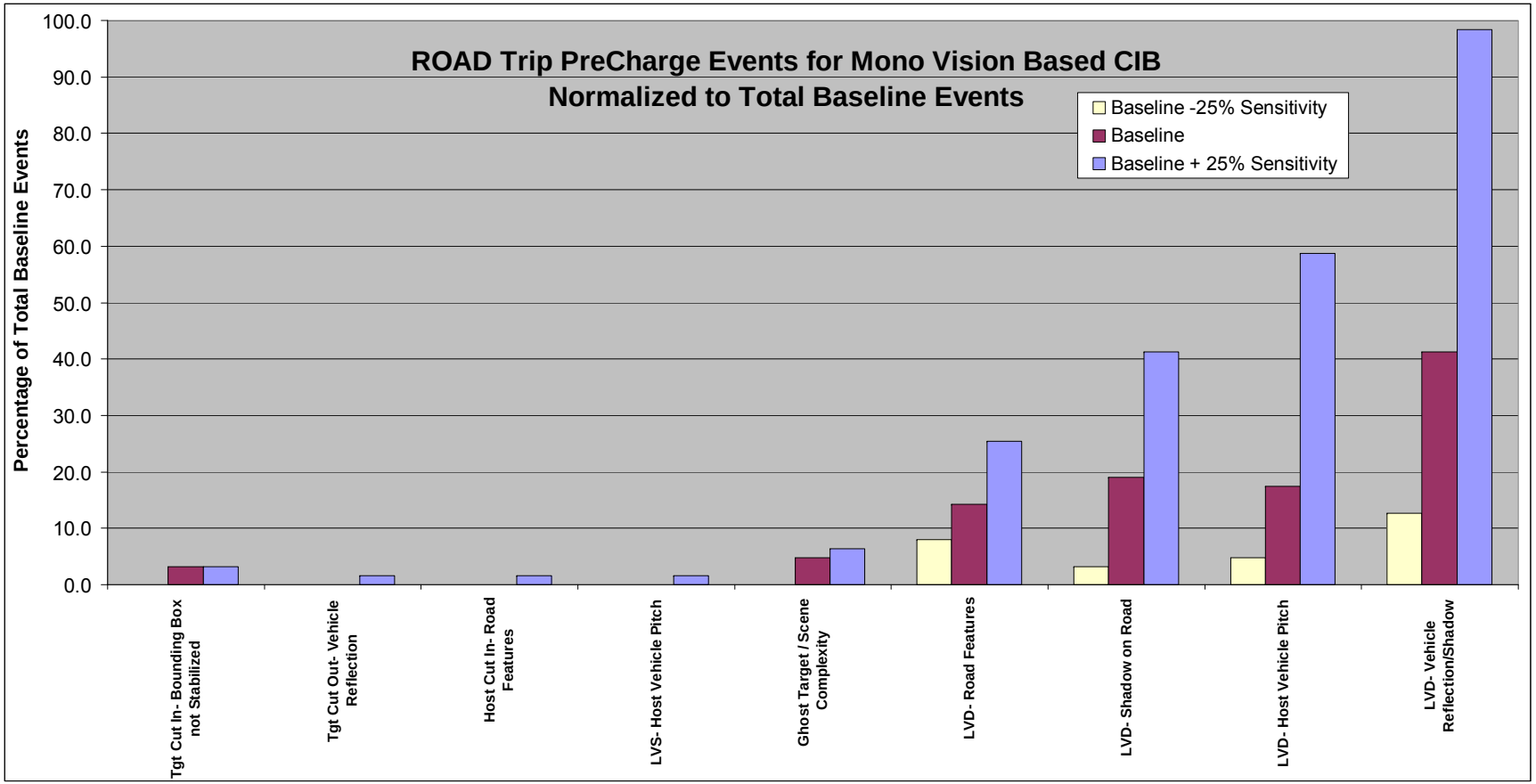

Figure 135: Scenario Classifications for Mono-Vision-Only, False, Precharge Events

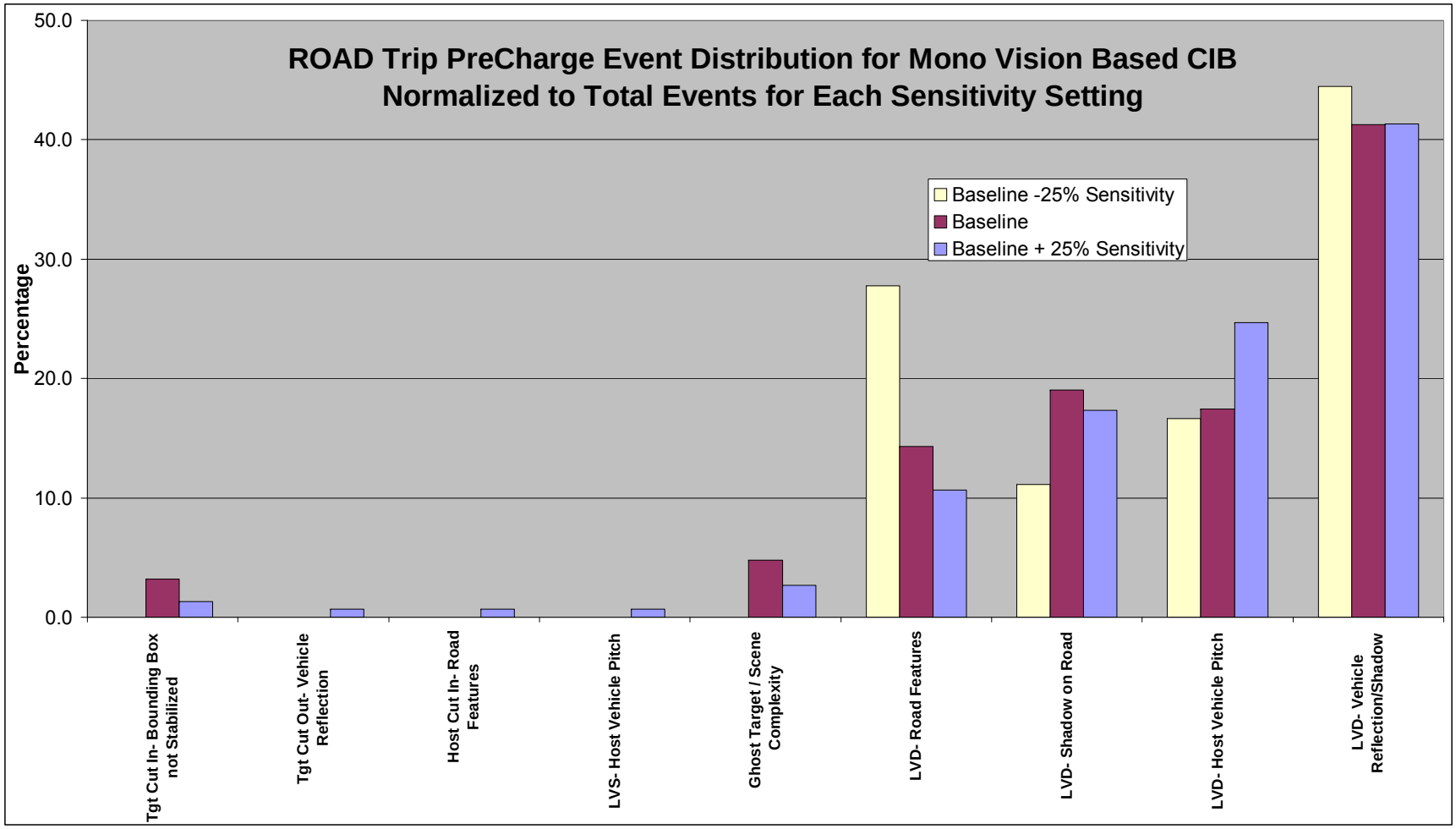

Figure 136: Scenario Distribution for Mono-Vision-Only, False, Precharge Events

N.2.2.1 Scenario Descriptions

The preceding figures addressing the scenario distribution of Mono-Vision indicate that the false events primarily occurred during Lead Vehicle Decelerating (LVD) Scenarios.These false event conditions can also be influenced and exacerbated by the deceleration profile of the lead vehicle.

N.2.2.1.1 LVD – Road-Features

The LVD Road-Feature events occurred when the target vehicle passed over a feature on the roadway surface, such as a crosswalk marking, turn-lane arrow, or discolorations on the road surface. Figure 137 and Figure 138 show examples of this type of false event.

Figure 137: Turn-Lane Arrow Influencing Vision Measurement

Figure 138: Line on Road Influencing Vision Measurement

Roadway surface features were sometimes misinterpreted as part of the target vehicle, which in turn influenced the Mono-Vision system's target size and position estimates and, thereby, the threat potential of the target vehicle. Consequently, the threat assessor may falsely report the target vehicle under these conditions as an imminent threat.

Figure 134 indicated that LVD Road Features accounted for approximately 15% of the false intervention events for both the Baseline and increased sensitivity settings (there were no false interventions with decreased sensitivity). Of the false precharge events shown in Figure 136, road features accounted for approximately 25% of the total events for the decreased sensitivity setting and approximately 10% of the total for the increased sensitivity setting.

N.2.2.1.2 LVD – Shadow-on-Road

LVD Shadow-on-Road-related events occurred when the target vehicle passed over a shadow on the roadway surface, such as those created by roadside objects like trees or buildings. Figure 139 shows an example of this type of false event.

Figure 139: Shadow-on-Road Influencing Vision Measurement

As with the LVD Road-Features events, the shadow was sometimes misinterpreted as part of the target vehicle, which in turn influenced the Mono-Vision system's target size and position estimates and, thereby, the threat potential of the target vehicle.

Figure 134 indicates this type of event did not occur at the baseline and decreased sensitivity settings and accounted for 20% of the false intervention events for the increased sensitivity setting. Of the false precharge events shown in Figure 136, shadows on the road accounted for approximately 10% of the total events for the decreased sensitivity settings and increased to approximately 15-20% of the total events for the baseline and increased sensitivity settings.

N.2.2.1.3 LVD – Host-Vehicle-Pitch

The LVD Host-Vehicle-Pitch events occurred when the target vehicle passed over a discontinuity on the roadway surface, such as those created by driving through intersections while going up or down a hill. Figure 140 shows an example of a large pitch change that led to this type of false event.

Figure 140: Change-in-Vehicle Pitch Influencing Vision Measurement

The resulting vehicle pitch change momentarily moves the horizon line and, thus, the position of the target vehicle in the image. This sudden movement of the target vehicle may temporarily distort the perceived size and position of the target vehicle.

Figure 134 illustrates that this type of event accounted for none of the events on the baseline and decreased sensitivity settings (there were no false interventions with decreased sensitivity) and increased to approximately 15% of the false intervention events for the increased sensitivity setting. Of the false precharge events shown in Figure 136, changes in host vehicle pitch accounted for approximately 15-20% of the total events for the decreased sensitivity and baseline settings and increased to approximately 25% of the total for the increased sensitivity settings.

N.2.2.1.4 LVD – Target-Vehicle-Reflection/Shadow

The LVD Target-Vehicle-Reflection/Shadow events occurred when the target vehicle casts a long, high-contrast shadow on the roadway surface, such as those created when the sun is relatively low in the sky. Figure 141 and Figure 142 show examples of this type of false event.

Figure 141: Vehicle Reflection Influencing Vision Measurement

Figure 142: Vehicle Shadow Influencing Vision Measurement

As with the LVD Road Feature events, the shadow was inadvertently associated with the target vehicle. However, in these cases the shadow moved with the target vehicle. At longer ranges when the visual angle subtended by the shadow was lower, the shadow had little effect on the perceived size of the target vehicle. However, as the range to the target

vehicle decreased, when the visual angle subtended by the shadow was higher, the shadow influenced the perceived size and position of the target vehicle.

Figure 134 indicates this type of event did not occur with the decreased sensitivity setting and increased to nearly 60% of the false intervention events for the baseline setting and decreased to nearly 30% of the increased sensitivity false intervention events. Of the false precharge events shown in Figure 136, target vehicle reflections/shadows accounted for approximately 40% of the total events for each of the sensitivity settings.

N.2.2.1.5 Ghost-Targets and Scene-Complexity

Ghost-Target and Scene-Complexity events occurred when the vision algorithm incorrectly interpreted non-vehicle elements in the scene as a vehicle. When this condition lasts for a sufficient amount of time, it can cause false events. Figure 143 and Figure 144 show examples of these types of false event.

Figure 143: Ghost Targets

Figure 144: Scene Complexity Influencing Vision Measurement

Figure 134 illustrates that this type of event did not occur at the decreased sensitivity settings and increased to nearly 30% of the false intervention events for the baseline setting and decreased to approximately 15% of the increased sensitivity false intervention events. Of the false precharge events shown in Figure 136, target vehicle

reflections/shadows accounted for less than 5% of the total events for each of the sensitivity settings.

N.2.2.2 Kinematics Analysis of Mono-Vision False-Events

The majority of the Mono-Vision-based false events were the result of incorrect TTC calculations caused by misinterpretations of the visual scene which generated erroneous TTC estimates. In order to further characterize the scenarios in which these false events took place, radar range and range rate values were manually correlated to the vision target for each false event. These radar-based calculations were used in the characterizations described below.

N.2.2.2.1 Host-Vehicle Speed Characterization

For the Mono-Vision only sensing system configuration, analysis of the false event scenarios indicated that the kinematics of the false events, in general, were similar for the majority of these scenarios. A large number of the false-events scenarios involved a misinterpretation of the target vehicle's threat potential when the target vehicle was coming to a stop at an intersection. This is supported by results shown in Figure 145 and Figure 146, which provide the distribution of host vehicle speeds for all false events (i.e., intervention and precharge). In these plots, the majority of events occurred when the host vehicle speed was between 9 and 25 mph.

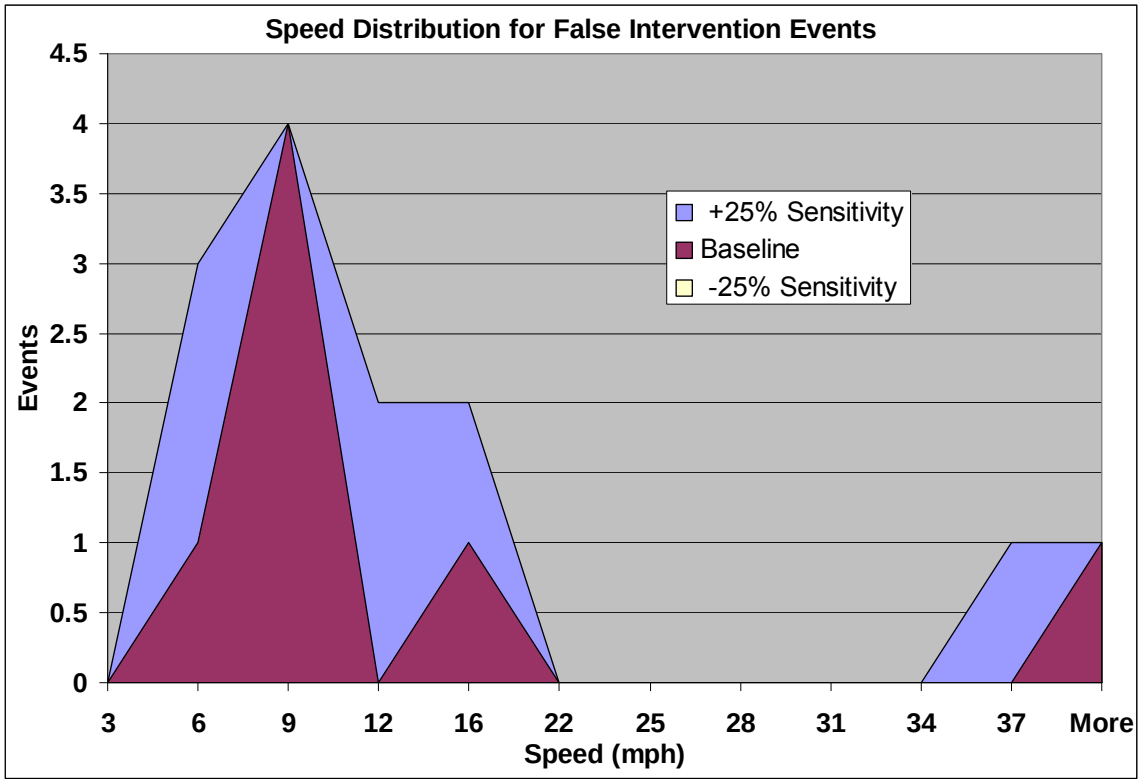

Figure 145: Speed Distribution for Mono-Vision-Based, False-Intervention Events

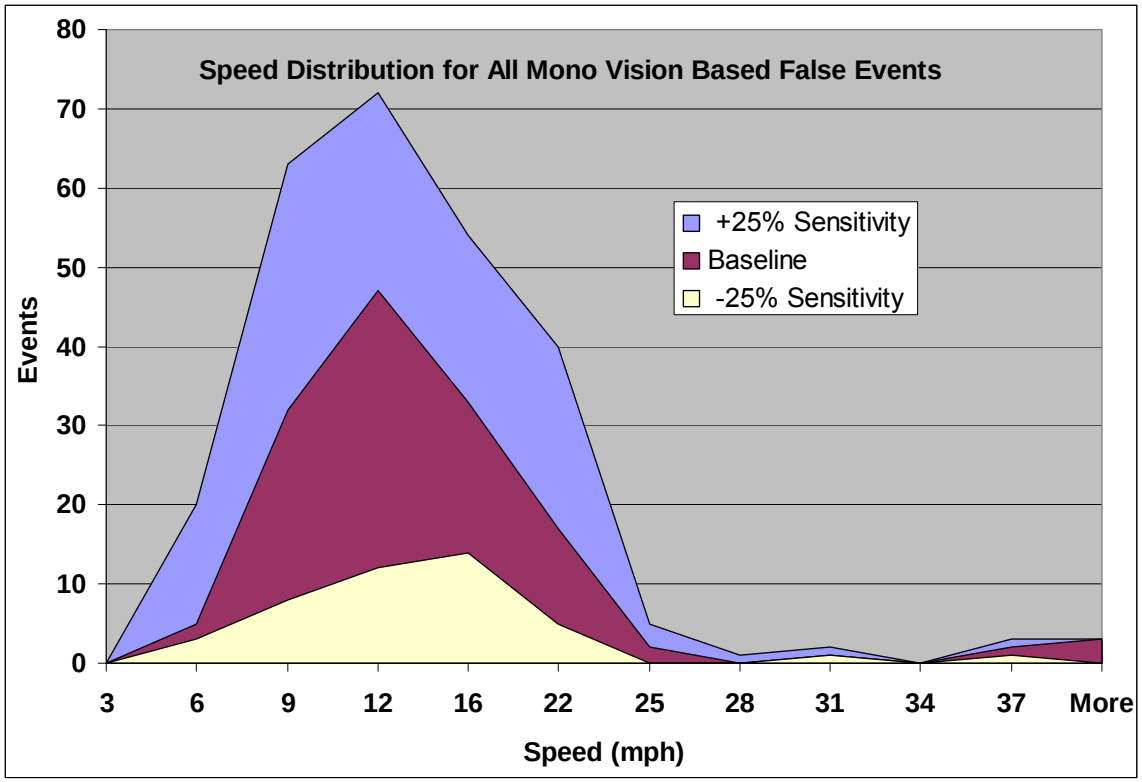

Figure 146: Speed Distribution for All Mono-Vision-Based False Events

N.2.2.2.2 Host Vehicle Yaw Rate Characterization

Figure 147 provides the distributions of the host vehicle's measured yaw rate at the time of the false event and indicates that for the majority of Mono-Vision-based false events the yaw rate ranged between -1 deg/sand 1 deg/s.

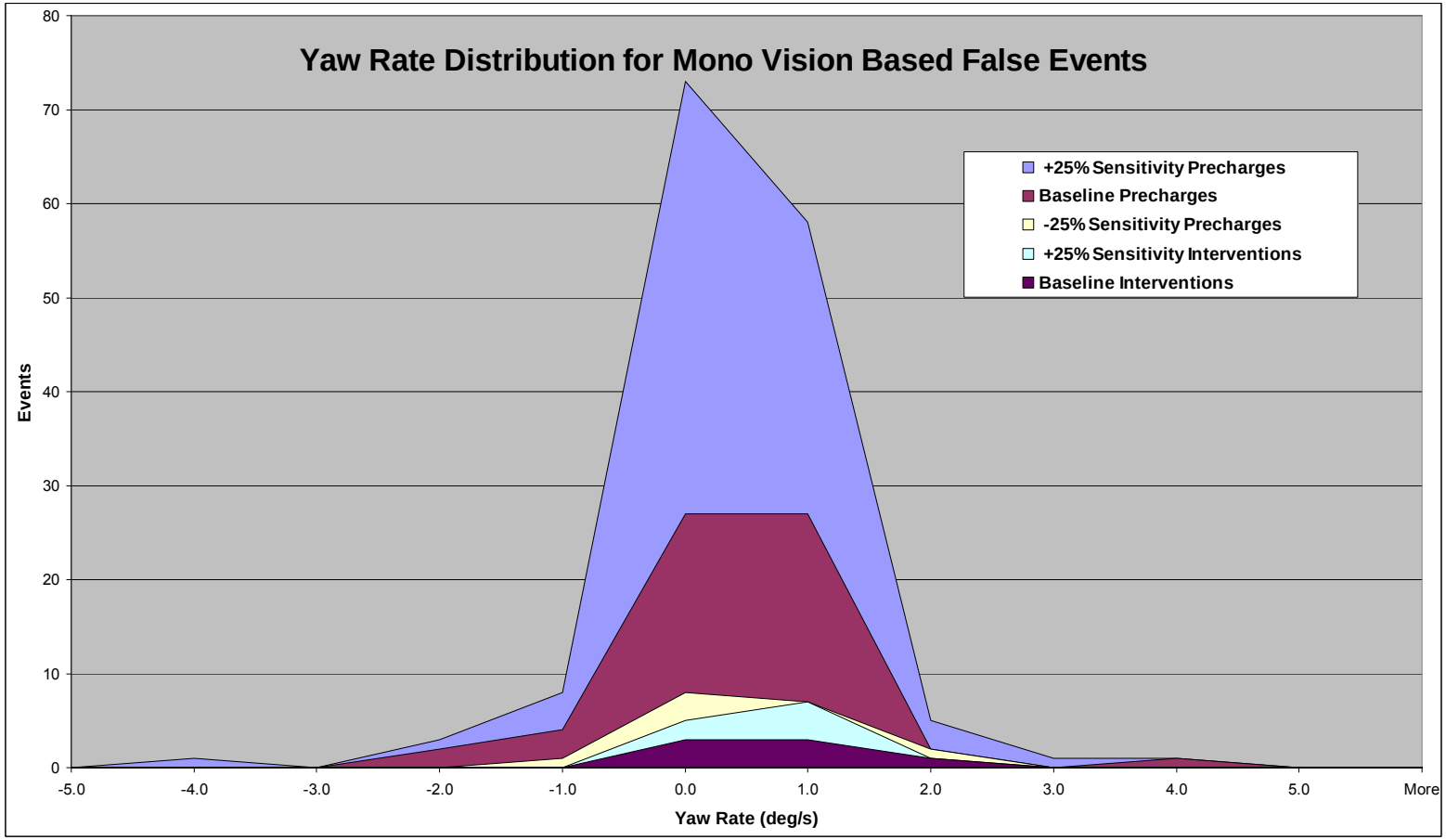

Figure 147: Yaw Rate for Mono-Vision False Events

N.2.2.2.3 Time- to-Collision (TTC) Characterization

The algorithms used to determine the level of threat in the Mono-Vision-only system configuration relied on more information than just the TTC calculation (whether simple range divided by range rate or a more complex formulation) described earlier. Consequently, sensitivity settings are specified as “Baseline” and “Baseline” plus or minus a percentage of sensitivity.

After correlating the vision targets to their corresponding radar targets in the dataset, a distribution of the radar-based simple TTC values observed was created. This information is shown to provide an approximation of the correlation of TTC to system sensitivity. This distribution is shown in Figure 148 and indicated that the majority of Mono-Vision-based false events took place when the simple TTC values were in the range of 2.0 to 3.5 seconds.

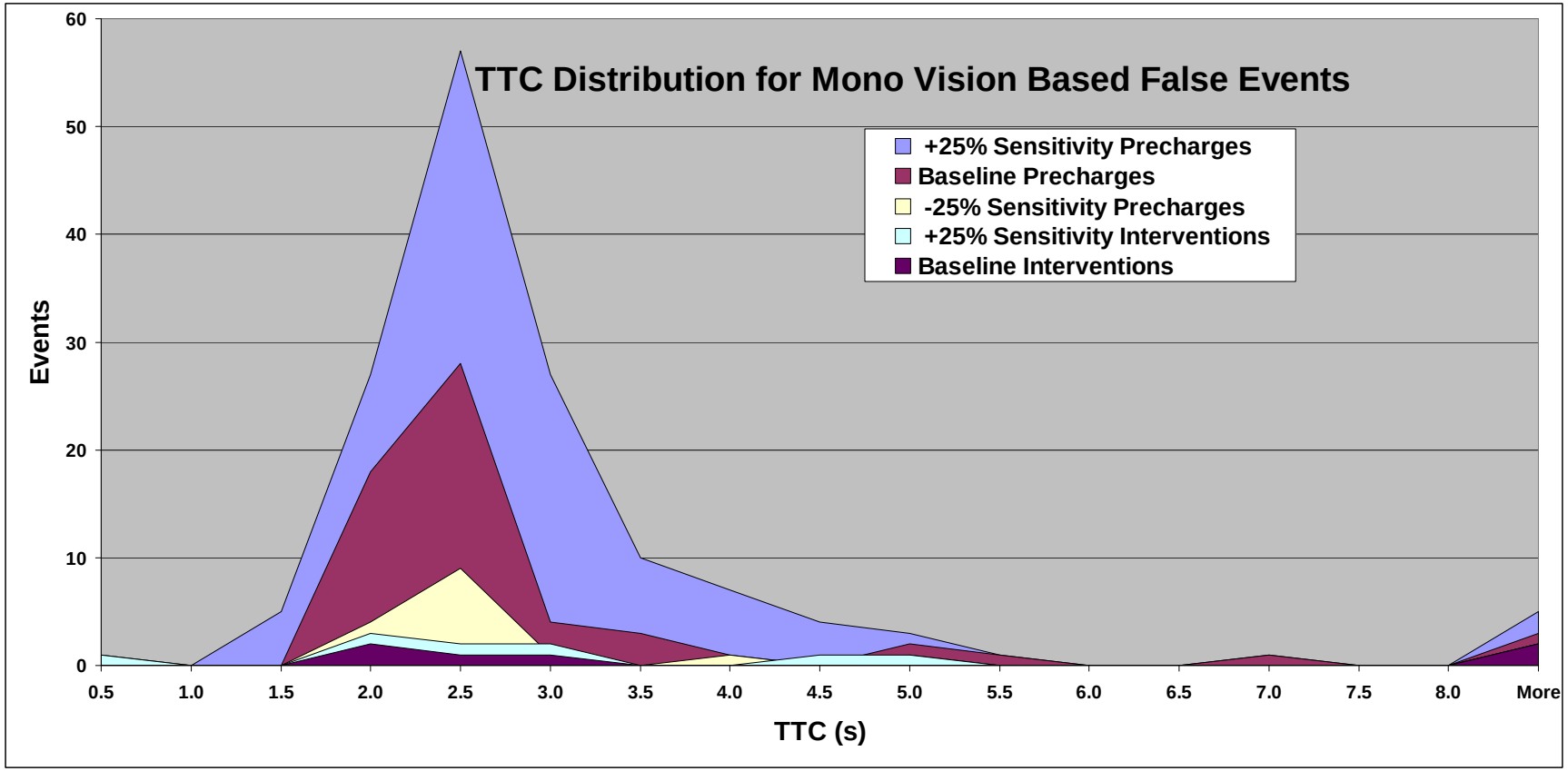

Figure 148: TTCs for Mono-Vision-Based False Events

N.2.2.2.4 Target-Range Characterization

As indicated above, the vision targets for each false event was manually correlated with their corresponding radar target in the dataset. Figure 149 illustrates the resulting distribution of the radar-based target ranges for all of the Mono-Vision-based, False-Precharge and False-Intervention events. This data shows that for each of the sensitivity cases, the mode of the target range distribution for Mono-Vision-related precharge and intervention false events was between 9 and 15 meters.

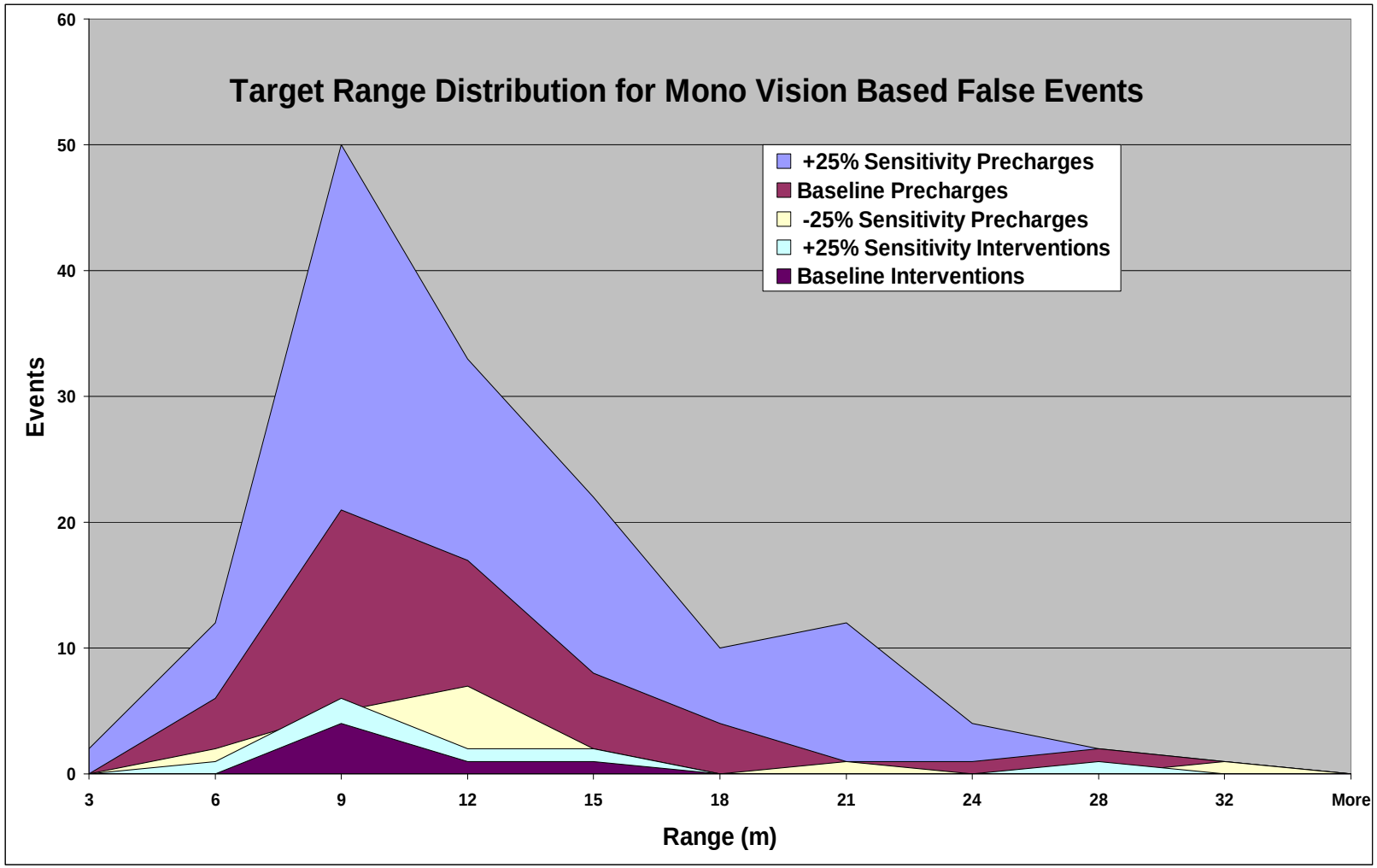

Figure 149: Target Range for Mono-Vision-Based False Events

N.2.2.2.5 Target-Range Rate Characterization

Once again, the vision targets for each event were manually correlated with their corresponding radar target in the dataset. Figure 150 provides the distribution of the radar-measured, target-range rate values for the Mono-Vision-based False-Precharge and False-Intervention events. These results indicate that majority of the target-range rate values at the time of the event ranged between -2 m/s to -6 m/s.

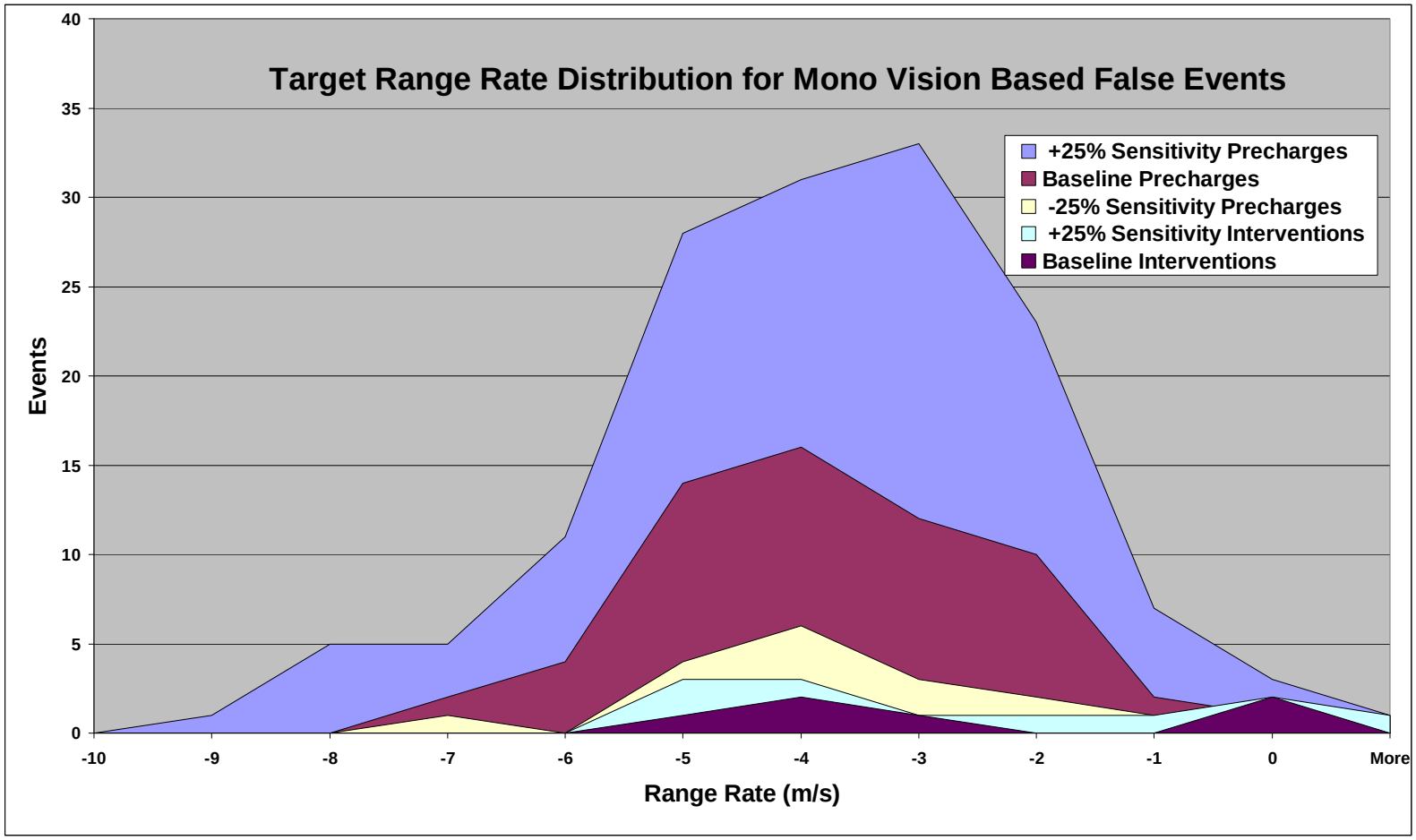

Figure 150: Target-Range Rate for Mono-Vision-Based False Events

N.2.2.2.6 Target-Vehicle-Deceleration Characterization

Unfortunately, particularly in light of the preponderance of Mono-Vision false events involving LVD scenarios, data for measuring the deceleration level of the target vehicles for these events was not directly available in the dataset. While an analysis of the change in target range rate versus the host vehicle deceleration could potentially be inferred from existing data, it was felt that such processes could add an unacceptable amount of noise to the resulting data. With that said, it is important to note that the majority of these false event cases were the result of following the lead vehicle to a stop in normal traffic, such as at an intersection or stop sign. This type of scenario typically involves deceleration in the range of 0.2 to 0.3g.

N.2.3 Analysis of Fused, Mono-Vision/Radar Sensing

The concept of "fused" sensing generally refers to using information from two or more different sensing systems (e.g., radar and vision) to obtain a more complete understanding of the environment that would be possible with either system's information alone. In the case of the both vehicles used in the ROAD Trip, this consisted of the fusion of the Long/Mid Range radar and Mono-Vision systems. The precise advantages of this combination of sensors depend on the exact nature of the fusion implementation. Because each of these two sensing systems have well understood strengths and weaknesses in different areas (e.g., range estimates versus target classification), the information provided by the combination of these sensors can be used in a complementary fashion to strengthen overall system performance. In some cases, information from one of the sensing systems can be used to augment the performance of the other. For example, the fusion algorithm can use the target classification information from a vision sensing system to confirm targets identified by the radar sensing system.

The raw data that was collected during the ROAD Trip was "fused" data (i.e., Mono-Vision and Radar). This data served as the "Baseline" for the fusion analysis. Much like the radar only and camera only methods, an analysis was performed at varying sensitivities in order to better understand system performance (see Figure 151 and Figure 152). These additional sensitivities were set to +25% and +50%. The raw data was resimulated at these sensitivity levels to produce comparative data sets.

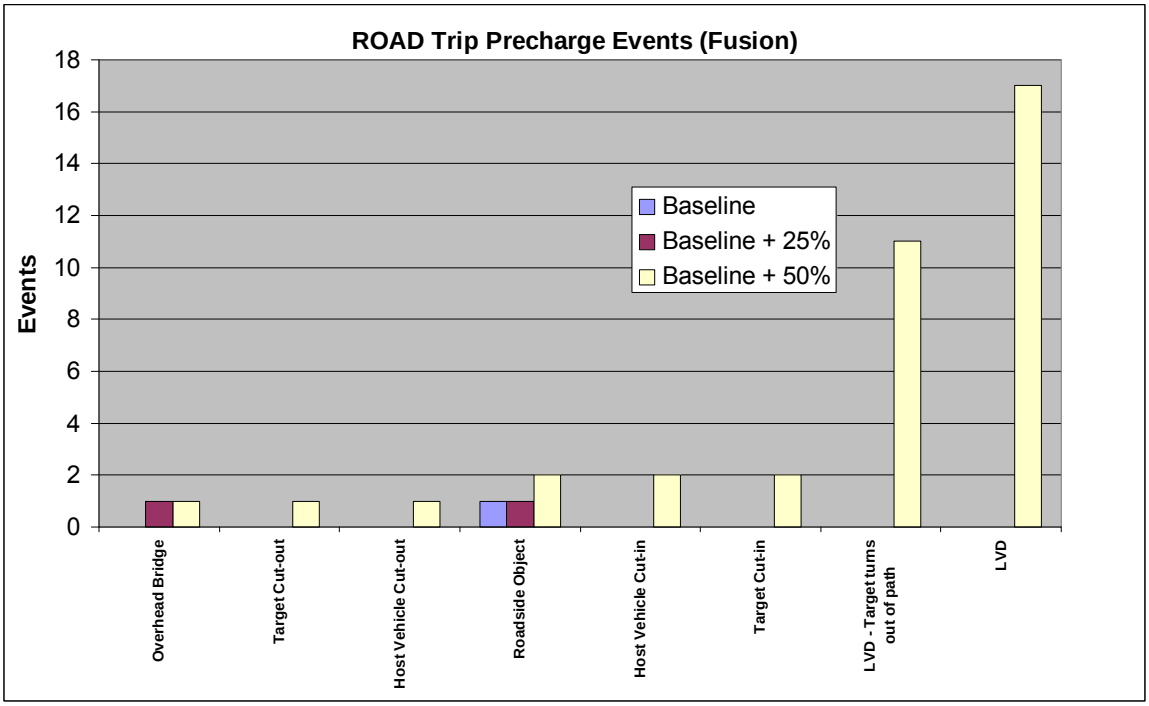

Figure 151: Scenario Classifications for Fusion False Precharge Events

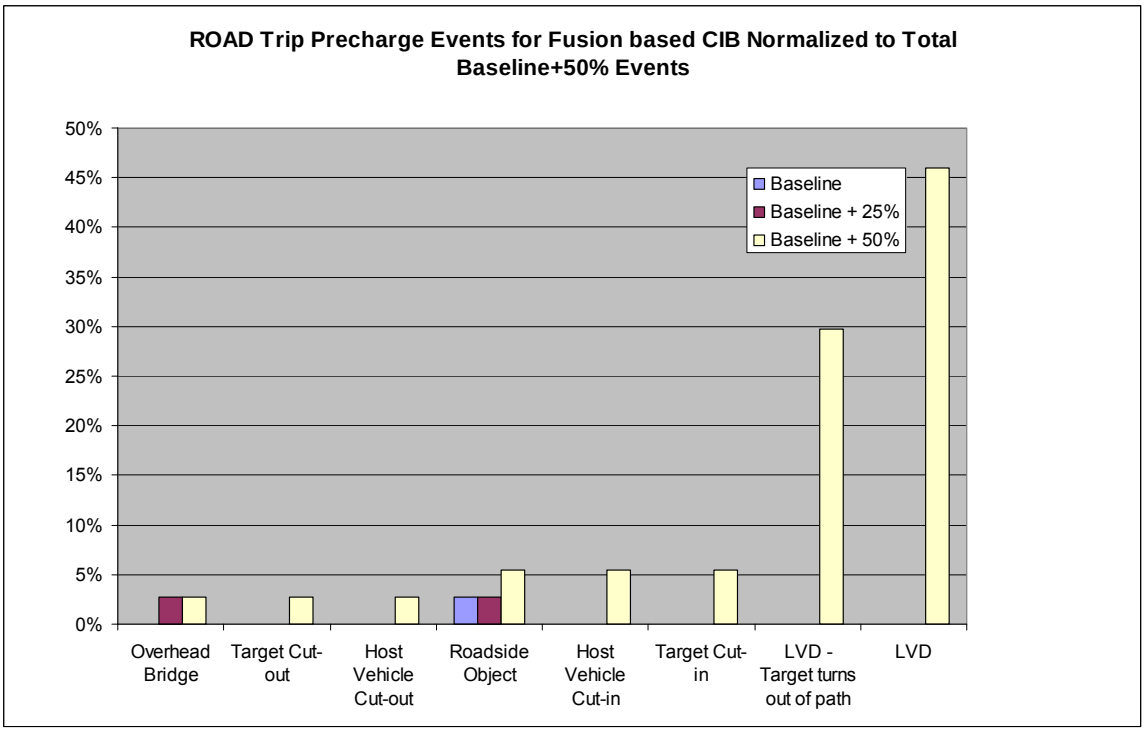

Figure 152: Scenario Classifications for Fusion False Precharge Events (Normalized)

N.2.3.1 Scenario Descriptions

These results indicate that combining both radar and camera data into a fused system dramatically reduced the total number of false events decreases over the stand-alone sensors used in the current testing. False interventions were eliminated entirely, and at the Baseline sensitivity level, false Precharge events were reduced almost completely. Only by adjusting the sensitivity level significantly did the occurrence of false Precharge events increase. Results from the +50% sensitivity level event distribution shows indicate the prominence of two types of scenarios: LVD, and LVD–Target Turns Out of Path.

N.2.3.1.1 Roadside Object

The only Roadway Object event at the Baseline sensitivity level was a “Roadside-Object” Precharge event. Figure 153 depicts this event in which the radar picks up a row of concrete posts along the lane edge as a stationary target. This information may have been fused with “moving” vision data, which in turn created a false valid target to which the system then reacted.

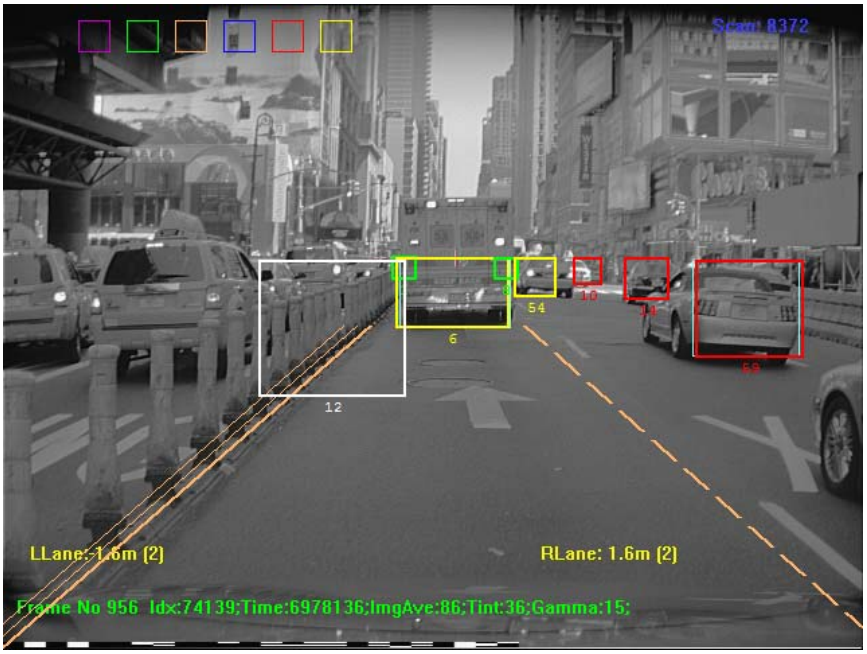

Figure 153: False Precharge Event at Baseline Sensitivity Due to Roadside Object

N.2.3.1.2 Lead Vehicle Decelerating (LVD)

Upon reviewing the LVD events, it was observed that most of the occurrences were a direct result of the increased sensitivity level rather than a misinterpretation of the sensor data or detection of a false target. Both the range and range-rate information recorded during these events support that under Baseline sensitivity levels, a Precharge event would not occur.

Figure 154 illustrates a case during normal highway driving where traffic was forced to reduce speed at a moderate deceleration level and a legitimate system Precharge event was triggered (but only at the + 50% sensitivity level).

Figure 154: "LVD" Precharge Event at Baseline + 50%

N.2.3.1.3 LVD – Target Turns Out-of-Path

Reviewing the "LVD – Target Turns Out-of-Path" subset of events produced a similar set of results as found in the LVD analysis. In general, these events were deemed to be strictly a result of the increased sensitivity level and judged as either unnecessary or "unwanted" from the driver perspective.

Figure 155 illustrates the case in which the target vehicle decelerates before turning out of the path of the host vehicle. The host vehicle's range and range-rate information supported the trigger of early Precharge event.

Figure 155: "LVD - Target Turns Out-of-Path" Precharge Event at Baseline + 50%

N.2.3.2 Kinematic Analysis of Fused Mono-Vision/Radar Sensing False-Events

Similar to the sections above, reviewing the baseline + 50% sensitivity level provides some basic knowledge on the host vehicle's kinematics.

N.2.3.2.1 Speed Characterization

Figure 156 below shows the speed distribution for all Precharge events at all three sensitivity levels. Focusing on the +50% data, it is clear from this plot that the majority of false events occurred below about 30 mph. This trend is also evident for the two scenarios with the highest occurrence, LVD and LVD – Target Turns Out-of-Path (see Figure 157 and Figure 158).

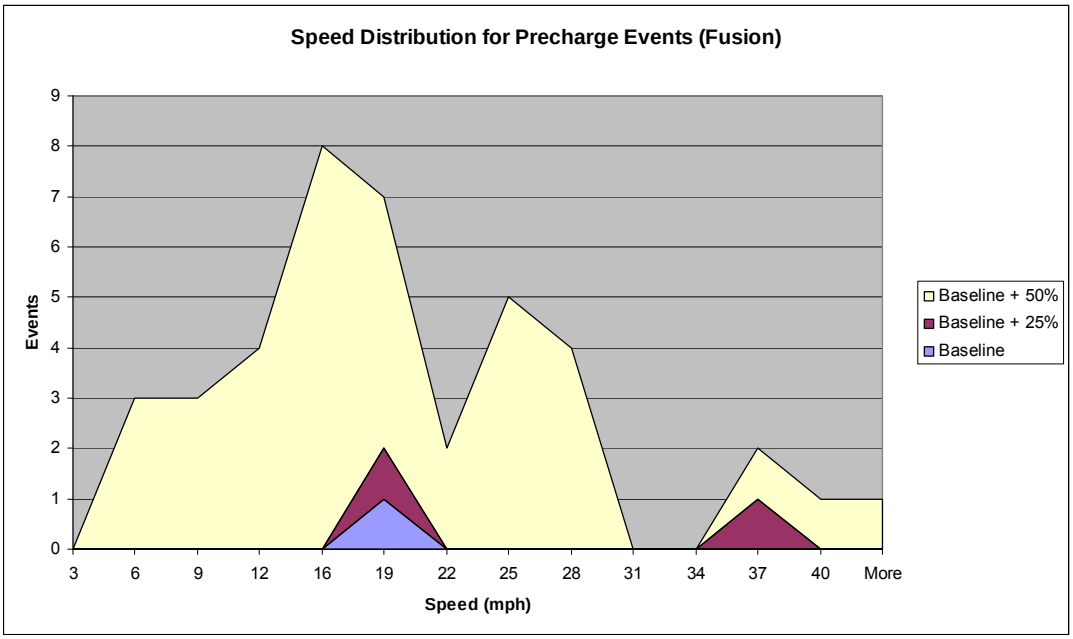

Figure 156: Speed Distribution for Fusion Precharge Events

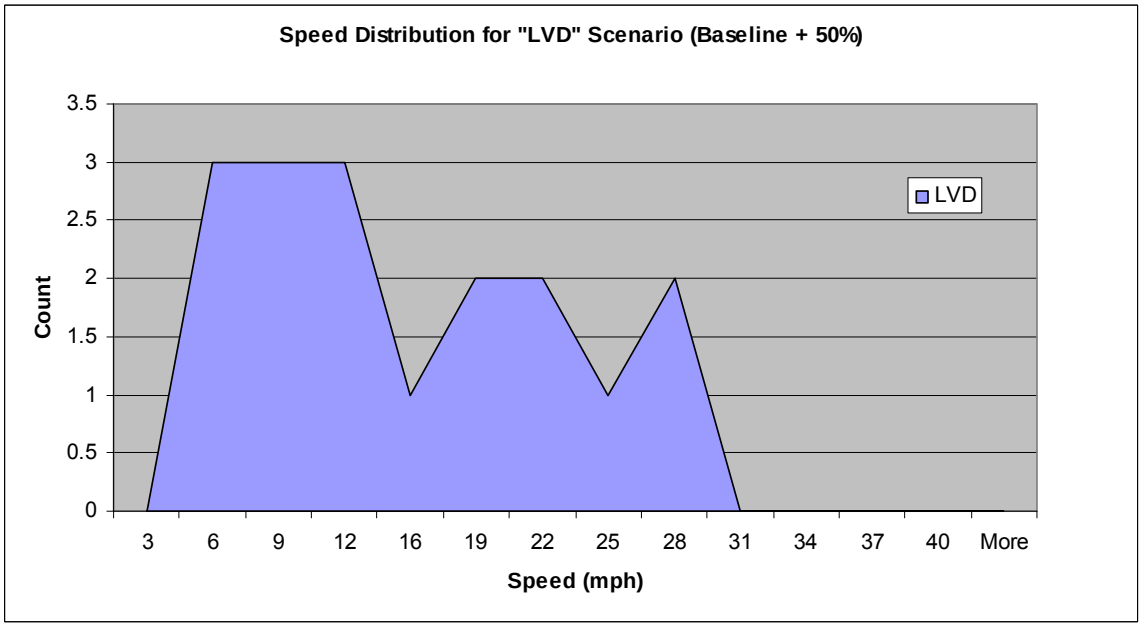

Figure 157: Speed Distribution for LVD Events

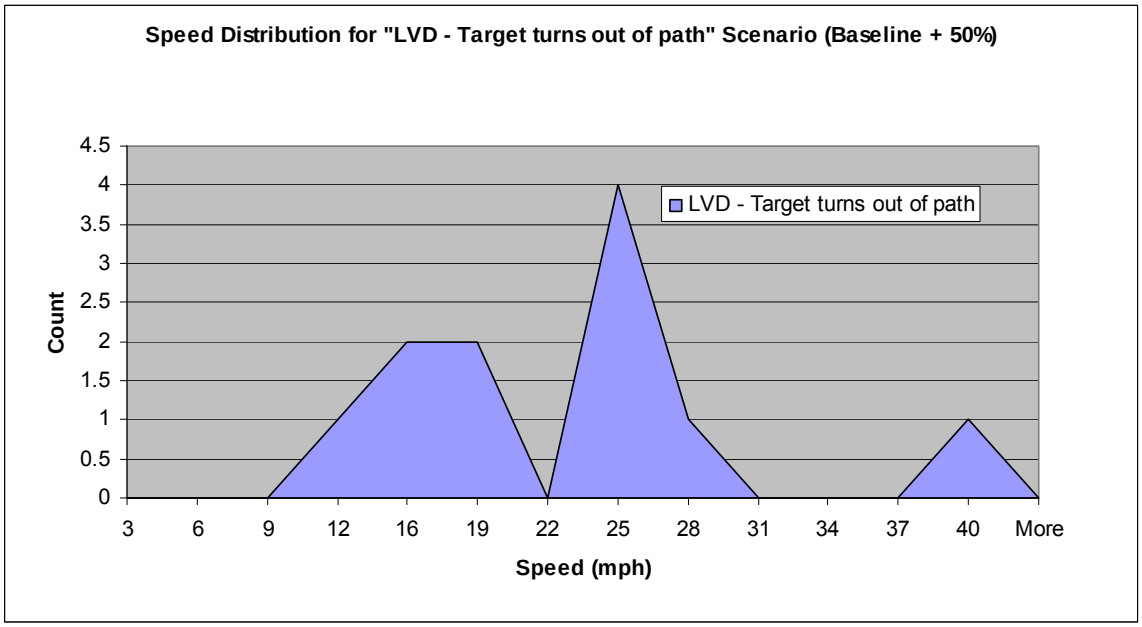

Figure 158: Speed Distribution for LVD – Target Turns Out-of-Path Events

N.2.3.2.2 Yaw Rate Characterization

Figure 159 provides the distribution of the host vehicle's measured yaw rate at the time of the false event. These results indicate that for the majority of fusion-based false events (all occurring the Baseline + 50% condition), the yaw rate was measured to be between - 1 deg/s and 1 deg/s.

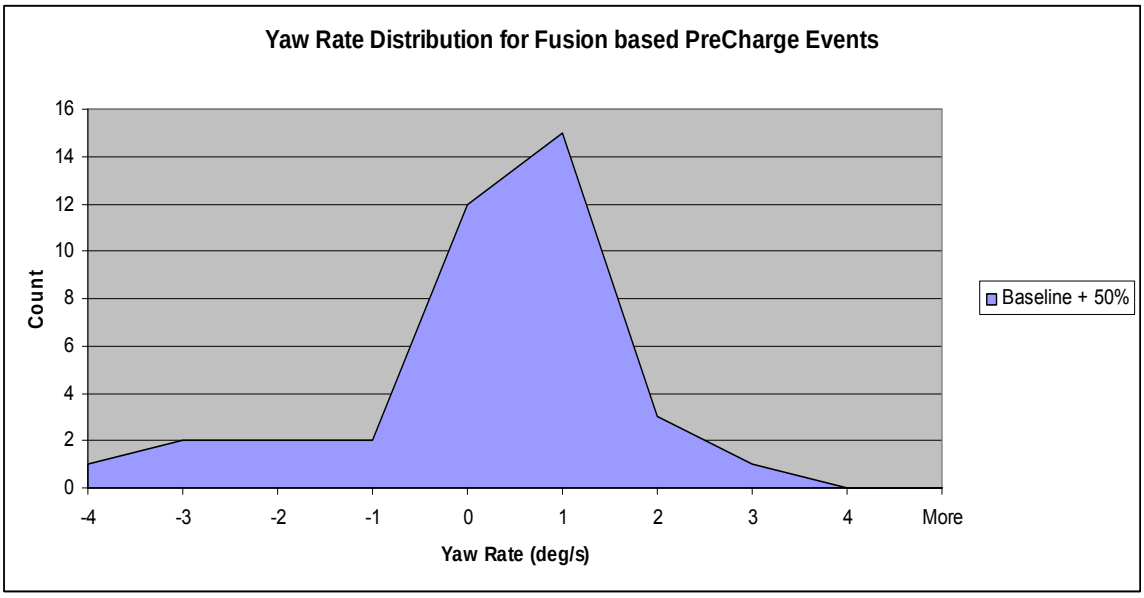

Figure 159: Yaw Rate Distribution for Fusion Precharge Events

N.2.4 Analysis of Stereo-Vision Based System

N.2.4.1 Data Collection

The data collected from the Stereo-Vision system provided a number of challenges that required developing a different analysis approach than was used for the other sensor configurations. First, the Stereo-Vision sensing system generated extremely large video file sizes, which prohibited continuous video data collection. Instead, target report data was transmitted from the sensors to the vehicle CAN where it was recorded continuously to the high-capacity data drive used for the other CIB system installed on the vehicle. Additionally, trigger points were established which initiated video data recordings surrounding CIB activation events identified by the Stereo-Vision system. These data recordings were triggered at both 0.6 sec and 0.3 sec simple TTC thresholds. Event data, including vehicle CAN, GPS, and target identifier information was recorded with these videos 16 seconds before and 4 seconds after the trigger event, which was not based upon any optimization of Stereo-Vision system. These triggers were selected based solely on the estimated amount of data storage space needed for the video recordings, which was based on an estimate of the number of recordings (i.e., trigger events) expected.

N.2.4.2 Data Analysis

Data from 258 event triggers were recorded over the ROAD Trip. An initial, post-trip, data review revealed that a large number of these recorded events included images which were either over-saturated (i.e., washed out), under bright, daytime conditions or under-saturated (i.e., too dark), under nighttime conditions. A subsequent review with the Stereo-Vision supplier revealed that a faulty “Automatic Aperture Control Algorithm” was loaded into the Stereo-Vision control module. This algorithm’s function is to appropriately adjust the camera imager’s aperture settings in response to ambient lighting conditions. Unfortunately, since the faulty algorithm failed to make these adjustments, a constant aperture setting was used during the entire ROAD Trip. This malfunction also resulted in data synchronizing issues between the vehicle CAN data, sensor target report data, and raw sensor video data. Once this issue was identified, the supplier attempted to reprocess the raw data through a system simulator.

Of the original 258 data recordings, 157 files could not be processed by the simulator. From the resimulation of the remaining 101 files, additional system performance issues were uncovered. First, due to the developmental nature of the Stereo-Vision system, the “Horizon Line Estimator” (HLE) function was deemed unreliable by the system supplier and deactivated during the ROAD Trip. Since this function provides an estimate of the road surface location, it can provide a potential means of minimizing false activations caused by road surface changes, shadows, hills, etc. Figure 160 and Figure 161 below contain sample event recordings that were deemed to be triggered as a result of this HLE function removal.

Figure 160: Example Recording #1 Triggered as a Result of the "Horizon Line Estimator" Function Removal

Figure 161: Example Recording #2 Triggered as a Result of the "Horizon Line Estimator" Function Removal

An additional performance issue discovered through the resimulation process was in the path estimation functionality. An error was found in the Stereo-Vision control algorithm

related to the sign (+/-) associated with left and right turns derived from the vehicle yaw rate measurement. This error adversely affected system performance associated with objects and vehicles detected in curves and turning situations. This resulted in the system triggering for objects it determined the vehicle was turning toward when, in fact, the vehicle was actually turning away. Figure 162 illustrates such a path estimation error case.

Figure 162: Example Recording Triggered as a Result of the Path Estimation Error

The resimulation process also uncovered recordings that were primarily triggered by either overestimated longitudinal velocity or by erratic Electronic Control Unit (ECU) frame rates. Figure 163 below contains a sample recording triggered as a result of overestimated longitudinal velocity in a traffic situation. Overestimations of longitudinal velocity are due to the fluid (developmental) nature of the current system calibration procedures, whereas erratic frame rates affect the ECU real-time performance. Improvements in both of these areas are under development by the Stereo-Vision supplier.

Figure 163: Example Recording Triggered as a Result of Overestimated Longitudinal Velocity

Figure 164 below provides the distribution of the 101 Stereo-Vision system resimulations based on the categories described above, and indicated that the largest number of data recordings were triggered either by overestimated longitudinal velocity or a path estimation error. The removal of the HLE function and the real-time performance caused by erratic ECU frame rates also contributed significant numbers of the triggered recordings. Most of the remaining recordings were triggered by variations of the calibration issues described previously.

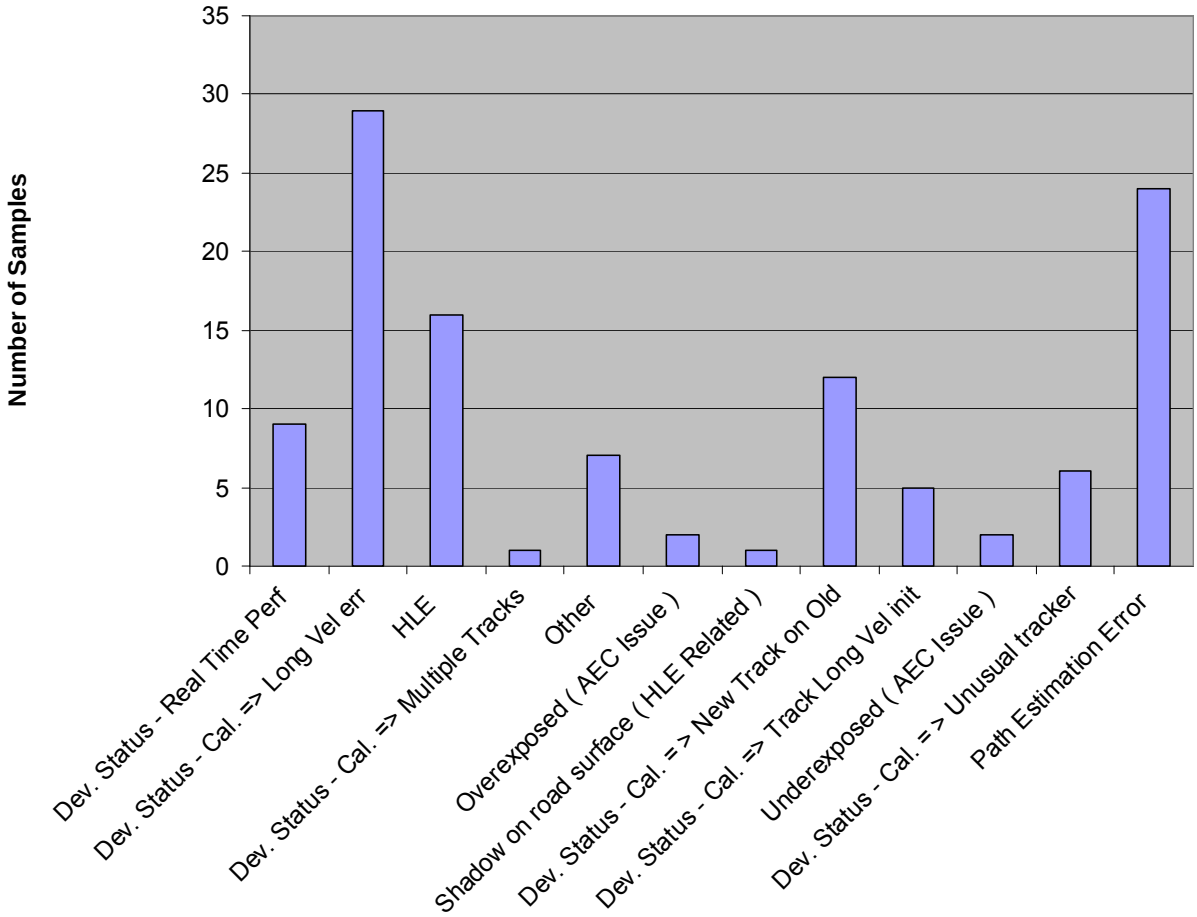

Figure 164: Distribution of Resimulated Stereo Vision System Recordings

N.2.4.3Supplier-Recommended Operational Test Scenarios for Stereo-Vision:

Based on the resimulation of the recorded video files, none of the false positive conditions observed lead to specific tests to verify against potential core systemic Stereo-Vision system issues. However, the system supplier recommended a few situational scenarios that tend to be generally challenging for vision-based sensing systems, including inclement weather and low-light conditions (which are shown in Figure 165 and Figure 166, respectively).

These conditions could be addressed as an adaptation to the operational tests for Mono-Vision systems outlined in Appendix O, incorporating low-light or simulated-rain conditions using, for example, an overhead sprinkler system.

Furthermore, visually repeating patterns (e.g., trees, bushes, and fences) may be particularly challenging for Stereo-Vision systems. In addition, to verify the performance of a vision systems “Horizon Line Estimator,” the supplier suggests that roadway inclines and/or declines may be considered within operational test scenarios. This type of test is consistent with the Host Vehicle Pitch Change and Shadow-on-Road tests described for the Mono-Vision-based system in Appendix O.

Figure 165: Example Image from an Event Recording Obstructed by Rain

Figure 166: Example Image from an Event Recorded in Low-Light Conditions

N.3 Environmental Conditions Not Assessed by the ROAD Trip

Due to program timing limitations, it was not possible to expose the vehicles driven on the ROAD Trip to winter driving conditions. Therefore, it is likely that there are winter-driving scenarios that could cause false events that were not captured on this trip. One such scenario that has been observed by an OEM consortium member has been caused by formation of icicles in front of a radar range sensor, as shown in Figure 167 and Figure 168.

Figure 167: No Evidence of Obstruction on the Outside of the Fascia

Figure 168: One Icicle on the Inside of the Foam Block

Formation of an icicle in front of the radar aperture can have the effect of distorting the perceived direction of the returned radar signal without attenuating it appreciably. When this happens the reported angles to targets can be altered such that an out of path target can be reported as in path, or, an in path target can be reported as out of path. An actual occurrence of this phenomenon is illustrated in Figure 169.

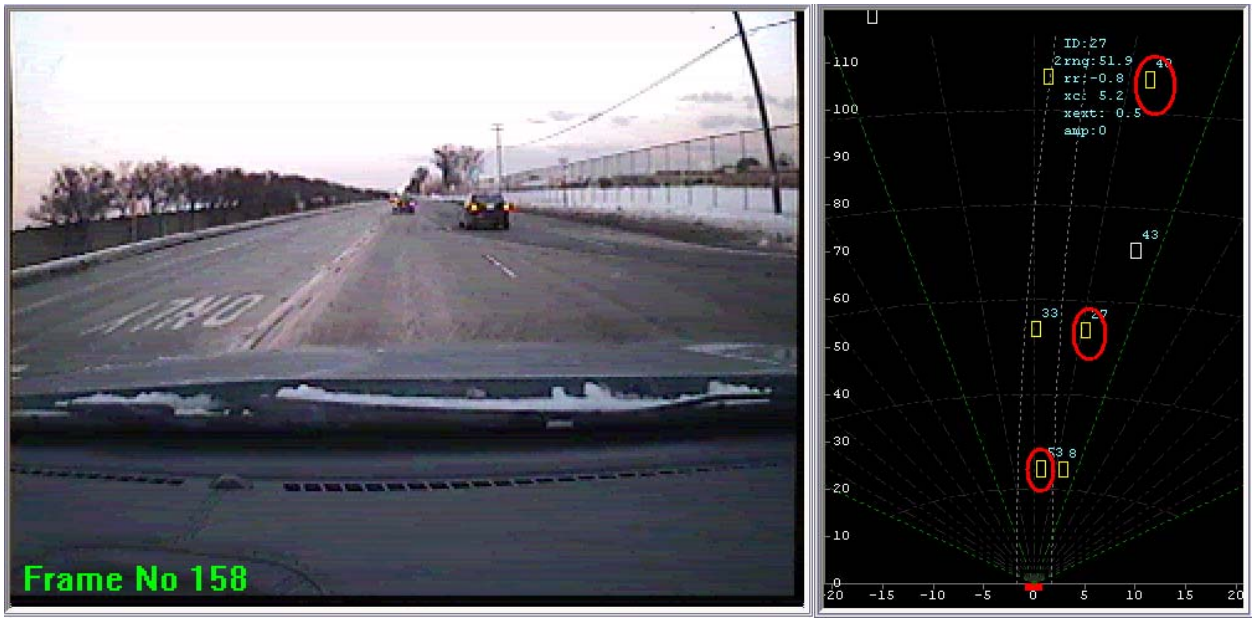

Figure 169: False Targets are Circled in Red

As can be seen in Figure 169, multiple “sidelobe” false tracks (circled in the plan view above) appear throughout the scene while the icicle is present. These tracks can appear

next to real objects and can be aliased into the host's path (for adjacent lane real objects) or out of the host's path when the real object is in the host's lane. These false radar tracks are eliminated when the icicle is removed.

This type of event could potentially cause a false event in a radar only CIB system. It can also cause false events in fused-vision and radar systems if a decelerating vehicle in the adjacent lane is incorrectly fused with a non-threat vehicle in the host's path. Additionally, because ice represents a phase shift in the RF rather than an attenuator, it can be difficult for the radar to detect as a fault condition.

It has been found that partial blockage due to ice can be emulated with plastic strips placed in front of the antenna aperture (either on the radome of the antenna or the fascia), as illustrated in Figure 170. This has been verified by correlating antenna patterns from a radar blocked with ice with antenna patterns from a radar blocked with plastic sheets.

Figure 170: Plastic Strips Used to Emulate Partial Ice Blockage

Appendix O Operational Test Scenarios

For the Operational Test Scenarios, the requirements for standard test conditions and equipment are listed in Appendix K.

The functional test methods were based upon the priority crash scenarios. These test methods address the actuation of the CIB system where the application of the brakes is necessary to mitigate the harm caused by a valid threat. Operational scenarios are the set of tests defined to test CIB system performance in the presence of targets that do not represent an actual vehicle threat. The operational tests examine the propensity of a CIB system for undesirable false CIB activations. The operational test methods were developed from data acquired during the ROAD Trip. A suite of tests has been developed for assessing the robustness of a CIB system to reject a variety of non-threatening targets that appear to be a threat due to environmental circumstances.

The following Operational Test Scenarios have been developed and evaluated during the project. However, these scenarios were not deemed validated since there was not sufficient data to categorize them as “validated” due to the observed lack of repeatability and inability to discriminate the differences between varying levels of CIB performance.

In order to evaluate the propensity of CIB systems to inappropriately engage due to the types of false-event scenarios observed during the ROAD Trip, a set of operational (false event) “on track” tests were devised that are intended to provide a first-order check for these false activation scenarios. It is important to stress that while these tests are recommended as an element of assessing CIB system performance, they are not considered a substitute for many miles of real-world evaluation. In the real world, false activations are typically rare and are not always repeatable. Unlike the Functional test scenarios, the test requirements below have been specified with the intent to replicate a range of values observed in the field rather than a specific value or criteria. Furthermore, it is recommended that the tests described below be run as a series of repeated tests that exercise system performance over the wide ranges provided (i.e., rather than repeating the tests at a single speed condition). The set of Operational Test Scenarios are the following:

- Object in Roadway
- Object in Roadway at Curve Entrance
- Object in Roadway at Curve-Exit
- Roadside Stationary Object
- Overhead Signs / Bridges
- Short Radius Turns
- LVD Operational Scenarios:
    - Road Markings
    - Shadows on Road – Non Vehicle

- Pitch
- Target Vehicle Shadows
- LVD – Target Turns Out of Path

O.1 Operational Test Procedure for Objects-in-Roadway

O.1.1 Test Description

The Object-in-Roadway event can be replicated on a test-track environment with the test arrangement illustrated in Figure 171. In-Road objects may be represented by placing radar reflective object (e.g., Bott's dot or corner cube) on the ground in the vehicle's path. Although reflectivity data for the in-roadway objects were not readily available from the ROAD Trip results, many of these events were caused by reflectors embedded in the roadway (e.g., Bott's dots). Therefore, the object recommended for this event is either a commercially available in-road reflector, or alternatively, to characterize the radar reflectivity of such a reflector and substitute an appropriately-sized corner cube.

To test the operational capability of the test vehicle CIB system in an Objects-in-Roadway Operational Scenario, the test vehicle is driven in a straight and level lane over a small stationary target at a constant forward velocity. The test vehicle brakes must not be manually applied until the test vehicle as passed over the target.

O.1.2 Instrumentation and Test Conditions

- Instrumentation and general testing conditions are described in Appendix K
- Test track configuration is comprised of one lane of a straight, flat testing area with a length of 350 meters

O.1.3 Test Procedure

- Place the target object in the center of the test vehicle lane with the reflective axis orientated parallel to the lane, toward the test vehicle (see Figure 171)
- The minimum starting separation distance between the test vehicle and the target is 300 meters. For each individual test, a vehicle test speed shall be selected from the range of speeds defined in Table 63. The test vehicle must reach and maintain the selected test speed for a distance of at least 100 meters before the target location.
- The test vehicle is driven straight toward the target at constant speed
- During test execution, yaw rate, vehicle acceleration and lateral offset should be maintained within the ranges indicated (see Table 63)
- The test vehicle brakes must not be applied by the operator until the test has passed over the target
- The test will be repeated within the specified speed range until 15 valid runs are recorded. A different speed shall be used for each test within the limits described in Table 63. A valid run is one in which all specified parameters fall within the limits described and all test results identified below are recorded.

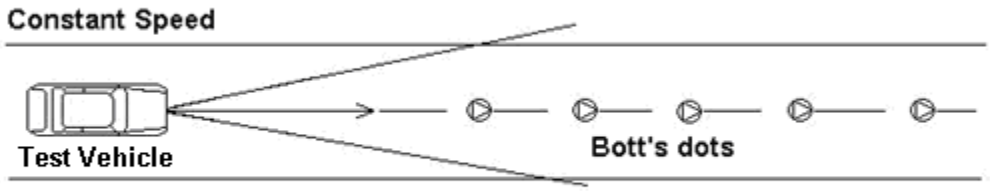

Figure 171: Test Vehicle with Objects-in-Roadway

Table 63: Parameters for Objects-in-Roadway Operational Test

Parameter	Min	Max
Test Vehicle Speed (mph)	30	75
Test Vehicle Yaw Rate (deg/s)	-2	2
Test Vehicle Longitudinal Acceleration (m/s^2)	-0.3	0.3
Heading Lateral Offset from Target (m)	-1.5	1.5

O.1.4 Test Results

The following data shall be recorded for each valid test run:

- Test vehicle speed versus time
- Test vehicle acceleration versus time
- Test vehicle position versus time
- Test vehicle yaw versus time
- Position of target system
- Test vehicle autonomous braking activated: yes/no

The following criteria shall be used to determine the pass/fail status:

- Autonomous tests vehicle deceleration during this test shall not exceed 0.5 m/s^2 on all tests

O.2 Operational Test Procedure for Stationary Object at Curve Entrance

O.2.1 Test Description

In order to replicate the Curve-Entry False-Event Scenario, the test vehicle shall drive on a straight section of roadway and then approach a curve (as illustrated in Figure 172). A stationary target shall be placed just past the curve exit on the outside of the curve. Target placement at the entrance shall be on the side of the roadway after it becomes straight, such that continuation of the straight-line path would intersect the target. Since this type of event can also affect Fusion-based systems, it is suggested that the stationary target used for this test be a midsize passenger sedan rather than a corner cube or other radar reflective device. Using a midsized sedan will also make the same test method valid for both Radar and Fusion systems.

O.2.2 Instrumentation and Test Conditions

Instrumentation and general testing conditions are described in Appendix K.

- Test track configuration is comprised of one lane of a straight, flat testing area with a length of 350 meters, with a flat curved section whose radius of curvature falls within the values specified in Table 64

O.2.3 Test Procedure

- Place the target vehicle at side of the road and just beyond the entrance of the curve, such that the continuation of the straight-line path intersects with the target vehicle (see Figure 172)
- The minimum starting separation distance between the test vehicle and the target is 300 meters. The test vehicle must reach and maintain the defined test speed (see Table 64) for a distance of at least 100 meters before the target location.
- The test vehicle is driven straight toward the target at constant speed
- The test vehicle brakes must not be applied by the operator until the test has passed by the target
- The test will be repeated within the specified speed range until 15 valid runs are recorded. A different speed shall be used for each test within the limits described in Table 64. A valid run is one in which all specified parameters fall within the limits described and all test results identified below are recorded.

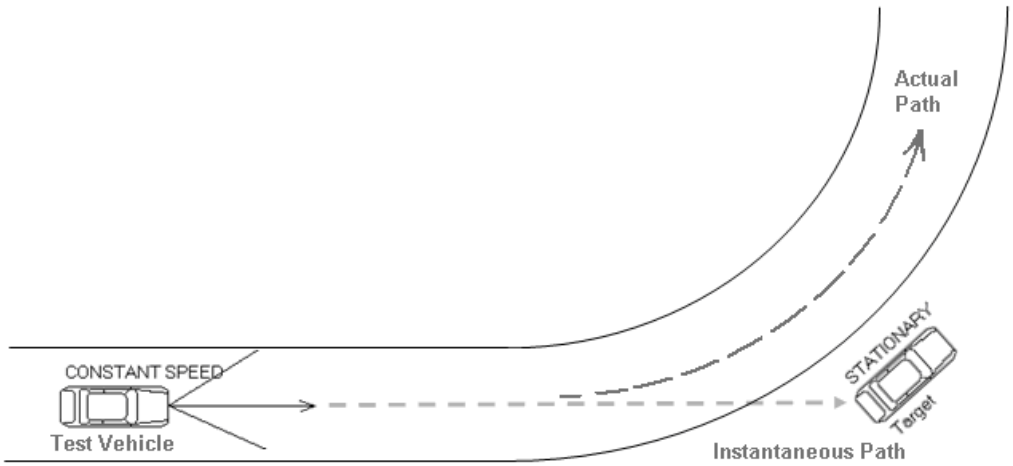

Figure 172: Stationary Vehicle Located at Curve Entrance

Table 64: Test Parameters for Curve-Entrance Operational Test

Parameter	Min	Max
Test Vehicle Speed (mph)	20	55
Curve Radius of Curvature (m)	600	800
Test Vehicle Yaw Rate Before Curve Entrance (deg/s)	-2	2
Test Vehicle Yaw Rate After Curve Entrance (deg/s)	-15	15
Test Vehicle Longitudinal Acceleration (m/s^2)	-0.5	0.5
Test Vehicle Lateral Acceleration Before Curve Entrance(m/s^2)	-1.0	1.0
Test Vehicle Lateral Acceleration After Curve Entrance (m/s^2)	-3.5	3.5
Heading Lateral Offset from Target Before Curve Entrance (m)	-1.5	1.5

O.2.4 Test Results

The following data shall be recorded for each valid test run:

- Test vehicle speed versus time
- Test vehicle acceleration versus time
- Test vehicle position versus time
- Test vehicle yaw versus time

- Position of target system

The following criteria shall be used to determine the pass/fail status:

- Autonomous test vehicle deceleration during this test shall not exceed 0.5 m/s^2 on all tests

O.3 Operational Test Procedure for Stationary Object at Curve-Exit

O.3.1 Test Description

In order to replicate the Curve-Exit False-Event Scenario, the test vehicle shall drive on a section of roadway of constant curvature and approach the end of the curve as illustrated in Figure 173. A stationary target vehicle shall be placed just past the curve exit on the inside of the curve.

Target placement at the curve exit shall be on the side of the roadway after it becomes straight, such that continuation of the curve would intersect the target. Since this type of event can also affect Fusion-based systems, it is suggested that the stationary target used for this test be an actual car rather than a corner cube or other radar reflective device. This will also make the same test method valid for both Radar and Fusion systems.

O.3.2 Instrumentation and Test Conditions

- Instrumentation and general testing conditions are described in Appendix K
- Test track configuration is comprised of one flat curved lane whose radius of curvature falls within the range of values specified in Table 65, with a length of 350 meters

O.3.3 Test Procedure

- Place the target vehicle at side of the road and just beyond the exit of the curve, such that the continuation of the curved line path intersects with the target vehicle (see Figure 173)
- The minimum starting separation distance between the test vehicle and the target is 300 meters along the defined path. The test vehicle must reach and maintain the defined test speed (see Table 65) for a distance of at least 100 meters before the target location. The test vehicle must remain in the center of the lane until it passes the stationary vehicle.
- The test vehicle is driven along the defined path at constant speed
- The test vehicle brakes must not be applied by the operator until the test vehicle has passed by the target
- The test will be repeated within the specified speed range until 15 valid runs are recorded. A different speed shall be used for each test within the limits described in Table 65. A valid run is one in which all specified parameters fall within the limits described and all test results identified below are recorded.

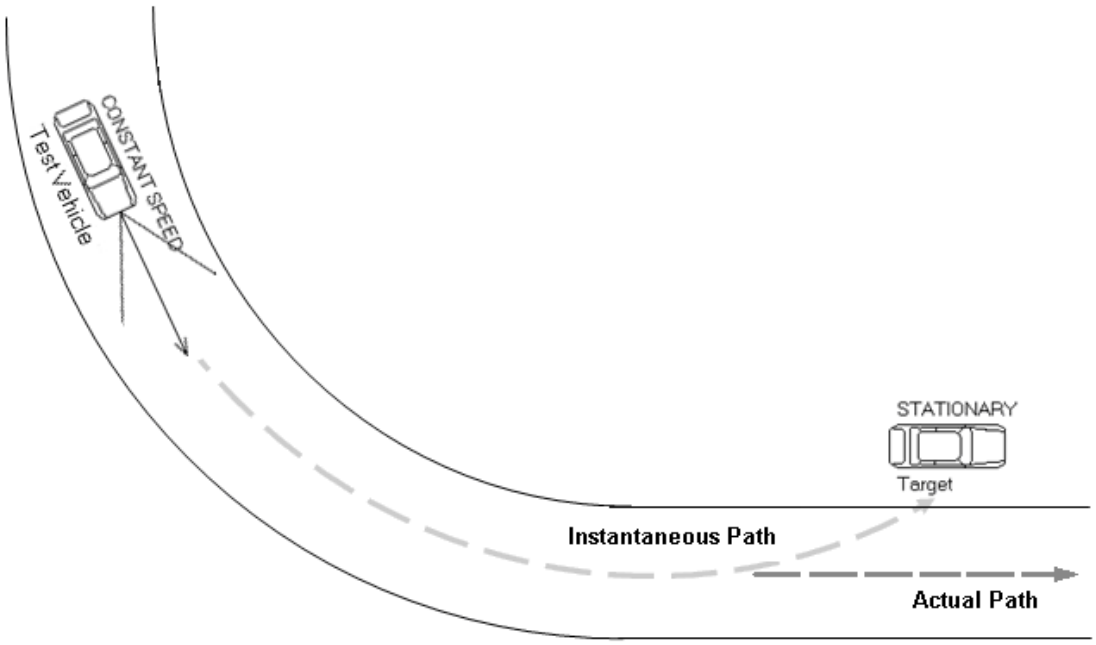

Figure 173: Stationary Vehicle at Curve Exit

Table 65: Test Parameters for Curve-Exit Operational Test

Parameter	Min	Max
Test Vehicle Speed (mph)	20	55
Curve Radius of Curvature (m)	600	800
Test Vehicle Yaw Rate Before Curve Exit (deg/s)	-10	10
Test Vehicle Yaw Rate After Curve Exit (deg/s)	-2	2
Test Vehicle Longitudinal Acceleration (m/s²)	-0.5	0.5
Test Vehicle Lateral Acceleration Before Curve Exit (m/s²)	-3.5	3.5
Test Vehicle Lateral Acceleration After Curve Exit (m/s²)	-1.0	1.0

O.3.4 Test Results

The following data shall be recorded for each valid test run:

- Test vehicle speed versus time
- Test vehicle acceleration versus time
- Test vehicle position versus time

- Test vehicle yaw versus time
- Position of target system

The following criteria shall be used to determine the pass/fail status:

- Autonomous test vehicle deceleration during this test shall not exceed 0.5 m/s^2 on all tests

O.4 Operational Test Procedure for Roadside Stationary Objects

O.4.1 Test Description

In order to replicate the Roadside-Object False-Event Scenario, the test vehicle shall drive on a straight section of roadway and approach a row of stationary objects as illustrated in Figure 174. As it approaches the stationary objects, the test vehicle would perform a mild lane change towards them (see test parameters in Table 66).

Target placement shall be on the side of the roadway with an open lane between the test vehicle's starting lane and the stationary targets. Since this type of event can also affect Fusion-based systems, it is suggested that the stationary targets used for this test be midsize passenger sedans rather than corner cubes or other radar reflective devices. Use of actual cars will also allow the test method to be valid for both Radar and Fusion systems.

O.4.2 Instrumentation and Test Conditions

- Instrumentation and general testing conditions are described in Appendix K
- Test track configuration is comprised of two lanes of a straight, flat testing area with a length of 350 meters. The lane width should be nominally 3 to 3.5 m.

O.4.3 Test Procedure

- A minimum of three targets is required. Place the targets at side of the road (see Figure 174 which illustrates the test procedure using stationary vehicles as targets). Targets shall be located 1 to 2 m from the lane boundary and separated by 1 to 3 m.
- The minimum starting separation distance between the test vehicle and the target is 300 meters along the defined path. The test vehicle must reach and maintain the defined test speed (see Table 66) for a distance of at least 100 meters before the target location.
- Initial lateral positioning of the test vehicle shall be such that there is one open lane between the test vehicle and the stationary targets
- When the separation distance is within the range specified in Table 66, the test vehicle shall initiate a mild lane change maneuver such that the lateral acceleration limits given in Table 66 are not exceeded
- The lane change maneuver shall be initiated such that the test vehicle's heading temporarily intersects with one or more of the stationary targets during the lane change
- The test vehicle is driven along the defined path at constant speed
- The test vehicle brakes must not be applied by the operator until the test has passed by the targets
- The test will be repeated within the specified speed range until 15 valid runs are recorded. A different speed shall be used for each test within the limits described

in Table 66. A valid run is one in which all specified parameters fall within the limits described and all test results identified below are recorded.

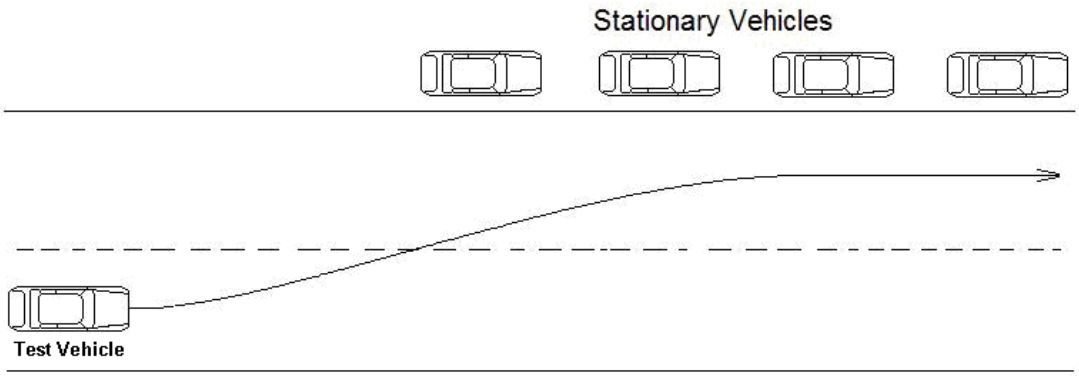

Figure 174: Roadside Stationary Vehicles

Table 66: Test Parameters for Roadside-Object Operational Test

Parameter	Min	Max
Test Vehicle Speed (mph)	50	75
Test Vehicle Yaw Rate (deg/s)	-5	5
Test Vehicle Longitudinal Acceleration (m/s²)	-0.3	0.3
Separation Distance to Stationary Vehicles at Initiation of Lane Change (m)	40	80
Test Vehicle Lateral Acceleration (m/s²)	-1	1

O.4.4 Test Results

The following data is to be recorded for each valid test run:

- Test vehicle speed versus time
- Test vehicle acceleration versus time
- Test vehicle position versus time
- Test vehicle yaw versus time
- Position of target system

The following criteria shall be used to determine the pass/fail status:

- Autonomous test vehicle deceleration during this test shall not exceed 0.5 m/s² on all tests

O.5 Operational Test for Overhead Signs and Bridges

O.5.1 Test Description

In order to replicate the Overhead Signs and Bridges False-Event Scenario, the test vehicle shall drive on a straight section of roadway and approach a bridge underpass or an overhead sign as illustrated in Figure 175. The bridge or sign shall have a metallic structure.

O.5.2 Instrumentation and Test Conditions

- Instrumentation and general testing conditions are described in Appendix K
- Test track configuration is comprised of two lanes of a straight, flat testing area with a length of 350 meters

O.5.3 Test Procedure

- The minimum starting separation distance between the test vehicle and the target shall be 300 meters along the defined path. The test vehicle must reach and maintain the defined test speed (see Table 67) for a distance of at least 100 meters before the target location.
- The test vehicle is driven along the defined path at constant speed
- The test vehicle brakes must not be applied by the operator until the test has passed by the target
- The test will be repeated within the specified speed range until 15 valid runs are recorded. A different speed shall be used for each test within the limits described in Table 67.
- A valid run is one in which all specified parameters fall within the limits described and all test results identified below are recorded

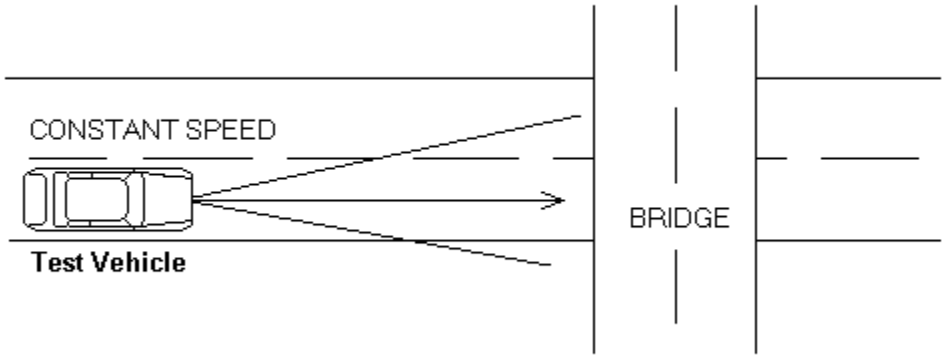

Figure 175: Overhead Sign/Bridge

Table 67: Test Parameters for Overhead Sign/Bridge Operational Test

Parameter	Min	Max
Test Vehicle Speed (mph)	50	75
Test Vehicle Yaw Rate (deg/s)	-5	5
Test Vehicle Longitudinal Acceleration (m/s^2)	-0.3	0.3
Clearance Height from Roadway to Bottom of Sign/Bridge (ft)	15	17

O.5.4 Test Results

The following data is to be recorded for each valid test run:

- Test vehicle speed versus time
- Test vehicle acceleration versus time
- Test vehicle position versus time
- Test vehicle yaw versus time
- Position of target system

The following criteria shall be used to determine the pass/fail status:

- Autonomous test vehicle deceleration during this test shall not exceed 0.5 m/s^2 on all tests

O.6 Operational Test Procedure for Short-Radius-Turns

O.6.1 Test Description

In order to replicate the Short-Radius-Turn False-Event Scenario, the test vehicle shall perform a short-radius, low-speed turn next to a row of stationary vehicles (as illustrated in Figure 176). Target placement shall be on the side of the roadway and out of the actual path of the turning test vehicle. Since this type of event can also affect Fusion-based systems, it is suggested that the stationary targets used for this test be mid-sized passenger sedans rather than corner cubes or other radar reflective devices. Use of mid-sized passenger cars will also allow the same test method to be valid for both Radar and Fusion systems.

O.6.2 Instrumentation and Test Conditions

- Instrumentation and general testing conditions are described in Appendix K
- Test track configuration is comprised of two perpendicular intersecting lanes of a straight, flat testing area, each with a length of 50 meters

O.6.3 Test Procedure

- The minimum starting separation distance between the test vehicle and the target is 50 meters along the defined path. The test vehicle must reach and maintain the defined test speed (see Table 68) for a distance of at least 50 meters before the target location.
- A minimum of three targets is required. Place the targets at the side of the road as shown in Figure 176 (which illustrates the test procedure using stationary vehicles as targets). Targets shall be located 1 to 2 m from the lane boundary and separated by 1 to 3 m.
- The test vehicle is driven along the defined path at constant speed
- The test vehicle brakes must not be applied by the operator until the test has passed by all of the targets
- The test shall be repeated within the specified speed range until 15 valid runs are recorded. A different speed shall be used for each test within the limits described in Table 68. A valid run is one in which all specified parameters fall within the limits described and all test results identified below are recorded.

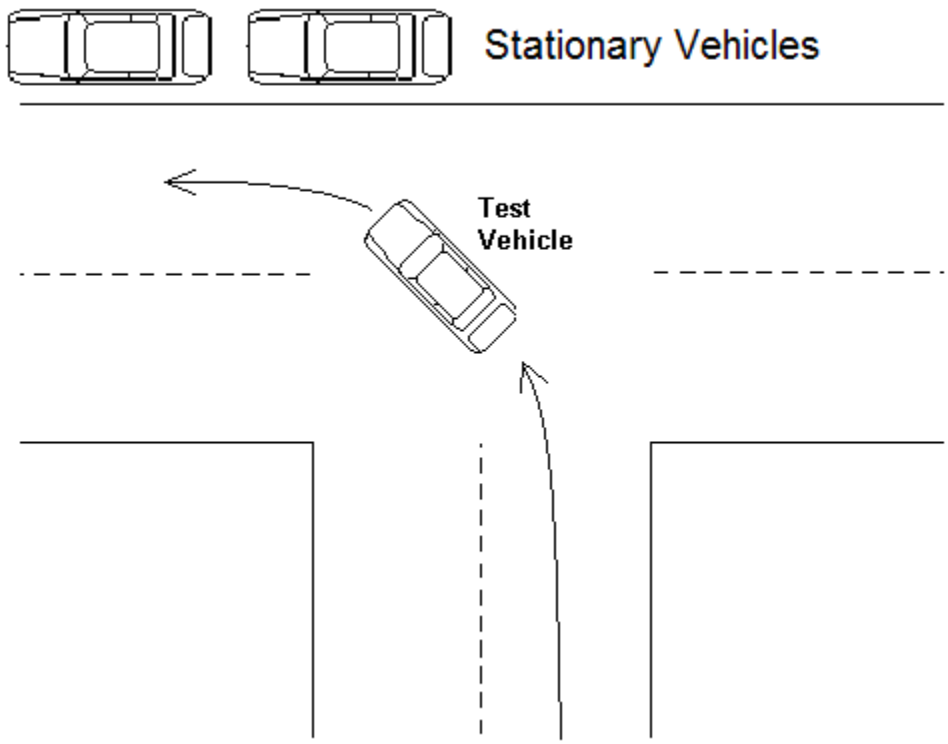

Figure 176: Short-Radius Turn

Table 68: Test Parameters for Short-Radius-Turn Operational Test

Parameter	Min	Max
Test Vehicle Speed (mph)	5	15
Radius of Curvature of Turn (m)	10	50

O.6.4 Test Results

The following data is to be recorded for each valid test run:

- Test vehicle speed versus time
- Test vehicle acceleration versus time
- Test vehicle position versus time
- Test vehicle yaw versus time
- Position of target system

The following criteria shall be used to determine the pass/fail status of each test:

- Autonomous test vehicle deceleration during this test shall not exceed 0.5 m/s² on all tests

O.7 Operational Test Procedure for Lead Vehicle Deceleration (LVD)

O.7.1 Test Description

The majority of vision-related false events from the systems evaluated were found to be due to various visual cues interfering with system performance. In order to replicate these false-event scenarios, a test similar to the LVD positive performance test can be used, while introducing representations of the various visual cues that have been observed to be potentially problematic.

The test vehicle shall be driven on a straight section of roadway while following the target vehicle as described in Sections O.7.3.1 through O.7.3.5. The target vehicle shall then decelerate at a rate that falls within the values specified in Table 69, while encountering one of the visual cues described in the operational LVD tests below.

O.7.2 Instrumentation and Test Conditions

- Instrumentation and general testing conditions are described in Appendix K
- Test track configuration is comprised of two lanes of a straight, flat testing area with a length of 350 meters

O.7.3 Test Procedure

Figure 177 through Figure 182 in the following sections illustrate the LVD Operational Test Scenarios. For the affected vision systems, the test scenarios assess performance during Lead Vehicle Decelerating scenarios and are designed such that a collision does not take place, thus, allowing the use of a real vehicle for the leading target. These four tests involve variations on the test scenario for LVD. The test procedures for these are the same for all four with differences in visual cues represented in each test. The reader is referred to Appendix L, Section L.3 for the description of the LVD test procedure.

O.7.3.1 Operational Test for LVD On-Road Features

As illustrated in Figure 177 for the LVD On-Road Features Operational Test Scenario, the lead vehicle shall start its deceleration just prior to traversing over a series of on-road markings that were observed to be potentially challenging for the Mono-Vision systems evaluated.

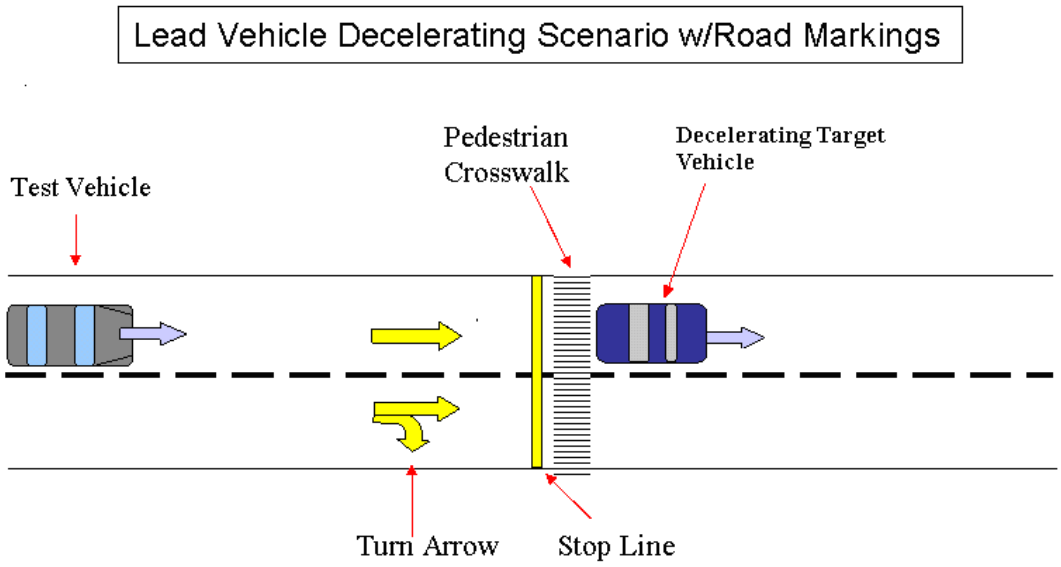

Figure 177: Operational Test for LVD On-Road Features

O.7.3.2 Operational Test for LVD Over Shadows-On-Road

As illustrated in Figure 178, for the LVD Over Shadows-on-Road Operational Test Scenario, the lead vehicle shall start its deceleration just before driving over a series of shadows cast onto the road.

The shadows cast on the roadway should have the following characteristics, as illustrated in Figure 179:

- The shadow should be cast such that it covers the entire lane to be occupied by the target vehicle
- The Shadow should be perpendicular to the direction of travel of the lane to be occupied by the target vehicle within ±5 degrees
- The shadow should be 1.5 to 3 meters wide

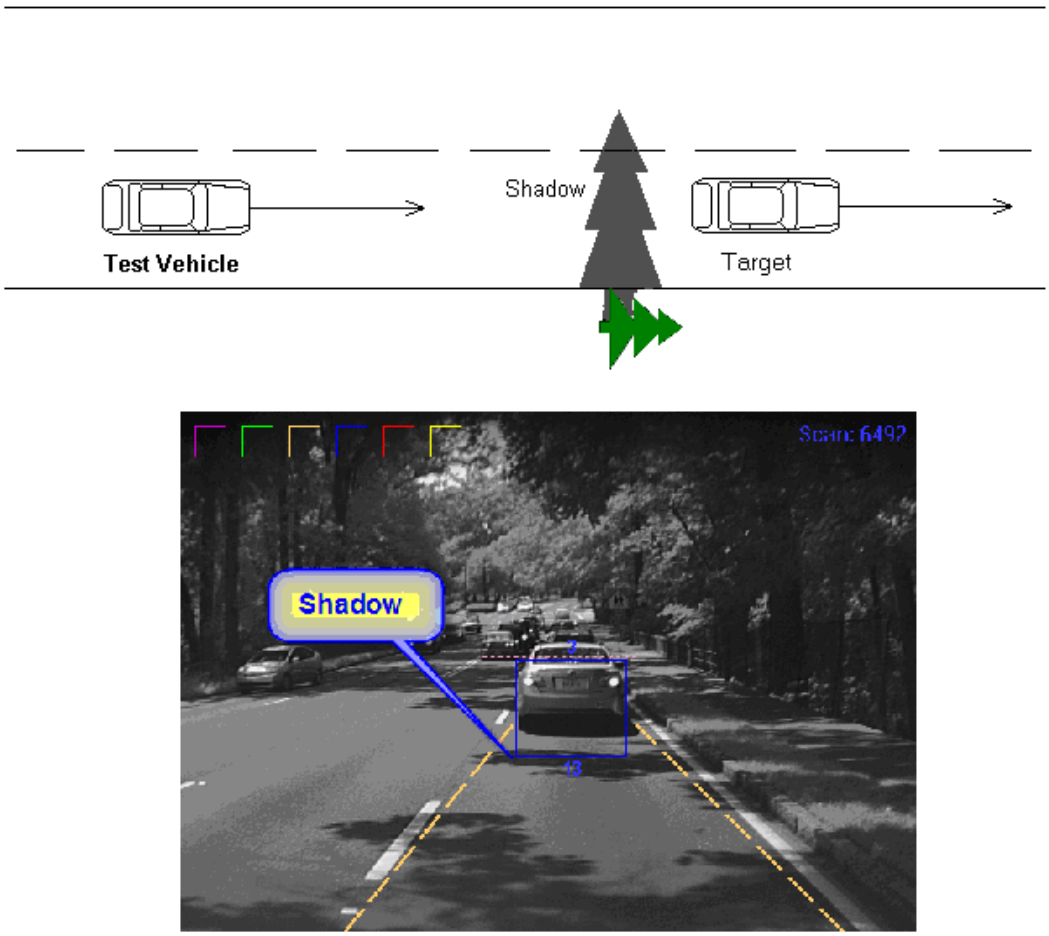

Figure 178: Operational Test for LVD Over Shadows-on-Road

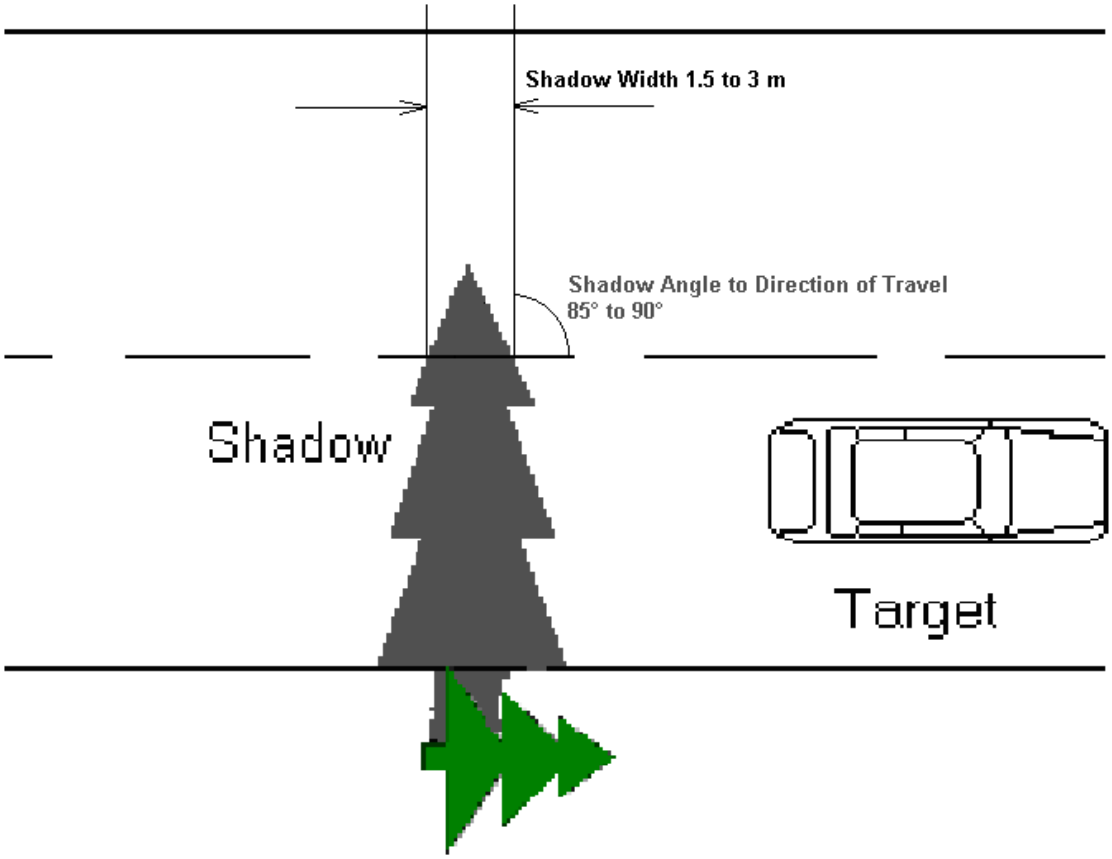

Figure 179: Detail of Shadow on Road

O.7.3.3 Operational Test for LVD during CIB-Vehicle-Pitch-Change

As illustrated in Figure 180, for the LVD During CIB-Vehicle-Pitch-Change Operational Test Scenario, the lead vehicle shall start its deceleration as the test vehicle is about to undergo a change in pitch. The designated pitch change for this test is presented in Table 69.

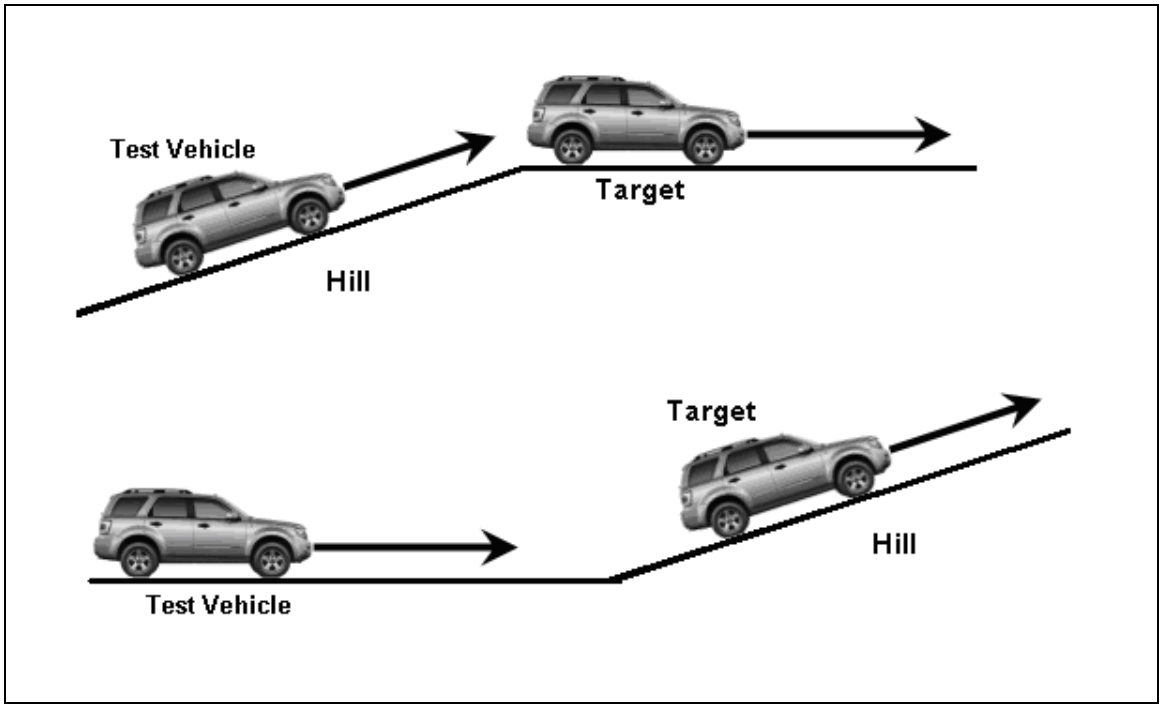

Figure 180: Operational Test for LVD During CIB-Vehicle-Pitch-Change

O.7.3.4 Operational Test for LVD with Target-Vehicle-Shadow

As illustrated in Figure 181, for the LVD with Target-Vehicle-Shadow Operational Test Scenario, the test shall be run during low-sun angle conditions such that a shadow is cast extending 2 m to 3 m behind the rear of the target vehicle.

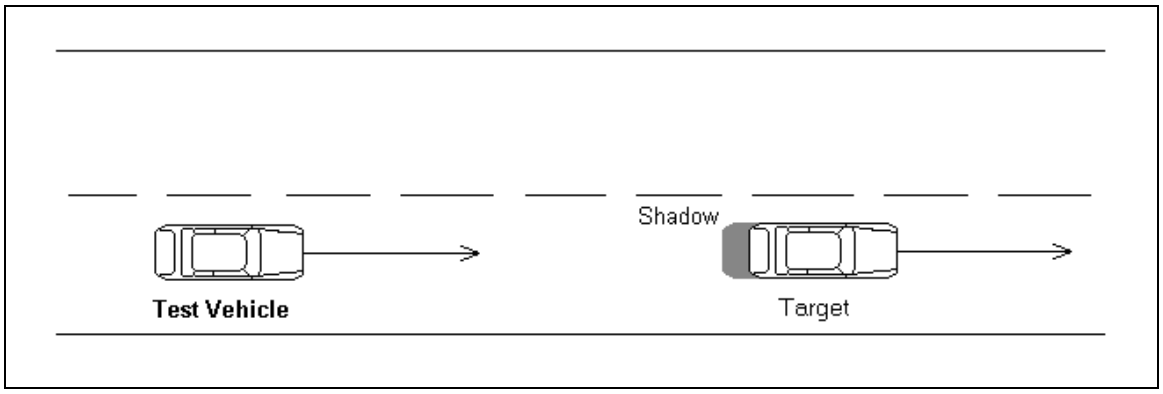

Figure 181: Operational Test for LVD with Target-Vehicle-Shadows

O.7.3.5 Operational Test for LVD and Target Turns Out-of-Path

The events that were observed for the "LVD and Target Turns Out-of-Path" scenario had very similar kinematic values to those found in the other LVD false events. As such,

these events could be replicated by using the operational test procedures as described in this section, with the modification that the lead vehicle turns “Out-of-Path” (e.g., makes a right turn) while decelerating, as is illustrated in Figure 182.

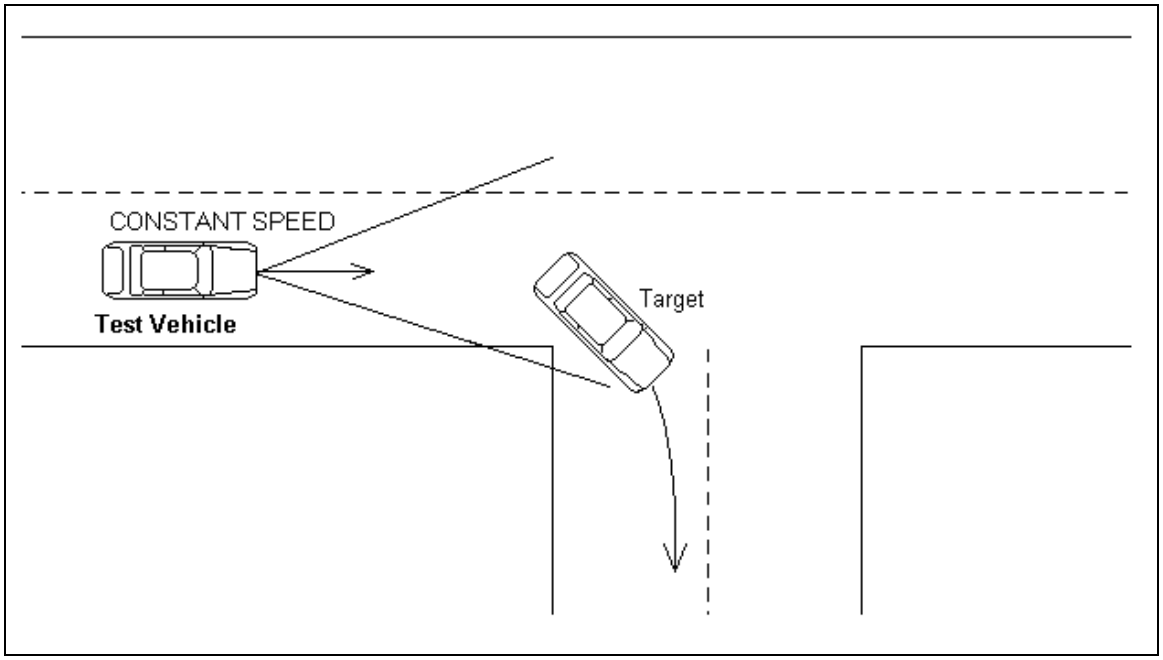

Figure 182: LVD Target Turns Out-of-Path Operational Test

Since these operational tests are variations on the same LVD scenario, it is recommended that these scenarios all be performed using the testing conditions specified in Table 69. Since it is recommended to vary the deceleration levels of the lead vehicle within the limits stated in Table 69, it is important for safety reasons to ensure that the resulting scenario does not result in a collision. The starting separation (or headway) distance is dependent on the level of deceleration chosen for the lead vehicle. Additionally, this separation distance shall be chosen to ensure that the resulting scenario falls in the range of values found during the ROAD Trip (see Table 69).

The following describes how the starting range for each scenario shall be derived. Initially, start with a minimum Simple (i.e., Momentary) Time to Collision (i.e., TTC = Range/Range Rate) that defines the end of the test. This value has been chosen to reflect the values observed in the ROAD test, and once this minimum TTC value is reached, the driver of the test vehicle shall immediately decelerate or steer around the target vehicle to avoid collision.

O.7.4 Derivation of Test Parameters

To calculate the starting separation distance for the test, the final separation distance (r_e) shall be specified from the values given in Table 69 and the final closing velocity ($\dot{r}_e$) shall be calculated from this:

$$\dot{r}_e = r_e / TTC \qquad (1)$$

Where:

$\dot{r}_e$ = Final Range Rate (closing velocity) to the target at the instance the min TTC is achieved (meters / second).

r_e = Range to the target (separation distance) at the instance the min TTC is achieved (meters). Min and Max Values are specified in Table 69

TTC = Time to Collision (seconds). Min Value is specified in Table 69

Given this information, calculate the starting separation distance from the following:

$$\dot{r}_e^{\,2} = \dot{r}_p^{\,2} + 2ar_d \qquad (2)$$

Where:

a = brake deceleration of the primary target (m/s^2). Min and Max values are specified in Table 69. This represents the actual value used within that range for each individual test.

$\dot{r}_p$ = Initial Range Rate to the target (meters / second)

r_d = Range gained on the primary target during its brake acceleration

Since the speeds of the test and target vehicle are initially equal, $\dot{r}_p$ is zero, thus:

$$r_d = \frac{\dot{r}_e^{\,2}}{2a} \qquad (3)$$

Combining elements from (1) and (3),

$$r_{start} = r_e + r_d \qquad (4)$$

Where

r_{start} = starting range (separation distance) for the test

Finally, in order to ensure that the target vehicle does not come to a stop during the test, the initial test and target velocities should be chosen such that:

$$v_0 \geq \dot{r}_e$$

Where

v_0 = the initial speed for both the test and target vehicle

Table 69: LVD Scenario Physical Conditions

Parameter	Min	Max
Test Vehicle Speed (v_0)	15 mph (6.7 m/s)	25mph (11.2m/s)
Test Vehicle Yaw Rate	-1 deg/s	1 deg/s
Initial Target Vehicle Speed (v_0)	same as test vehicle	
Test Vehicle to Target Spacing at End of Test (r_e)	9m	15m
Target Vehicle Deceleration (a)	1 m/s ^{2}	3 m/s ^{2}
Simple TTC at end of test (TTC)	2 sec	-
Roadway Pitch Change (degrees - pitch change tests only)	5	7

O.7.5 Choosing Parameter Values for an Individual Test

To determine specific test values for an individual test, follow the following steps:

- Pick a value for the Initial Test Vehicle Speed (v_0) from the range specified in Table 69
- Pick a value for Test Vehicle to Target Spacing at End of Test (r_e) from the range specified in Table 69, such that:

  $$v_0 \geq r_e / TTC$$

  using the min TTC specified in Table 69.
- Pick a value for Target Vehicle Deceleration (a) from the range specified in Table 69
- Calculate the Initial Test Vehicle to Target Vehicle Range Separation (r_{start}) from

  $$r_{start} = r_e + \frac{r_e^2}{TTC^2 2a}$$

using the min TTC specified in Table 69

Each series of tests will be repeated within the range of values specified until 15 valid runs are recorded. A valid run is one in which all specified parameters fall within the limits described and all test results identified below are recorded.

O.7.6 Test Results

The following data is to be recorded for each valid test run:

- Test vehicle speed versus time
- Test vehicle acceleration versus time
- Test vehicle position versus time
- Test vehicle yaw versus time
- Position of target system

The following criteria shall be used to determine the pass/fail status:

- Autonomous Test vehicle deceleration during this test shall not exceed 0.5 m/s^2 on all tests

DOT HS 811 521A
September 2011

U.S. Department
of Transportation
**National Highway
Traffic Safety
Administration**

NHTSA
www.nhtsa.gov